



## Durham E-Theses

---

### *Fluorometabolite biosynthesis in streptomyces cattleya*

Moss, Steven J.

#### How to cite:

---

Moss, Steven J. (1999) *Fluorometabolite biosynthesis in streptomyces cattleya*, Durham theses, Durham University. Available at Durham E-Theses Online: <http://etheses.dur.ac.uk/4603/>

#### Use policy

---

The full-text may be used and/or reproduced, and given to third parties in any format or medium, without prior permission or charge, for personal research or study, educational, or not-for-profit purposes provided that:

- a full bibliographic reference is made to the original source
- a [link](#) is made to the metadata record in Durham E-Theses
- the full-text is not changed in any way

The full-text must not be sold in any format or medium without the formal permission of the copyright holders.

Please consult the [full Durham E-Theses policy](#) for further details.

# Fluorometabolite Biosynthesis in *Streptomyces cattleya*

Steven J Moss

Nature has evolved the ability to form a C-F bond, as exemplified by the bacterium *Streptomyces cattleya*, which elaborates fluoroacetate (**FAc**) and 4-fluorothreonine (**4-FT**). The mechanism of this bond formation are unknown. This thesis probes the biosynthesis of fluoroacetate and 4-fluorothreonine and in doing so explores the C-F bond forming process.

Feeding stable isotope enriched primary metabolites to *S. cattleya*, followed by  $^{19}\text{F}$  NMR and GCMS analysis of the resultant fluorometabolites, highlights the role of the glycolytic pathway in delivering a substrate for fluorination. 3-Fluoro-1-hydroxypropan-2-one was synthesised and feeding studies eliminate this as the initial product of fluorination.

Fluoroacetaldehyde was identified as a common fluorinated intermediate in the biosynthesis of both **FAc** and **4-FT**. Whole cell studies demonstrate the rapid oxidation of fluoroacetaldehyde to **FAc**. **4-FT** is produced in low quantities by *S. cattleya* incubated with fluoroacetaldehyde. The synthesis and feeding of  $[1-^2\text{H}]$ -fluoroacetaldehyde provide evidence that the resultant **4-FT** is biosynthesised from fluoroacetaldehyde. The biotransformation from fluoroacetaldehyde to **FAc** was shown in cell free studies to be mediated by an aldehyde dehydrogenase, requiring  $\text{NAD}^+$  as a co-factor. The substrate specificity of fluoroacetaldehyde dehydrogenase was probed by spectrophotometrically monitoring the production of NADH in the presence of different aldehydes.

Further cell free experiments probed the biosynthetic origins of fluoroacetaldehyde. Glycolaldehyde phosphate and various phosphorylated glycolytic intermediates were incubated with cell free extracts of *S. cattleya* and a plethora of co-factors. In the absence of observing fluorination activity, it was shown that the cell free extract acts to dephosphorylate the substrates. The putative role of glycolaldehyde phosphate was explored by feeding isotopically labelled glycolaldehydes to whole cells of the bacterium. The results were not consistent with direct conversion from glycolaldehyde phosphate to fluoroacetaldehyde.

**Fluorometabolite Biosynthesis**  
**in *Streptomyces cattleya***

**Steven James Moss**

**PhD Thesis      1999**

**University of Durham**  
**Department of Chemistry**

The copyright of this thesis rests with the author. No quotation from it should be published without the written consent of the author and information derived from it should be acknowledged.

27 JAN 2000

## ***Declaration***

The work contained in this thesis was carried out by the author in the Department of Chemistry, University of Durham between October 1996 and July 1999. The work was conducted in collaboration with the Queen's University of Belfast. GC-MS analyses, on samples submitted by the author, were performed by Dr Jack Hamilton at the Queen's University of Belfast.

## ***Copyright***

The copyright of this thesis rests with the author. No quotation from it should be published without their prior written consent and information derived from it should be acknowledged

## *Acknowledgements*

I wish to thank my supervisor, Professor David O'Hagan, not only for the continued support and enthusiasm that he has dedicated to the project, but also for the opportunities that he has given me.

Professor David Harper and Dr Cormac Murphy, at the Queen's University of Belfast, provided both technical assistance in developing the resting cell methodology in Durham and hospitality during my stay in Belfast. Sincere thanks go to Dr Jack Hamilton for the GCMS analysis that makes this project possible and for his candid discussions of the results.

I acknowledge British Nuclear Fuels Ltd and the BBSRC who provided CASE funding for this work and I thank Dr Peter Binks, Dr Roy Bowden, Mr Martin Green and Dr Harry Eccles, all from BNFL, for the interest that they have shown in the project.

High field  $^{19}\text{F}$  NMR analysis was performed by Mr Ian McKeag and I thank him and the technical support staff in the Department of Chemistry.

The O'Hagan group, past and present, made the lab a vibrant and interesting place to work. I specifically would like to acknowledge Dr Jens Nieschalk and Dr Jens Fuchser, for the help and advice they imparted during this project.

Finally, I would like to thank my parents for encouraging me throughout my PhD studies and education before that.

## *List of Contents*

<b>Table of Contents</b>	<b>v</b>
<b>List of Figures</b>	<b>x</b>
<b>List of Tables</b>	<b>xvi</b>
<b>List of Abbreviations</b>	<b>xix</b>

### *Chapter 1: Introduction*

<b>1.1 Secondary metabolism</b>	<b>1</b>
1.1.1 Primary and secondary metabolism	1
1.1.2 Fatty acid biosynthesis and $\beta$ -oxidation	4
1.1.3 Microbial secondary metabolism	5
<b>1.2 Elucidation of metabolic pathways</b>	<b>7</b>
1.2.1 Biological methods	7
1.2.1.1 Mutant studies	7
1.2.1.2 Inhibition of protein biosynthesis	8
1.2.1.3 Cell free studies	8
1.2.2 Chemical methods	8
1.2.2.1 Radioisotopes	9
1.2.2.2 Stable isotopes	10
1.2.2.3 Single label feeding experiment studies	10
1.2.2.4 Double label feeding studies: 'bond labelling'	10
<b>1.3 Halogenated secondary metabolites</b>	<b>12</b>
1.3.1 Distribution of halogenated metabolites	12
1.3.2 Mechanisms for biohalogenation	13
<b>1.4 Fluorinated secondary metabolites</b>	<b>15</b>
1.4.1 Fluorine bioavailability	15
1.4.2 The Nature of the C-F bond	15
1.4.3 Fluorinated natural products in plants	17
1.4.3.1 Fluoroacetate	17
1.4.3.2 $\omega$ -Fluorinated fatty acids	18
1.4.3.3 Fluoroacetone	19
1.4.4 Fluoroacetate metabolism: (2 <i>R</i> , 3 <i>R</i> )-2-fluorocitrate	20
1.4.5 Resistance to fluoroacetate poisoning	23
1.4.6 Fluorometabolites from microorganisms	25
1.4.6.1 Nucleocidin	25

1.4.6.2	4-Fluorothreonine and fluoroacetate	26
<b>1.5</b>	<b>Biological fluorination - proposed mechanisms</b>	<b>27</b>
1.5.1	Addition to a carbon-carbon multiple bond	27
1.5.1.1	Pyridoxal phosphate assisted addition of fluoride	27
1.5.1.2	Ethylene and ethylene oxide as putative precursors	30
1.5.1.3	Nucleophilic attack on a halonium ion	30
1.5.2	Fluorination <i>via</i> nucleophilic substitution	32
<b>1.6</b>	<b><i>Streptomyces cattleya</i> and the fluorometabolites</b>	<b>33</b>
1.6.1	The Streptomycetes	33
1.6.2	<i>Streptomyces cattleya</i>	33
1.6.3	Fluoroacetate and 4-fluorothreonine	35
1.6.4	The biosynthetic relationship between fluoroacetate and 4-fluorothreonine	38
1.6.5	Incorporation of stable isotope enriched glycolate, glycine and pyruvate	39
1.6.6	The stereochemical processing of glycerol	41
1.6.7	Overview	43

## ***Chapter 2: Fluorometabolite biosynthesis and primary metabolism***

<b>2.1</b>	<b>Maintenance and growth of <i>Streptomyces cattleya</i></b>	<b>45</b>
2.1.1	Preparation of a starter culture of <i>Streptomyces cattleya</i>	46
2.1.2	Preparation of batch cultures of <i>Streptomyces cattleya</i>	46
2.1.3	Time course study on fluorometabolite biosynthesis	47
2.1.3.1	Results: pH analysis	47
2.1.3.2	Results: fluoride analysis	48
2.1.3.3	Discussion	49
<b>2.2</b>	<b>Studying fluorometabolite biosynthesis</b>	<b>50</b>
2.2.1	Preparation of resting cells of <i>Streptomyces cattleya</i>	50
2.2.1.1	Resting cell experiments: controls	51
2.2.2	Studying fluoroacetate and 4-fluorothreonine with <sup>19</sup> F NMR	51
2.2.2.1	Feeding <sup>2</sup> H <sub>2</sub> O	54
2.2.2.2	Incorporation of [2- <sup>13</sup> C]-glycine into the fluorometabolites: <sup>19</sup> F NMR analysis	56
2.2.3	GCMS analysis of fluoroacetate and 4-fluorothreonine	57
2.2.3.1	GCMS analysis of fluoroacetate	57
2.2.3.2	GCMS analysis of 4-fluorothreonine	58
<b>2.3</b>	<b>Resting cell incorporation studies</b>	<b>60</b>
2.3.1	[6,6- <sup>2</sup> H <sub>2</sub> ]-Glucose	60

2.3.1.1	Background	60
2.3.1.2	Results and discussion	62
2.3.2	Isotopically labelled acetates	66
2.3.2.1	Background	66
2.3.2.2	Results and discussion	66
2.3.3	[2- <sup>2</sup> H]-Glycerol and [2- <sup>2</sup> H]-glycerate	71
2.3.3.1	Background	71
2.3.3.2	Results and discussion	72
<b>2.4</b>	<b>Synthesis and feeding of 3-fluoro-1-hydroxypropanone</b>	<b>75</b>
2.4.1	Background	75
2.4.2	3-Fluoro-1-hydroxypropanone	77
2.4.3	Synthesis of 3-fluoro-1-hydroxypropanone	78
2.4.4	Biotransformation of 3-fluoro-1-hydroxypropanone	81
2.5	Conclusions	87

### *Chapter 3: A role for fluoroacetaldehyde*

<b>3.1</b>	<b>Fluoroacetaldehyde</b>	<b>89</b>
3.1.1	Synthesis of fluoroacetaldehyde	89
<b>3.2</b>	<b>Whole cell studies on fluoroacetaldehyde</b>	<b>92</b>
3.2.1	Preliminary studies	92
3.2.1.1	Introduction	92
3.2.1.2	Results and discussion	92
3.2.2	Oxygen requirements of fluoroacetaldehyde metabolism	95
3.2.2.1	Fluoroacetaldehyde metabolism under nitrogen	95
3.2.2.2	Fluoroacetaldehyde metabolism under <sup>18</sup> O <sub>2</sub>	96
3.2.2.3	Conclusions	97
<b>3.3</b>	<b>Fluoroacetaldehyde in fluorometabolite biosynthesis</b>	<b>98</b>
3.3.1	Fluoroacetaldehyde metabolism by other <i>Streptomyces</i> spp.	98
3.3.1.1	Growth of <i>Streptomyces cinnamonensis</i>	98
3.3.1.2	Feeding fluoroacetaldehyde to resting cells of <i>Streptomyces cinnamonensis</i>	99
3.3.2	Fluoroacetaldehyde: incubation with alanine and serine	100
3.3.2.1	Experimental considerations	100
3.3.2.2	Results and discussion	101
3.3.3	The synthesis and feeding of [1- <sup>2</sup> H]-fluoroacetaldehyde	101
3.3.3.1	Synthesis of [1- <sup>2</sup> H]-fluoroacetaldehyde	103
3.3.3.2	Feeding [1- <sup>2</sup> H]-fluoroacetaldehyde	108
3.3.3.3	Conclusions	113
<b>3.4</b>	<b>Cell free studies on fluoroacetaldehyde metabolism</b>	<b>114</b>



3.4.1 Protein determination	114
3.4.2 Disruption of the cells by sonication	115
3.4.2.1 Maximising the protein yield	115
3.4.2.2 Fluoroacetaldehyde metabolism	115
3.4.3 Disruption of the cells with a French Press	116
3.4.3.1 Fluoroacetaldehyde metabolism	116
3.4.3.2 Results and discussion	117
3.4.3.3 Conclusions	117
3.4.4 Co-factor dependence	118
3.4.4.1 Experimental protocol	118
3.4.4.2 Results and discussion	119
3.4.5 Substrate specificity	122
3.4.5.1 Experimental protocol	123
3.4.5.2 Results and discussion	123
3.4.5.3 Conclusions	125
3.4.6 Fluoroacetaldehyde dehydrogenase: membrane bound or soluble?	125
3.4.6.1 Experimental protocol	125
3.4.6.2 Results and discussion	126
<b>3.5 Cell free studies on 4-fluorothreonine biosynthesis</b>	<b>127</b>
3.5.1 Synthesis of aminomalonate	128
3.5.2 Cell free studies with aminomalonate	128
3.5.3 Conclusions	129
<b>3.6 Conclusions</b>	<b>130</b>

### *Chapter 4: Cell free investigation of the fluorination event*

<b>4.1 Cell free studies with phosphorylated intermediates</b>	<b>136</b>
4.1.1 Synthesis of glycolaldehyde phosphate	136
4.1.2 Preliminary cell free experiments	137
4.1.3 Cell free experiments with SAM, methionine, cysteine and glutathione	139
4.1.4 Cell free studies with pyridoxamine	143
4.1.5 Conclusions	144
<b>4.2 Assessing phosphatase activity in the cell free extract</b>	<b>146</b>
4.2.1 Phosphate assay	146
4.2.2 Preliminary dephosphorylation studies	147
4.2.3 Partial purification of the cell free extract	151
4.2.4 Partial purification of fluoroacetaldehyde dehydrogenase	153

4.2.5 Conclusions	156
<b>4.3 Synthesis and evaluation of isotope enriched glycolaldehydes</b>	<b>157</b>
4.3.1 Synthesis of isotope enriched glycolaldehydes	157
4.3.2 Feeding isotope enriched glycolaldehydes	159
<b>4.4 Conclusions</b>	<b>164</b>

## *Chapter 5: Experimental*

<b>5.1 Chemical Syntheses</b>	<b>167</b>
5.1.1 General Details	167
5.1.2 Preparation of 3-fluoro-1-hydroxypropanone	167
5.1.3 Preparation of fluoroacetaldehyde	171
5.1.4 Preparation of [1- <sup>2</sup> H]-fluoroacetaldehyde	173
5.1.5 Preparation of aminomalonate	175
5.1.6 Preparation of glycolaldehyde phosphate	175
5.1.7 Preparation of [1- <sup>13</sup> C]- and [1- <sup>13</sup> C, 2,2- <sup>2</sup> H <sub>2</sub> ]-glycolaldehyde	178
<b>5.2 Biological Preparations</b>	<b>183</b>
5.2.1 General details	183
5.2.1.1 <sup>19</sup> F NMR analysis of resting cell experiments	183
5.2.1.2 GCMS analysis of resting cell feeding studies	184
5.2.2 Microorganism maintenance and growth	185
5.2.2.1 Variations of pH and fluoride uptake during growth of <i>S. cattleya</i>	186
5.2.3 Resting cell experiments with <i>Streptomyces cattleya</i>	186
5.2.4 Whole cell studies with fluoroacetaldehyde	191
5.2.5 Cell free studies with <i>Streptomyces cattleya</i>	196
5.2.5.1 Protein concentration determination	196
5.2.5.2 Cell disruption by sonication	196
5.2.5.3 Cell disruption using the french press	197
5.2.5.4 Phosphate release assay	198
<b>References</b>	<b>199</b>
<b>Appendix I</b> List of Conferences attended	<b>206</b>

## List of Figures

<b>Fig. 1.1</b>	Penicillin, coniine and $\alpha$ -pinene.	2
<b>Fig. 1.2</b>	The major secondary metabolic precursors. The arrows represent multiple step transformations.	4
<b>Fig. 1.3</b>	Fatty acid biosynthesis and $\beta$ -oxidation.	5
<b>Fig. 1.4</b>	Cholesterol biosynthesis, topological mapping by [1- $^{14}$ C]-acetate.	9
<b>Fig. 1.5</b>	Thyroxine, vancomycin & tyrian purple dye.	12
<b>Fig. 1.6</b>	Monochlorodimedone assay for haloperoxidases activity.	14
<b>Fig. 1.7</b>	NADH-dependent halogenase in pyrrolnitrin (32) biosynthesis	14
<b>Fig. 1.8</b>	Fluoroacetate.	17
<b>Fig. 1.9</b>	$\omega$ -Fluorinated fatty acids.	18
<b>Fig. 1.10</b>	Fluoroacetone, and its putative biosynthesis from fluoroacetate.	20
<b>Fig. 1.11</b>	Lethal synthesis of 2-fluorocitrate from fluoroacetate, mediated by citrate synthase.	21
<b>Fig. 1.12</b>	Metabolism of (2 <i>R</i> , 3 <i>R</i> )-2-fluorocitrate to 4-hydroxy- <i>trans</i> -aconitate.	22
<b>Fig. 1.13</b>	Proposed mechanism for microbial fluoroacetate defluorination to yield glycolate.	23
<b>Fig. 1.14</b>	Fluoroacetate defluorination in <i>Moraxella</i> spp. B.	24
<b>Fig. 1.15</b>	Nucleocidin.	25
<b>Fig. 1.16</b>	Fluoroacetate and 4-fluorothreonine.	26
<b>Fig. 1.17</b>	Biosynthesis of $\beta$ -substituted alanines by the Leguminales.	27
<b>Fig. 1.18</b>	Putative biosynthesis of fluoroacetate, Mead and Segal.	28
<b>Fig. 1.19</b>	The decarboxylation of $\beta$ -fluoropyruvate by <i>Dichapetalum cymosum</i> .	29
<b>Fig. 1.20</b>	Putative pathways to fluoroacetate from ethylene.	30
<b>Fig. 1.21</b>	<i>In vitro</i> formation of a halonium ion and subsequent nucleophilic attack.	31
<b>Fig. 1.22</b>	The <i>in vitro</i> synthesis of 2,3-fluoroiodopropan-1-ol.	31
<b>Fig. 1.23</b>	The putative biosynthesis of fluoroacetate <i>via</i> an $\omega$ -fluorinated fatty acid.	31
<b>Fig. 1.24</b>	Nucleophilic substitution of a phosphate group by fluoride.	32
<b>Fig. 1.25</b>	Geosmin.	33

<b>Fig. 1.26</b>	Thienamycin, imipenem and meropenam.	34
<b>Fig. 1.27</b>	Cephamycin C, 2-hydroxy-2-hydroxymethylcyclo-pent-4-ene, penicillin N and 3-ethynyl serine.	34
<b>Fig. 1.28</b>	Proposed biosynthesis of fluoroacetate and 4-fluorothreonine, Sanada <i>et al</i>	35
<b>Fig. 1.29</b>	[2- <sup>13</sup> C]-glycerol incorporation into fluoroacetate, Soda <i>et al</i> .	37
<b>Fig. 1.30</b>	Putative conversion of β-hydroxypyruvate to fluoroacetate, Soda <i>et al</i> .	38
<b>Fig. 1.31</b>	Fluoroacetate is not a precursor of 4-fluorothreonine, Reid <i>et al</i> .	39
<b>Fig. 1.32</b>	Recombination of label from [2- <sup>13</sup> C]-glycine into both fluoroacetate and 4-fluorothreonine.	40
<b>Fig. 1.33</b>	Glycine recombination <i>via</i> serine.	40
<b>Fig. 1.34</b>	Incorporation of [2- <sup>13</sup> C]- & [3- <sup>13</sup> C]-pyruvate into fluoroacetate and 4-fluorothreonine.	41
<b>Fig. 1.35</b>	The feeding of chiral glycerols to <i>S. cattleya</i> , Nieschalk <i>et al</i> .	42
<b>Fig. 1.36</b>	The metabolic relationship between primary metabolites that contribute to fluorometabolite biosynthesis.	43
<b>Fig. 2.1</b>	Growth of <i>S. cattleya</i> and fluorometabolite production.	45
<b>Fig. 2.2</b>	Fluoroacetate and 4-fluorothreonine production in <i>S. cattleya</i> .	45
<b>Fig. 2.3</b>	The variation of pH with time in batch cells of <i>S. cattleya</i> .	47
<b>Fig. 2.4</b>	Calibration curve for fluoride selective electrode.	48
<b>Fig. 2.5</b>	Fluoride uptake by batch cells of <i>S. cattleya</i>	49
<b>Fig. 2.6</b>	Potential patterns of deuterium labelling in 4-FT.	52
<b>Fig. 2.7</b>	<sup>19</sup> F { <sup>1</sup> H} NMR of FAc and 4-FT labelled <i>via</i> [2,2,3,3- <sup>2</sup> H <sub>4</sub> ]-succinate metabolism.	53
<b>Fig. 2.8</b>	<sup>19</sup> F { <sup>1</sup> H} NMR of FAc and 4-FT labelled <i>via</i> [3- <sup>13</sup> C]-pyruvate metabolism.	54
<b>Fig. 2.9</b>	<sup>19</sup> F { <sup>1</sup> H} NMR analysis of resting cells of <i>Streptomyces cattleya</i> incubated in the presence of <sup>2</sup> H <sub>2</sub> O.	55
<b>Fig. 2.10</b>	<sup>19</sup> F { <sup>1</sup> H} NMR analysis of resting cells of <i>Streptomyces cattleya</i> incubated with [2- <sup>13</sup> C]-glycine.	56
<b>Fig. 2.11</b>	Derivatisation of fluoroacetate with 2-bromo-4'-phenacetophenone.	57
<b>Fig. 2.12</b>	Cleavage of per-trimethylsilylated derivative of 4-fluorothreonine.	58
<b>Fig. 2.13</b>	The glycolytic pathway	61

<b>Fig. 2.14</b>	$^{19}\text{F}$ $\{^1\text{H}\}$ NMR of fluoroacetate and 4-fluorothreonine, following incubation of resting cells of <i>S. cattleya</i> with 5 mM $[6,6\text{-}^2\text{H}_2]$ -glucose.	62
<b>Fig. 2.15</b>	Labelling pattern in the fluorometabolites from $[6,6\text{-}^2\text{H}_2]$ -glucose.	63
<b>Fig. 2.16</b>	The pentose phosphate pathway.	65
<b>Fig. 2.17</b>	$^{19}\text{F}$ $\{^1\text{H}\}$ NMR analysis of resting cells of <i>S. cattleya</i> fed with $[1\text{-}^{13}\text{C}]$ -acetate.	66
<b>Fig. 2.18</b>	$^{19}\text{F}$ $\{^1\text{H}\}$ NMR analysis of resting cells of <i>S. cattleya</i> fed with $[1,2\text{-}^{13}\text{C}_2]$ -acetate.	67
<b>Fig. 2.19</b>	$^{19}\text{F}$ $\{^1\text{H}\}$ NMR analysis of resting cells of <i>S. cattleya</i> fed with $[2,2,2\text{-}^2\text{H}_3]$ -acetate.	67
<b>Fig. 2.20</b>	The TCA cycle, demonstrating both the fate of $[2\text{-}^{13}\text{C}]$ -acetate and $[^2\text{H}_3]$ -acetate, including the scrambling of label through fumarate.	70
<b>Fig. 2.21</b>	Oxidation state at C-2 of the glycolytic intermediates on either side of DHAP, P = phosphate.	71
<b>Fig. 2.22</b>	The removal of deuterium from glyceraldehyde <i>via</i> triose phosphate isomerase.	73
<b>Fig. 2.24</b>	Working hypothesis for fluorometabolite biosynthesis <i>via</i> a fluorinated $\text{C}_3$ unit.	75
<b>Fig. 2.25</b>	Putative post fluorination products synthesised and fed by Amin and Murphy	76
<b>Fig. 2.26</b>	3-Fluoro-1-hydroxypropanone and DHAP.	76
<b>Fig. 2.27</b>	Synthesis of 3-fluoro-1-hydroxypropan-2-one by Kozarich.	77
<b>Fig. 2.28</b>	Putative synthesis of $[3\text{-}^2\text{H}_2]$ -3-fluoro-1-hydroxypropanone from 3-fluoro-1-hydroxypropanone benzyl ether.	77
<b>Fig. 2.29</b>	Synthesis of 3-fluoro-1-hydroxypropan-2-one benzyl ether.	78
<b>Fig. 2.30</b>	Ring opening of glycidol benzyl ether with $\text{KHF}_2$ .	79
<b>Fig. 2.31</b>	$^{19}\text{F}$ NMR of 3-fluoro-1-hydroxypropanone.	80
<b>Fig. 2.32</b>	Putative mechanism for 3-fluoro-1-hydroxypropanone DNP defluorination.	81
<b>Fig. 2.33</b>	$^{19}\text{F}$ NMR spectrum of the resultant supernatant from incubating resting cells of <i>S. cattleya</i> for 18 hours with 3-fluoro-1-hydroxypropanone ( <b>experiment 1</b> ).	82
<b>Fig. 2.34</b>	$^{19}\text{F}$ NMR spectrum of the resultant supernatant from incubating resting cells of <i>S. cattleya</i> for 18 hours with 3-fluoro-1-hydroxypropanone ( <b>experiment 2</b> ).	82
<b>Fig. 2.35</b>	$^{19}\text{F}$ NMR spectrum of the resultant supernatant from incubating resting cells of <i>S. cattleya</i> for 48 hours with 3-fluoro-1-hydroxypropanone ( <b>experiment 1</b> ).	83

<b>Fig. 2.36</b>	<sup>19</sup> F NMR spectrum of the resultant supernatant from incubating resting cells of <i>S. cattleya</i> for 48 hours with 3-fluoro-1-hydroxypropanone ( <b>experiment 2</b> ).	83
<b>Fig. 2.37</b>	Putative conversion of 3-fluoro-1-hydroxypropanone to 3-fluoroglyceraldehyde.	85
<b>Fig. 2.38</b>	Coupling constants in 3-fluoroglyceraldehyde, Effenberger.	85
<b>Fig. 3.1</b>	<sup>19</sup> F NMR spectrum of fluoroacetaldehyde and 2-fluoroethanol.	90
<b>Fig. 3.2</b>	<sup>19</sup> F NMR, fluoroacetaldehyde (2.0 mM) fed to <i>Streptomyces cattleya</i> , Time = 0 minutes.	93
<b>Fig. 3.3</b>	<sup>19</sup> F NMR, fluoroacetaldehyde (2.0 mM) fed to <i>Streptomyces cattleya</i> , Time = 10 minutes.	93
<b>Fig. 3.4</b>	<sup>19</sup> F NMR, fluoroacetaldehyde (2.0 mM) fed to <i>Streptomyces cattleya</i> , Time = 30 minutes.	94
<b>Fig. 3.5</b>	<sup>19</sup> F NMR, fluoroacetaldehyde (2.0 mM) fed to <i>Streptomyces cattleya</i> , Time = 40 minutes.	94
<b>Fig. 3.6</b>	Conversion of fluoroacetaldehyde to fluoroacetate, by resting cells of <i>S. cattleya</i> .	95
<b>Fig. 3.7</b>	Fluoroacetaldehyde under a N <sub>2</sub> atmosphere, in resting cells of <i>S. cattleya</i> .	96
<b>Fig. 3.8</b>	Incubation of fluoroacetaldehyde in an <sup>18</sup> O <sub>2</sub> atmosphere, with resting cells of <i>S. cattleya</i> .	97
<b>Fig. 3.9</b>	Retrosynthetic analysis of [1- <sup>2</sup> H]-fluoroacetaldehyde.	103
<b>Fig. 3.10</b>	Synthesis of [1- <sup>13</sup> C, 1,1- <sup>2</sup> H <sub>2</sub> ]-ethanol, Rogers.	103
<b>Fig. 3.11</b>	Synthesis of <i>para</i> -phenylphenacyl fluoroacetate.	104
<b>Fig. 3.12</b>	Synthesis of fluoroacetaldehyde from phenylphenacyl fluoroacetate.	105
<b>Fig. 3.13</b>	Synthesis of [1- <sup>2</sup> H]-fluoroacetaldehyde from <i>para</i> -phenylphenacyl fluoroacetate.	106
<b>Fig. 3.14</b>	<sup>19</sup> F NMR of [1- <sup>2</sup> H]-fluoroacetaldehyde and [1,1- <sup>2</sup> H <sub>2</sub> ]-2-fluoroethanol.	106
<b>Fig. 3.15</b>	Putative reduction of ethyl fluoroacetate with LiAlH <sub>4</sub> .	107
<b>Fig. 3.16</b>	Potential labelling patterns in 4-fluorothreonine from feeding both [1- <sup>2</sup> H]-fluoroacetaldehyde and [2- <sup>13</sup> C]-glycine (91), to resting cells of <i>S. cattleya</i> .	109
<b>Fig. 3.17</b>	Comparison of populations of none (M), single (M+1), double (M+2) and triple (M+3) label in positions 2, 3 & 4 of fluorothreonine resultant from incubating [1- <sup>2</sup> H]-fluoroacetaldehyde and 10 mM [2- <sup>13</sup> C]-glycine with resting cells of <i>S. cattleya</i> , <b>Experiment 1</b> .	111

<b>Fig. 3.18</b>	Comparison of populations of none (M), single (M+1), double (M+2) and triple (M+3) label in positions 2, 3 & 4 of fluorothreonine resultant from incubating [1- <sup>2</sup> H]-fluoroacetaldehyde and 1.0 mM [2- <sup>13</sup> C]-glycine with resting cells of <i>S. cattleya</i> , <b>Experiment 2</b> .	112
<b>Fig. 3.19</b>	Standard curve for protein (BSA) determination using the Bradford assay.	114
<b>Fig. 3.20</b>	Action of NAD <sup>+</sup> on the fluoroacetaldehyde dehydrogenase.	120
<b>Fig. 3.21</b>	Graphical representation of conversion of fluoroacetaldehyde to fluoroacetate and the variation of absorbance, measured at $\lambda = 310$ nm.	121
<b>Fig. 3.22</b>	Decrease in rate of NADH production with time. All samples are cell free extract, 2 mM fluoroacetaldehyde and 2 mM NAD <sup>+</sup> .	122
<b>Fig. 3.23</b>	Putative biosynthesis of 4-fluorothreonine from fluoroacetaldehyde and 2-aminomalonate.	127
<b>Fig. 3.24</b>	Synthesis of potassium 2-aminomalonate.	128
<b>Fig. 3.25</b>	Putative relationship between molecular oxygen and fluoroacetaldehyde oxidation in <i>S. cattleya</i> .	130
<b>Fig. 3.26</b>	The pivotal role of fluoroacetaldehyde in fluorometabolite biosynthesis in <i>S. cattleya</i> .	131
<b>Fig. 3.27</b>	Hypothetical role of channelled fluoroacetaldehyde in fluorometabolite biosynthesis, in <i>S. cattleya</i> .	132
<b>Fig. 4.1</b>	Oxidative bond cleavage and fluorination are required to synthesis fluoroacetaldehyde from a glycolytic intermediate.	134
<b>Fig. 4.2</b>	Putative role of glycolaldehyde phosphate in fluoroacetaldehyde biosynthesis.	134
<b>Fig. 4.3</b>	Putative substrates for the fluorination event in <i>S. cattleya</i> .	135
<b>Fig. 4.4</b>	Synthetic scheme to glycolaldehyde phosphate, Eschenmoser <i>et al.</i>	136
<b>Fig. 4.5</b>	Putative mechanism for fluorination <i>via</i> nucleophilic displacement of phosphate by a thiol, followed by nucleophilic attack by fluoride. Glycolaldehyde phosphate is used as the substrate by way of example.	139
<b>Fig. 4.6</b>	SAM, methionine, cysteine and glutathione.	140
<b>Fig. 4.7</b>	Putative mechanism for fluoroacetaldehyde defluorination by cysteine.	143
<b>Fig. 4.8</b>	Putative mechanism involving pyridoxamine phosphate (PMP).	143
<b>Fig. 4.9</b>	Standard curve for phosphate assay, absorbance @ $\lambda = 310$ nm.	147

<b>Fig. 4.10</b>	SDS-PAGE electrophoresis analysis of crude and partially purified cell free extract of <i>S. cattleya</i> . Lane 1, molecular weight markers; Lane 2, 10 $\mu$ l crude CFE; Lane 3, 17 $\mu$ l crude CFE; Lane 4, 10 $\mu$ l partially purified CFE; Lane 5, 17 $\mu$ l partially purified CFE.	155
<b>Fig. 4.11</b>	Putative conversion of glycolaldehyde to fluoroacetaldehyde via glycolaldehyde phosphate.	157
<b>Fig. 4.12</b>	Kiliani-Fischer type synthesis to prepare glycolaldehyde.	157
<b>Fig. 4.13</b>	Synthesis of [1- $^{13}$ C, 2,2- $^2$ H $_2$ ]-glycolaldehyde.	159
<b>Fig. 4.14</b>	$^{19}$ F { $^1$ H} NMR of fluoroacetate and 4-fluorothreonine, following incubation of resting cells of <i>S. cattleya</i> with 10 mM [1- $^{13}$ C, 2,2- $^2$ H $_2$ ]-glycolaldehyde.	161
<b>Fig. 4.15</b>	Labelling observed in fluoroacetate and 4-fluorothreonine resulting from incubation of resting cells of <i>S. cattleya</i> with [1- $^{13}$ C, 2,2- $^2$ H $_2$ ]-glycolaldehyde.	161
<b>Fig. 4.16</b>	The biosynthesis of activated glycolaldehyde by thiamine pyrophosphate and transketolase.	162
<b>Fig. 4.17</b>	Putative assimilation of [1- $^{13}$ C, 2,2- $^2$ H $_2$ ]-glycolaldehyde into [2- $^{13}$ C, 1,1- $^2$ H $_2$ ]-fructose-6-phosphate and [2- $^{13}$ C, 1,1- $^2$ H $_2$ ]-xylulose-5-phosphate.	163



## *List of Tables*

<b>Table 1.1</b>	Properties of isotopes used in biosynthetic studies.	9
<b>Table 1.2</b>	Fluoride and chloride concentrations in the Earth's crust and sea water.	15
<b>Table 1.3</b>	Physicochemical parameters of the halogens.	16
<b>Table 1.4</b>	Van der Waal's radius and bond length of C-H and other substituents.	16
<b>Table 1.5</b>	Heat of hydration and standard redox potential for the halogens.	17
<b>Table 2.1</b>	Calibration data for the fluoride selective electrode.	48
<b>Table 2.2</b>	Upfield shifts observed in $^{19}\text{F}$ $\{^1\text{H}\}$ NMR due to $^2\text{H}$ and $^{13}\text{C}$ in both fluoroacetate and 4-fluorothreonine.	52
<b>Table 2.3</b>	GCMS analysis of 4-fluorothreonine, following incubation of resting cells of <i>S. cattleya</i> with 5 mM $[6,6\text{-}^2\text{H}_2]$ -glucose.	62
<b>Table 2.4</b>	GCMS analysis of fluoroacetate, following incubation of resting cells of <i>S. cattleya</i> with 5 mM $[6,6\text{-}^2\text{H}_2]$ -glucose.	63
<b>Table 2.5</b>	GCMS analysis of fluoroacetate, following incubation of resting cells of <i>S. cattleya</i> with isotopically enriched acetates.	68
<b>Table 2.6</b>	GCMS analysis of 4-fluorothreonine, following incubation of resting cells of <i>S. cattleya</i> with $[2\text{-}^2\text{H}]$ -glycerate.	72
<b>Table 2.7</b>	GCMS analysis of 4-fluorothreonine, following incubation of resting cells of <i>S. cattleya</i> with $[2\text{-}^2\text{H}]$ -glycerate.	74
<b>Table 3.1</b>	Percentage conversion of fluoroacetaldehyde to fluoroacetate by resting cells of <i>Streptomyces cinnamomensis</i> .	99
<b>Table 3.2</b>	Fluorometabolite production resultant from feeding fluoroacetaldehyde to resting cells of <i>Streptomyces cattleya</i> , Murphy.	102
<b>Table 3.3</b>	% Incorporation into positions 2, 3 & 4 of 4-fluorothreonine, resulting from feeding $[1\text{-}^2\text{H}]$ -fluoroacetaldehyde, to resting cells of <i>S. cattleya</i> .	108
<b>Table 3.4</b>	Incorporation of $^{13}\text{C}$ & $^2\text{H}$ into positions 2, 3 & 4 of 4-fluorothreonine, resulting from incubating $[1\text{-}^2\text{H}]$ -fluoroacetaldehyde and $[2\text{-}^{13}\text{C}]$ -glycine with resting cells of <i>S. cattleya</i> .	110
<b>Table 3.5</b>	The experimental protocol for studies into fluoroacetaldehyde metabolism by cell free extracts of <i>S. cattleya</i> . Numbers refer to volume (ml).	116

<b>Table 3.6</b>	Conversion of fluoroacetaldehyde to fluoroacetate by cell free extracts of <i>S. cattleya</i> . % Conversion determined from integrals of $^{19}\text{F}$ NMR analysis.	117
<b>Table 3.7</b>	Experimental protocol for co-factor dependence studies. Numbers refer to volume (ml).	118
<b>Table 3.8</b>	Percentage conversion of fluoroacetaldehyde to fluoroacetate as determined from integrals of $^{19}\text{F}$ NMR analysis. The bracketed abbreviations refer to the co-factor that was absent in that experiment.	119
<b>Table 3.9</b>	Experimental protocol for spectrophotometric analysis of fluoroacetate production in cell free extracts of <i>S. cattleya</i> incubated with fluoroacetaldehyde and $\text{NAD}^+$ . Numbers refer to volume (ml).	120
<b>Table 3.10</b>	% conversion and % absorbance of experiments to determine fluoroacetate and NADH production in cell free extracts of <i>S. cattleya</i> .	121
<b>Table 3.11</b>	Relative rate of aldehyde oxidation by the crude cell free extract of <i>S. cattleya</i> and $\text{NAD}^+$ .	124
<b>Table 3.12</b>	Experimental protocol for membrane bound study. Numbers refer to volume (ml).	126
<b>Table 3.13</b>	$^{19}\text{F}$ NMR analysis of membrane bound study for fluoroacetaldehyde dehydrogenase in <i>S. cattleya</i> , the figures refer to % conversion of a 2 mM fluoroacetaldehyde solution.	126
<b>Table 3.14</b>	Experimental protocol for 2-aminomalonate incubations in cell free extracts of <i>S. cattleya</i>	129
<b>Table 4.1</b>	Experimental protocol for preliminary fluorination event studies in cell free extracts of <i>S. cattleya</i> . Numbers refer to volume (ml)	138
<b>Table 4.2</b>	Experimental protocol for cell free study. <b>Experiment 1:</b> Co-factor soup was supplemented with 2 mM SAM and 2 mM methionine. <b>Experiment 2:</b> Co-factor soup was supplemented with 2 mM cysteine and 2 mM glutathione. Numbers refer to volume (ml).	140
<b>Table 4.3</b>	Experimental protocol for defluorination studies with cysteine and glutathione.	142
<b>Table 4.4</b>	Experimental protocol on pyridoxamine co-factor study. Numbers refer to volume (ml).	144
<b>Table 4.5</b>	Experimental protocol for preliminary dephosphorylation studies. Numbers refer to volume (ml).	148

<b>Table 4.6</b>	Phosphate release (mM) from glycolytic intermediates and glycolaldehyde phosphate incubated with crude cell free extract of <i>S. cattleya</i> .	148
<b>Table 4.7</b>	Experimental protocol for dephosphorylation studies on glycolaldehyde phosphate and glyceraldehyde-3-phosphate. Numbers refer to volume (ml).	149
<b>Table 4.8</b>	Phosphate release (mM) from glyceraldehyde-3-phosphate and glycolaldehyde phosphate.	150
<b>Table 4.9</b>	Experimental protocol for assay of partially purified CFE. Numbers refer to volume (ml).	152
<b>Table 4.10</b>	Phosphate release (mM) from glyceraldehyde-3-phosphate when incubated with fractions a → d of the CFE of <i>S. cattleya</i> .	152
<b>Table 4.11</b>	Conversion from fluoroacetaldehyde to fluoroacetate by fractions a → d of the CFE of <i>S. cattleya</i> . Estimated from integrals of <sup>19</sup> F NMR.	153
<b>Table 4.12</b>	Experimental protocol for partial purification of fluoroacetaldehyde dehydrogenase. Numbers refer to volume (ml)	154
<b>Table 4.13</b>	Conversion from fluoroacetaldehyde to fluoroacetate by fractions a → c of the CFE of <i>S. cattleya</i> . Estimated from integrals of <sup>19</sup> F NMR.	154
<b>Table 4.14</b>	Experimental protocol for feeding isotope enriched glycolaldehydes to resting cells of <i>S. cattleya</i> . Numbers refer to volume (ml). The concentration of both glycolaldehydes was estimated to be 200 mM, therefore their final concentration was approximately 10 mM and 20 mM (from 1 ml and 2 ml respectively).	160
<b>Table 4.15</b>	GCMS analysis of 4-fluorothreonine (positions 2, 3 & 4) resulting from incubation of resting cells of <i>S. cattleya</i> with isotopically labelled glycolaldehydes.	160

### *List of abbreviations*

•	Carbon-13 label
4-FT	4-Fluorothreonine
Abs	Absorbance
ATP	Adenosine 5'-triphosphate
Br.	Broad
BSA	Bovine serum albumin
CFE	Cell free extract
CI	Chemical ionisation
CoA	Coenzyme A
d	Doublet
D	Deuterium atom
DCM	Dichloromethane
DHAP	Dihydroxyacetone phosphate
DMS	Dimethyl sulfide
DMSO	Dimethyl sulfoxide
DNP	Dinitrophenylhydrazine
DTT	Dithiothreitol
EI	Electron impact
FAc	Fluoroacetate
FAD	Flavin adenine dinucleotide
FADH <sub>2</sub>	Flavin adenine dinucleotide, reduced form
FMN	Flavin mononucleotide
G-3-P	Glyceraldehyde-3-phosphate
GC-MS	Gas chromatography - mass spectroscopy
HPLC	High pressure liquid chromatography
i.d.	Inner diameter
LD <sub>50</sub>	Lethal dose (50 %)
m	Multiplet
MES	2-( <i>N</i> -Morpholino)ethanesulfonic acid
MS	Mass spectroscopy
MSTFA	<i>N</i> -Methyl- <i>N</i> -(trimethylsilyl)trifluoroacetamide
NAD <sup>+</sup>	Nicotinamide adenine dinucleotide

NADH	Nicotinamide adenine dinucleotide, reduced form
NADP <sup>+</sup>	Nicotinamide adenine dinucleotide phosphate
NADPH	Nicotinamide adenine dinucleotide phosphate, reduced form
NMR	Nuclear magnetic resonance spectroscopy
PDC	Pyruvate dehydrogenase complex
PDC	Pyridinium dichromate
PLP	Pyridoxal phosphate
PMP	Pyridoxamine phosphate
ppm	Parts per million
rpm	Revolutions per minute
s	Singlet
SAM	S-adenosyl-L-methionine
SDS-PAGE	Sodium dodecyl sulfate-polyacrylamide gel electrophoresis
Sh.	Shoulder
SIM	Selected ion monitoring
Sp.	Species
Spp.	Species (plural)
t	Triplet
TCA (cycle)	Tricarboxylic acid
tlc	Thin layer chromatography
TMS-	Trimethylsilyl-
TPP	Thiamine pyrophosphate

Now, ever since Perkin, failing to make quinine, founded the dyestuffs industry, the organic chemists have found the study of 'natural products' an inexhaustible source of exercises, which can be performed out of pure curiosity even when paid for in the hope of a more commercial reward. As a result, the organic chemist's view of nature is unbalanced, even lunatic, but still in some ways more exciting than that of the biochemist. While the enzymologist's garden is a dream of uniformity, a green meadow where the cycles of Calvin and Krebs tick round in a disciplined order, the organic chemist walks in an untidy jungle of uncouthly named extractives, rainbow displays of pigments, where in every bush there lurks the mangled shape of some alkaloid, the exotic perfume of some new terpene, or some shocking and explosive polyacetylene. To such a visionary, both the diatretynes are equal prizes, to be set together as 'natural products.' We shall do the same, but since to a more sober eye both are in a sense less 'natural' than, say, glycine or adenosine triphosphate, we may prefer the term '**secondary metabolites.**'

J. D. Bu'lock, *Adv. Appl. Microbiol.*, **3** (1961), 293

*Chapter 1*

*Introduction*

## ***Chapter 1: Introduction***

Over half a century has elapsed since the toxin fluoroacetate (1) was first identified as a natural product of the South African plant *Dichapetalum cymosum*.<sup>1</sup> Since then a further twelve naturally occurring compounds containing a C-F bond have been discovered. To date the mechanism and enzymology of Nature's fluorination reactions remain largely unknown.<sup>2</sup> To provide a framework for discussion of fluoroacetate (1) and 4-fluorothreonine (2) biosynthesis, it is first necessary to introduce the concept of secondary metabolism and review to some extent the methods by which the other halogens are introduced into natural products.

### ***1.1 Secondary Metabolism***

#### ***1.1.1 Primary and secondary metabolism***

Metabolism is classically delineated into two general categories. Primary metabolism defines the metabolic pathways common to all living organisms, such as the pathways that produce and utilise carbohydrates, amino acids, nucleic acids and fatty acids. These pathways are similar, though not identical, across the wide genus and species spectrum. Primary metabolites are manipulated by both anabolic and catabolic processes.<sup>3</sup> These synthesise and degrade, respectively, the primary metabolites and biopolymers (DNA, RNA, proteins, polysaccharides and lipids) derived from them. Primary metabolites are essential for the efficient functioning of all organisms.<sup>4</sup>

Many species also operate metabolic pathways other than those directly involved in primary metabolism. These pathways utilise primary metabolites to deliver often structurally unique compounds. Such natural products are termed secondary metabolites as the pathways that create them are peripheral to primary metabolism. The border between primary and secondary metabolism is ill-defined with no universally satisfactory definition. Rigid definitions tend to exclude known secondary metabolites and occasionally preclude primary metabolites. A generally accepted and useful definition is that secondary metabolites have a limited distribution, usually restricted to a genus or species.<sup>5</sup>



Microbial secondary metabolites display phase dependent growth and are irrelevant to the growth of the organism (section 1.1.3).<sup>6</sup> It is of great interest that secondary metabolites do not appear to be essential for the survival of the producer organism. The biosynthetic pathways to secondary metabolites tend to be long and complex, so the production of a secondary metabolite must infer some selective advantage over nonproducing strains of the same species for their biosynthesis to be conserved through evolution.<sup>7</sup> In antibiotic production, this may be easy to rationalise, however where physiological roles have not been assigned to specific secondary metabolites their *raison d'être* is not so obvious.

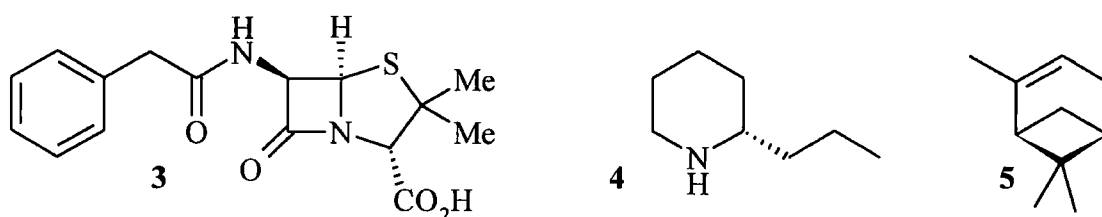


**Fig. 1.1:** Penicillin G (3), coniine (4) and  $\alpha$ -pinene (5).

The structures of secondary metabolites are characteristically ornate and this is reflected in their diversity of biological functions and uses by man.<sup>8</sup> They may have, for example, antibiotic activity, high toxicity or pheromonal action such as in penicillin (3), coniine (4) and  $\alpha$ -pinene (5) respectively. Due to their diverse biological activities secondary metabolites have been used by man as poisons, narcotics, stimulants, flavours, fragrances and pharmaceuticals. Crude preparations of secondary metabolites have been used in folklore medicine and much has been learnt through ethnopharmacology (studying the crude plant preparations used by indigenous people for their biological activity; be it medicinal, poison or hallucinogenic).<sup>9,10</sup> It is envisaged that secondary metabolites will continue to supply new lead compounds for the pharmaceutical industry, through both the identification of new natural product chemotypes and through biotechnological exploitation of existing natural products.<sup>11</sup> Secondary metabolites have had a large impact on contemporary society, both positively through pharmaceuticals, flavours and fragrances and negatively through their use and associated crime in the illegal drugs market, which is largely based on natural products.

The reason why an organism produces secondary metabolites has been much debated. Even though many secondary metabolites have physiological roles assigned to them, these are pharmaceutical descriptors (*e.g.*, antibiotic) and may not reveal the fundamental role of the metabolite. It has been noted and accorded some significance that many secondary metabolites have activities in species other than the producing organism. However, it may be that secondary metabolites originally had a role in the internal physiology of the producing organism. This ancestral function may now be disguised by evolutionary development where such compounds have refined specialised interactions with other species.<sup>12</sup>

Secondary metabolites are broadly classified by their biosynthetic origin. Fatty acids and derivatives (*e.g.* polyacetylenes and prostaglandins) originate from the condensation from acetate (6) (see section 1.1.2). Similarly, polyketides originate from acetate (6) and partial reduction of the resultant 'polyketone' chains that may condense and cyclise. Shikimate (7) provides a start point for the biosynthesis of many phenols, lignans and flavanoids. Alkaloids originate from the amino acid pool, as do the non-ribosomal peptides. The isoprenoids (terpenes and sterols) are derived from deoxyxylulose-5-phosphate and mevalonic acid (8) in two separate pathways. In Fig. 1.2 the relationship between these key intermediates and primary metabolism is demonstrated. Primary metabolism supplies the necessary intermediates through glycolysis (minimally represented here by the conversion of glucose (9) to pyruvate (10), *via* glyceraldehyde-3-phosphate (11) and phosphoenol pyruvate (12)) and subsequent incorporation of acetyl-S-CoA (13) into the tricarboxylic acid (TCA) cycle. The diagram has been modified (from Mann,<sup>8</sup> 1994) to show a newly realised pathway to the isoprenoids *via* 1-deoxyxylulose phosphate (14), which operates independent of the well established mevalonate pathway.<sup>13,14</sup> In the following section fatty acid biosynthesis and  $\beta$ -oxidation will be discussed in some detail as these pathways are relevant to the origin of some of the known fluorinated metabolites.

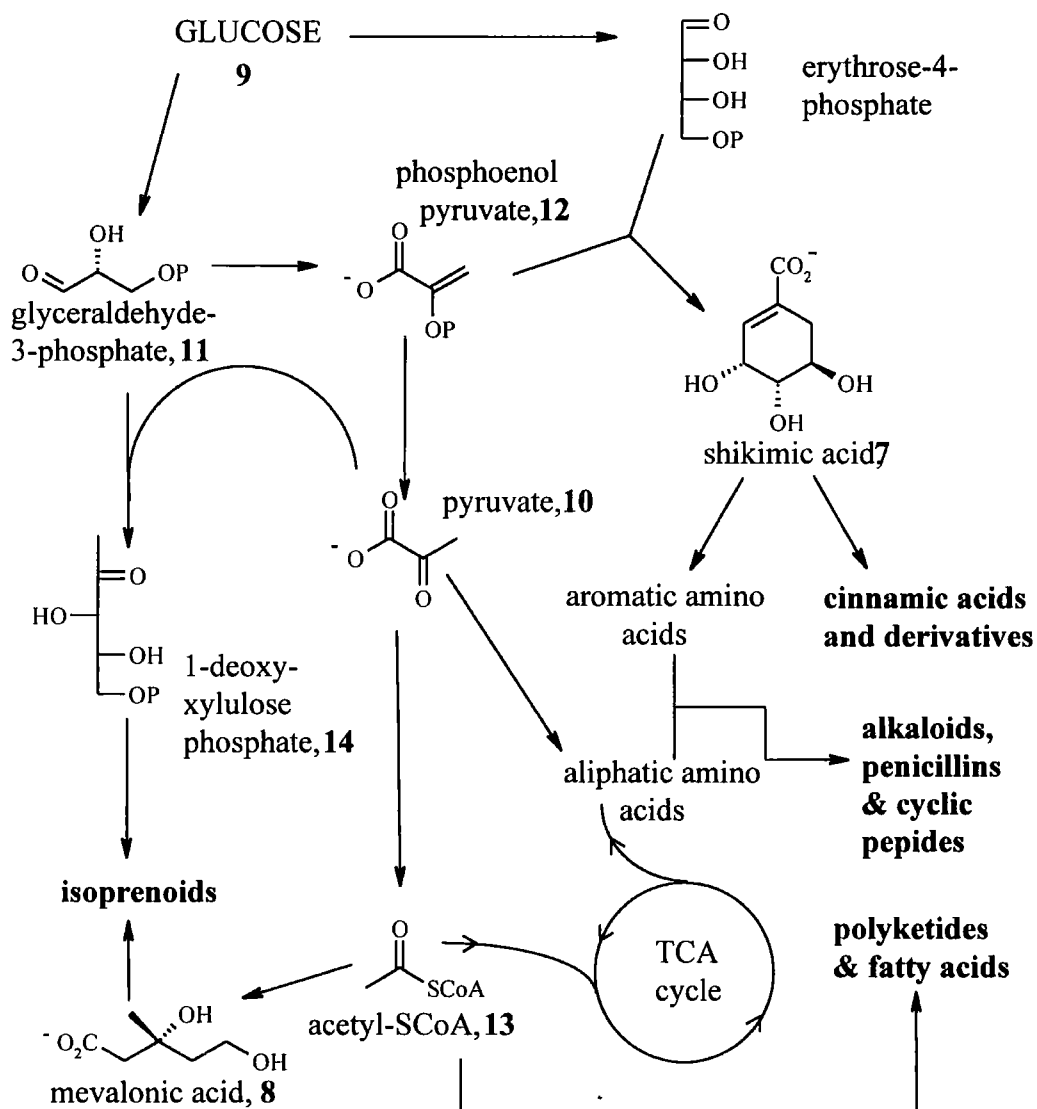
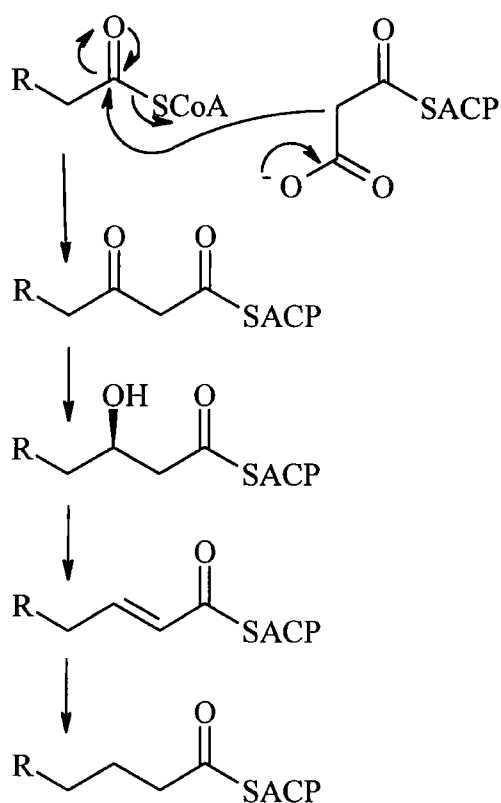


**Fig. 1.2:** The major secondary metabolic precursors. The arrows represent multiple step transformations.

### 1.1.2 Fatty acid biosynthesis and $\beta$ -oxidation<sup>15</sup>

Fatty acids are biosynthesised by the repeated decarboxylative condensation of malonyl-S-CoA (15), extending the chain by two carbons with each condensation. The resultant  $\beta$ -keto thioester is reduced by a series of enzymes to  $\text{CH}_2$  before the next condensation cycle starts (see Fig. 1.3). The starter unit is generally acetyl-S-CoA (13), although not exclusively so. In a variety of secondary metabolites, particularly in bacteria, other carboxylic acids can become incorporated as their coenzyme A ester.  $\beta$ -Oxidation is essentially the reverse of this process (though it is mediated by different enzymes and cofactors and in eukaryotes it occurs in a different cellular location).  $\beta$ -Oxidation is the process of fatty acid catabolism and generates acetyl-S-CoA (13).

### fatty acid biosynthesis



### β-oxidation

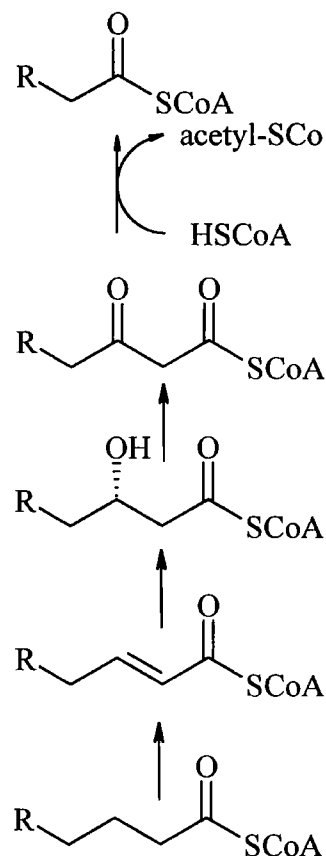


Fig. 1.3: Fatty acid biosynthesis and β-oxidation.

#### 1.1.3 Microbial secondary metabolism

Phase dependent biosynthesis is a characteristic of microbial secondary metabolism. In bacterial systems there are well-defined stages of growth and these correlate with the organism's biosynthetic capabilities.<sup>16</sup> If cell growth in a complex medium is considered, the cells in the initial inoculum may not be fully established in primary metabolism. There is a lag period before cell growth commences. The rate of growth then becomes exponential as healthy cells divide. During this phase primary metabolism dominates as the cells maximise use of available resources. This is known as the *trophophase*, and continues until there is a deficit in nutrients. At this point cell growth ceases and cell death begins as the organism takes steps to maximise its chance of survival. Two characteristics of this next phase, the *idiophase*, are secondary metabolism and sporulation. Sporulation is a mechanism by which the microorganism generates heat resistant cells. Spores can remain dormant until such a time as they are once again in a favourable environment for growth. Concurrent with sporulation is the onset of secondary metabolism.

It is perhaps poignant that secondary metabolism occurs so late in the life cycle of microorganisms and this led to the early hypothesis that some secondary metabolites were merely 'shunt' metabolites, secreted to prevent the accumulation of potential toxic primary metabolites.<sup>6</sup> This is no longer a generally accepted argument. The complexity of the signalling required to initiate secondary metabolite biosynthesis suggests a level of sophistication that would rule out a mere accumulation. Also the biosynthesis of aerial mycelium (sporulation) requires a level of primary metabolism that would prevent this accumulation.<sup>17</sup> The concurrent events of secondary metabolism and sporulation may indicate a dedicated defence system for the organism. There is evidence in *Streptomyces* spp. that the concurrent activities of secondary metabolism and sporulation are not linked by chance, but that these events are controlled by the same genes, referred to as pleiotropic switches. Therefore, the organism prepares to enhance its long-term survival by producing heat resistant spores, whereas natural product biosynthesis may protect the organism during its idiophase.

The accumulation of secondary metabolites after the cessation of cell growth provides another definition of secondary metabolism. As primary metabolites generally do not accumulate, and are in a low steady state concentration, any metabolite that does accumulate after the cessation of growth may be defined as a secondary metabolite. Interestingly this definition includes many *bona fide* primary metabolites, *e.g.* citrate, malate and shikimate. Perhaps a better definition of microbial secondary metabolism was proposed by Duclaux (1925)<sup>18</sup> that the accumulated metabolites are 'produits de souffrance', that is secondary metabolites are produced when the organism is under stress, a state other than its physiological optima.

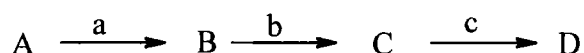
## 1.2 Elucidation of Metabolic Pathways

Following structural elucidation it is usually possible to propose a biosynthesis for a given secondary metabolite, often by analogy to other known natural products. To set about establishing a biosynthetic pathway a variety of techniques are available. Two general strategies are adopted. Either putative intermediates are fed carrying an isotopic label, to the producing organism to determine if it is carried through to the final product. Alternatively the pathway may be blocked, by mutation, to observe the accumulation of any intermediates. Although these studies require a synergy of biological and chemical techniques, the former is largely chemical and the latter, biological.

### 1.2.1 Biological methods

#### 1.2.1.1 Mutant studies

Consider a hypothetical biosynthetic pathway to D, through the putative intermediates A, B and C, catalysed by the enzymes a, b and c.



There are two general methods of blocking individual steps to observe accumulation of intermediates. Either the enzyme is prevented from being expressed at the genetic level or its action is inhibited by the addition of a chemical inhibitor. Chemical inhibitors used *in vivo* are generally not so effective as the inhibitor may interfere with other metabolic processes.<sup>19</sup> On the other hand, preventing the production of the enzyme, by mutation, can be an effective tool. If the culture is irradiated with UV or X-rays, or treated with a chemical mutagen, then random genetic mutations will occur. If these mutations affect the expression of enzymes involved in primary metabolism then the growth of the organism will be adversely effected. If however the mutation affects the expression of an enzyme involved in secondary metabolism then the organism will grow and any novel metabolites that accumulate can be analysed.<sup>20</sup> Approaches using this method have become increasingly sophisticated. The genes that encode for the enzymes required for the production of certain secondary metabolite are often clustered. This is especially the case in the polyketide antibiotics. The function of many of these genes can be proposed by sequence homology to enzymes of known function. By introducing a mutation directly into a gene, the substrate for the enzyme that it encodes can be identified as it accumulates. Not only is this powerful methodology furthering the

knowledge of individual biosynthetic pathways, but it also produces novel, potentially biologically active compounds, for pharmaceutical screening.

#### ***1.2.1.2 Inhibition of protein biosynthesis***

Cycloheximide (**16**) has been used to inhibit the production of enzymes necessary for secondary metabolism.<sup>19</sup> This compound inhibits protein biosynthesis, and if added just prior to the onset of secondary metabolism it can influence the expression of target pathways. Such studies have demonstrated that enzymes of secondary metabolism are not constitutive and that there is a chemical signal that initiates gene expression. Conversely secondary metabolite production in the presence of cycloheximide (**16**) show that the required enzymes are constitutive and have been biosynthesised prior to the onset of secondary metabolism.

#### ***1.2.1.3 Cell free studies***

Once key steps in a biosynthetic pathway have been identified then *in vitro* studies can provide further information, for example, on substrate specificity or cofactor requirements. These experiments can be conducted on crude cell free extracts prepared by disrupting the cell walls by pressure, sonication or lytic enzymes. Such studies constitute part of this thesis.

#### ***1.2.2 Chemical methods***

The use of both stable and radioactive isotopes, in the elucidation of metabolic pathways is well established. The main isotopes used in this context are listed in below (Table 1.1).

Isotope	Relative natural abundance, %	Radiation emitted	Half-life	Spin
$^2\text{H}$	0.015		stable	1
$^3\text{H}$		$\beta$	12.1 years	$\frac{1}{2}$
$^{13}\text{C}$	1.1		stable	$\frac{1}{2}$
$^{14}\text{C}$		$\beta$	5700 years	
$^{15}\text{N}$	0.37		stable	$\frac{1}{2}$
$^{18}\text{O}$	0.20		stable	
$^{32}\text{P}$		$\beta$	14.3 days	

**Table 1.1:** Properties of isotopes used in biosynthetic studies.

### 1.2.2.1 Radioisotopes

Radioisotopes have been used to great effect in understanding some of the fundamental pathways in primary metabolism. The application of radioisotopes to biochemistry was pioneered in the 1920's by Hevesy (Copenhagen) and 1940's by Schoenheimer (New York). Their work led to the fundamental realisation that biomolecules are in a constant state of flux, being produced on demand.<sup>21</sup> Using  $^{14}\text{CO}_2$  Calvin showed that the first stable intermediate of  $\text{CO}_2$  fixation in plants was 3-phosphoglyceric acid (17). The use of radioisotopes can require degradation studies to deduce the regiochemistry of labelling. This was elegantly used by Cornforth *et al*<sup>22,23</sup> to demonstrate that cholesterol (19) is biosynthesised ultimately from acetate, by tracing the path of  $[1-^{14}\text{C}]$ -acetate (18) through the mevalonic acid pathway into the lipid.

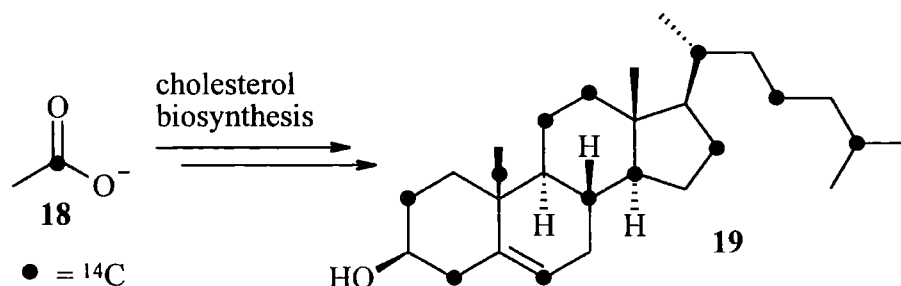


**Fig. 1.4:** Cholesterol (19) biosynthesis, topological mapping by  $[1-^{14}\text{C}]$ -acetate (18).



A disadvantage of using radioisotopes, beyond radiation exposure issues, is the approach offers limited regiochemical information, unless chemical degradation studies are employed.

#### **1.2.2.2 Stable isotopes**

Stable isotopes are now used widely and effectively as a biosynthetic tool. Advances in spectroscopic methods over the last thirty years, particularly  $^{13}\text{C}$  and  $^2\text{H}$  NMR, have ensured that stable isotope feeding experiments cannot only demonstrate incorporation of putative intermediates but can also resolve regiochemical and stereochemical issues.<sup>24</sup> One of the many benefits of using radioisotopes was accurate incorporation determination. This accuracy is now possible with stable isotope incorporation through GC-MS and  $^{13}\text{C}$  NMR analysis.<sup>25</sup>

There are many different types of feeding experiment that can be conducted. Initial studies into the biosynthesis of a secondary metabolite usually focus on understanding the construction of the carbon skeleton. This is carried out, most straightforwardly, by feeding isotopically labelled primary metabolites, such as  $[1-^{13}\text{C}]$ -acetate (**20**). Once an understanding of the connectivity of the carbon skeleton has been gained then more specific labelling strategies are employed, usually requiring synthetic chemistry to prepare appropriate precursors.

#### **1.2.2.3 Single label feeding experiment studies<sup>25</sup>**

The analysis of feeding putative precursors containing only a single stable isotope generally relies on the assessment of enrichments in the NMR spectrum relative to that of the unlabelled compound. This is particularly relevant for  $^{13}\text{C}$  and  $^2\text{H}$  labelling. It is becoming increasingly common now to investigate the incorporation of low levels of  $^2\text{H}$  due to its low natural abundance (0.01 %)

#### **1.2.2.4 Double label feeding studies: 'bond labelling'<sup>25,24</sup>**

Double label feeding experiments are particularly powerful as they directly demonstrate bond connectivity. For example, in  $[1,2-^{13}\text{C}_2]$ -acetate (**21**), the two carbon nuclei couple to each other, and if the bond is not broken through the biosynthetic pathway the coupling is retained in the isolated metabolite. This technique is widely applied as an initial experiment in many biosynthetic investigations. Other connectivities can be

demonstrated, by an extension of this strategy, either by coupling between magnetically active nuclei or by observing a heavy atom induced upfield shift of *e.g.*  $^{18}\text{O}$  or  $^2\text{H}$  bonded to  $^{13}\text{C}$ . As the isotopes used in such labelling studies are heavier than their 'natural' counterparts, the bonds that they form are slightly shorter than those in the unlabelled isotopomer, and therefore the chemical environment of neighbouring nuclei is perturbed. In a  $^{13}\text{C}$  NMR spectrum a heavy isotope bonded to  $^{13}\text{C}$  will shift its resonance to a lower frequency. Using these techniques the following bonds can be mapped through biosynthesis:  $^{13}\text{C}$ - $^{13}\text{C}$ ,  $^{13}\text{C}$ - $^{12}\text{C}$ - $^{13}\text{C}$ ,  $^{13}\text{C}$ - $^{15}\text{N}$  (by observing coupling);  $^{13}\text{C}$ - $^2\text{H}$  (by observing coupling and an upfield shift);  $^{13}\text{C}$ - $^{12}\text{C}$ - $^2\text{H}$ ,  $^{13}\text{C}$ - $^{18}\text{O}$  (by observing the an upfield shift).

The magnitude of the upfield shift is dependent on the stable isotope and its distance from the observed  $^{13}\text{C}$  nuclei. Some of the largest  $^{13}\text{C}$ -NMR shifts to lower frequency are observed with  $\alpha$ -deuteriums, which can be of  $\sim 0.6$  ppm in magnitude for each deuterium.

Recently  $^3\text{H}$  labelling has had a resurgence due to increased access to  $^3\text{H}$  NMR. As  $^3\text{H}$  is not quadrupolar the line broadening inherent in  $^2\text{H}$  NMR is absent and the extremely low natural abundance of  $^3\text{H}$  allows very low levels of incorporation to be studied.<sup>20</sup>

## 1.3 Halogenated Secondary Metabolites

### 1.3.1 Distribution of halogenated metabolites

Halogenated secondary metabolites were considered to be somewhat rare in Nature. A comprehensive review<sup>26</sup> in 1968 listed no more than 30 naturally occurring halometabolites, however now the total number of halometabolites exceeds 2900.<sup>27</sup> Chlorine is the most common halogen found in secondary metabolites,<sup>28</sup> although there are metabolites reported for all of the stable halogens.<sup>29</sup> The thyroid hormone thyroxine (22) is one of the few examples involving iodine.<sup>30</sup> Brominated metabolites are relatively sparsely distributed, although there are many in the marine environment and some have been generated by the replacement of chloride by bromide in culture media.<sup>31</sup> Chlorinated metabolites, perhaps not surprisingly considering the bioavailability of chloride, in *e.g.* seawater, are produced in both great number and large amounts. It is estimated that bacteria release *ca.*  $5 \times 10^6$  tonnes *per annum* of methyl chloride into the marine environment, compared with  $2.6 \times 10^4$  tonnes per year from man-made sources.<sup>32</sup> All of the classes of secondary metabolites demonstrate the ability to use halogens in natural product biosynthesis, although plant alkaloids have very few examples.

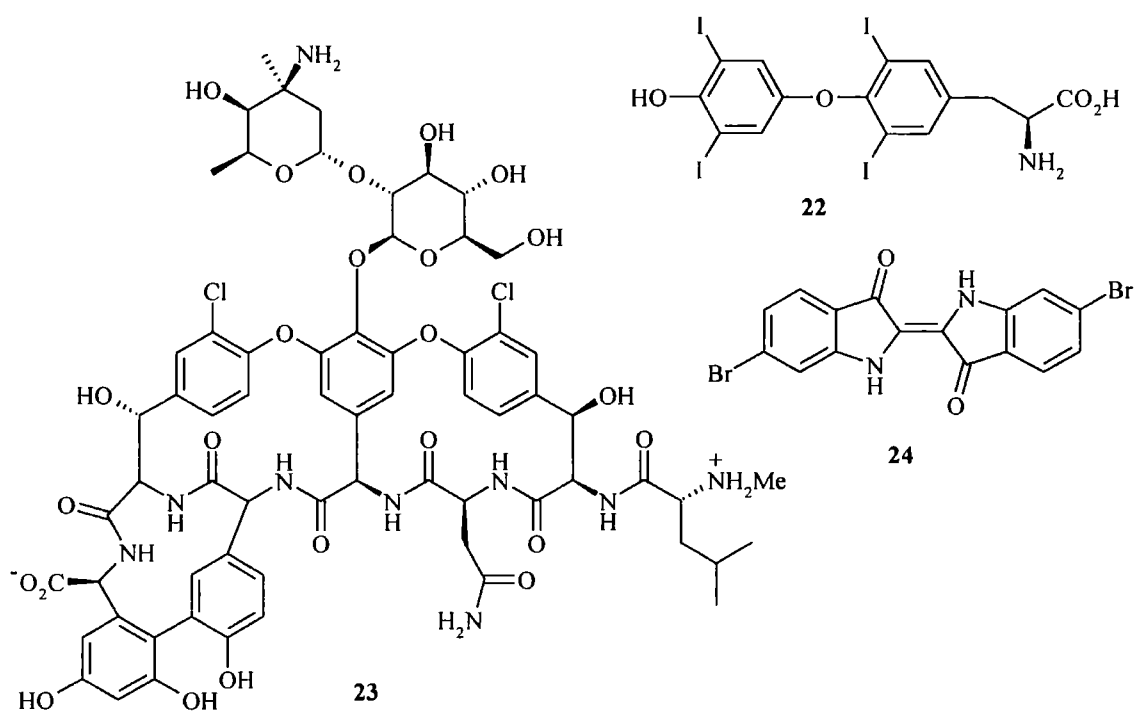
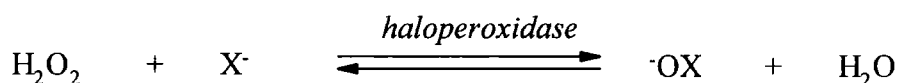


**Fig. 1.5:** Thyroxine (22), vancomycin (23) & tyrian purple dye (24).

It would appear that the ability to produce halogenated metabolites has survived the rigours of natural selection by conferring a selection advantage to the producing organism. As with other secondary metabolites these compounds are often utilised by man. One important example is the glycopeptide vancomycin (**23**), a last resort antibiotic used in the treatment of methicillin-resistant *Staphylococcus aureus*, where the chlorine atoms are important in displaying this biological activity.<sup>33</sup>

### 1.3.2 Mechanisms for biohalogenation

The biohalogenation of metabolites (primary and secondary) is generally thought to be catalysed by haloperoxidases. Haloperoxidases oxidise halide ions to form hypohalites, using hydrogen peroxide as the oxidant.<sup>34</sup>



The activated ( $\cdot\text{OX}$ ) species then halogenates an organic substrate often in a rather indiscriminate manner. The haloperoxidases are classified with regard to their oxidising capabilities. Chloroperoxidases oxidise chloride, bromide and iodide, whereas bromoperoxidases oxidise bromide and iodide, and iodoperoxidases only oxidise iodide. They are further classified by their active site, as either haem-containing, vanadium-containing or metal-free haloperoxidases.<sup>31</sup> A study on metal free bacterial haloperoxidases has shown that the oxidising species is peracetic acid generated from hydrogen peroxide and acetate present in the buffer. In this respect the enzyme appears to act as a hydrolase. Peracetic acid can then diffuse away from the active site to oxidise a halide.<sup>35</sup>

Haloperoxidases are generally monitored by a straightforward spectrophotometric assay. This involves the halogenation of synthetic monochlorodimedone (**25**) with the concomitant loss of absorbance at  $\lambda = 290 \text{ nm}$ , by the removal of the enolone moiety.<sup>36</sup>

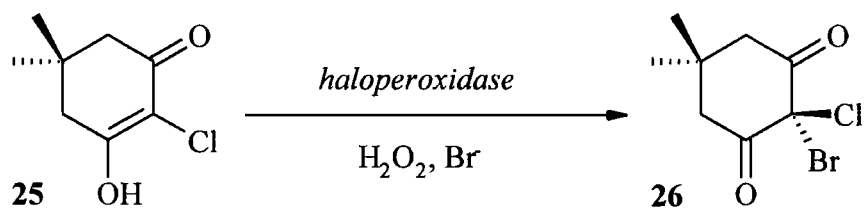


**Fig. 1.6:** Monochlorodimedone (25) assay for haloperoxidases activity.

Using this assay many haloperoxidases have been identified and isolated and again this indicates both the broad substrate and regiospecificity of haloperoxidases.

A recent genetic analysis of the chlorotetracycline (27)<sup>37</sup> and pyrrolnitrin (32)<sup>38</sup> gene clusters has failed to show the presence of haloperoxidases in their biosynthesis. This has led to the demonstration of an NADH-dependent halogenase, rather than haloperoxidase, activity in pyrrolnitrin (32) biosynthesis. It is proposed that instead of activating the halide (as in haloperoxidase catalysed biosynthesis) the organic substrate is activated as an epoxide, with nucleophilic attack of a halide ion.

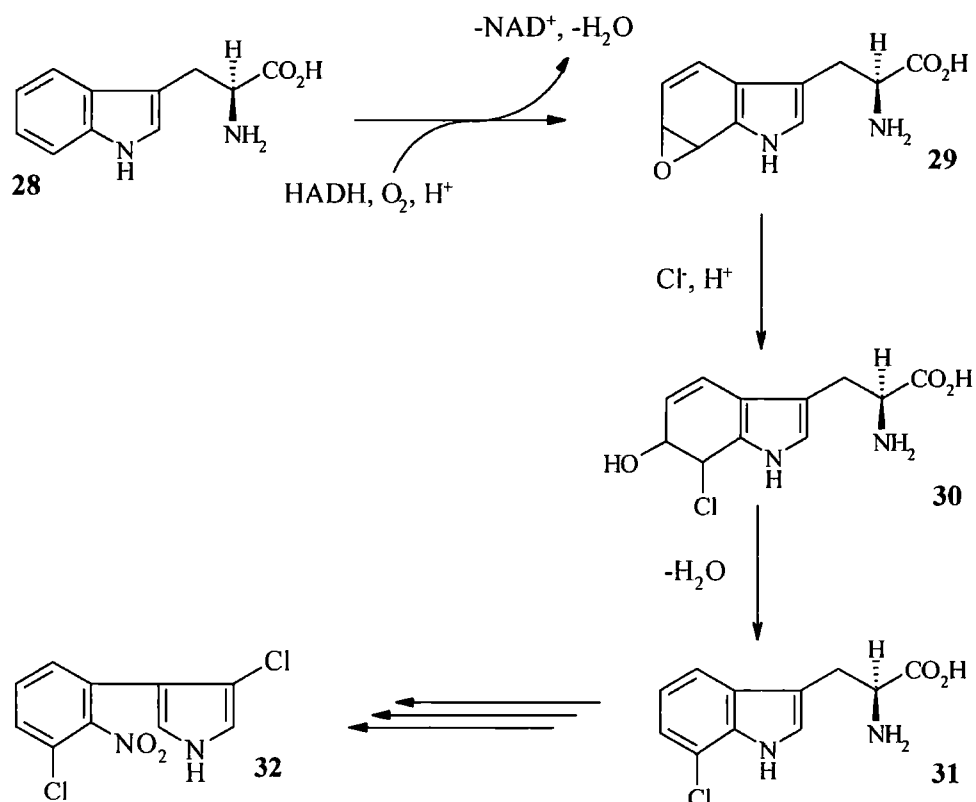


**Fig. 1.7:** NADH-dependent halogenase in pyrrolnitrin (32) biosynthesis

## 1.4 Fluorinated Secondary Metabolites

The occurrence of organo-fluorine compounds is rare in Nature. In fact there are only thirteen known natural products containing a C-F bond, isolated primarily from tropical and subtropical plants, but also microorganisms.<sup>2</sup> There are no known examples of organo-fluorine compounds in the animal kingdom or from the marine environment. This dearth of fluorometabolites is probably due to two main factors: the lack of bioavailable fluoride and the chemistry and thermodynamics of both fluoride and the C-F bond.

### 1.4.1 Fluorine bioavailability

As the most abundant halogen in the earth's crust and the 13<sup>th</sup> most abundant<sup>39</sup> of all elements, the poor bioavailability of fluoride is perhaps paradoxical. However, the minerals (*e.g.* fluor spar) that contain fluorine in the earth's crust are largely insoluble. This is exemplified by comparing the amount of fluoride and chloride in the earth's crust and its concentration in sea water.

	Concentration in the Earth's crust (ppm)	Concentration in sea water (ppm)
F	544	1.3
Cl	126	19 000

**Table 1.2:** Fluoride and chloride concentrations in the Earth's crust and sea water.<sup>39</sup>

Despite this lack of bioavailability some organisms have developed the capacity to tolerate and store large concentrations of fluoride, including the genus *Camellia*.<sup>40</sup> Commercial tea (of that genus) contains 70 - 180  $\mu\text{g g}^{-1}$  dry weight fluoride. Certain plant species growing on waste from fluor spar mining can accumulate fluoride to a concentration of 10 000  $\mu\text{g g}^{-1}$  dry weight<sup>41</sup> and the sponge *Halichondria moorei* can contain a remarkable 10 % of fluorine by dry mass, as potassium fluorosilicate.<sup>42</sup>

### 1.4.2 The Nature of the C-F bond

In the context of fluorinated secondary metabolites it is useful to discuss the nature of the C-F bond and fluorine chemistry in general. Fluorine chemistry began in the second half of the 18<sup>th</sup> Century, when Scheele produced a crude solution of hydrofluoric acid<sup>39</sup> (Scheele also isolated the first pure natural products, including some of the first

secondary metabolites), before that it was known to be a component of the mineral fluorspar, from which it got its name (fluorspar was used as a flux; latin *fluor*, flowing). The element itself was not isolated for a further one hundred years when H. Moissan succeeded in the electrolysis of a solution of  $\text{KHF}_2$  in HF. It was not until 1940 that  $\text{F}_2$  was prepared on an industrial scale, when it was required to produce  $\text{UF}_6$  for uranium enrichment for the nuclear industry.

When comparing the C-F bond with other C-X bonds it is noticeable how short, strong and polarised the bond is. In fact the C-F bond is the strongest single bond involving carbon, being 10 % stronger than the C-H bond. In Table 1.3 fluorine is compared with hydrogen and other halogens by way of some physical properties of the element and the bond.

X	Bond dissociation energy, $\text{CH}_3\text{-X}$ ( $\text{kJmol}^{-1}$ )	Bond Length, C-X (nm)	Dipole moment, $\text{CH}_3\text{-X}$ (Debye units)	Electronegativity (Pauling scale)
F	460	0.139	1.82	4.0
Cl	356	0.178	1.94	3.0
Br	297	0.193	1.97	2.8
I	238	0.214	1.64	2.5
H	414	0.109	0	2.2

**Table 1.3:** Physicochemical parameters of the halogens.<sup>43</sup>

Fluorine is both the most electronegative and the smallest halogen, this leads to a large polarisation of the C-F bond. The overall dimensions of a C-F bond is in between that of a C-H and a C-OH bond<sup>44</sup> (see Table 1.4)

Substituent, X	Bond length, C-X (nm)	Van der Waal's radius (nm)
H	0.109	0.120
F	0.139	0.135
O (in OH)	0.143	0.140
Cl	0.178	0.180
S (in SH)	0.182	0.185
Br	0.193	0.195
I	0.214	0.215

**Table 1.4:** Van der Waal's radius and bond length of C-H and other substituents.<sup>43</sup>

Halogens other than fluorine are introduced biosynthetically *via* haloperoxidases. However, this method is not applicable to fluorination as the redox potential for fluoride is too great to be oxidised by peroxide reduction. This high redox potential is in part due to the high heat of hydration, which renders fluoride heavily solvated in aqueous media. Also being heavily solvated, fluoride emerges as a particularly poor nucleophile in aqueous media.

X	Heat of hydration, X <sup>-</sup> (kJmol <sup>-1</sup> )	Standard redox potential, E <sup>0</sup> (V)
F	490	-3.06
Cl	351	-1.36
Br	326	-1.07
I	285	-0.54

**Table 1.5:** Heat of hydration and standard redox potential for the halogens.<sup>43</sup>

Fluoride is a poor leaving group due to the strength of the C-F bond, however its ability to stabilise  $\beta$ -carbanions and the high heat of hydration can assist in fluoride elimination.

### 1.4.3 Fluorinated natural products in plants

#### 1.4.3.1 Fluoroacetate (1)

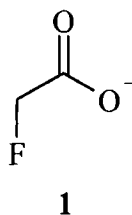


**Fig. 1.8:** Fluoroacetate (1).

By far the most abundant of the fluorometabolites is fluoroacetate (1), a toxin found in several species of tropical and subtropical plants.<sup>2</sup> The South African plant *Dichapetalum cymosum* was known to be highly poisonous (known locally as *Gifblaar*, from Afrikaans: *Gif* - poison). In 1943 fluoroacetate (1) was identified as the toxic principle,<sup>45,46</sup> where it was shown to accumulate to 2500  $\mu\text{g g}^{-1}$  dry weight in the young leaves of the plant. Fluoroacetate (1) has now been identified in tropical and subtropical plants in Africa, Australia, Asia and South America.<sup>43</sup> With the exception of



*Dichapetalum* spp., fluoroacetate (1) production is confined to the Leguminales. Not only does the level of fluoroacetate (1) vary greatly across all these species, but within each species there is variation depending on the geographic location, season and age of the plant. The changes with regard to geographical location could be due either to the availability of fluoride or genetic variation across the species. The mechanisms behind the toxic ability of fluoroacetate (1) and rationales for resistance in fluoroacetate (1) producing organisms will be discussed below (sections 1.4.4 and 1.4.5 respectively).

### 1.4.3.2 $\omega$ -Fluorinated fatty acids

The seeds of the fluoroacetate (1) producer *Dichapetalum toxicarium* are very toxic, but unlike the leaves, the seeds contain very little fluoroacetate (1). It has been shown that  $\omega$ -fluorooleic acid (33), makes up 3 % of the mass of the seed oil and accounts for 80 % of the organically bound fluorine.  $\omega$ -Fluoropalmitic acid (36),  $\omega$ -fluoromyristic acid (35) and  $\omega$ -fluorocapric acid (34) were also identified as components of the seed oil.<sup>47</sup> A more recent study has confirmed that these and a number of other fluorinated fatty acids are present.<sup>48</sup> They include  $\omega$ -fluoroarachidonic acid,  $\omega$ -fluoropalmitoleic acid,  $\omega$ -fluoroecosenoic acid,  $\omega$ -fluorostearic acid and  $\omega$ -fluorolinoleic acid. *Dichapetalum toxicarium* also displays the ability to biosynthesise *threo*-18-fluoro-9,10-dihydroxystearic acid (37). This is likely to form *via* the epoxidation and hydrolysis of  $\omega$ -fluorooleyl-SACP.

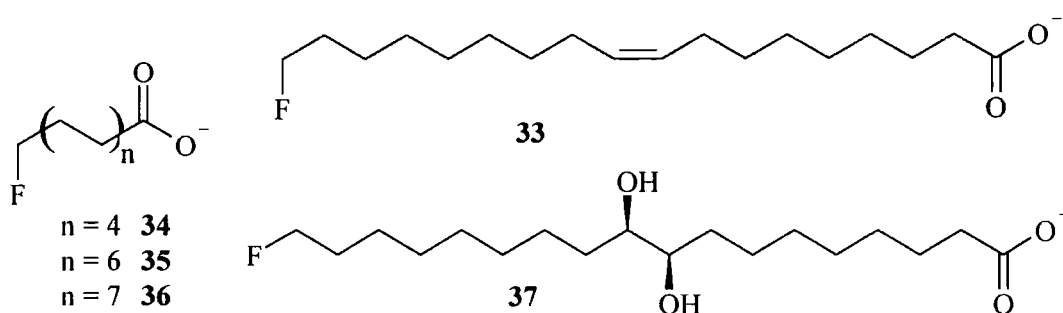


**Fig. 1.9:**  $\omega$ -Fluorinated fatty acids.

The biosynthetic origin of these  $\omega$ -fluorinated fatty acids can be readily explained by fatty acid biosynthesis that utilises fluoroacetyl-S-CoA (38) as a starter unit. As discussed previously fatty acid biosynthesis (section 1.1.2) proceeds from elongation of an acetyl-S-CoA (13) starter unit by condensation with malonyl-S-CoA (15). In the

terminal position the electronic effects of the fluorine clearly do not effect the chain elongation and presumably the subsequent enzymes do not discriminate the non-fluorinated from the fluorinated fatty acids and they are processed side by side.

#### 1.4.3.3 Fluoroacetone (39)

The Australian species *Acacia georginae* had already been shown to produce fluoroacetate (1), although when researchers studied the amounts of inorganic and organic fluorine they noticed a discrepancy,<sup>49</sup> which suggested loss of fluorine, possibly as a volatile. It was hypothesised that fluoroacetone (39) could be the volatile as it had been previously identified as a metabolite of fluoroacetate (1) in rat liver.<sup>50</sup> Fluoroacetone (39) was identified as its dinitrohydrazone (DNP) derivative. The volatiles were passed through a DNP solution, which was analysed by paper chromatography. It was shown that the derivative co-eluted with the DNP-derivative of synthetic fluoroacetone (39). However, the authors did state that the DNP-derivatives of fluoroacetone (39) and acetaldehyde could not be separated by their system and so by the same token fluoroacetaldehyde (40) could not be ruled out. The authors suggested however that fluoroacetaldehyde (40) was unlikely to form due to its inherent instability. Results presented in this thesis, weaken this conjecture and therefore the possibility of fluoroacetaldehyde (40) being the volatile produced in *A. georginae* remain.

Assuming that fluoroacetone (39) is a *bona fide* fluorometabolite, then its bio-origins can be rationalised from fluoroacetate (1). Following the early stages of  $\omega$ -fluorinated fatty acid biosynthesis, fluoroacetyl-SCoA (38) is condensed with malonyl-ACP (15) to form fluoroacetoacetyl-ACP (41). Hydrolysis and decarboxylation of 4-fluoroacetoacetate (41) would deliver fluoroacetone (39).

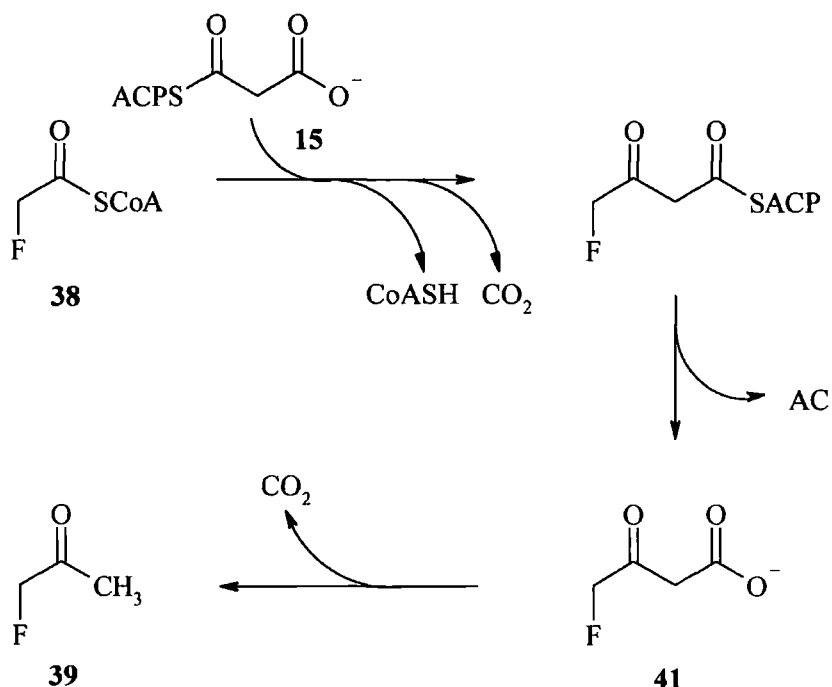


**Fig. 1.10:** Fluoroacetone (39), and its putative biosynthesis from fluoroacetate (1).

#### 1.4.4 Fluoroacetate (1) metabolism: (2R, 3R)-2-fluorocitrate (44)

The plants that produce fluoroacetate (1) are highly toxic and are responsible for large scale cattle losses in Africa and Australia, an observation which prompted the original studies into the toxic components of *Dichapetalum* spp. The toxicity of fluoroacetate (1) led to its sodium salt being licensed as a rat poison and it is still used as such in North America and particularly Australia under the trade name 'compound 1080'.

The physiological effect of fluoroacetate (1) poisoning is depressed levels of Ca<sup>2+</sup>, due to an increased level of citrate that is known to bind of Ca<sup>2+</sup> strongly.<sup>51</sup> The origins of this toxicity may lie in the ability of fluoroacetate (1) to inhibit the tricarboxylic acid cycle (TCA or Krebs's cycle). The TCA cycle is the end point of the catabolic processes that yield energy from fuel molecules by the complete oxidation of acetate (6) to CO<sub>2</sub>.<sup>3</sup> The TCA cycle is considered to be at the crossroads between catabolism and anabolism as it provides many precursors for both primary and secondary metabolism.

Acetyl-S-CoA (13) enters the TCA cycle from glycolysis by the oxidative decarboxylation of pyruvate (10) (mediated by pyruvate dehydrogenase), before being condensed with oxaloacetate (42) to form citrate (43). Fluoroacetate (1) is involved in the 'lethal synthesis'<sup>52</sup> of 2-fluorocitrate (44) by the analogous coupling of fluoroacetyl-

S-CoA (**38**) with oxaloacetate (**42**). The 2-*pro-R* proton from fluoroacetate (**1**) is abstracted and condensation with oxaloacetate (**42**) (attacking the *si* face), proceeds with inversion at C-2.<sup>53</sup> Therefore only (2*R*,3*R*)-2-fluorocitrate (**44**) is biosynthesised,<sup>54</sup> synthetic studies have shown that the other three diastereoisomers are not toxic.<sup>55</sup>

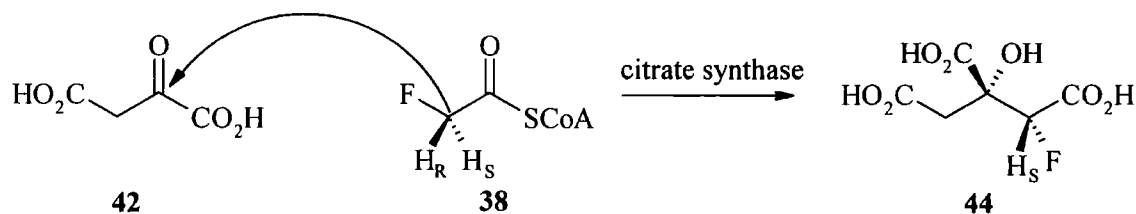


**Fig. 1.11:** Lethal synthesis of (2*R*,3*R*)-2-fluorocitrate (**44**) from fluoroacetate (**1**), mediated by citrate synthase.

It appears that (2*R*,3*R*)-2-fluorocitrate (**44**) has the ability to inhibit the next step in the TCA cycle, the conversion of citrate (**43**) to isocitrate (**45**) by aconitase (EC 4.2.1.3).<sup>56</sup> Citrate (**43**) is dehydrated to form *cis*-aconitate (**46**) before being rehydrated in an *anti*-Markovnikoff fashion to yield isocitrate (**45**). (2*R*, 3*R*)-2-Fluorocitrate (**44**) is accepted as a substrate for aconitase, to form 2-fluoroaconitate (**47**). The enzyme then mediates an S<sub>N</sub>2' hydroxyl attack to the 5 position, with concomitant fluoride release, to form 4-hydroxy-*trans*-aconitate (**48**), which binds strongly to the enzyme in a non-covalent manner. Recent crystallographic evidence<sup>56</sup> of the aconitase - 4-hydroxy-*trans*-aconitate (**48**) complex indicates that short hydrogen bonds keep (**48**) in the active site as a transition state analogue. The double bond in this complex cannot be hydrated and therefore remains at the active site, released only by a great excess (> 10<sup>4</sup>-fold) of substrate (**43**).

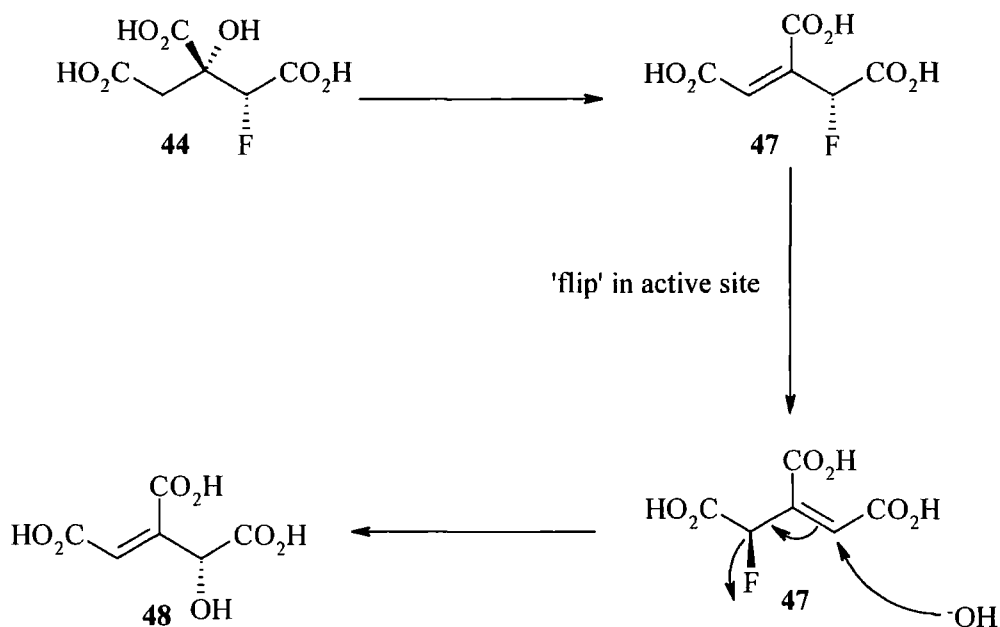


**Fig. 1.12:** Metabolism of (2*R*, 3*R*)-2-fluorocitrate (**44**) to 4-hydroxy-*trans*-aconitate (**48**).

Aconitase inhibition may only contribute partially to 2-fluorocitrate (**44**) toxicity. It appears that the  $K_i$  for aconitase inhibition is of the order of 1  $\mu\text{M}$ , but (2*R*, 3*R*)-2-fluorocitrate (**44**) is toxic at the  $10^{-4}$   $\mu\text{M}$  level. 2-Fluorocitrate (**44**) has been implicated in inhibiting citrate (**43**) transport across the mitochondrial membrane.<sup>56</sup>

The toxicity of the  $\omega$ -fluorinated fatty acids from *D. toxicarium* can also be explained in terms of the lethal synthesis of fluorocitrate (**44**), by  $\beta$ -oxidation (section 1.1.2) of the  $\omega$ -fluorinated fatty acids. Through this process the  $\omega$ -fluorinated fatty acids are catabolised to acetyl-S-CoA (**13**) and fluoroacetyl-S-CoA (**38**). Neatly this provides independent evidence for  $\beta$ -oxidation. The  $\omega$ -fluorinated fatty acids tend to be more toxic than fluoroacetate (**1**) itself and this may be because fluoroacetyl-S-CoA (**38**) is generated directly for 2-fluorocitrate (**44**) synthesis. Consistent with this only the  $\omega$ -fluorinated fatty acids with an even number of carbon atoms are toxic, if an odd number is present then  $\beta$ -oxidation presumably yields the non-toxic fluoropropionyl-S-CoA.<sup>51</sup>

### 1.4.5 Resistance to fluoroacetate (1) poisoning

Nature has developed a number of strategies for resistance to fluoroacetate (1) toxicity. As fluoroacetate (1) itself is relatively benign the ability to convert the active and potentially toxic (through the lethal synthesis) fluoroacetyl-S-CoA (38) to fluoroacetate (44) is an effective means of resistance. An *in vitro* activity has been identified in *D. cymosum* capable of hydrolysing fluoroacetyl-S-CoA (38), but not acetyl-S-CoA (13). This suggests that such a hydrolytic enzyme may be responsible for plant fluoroacetate (1) resistance.<sup>57</sup> It has also been suggested that plants have the ability to segregate fluoroacetate (1) remote from the mitochondria,<sup>58</sup> so that it is not processed to (2*R*, 3*R*)-2-fluorocitrate (44). It may be that some plant citrate synthases do not have the ability to process fluoroacetyl-S-CoA (38) through to 2-fluorocitrate.<sup>59</sup>

Microorganisms that are symbionts on plants that produce fluoroacetate (1) have developed a defluorination activity. Studies on *Pseudomonas* spp.<sup>60,61,62</sup> and the fungus *Fusarium solani*<sup>63</sup> have demonstrated the ability to defluorinate fluoroacetate (1) and this activity is inhibited by thiol blocking agents. It appears that a thiol group on the enzyme displaces fluoride to form a thioether (49), which is then hydrolysed to yield glycolate (50). When this hydrolysis is carried out in H<sub>2</sub><sup>18</sup>O the resultant glycolate (50) incorporates oxygen-18.<sup>61</sup>

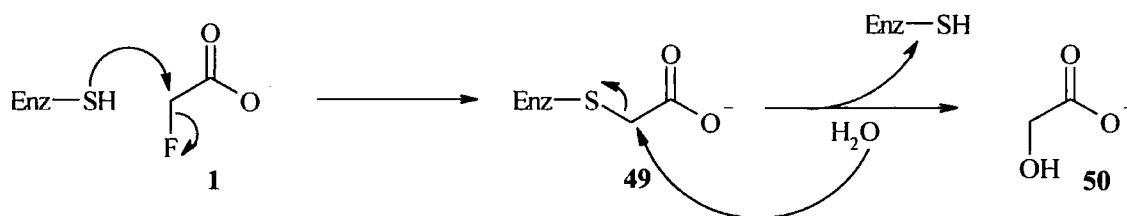


**Fig. 1.13:** Proposed mechanism for microbial fluoroacetate (1) defluorination to yield glycolate (50).

A different mechanism for microbial defluorination has recently been revealed in *Moraxella* Spp.<sup>64</sup> A fluoroacetate (1) dehalogenase has been shown to defluorinate fluoroacetate (1) *via* nucleophilic attack by a carboxylate group (from Asp105 in the enzyme), to generate an intermediate ester. This ester is hydrolysed, assisted by His272. Multiple turnover of the enzyme in the presence of H<sub>2</sub><sup>18</sup>O demonstrated that label was incorporated into the enzyme at position Asp105, rather than the product, supporting the mechanism (see Fig. 1.14).

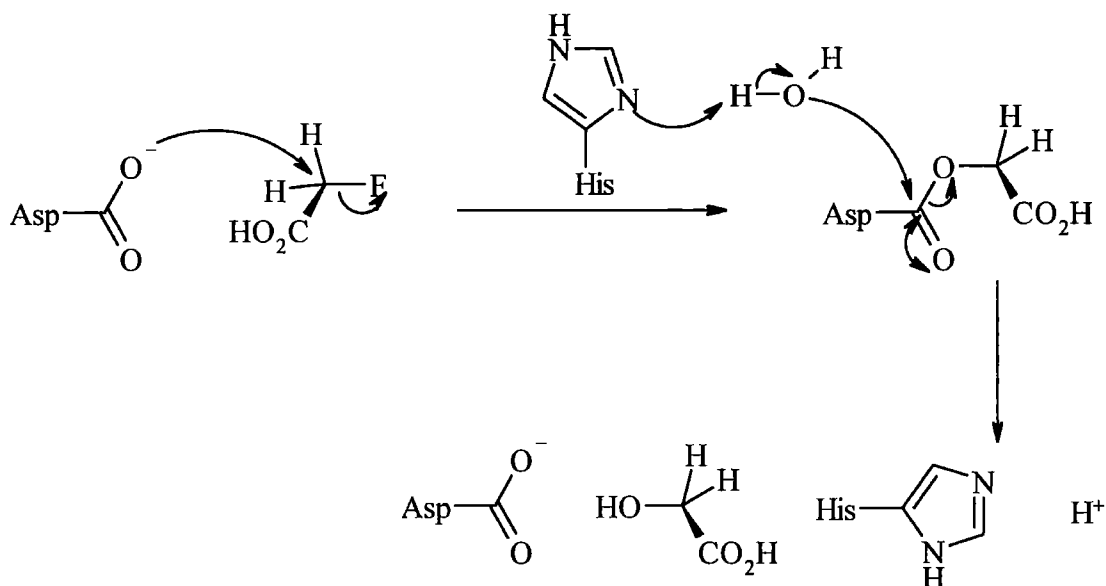


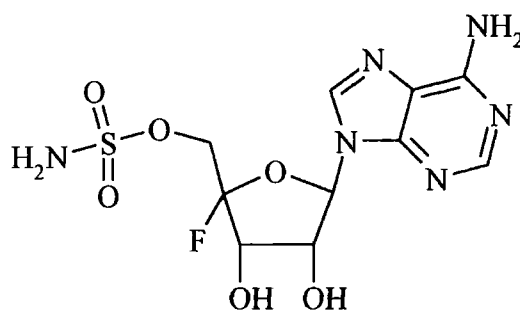
**Fig. 1.14:** Fluoroacetate (1) defluorination in *Moraxella* spp. B.

A similar defluorination activity appears in plants and animals. *In vitro* experiments on liver homogenates of the brush-tailed possum (*Trichosurus vulpecula*) demonstrated a defluorination based on nucleophilic attack from the free thiol from glutathione rather than a thiol on an enzyme.<sup>65</sup> This generates *S*-(carboxymethyl)glutathione which is metabolised to *S*-(carboxymethyl)cysteine. The presence of *S*-(carboxymethyl)cysteine following fluoroacetate (1) defluorination in mouse<sup>66</sup> and lettuce<sup>67</sup> suggest that this defluorination method operates in these systems.

### 1.4.6 Fluorometabolites from microorganisms

To date there are only two examples of microorganisms capable of fluorometabolite biosynthesis, both of which belong to the genus *Streptomyces*.

#### 1.4.6.1 Nucleocidin (51)



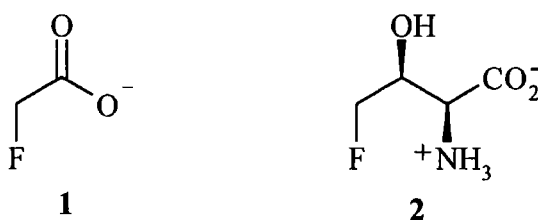
51

Fig. 1.15: Nucleocidin (51).

Nucleocidin (51) was isolated from the bacterium *Streptomyces calvus*, cultured from an Indian soil sample.<sup>68</sup> It demonstrated broad antibiotic and antitrypanosomal activity, although clinical use was curtailed due to its toxicity. Originally a partial structure was proposed from the empirical formula of  $C_{11}H_{16}N_6SO_8$ , however during the late sixties the proposed structure was revised twice. In 1968, on the basis of new chemical and spectroscopic evidence, it was proposed that the nucleocidin structure was 9-(4-O-sulfamoylpentofuranosyl)adenine ( $C_{10}H_{14}N_6SO_7$ ), before the same research group revised the structure to 9-(4-fluoro-5-O-sulfamoylpentofuranosyl)adenine ( $C_{10}H_{13}N_6SO_6F$ ) in 1969.<sup>69</sup> This structure has been confirmed through total synthesis.<sup>70</sup> Nucleocidin (51) is the only compound known to display a fluoro-sugar moiety and nothing is known about the biosynthesis of this C-F bond. It is not obvious that fluoroacetate (1) could be involved in nucleocidin (51) biosynthesis, suggesting a unique C-F bond forming process. Unfortunately recent attempts to re-establish nucleocidin (51) production in *Streptomyces calvus* have failed<sup>71</sup> and there is not a biological system available to pursue a biosynthetic study on this metabolite.



#### 1.4.6.2 Fluoroacetate (1) and 4-fluorothreonine (2)



**Fig. 1.16:** Fluoroacetate (1) and 4-fluorothreonine (2).

Fluoroacetate (1) and 4-fluorothreonine (2) are produced by *Streptomyces cattleya* and are the subject of this thesis. During fermentation studies<sup>72</sup> on the  $\beta$ -lactam antibiotic thienamycin (52) in *S. cattleya*, it was noticed that an antimetabolite was co-produced. The isolation and structural elucidation of this co-metabolite led to its identification as 4-fluorothreonine (2) and subsequent <sup>19</sup>F-NMR studies on the culture broth demonstrated the presence of fluoroacetate (1). 4-Fluorothreonine (2) was found to exhibit poor antibacterial properties and has an LD<sub>50</sub> of 320 mg/kg (intravenous administration) in mice. This compares with an LD<sub>50</sub> of 6.6 mg/kg for fluoroacetate (1) toxicity. Total synthesis has since confirmed that naturally occurring 4-fluorothreonine (2) is the (2*S*,3*S*)-4-fluorothreonine (2) isomer, with an identical stereochemistry to L-threonine.<sup>73</sup> The short highly stereoselective synthesis involved the condensation of fluoroacetyl chloride to a substituted imidazolidinone in an extension of Seebach's methodology for preparing  $\alpha$ -amino- $\beta$ -hydroxy acids.<sup>74</sup>

## 1.5 Biological fluorination - proposed mechanisms

Fluoride is heavily solvated and a poor nucleophile in aqueous media, but despite this the most probable mechanism for biological C-F bond formation is the nucleophilic attack of fluoride onto an activated carbon. Putative mechanisms for biological fluorination, specifically for the biosynthesis of fluoroacetate (1) in plants, have been proposed and are discussed below.

### 1.5.1 Addition to a carbon-carbon multiple bond

#### 1.5.1.1 Pyridoxal phosphate (53) assisted addition of fluoride

Mead and Segal<sup>75</sup> suggested that fluoroacetate (1) may be biosynthesised in a similar manner to  $\beta$ -substituted alanines in plants. The Leguminales, of which *Acacia* spp. are members, are capable of elaborating a variety of unusual  $\beta$ -substituted alanines. These amino acids arise by nucleophilic attack on  $\beta$ -position of serine (54) or cysteine (55), catalysed by pyridoxal phosphate (53). Seven such  $\beta$ -alanines (56  $\rightarrow$  61) have been isolated from *Acacia* spp.,<sup>76</sup> including  $\beta$ -cyanoalanine (56) which was shown to be synthesised by this method.<sup>77,78</sup>

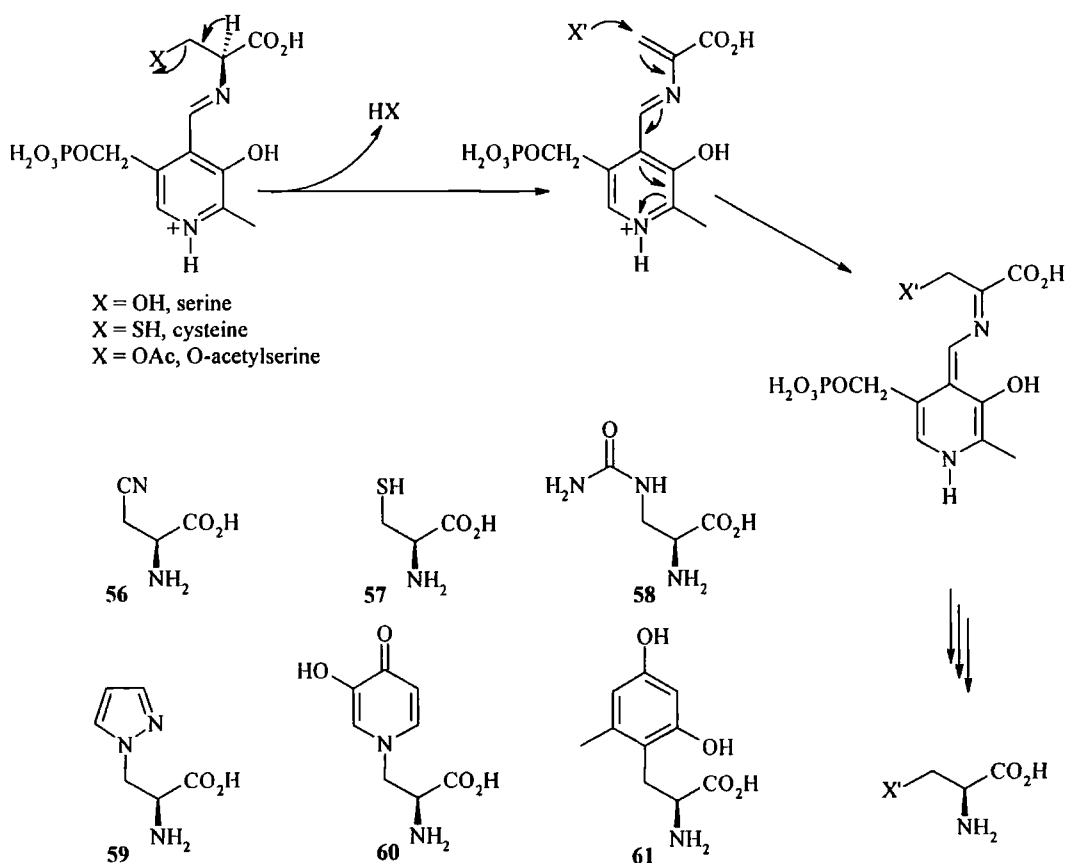
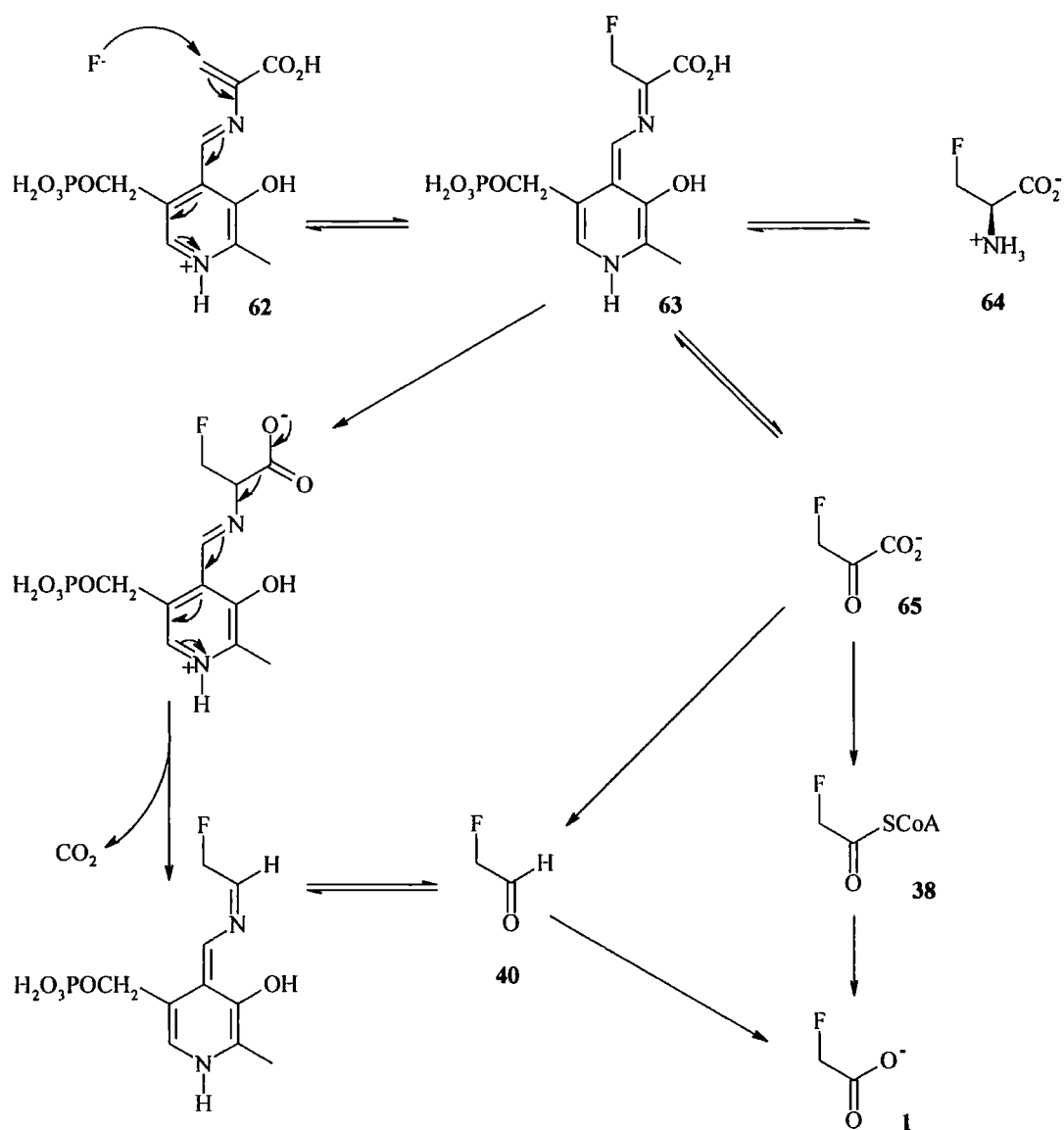


Fig. 1.17: Biosynthesis of  $\beta$ -substituted alanines (56  $\rightarrow$  61) by the Leguminales.

The product of elimination of serine or cysteine pyridoxal phosphate adducts (**62**) is subject to Michael-type attack. Hydrolysis of the resultant adducts liberates the  $\beta$ -substituted alanines as listed in Fig. 1.17. It is reasonable to suggest that a non-specific synthase catalyses this nucleophilic attack and may utilise fluoride as a nucleophile, to generate pyridoxal phosphate bound  $\beta$ -fluoroalanine (**63**). The biosynthesis of fluoroacetate (**1**) from this species could occur in one of two ways. Either  $\beta$ -fluoropyruvate (**65**) is liberated by hydrolysis and fluoroacetyl-SCoA (**38**) synthesised by oxidative decarboxylation mediated by a pyruvate decarboxylase or the pyridoxal phosphate complex (**63**) undergoes decarboxylation and releases fluoroacetaldehyde (**40**) which could be oxidised to fluoroacetate (**1**) by an aldehyde dehydrogenase.



**Fig. 1.18:** Putative biosynthesis of fluoroacetate (**1**), Mead and Segal.

The authors cite relevant analogous reactions from within phytochemistry, mostly based on known *S*-methylcysteine metabolism.<sup>79,80</sup> Mead and Segal examined the effect of fluoride and cyanide on extracts of *Acacia georginae* in order to test their hypothesis.<sup>81</sup> Cyanide was found to inhibit the formation of pyruvate (10) from cysteine (55) (a process catalysed by pyridoxal phosphate (53)), and  $\beta$ -cyanoalanine (56) was synthesised *in vitro*. However, in the presence of fluoride ion there was no production of either  $\beta$ -fluoropyruvate (65) or  $\beta$ -fluoroalanine (64).  $\beta$ -Fluoroalanine (64) is unstable above pH 7.0, decomposing to liberate inorganic fluoride.<sup>82</sup> Also, the pyruvate dehydrogenase complex (PDC) stoichiometrically defluorinates  $\beta$ -fluoropyruvate (65),<sup>83,84</sup> a process mediated by pyruvate decarboxylase. Therefore in cell-free extracts at pH 8.5  $\beta$ -fluoropyruvate (65) may have decomposed prior to detection. It is worth noting that the majority of fluoroacetate (1) producers are members of the Leguminales which demonstrate the phytochemistry necessary to produce  $\beta$ -substituted alanines, however *Dichapetalum* spp. to which many fluoroacetate (1) producers belong, falls outside of this group and generally they do not display  $\beta$ -substituted alanine chemistry.

Interestingly callus tissue of *Dichapetalum cymosum* has been shown to convert  $\beta$ -fluoropyruvate (65) to fluoroacetate (1).<sup>84</sup> This activity was only demonstrated in cell-free extracts of the callus tissue, in the presence of a PDC inhibitor, monomethyl acetylphosphonate (66),<sup>85</sup> demonstrating that  $\beta$ -fluoropyruvate (65) is not decarboxylated by PDC itself and that there is a high degree of compartmentalisation to separate the two activities. This biotransformation perhaps implies a role for  $\beta$ -fluoropyruvate (65) in fluoroacetate (1) biosynthesis in *Dichapetalum cymosum*.

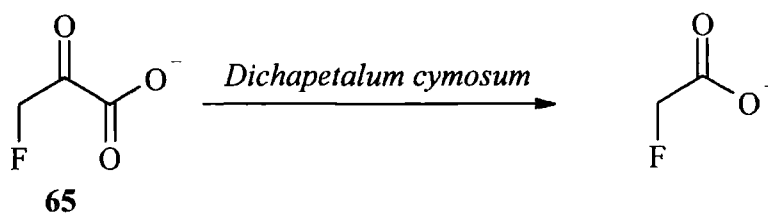


**Fig. 1.19:** The decarboxylation of  $\beta$ -fluoropyruvate (65) by *Dichapetalum cymosum*.

### 1.5.1.2 Ethylene (67) and ethylene oxide (70) as putative precursors

Ethylene (67) has been proposed as a potential precursor to fluoroacetate (1). The fluoroacetate (1) producer *Acacia georginae* has been shown to lose fluoride by producing a volatile organofluorine compound<sup>49</sup> and also produces the plant hormone ethylene (67)<sup>86</sup> (in bananas this hormone is responsible for the initiating ripening process,<sup>20</sup> and is now used to artificially ripen bananas once imported). Peters<sup>87</sup> hypothesised that fluoroacetate (1) could be produced *via* fluoroethane (68) or vinyl fluoride (69), although he did not suggest a plausible mechanism. By association ethylene oxide (70) has been proposed as an intermediate also,<sup>43</sup> which could generate fluoroethanol (71), prior to oxidation to fluoroacetate (1). However these routes are hypothetical and there is no experimental evidence to support these proposals.

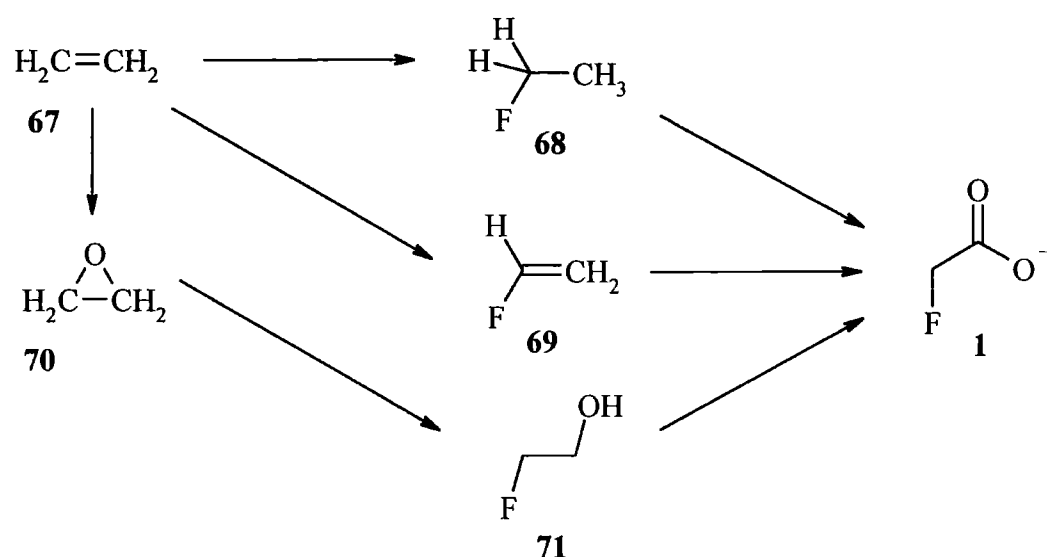
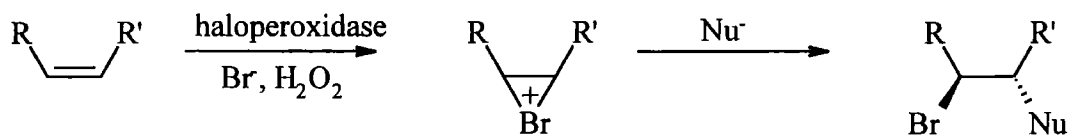


Fig. 1.20: Putative pathways to fluoroacetate (1) from ethylene (67).

### 1.5.1.3 Nucleophilic attack on a halonium ion

When a haloperoxidase reacts with an alkene then the reaction product is dependent on the relative anion concentrations. Usually a halohydrin species is formed by reaction with hydroxide in the buffer, although if there is a relatively high concentration of halide ion a 1,2-dihalo species may be formed.<sup>88</sup>



Nu: OH, Br, Cl, F<sup>-</sup>

**Fig. 1.21:** *In vitro* formation of a halonium ion and subsequent nucleophilic attack.

Using this methodology Neidleman and Geigert<sup>88</sup> prepared 2,3-fluoroiodopropan-1-ol (**73**), by the action of Horseradish peroxidase on allyl alcohol (**72**) and iodide in the presence of H<sub>2</sub>O<sub>2</sub> and fluoride, the first *in vitro* 'enzyme-associated' formation of a C-F bond.

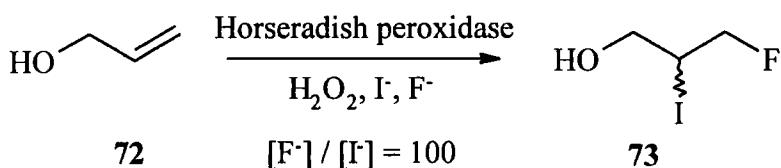


**Fig. 1.22:** The *in vitro* synthesis of 2,3-fluoroiodopropan-1-ol (**73**).

On the basis of this Neidleman and Geigert<sup>89</sup> speculated that fluoroacetate (**1**) could be biosynthesised by the iodofluorination of an ω-unsaturated fatty acid (**74**) which then undergoes de-iodination and degradation to fluoroacetate (**1**) *via* β-oxidation.

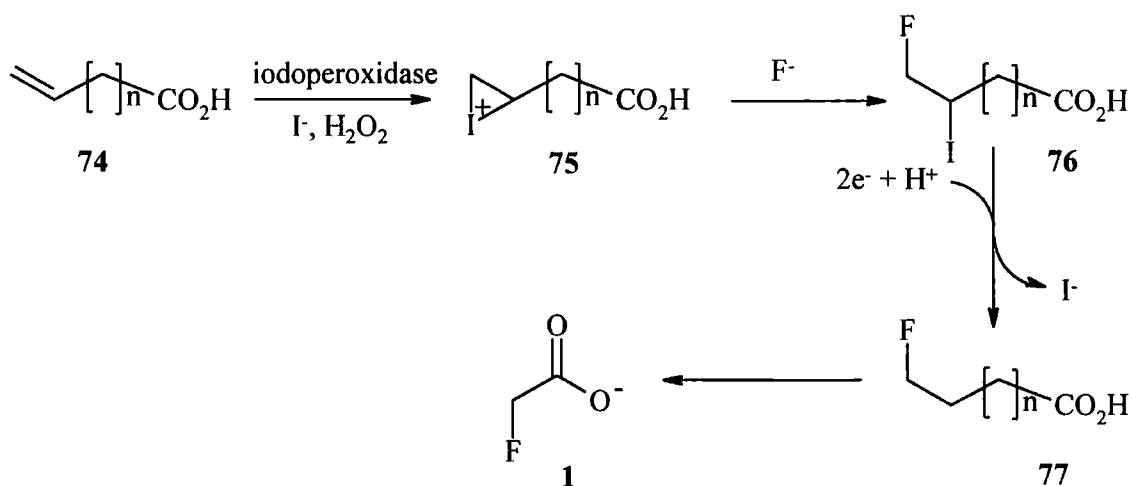


**Fig. 1.23:** The putative biosynthesis of fluoroacetate (**1**) *via* an ω-fluorinated fatty acid (**77**).

The authors presented no supporting evidence for this hypothesis, although they did suggest studying the iodine content of fluoroacetate (1) producers.

### 1.5.2 Fluorination via nucleophilic substitution

It is unlikely that fluoroacetate (1) is produced directly by substitution on acetate (6) as the methyl group is not activated to such attack. Incubation of the leaves of the fluoroacetate (1) producer *Dichapetalum cymosum* with [2-<sup>14</sup>C]-acetate did not result in incorporation into the resultant fluoroacetate (1).<sup>90</sup> This does not seem to inhibit the author of one secondary metabolite text<sup>91</sup> from implying that the origin of fluoroacetate (1) is known to be acetate (6), and also to introduce trifluoroacetic acid (78) as a constituent of *Dichapetalum* spp. This latter aberration arose as trifluoroacetic acid (78) was used as the internal reference added in a <sup>19</sup>F NMR study in the citation quoted.

The nucleophilic substitution of the hydroxyl group on glycolate (50) by fluoride to produce fluoroacetate (1), is an economical and attractive hypothesis. Due to the bond energy of the C-F bond in fluoroacetate (1), substitution could proceed under physiological conditions if it were coupled to a spontaneous reaction.<sup>92</sup> It is unlikely however that hydroxyl would act as a leaving group in this case, but a more realistic hypothesis emerges if it were activated, possibly by phosphorylation.<sup>43</sup>

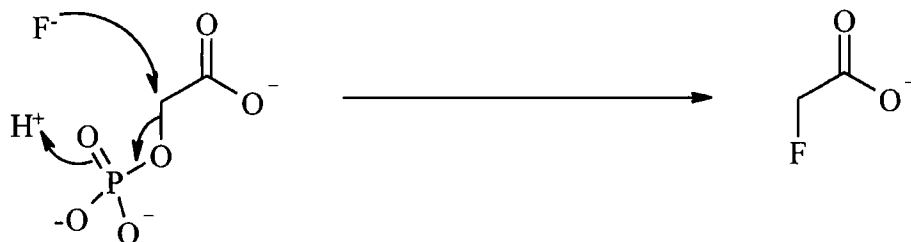


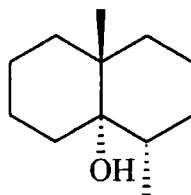
**Fig. 1.24:** Nucleophilic substitution of a phosphate group by fluoride.

The reverse of the reaction is well documented. Microorganisms that are capable of utilising fluoroacetate (1) as a sole carbon source have a haloacetate halohydrolyase that converts fluoroacetate (1) to fluoride and glycolate (50).<sup>60,61,63</sup> The reaction proceeds by the nucleophilic attack of an enzyme bound thiol to liberate fluoride and produce a thioether bond, which is hydrolysed to yield glycolate (50) (section 1.4.5). However the reversibility of this reaction has been studied by the incubation of glycolate (50) and fluoride in the presence of  $H_2^{18}O$ . Neither fluoroacetate (1) or glycolate (50) became labelled with oxygen-18.

## 1.6 *Streptomyces cattleya* and the fluorometabolites

### 1.6.1 *The Streptomyces*

The majority of *Streptomyces* spp. are restricted to soil (usually under alkaline or neutral conditions)<sup>93</sup> and are largely responsible for the 'earthy' smell of some soils as a consequence of the release of volatile metabolites such as geosmin (**79**).<sup>94</sup>



79

**Fig. 1.25:** Geosmin (**79**).

The genus *Streptomyces* is associated with two phenomenon; sporulation and antibiotic biosynthesis.<sup>95</sup> When grown on solid media mature *Streptomyces* display differentiated morphologies, consisting of a lower branching vegetative mycelium on which aerial hyphae form spores or conidia. Closely linked with the onset of sporulation is secondary metabolite biosynthesis and the *Streptomyces* produce a vast diversity of secondary metabolites. These include the polyether, macrolide, tetracycline, aminoglycoside and various  $\beta$ -lactam antibiotics. Many of the natural products isolated from *Streptomyces* have become commercially important being used in medicine and in agriculture as feed stock additives.

### 1.6.2 *Streptomyces cattleya*

*Streptomyces cattleya* is the thienamycin (**52**) producing organism isolated by Merck in New Jersey, USA.<sup>96</sup> Thienamycin (**52**) is a commercially important broad-spectrum antibiotic, active against many Gram-positive and some Gram-negative bacteria. It possesses a carbapenem ring system and as such is resistant to many  $\beta$ -lactamases which hydrolyse penicillins and cephalosporins. However, under physiological conditions, thienamycin is unstable, therefore the derivatives Imipenem (**80**) and Meropenam (**81**) are used in conjunction with Cilastatin which is an inhibitor of kidney dipeptidase, and so slows the degradation of the antibiotics.<sup>97</sup>



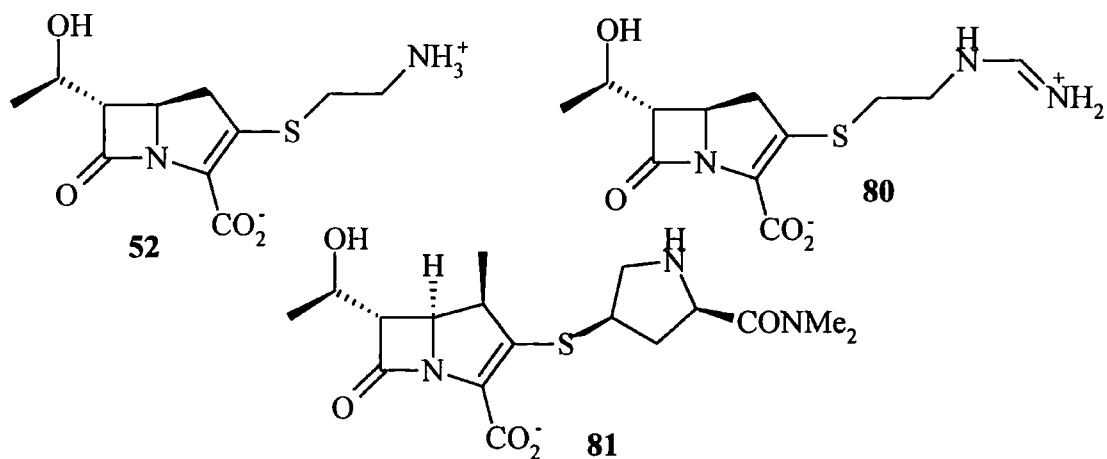


**Fig. 1.26:** Thienamycin (52), imipenem (80) and meropenam (81).

Biosynthetic studies<sup>98</sup> have shown that thienamycin (52) arises by a non-classical  $\beta$ -lactam biosynthesis. Stable isotope incorporation studies suggest that the pyrrolidine ring is derived from glutamate, and the other two carbons of the  $\beta$ -lactam originate from an acetate (6) unit. The hydroxyethyl side group is delivered by the consecutive addition of two methyl groups from methionine (SAM) and the cysteaminy side chain originates from cysteine.

*Streptomyces cattleya* also produces the  $\beta$ -lactams cephamycin C (82) and penicillin N (83) and the metabolites 2-hydroxy-2-hydroxymethylcyclopent-4-ene (84) and 3-ethynylserine (85).

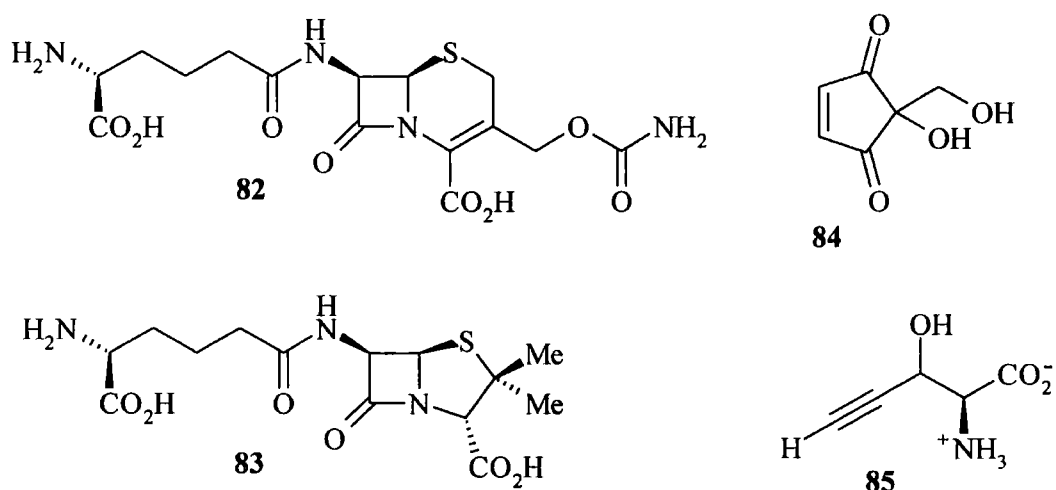


**Fig. 1.27:** Cephamycin C (82), 2-hydroxy-2-hydroxymethylcyclopent-4-ene (84), penicillin N (83) and 3-ethynylserine (85).

### 1.6.3 Fluoroacetate (1) and 4-fluorothreonine (2)

4-Fluorothreonine (2) was isolated and identified during studies to optimise thienamycin (52) production when the soybean casein in the media contained inorganic fluoride.<sup>72</sup> Fluoroacetate (1) was not isolated but was identified by <sup>19</sup>F NMR analysis of the culture broth. The authors suggested that fluoroacetate (1) might be an intermediate, that could be metabolised to fluoroacetaldehyde (40). 4-Fluorothreonine (2) could then be formed by the condensation of fluoroacetaldehyde (40) and glycine (86). No discussion on C-F bond formation was presented.

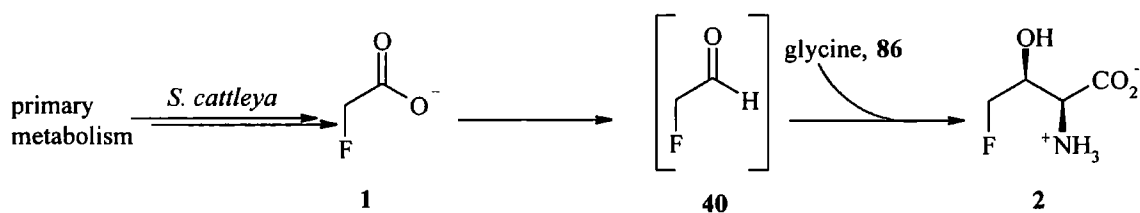


**Fig. 1.28:** Proposed biosynthesis of fluoroacetate (1) and 4-fluorothreonine (2), Sanada *et al.*<sup>72</sup>

Resting cells of *Streptomyces cattleya* were already known to produce thienamycin (52), so Sanada *et al.* used this system to study fluorometabolite production under a variety of fluorine sources. Resting cells are prepared when an organism is in its idiophase and the cells are harvested and suspended in a buffer. This allows the biosynthesis to be studied by supplementing the cells with putative precursors as the sole carbon source. Both of the fluorometabolites were produced by resting cells of *S. cattleya* in the presence of 4-fluoroglutamate, sodium fluoroacetate and potassium fluoride. They also noted that 4-fluorothreonine (2) when supplemented to resting cells, could support fluoroacetate (1) biosynthesis.

Reid *et al.*<sup>99</sup> in the first publication from a collaboration between The Queen's University of Belfast and The University of Durham, published a detailed account of fluorometabolite production in both growing and resting cells. The concentrations of the fluorometabolites were determined by <sup>19</sup>F-NMR analysis, by comparing integral heights with an internal standard (fluoroacetone (39)) for which a calibration curve had been obtained. It was noted that fluorometabolite production commenced just after maximum growth of the organism, in a classical manner. The onset of fluorometabolite production was characterised by the concurrent production of fluoroacetate (1) and

4-fluorothreonine (2), although the rate of fluoroacetate (1) production was greater. The culture medium when supplemented with 2 mM inorganic fluoride generated fluoroacetate (1) at 1.2 mM and 4-fluorothreonine (2) at 0.5 mM. In time, essentially all of the fluoride was utilised for fluorometabolite production and both of the fluorometabolites were excreted extracellularly.

Resting cells of *Streptomyces cattleya* were optimised for fluorometabolite production. It was noted that resting cells prepared from cells 6 - 10 days old were capable of fluorometabolites production. The pH optima in terms of fluoride uptake into the cells was pH 6.0, however there was a discrepancy between amount of fluoride taken into the cells and fluorometabolites excreted from the cells. Even though the rate of fluoride uptake was low at pH 6.5 (compared to pH 6.0) the fluorometabolites produced equated with the amount of fluoride removed from the buffer. Therefore these conditions revealed that the rate-limiting step is fluoride uptake by the cells.

Using these optimised resting cells (6 day old cultures, pH 6.5) various <sup>14</sup>C labelled putative intermediates were administered to the bacterium and specific incorporations into fluoroacetate (1) measured.<sup>99,100</sup> The best carbon source under these conditions was [U-<sup>14</sup>C]-glycolate (incorporation between 1.7 % and 4.1 %). D-[U-<sup>14</sup>C]-Glucose and [U-<sup>14</sup>C]-glycerol gave lower incorporations (1.6 % and 1.1 % respectively). However, it was suggested that these are such good carbon sources that they were also being utilised in primary metabolic processes. The relatively high incorporation of [U-<sup>14</sup>C]-glycolate could be consistent with fluoroacetate (1) being biosynthesised by the nucleophilic displacement of the alcohol group (most likely in an activated form) by inorganic fluoride (**section 1.5.2**)

In 1995 Soda *et al.*<sup>101</sup> published an account of the biosynthesis of fluoroacetate (1) and 4-fluorothreonine (2) in *Streptomyces cattleya*. They monitored the production of both fluoroacetate (1) and 4-fluorothreonine (2) by <sup>19</sup>F-NMR and noticed that fluoroacetate (1) started to accumulate earlier than 4-fluorothreonine (2). From this they conjectured that fluoroacetate (1) is metabolised to 4-fluorothreonine (2). However, the accumulation of a metabolite does not imply its position in a biosynthetic pathway as many intermediates exist only in low steady-state concentrations. In fact if the rate of the hypothetical conversion of fluoroacetate (1) to 4-fluorothreonine (2) was high then

the latter might be expected to accumulate first despite the former preceding it biosynthetically.

Soda *et al.* also reported feeding experiments with  $^{14}\text{C}$  labelled primary metabolite intermediates, in both growing and resting cell preparations, supplemented with 10 mM KF. These feeding studies were conducted using a mutant organism (*Streptomyces cattleya* NTG29), generated by treating the wild type (*S. cattleya* NRRL 8057) with *N*-methyl-*N'*-nitro-*N*-nitrosoguanidine. They surmised that fluoroacetate (**1**) was biosynthesised from glycerol (**87**) via  $\beta$ -hydroxypyruvate (**88**), a conclusion supported by relatively high incorporations of label from  $[\text{U-}^{14}\text{C}]$ -glucose,  $[\text{U-}^{14}\text{C}]$ -glycerol,  $[\text{U-}^{14}\text{C}]$ -serine and  $[\text{U-}^{14}\text{C}]$ - $\beta$ -hydroxypyruvate compared with lower incorporations from  $[\text{U-}^{14}\text{C}]$ -aspartate,  $[2,3\text{-}^{14}\text{C}]$ -succinate and  $[3\text{-}^{14}\text{C}]$ -pyruvate. A key experiment involved the feeding of  $[2\text{-}^{13}\text{C}]$ -glycerol (**89**). The resultant fluoroacetate was isolated and purified by preparative HPLC and was analysed by NMR ( $^1\text{H}$ ,  $^{13}\text{C}$  and  $^{19}\text{F}$ ) and GCMS of the methyl ester.  $[2\text{-}^{13}\text{C}]$ -Glycerol (**89**) labelled only C-1 of fluoroacetate (**1a**) at a high incorporation of 40 %.

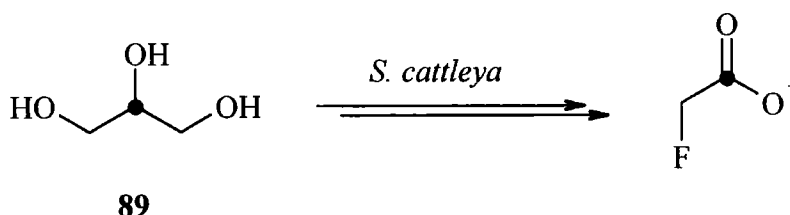


**Fig. 1.29:**  $[2\text{-}^{13}\text{C}]$ -glycerol (**89**) incorporation into fluoroacetate (**1a**), Soda *et al.*

The authors proposed that glycerol (**87**) is converted to  $\beta$ -hydroxypyruvate (**88**) which is processed through to fluoroacetate (**1**) by fluorination and decarboxylation.

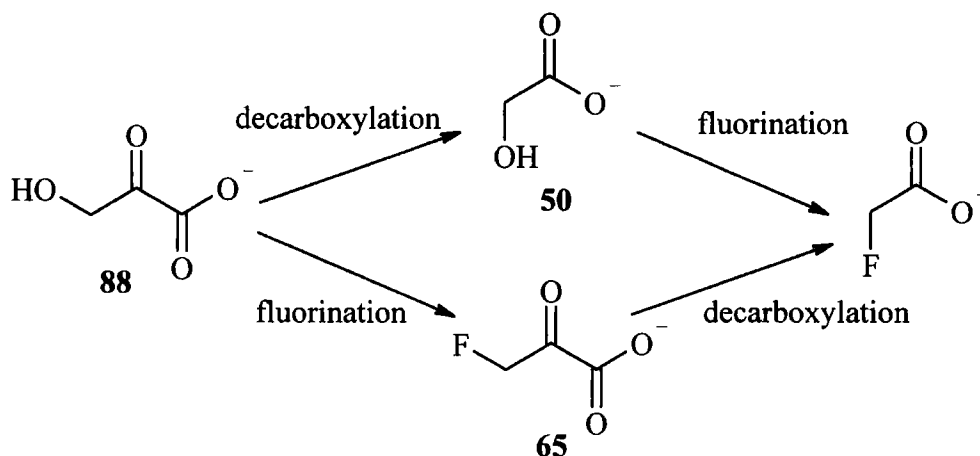


**Fig. 1.30:** Putative conversion of  $\beta$ -hydroxypyruvate (88) to fluoroacetate (1), Soda *et al.*

As there are two possible pathways there are two possible intermediates:  $\beta$ -fluoropyruvate (65) and glycolate (50). Feeding experiments with  $[2-^{14}\text{C}]$ -glycolate and  $[1,2-^{13}\text{C}_2]$ -glycolate resulted in low incorporations into fluoroacetate (1) (c.f. Reid *et al.*) and it was concluded that glycolate (50) is unlikely to be a direct intermediate. No experiments with commercially available  $\beta$ -fluoropyruvate (65) were reported, but this compound defluorinates rapidly *in vivo* by the action of pyruvate decarboxylase.

The authors suggested that as fluorination could not be catalysed by a haloperoxidase, the displacement of a leaving group by the fluoride anion was clearly a more satisfactory possibility.

#### 1.6.4 The biosynthetic relationship between fluoroacetate (1) and 4-fluorothreonine (2)

Both Sanada *et al.* and Soda *et al.* suggested that 4-fluorothreonine (2) was derived by fluoroacetate (1) metabolism. However, evidence now argues against this. Reid *et al.* incubated resting cells of *S. cattleya* with various organofluorine compounds including fluoroacetate (1) and 4-fluorothreonine (2). In both cases the rate of interconversion was estimated to be at least an order of magnitude too low to account for the levels of the fluorometabolites generated when the bacterium is grown in the presence of fluoride. The rate of interconversion from fluoroacetate to 4-fluorothreonine (2) was 20-fold too slow and when  $[2-^2\text{H}_2]$ -fluoroacetate (1b) was administered to the bacterium the isotope was not incorporated into 4-fluorothreonine (2).

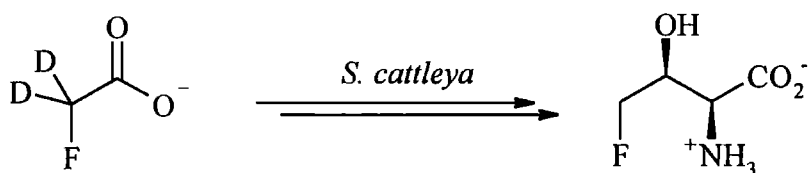


**Fig. 1.31:** [2-<sup>2</sup>H<sub>2</sub>]-Fluoroacetate (**1b**) does not label 4-fluorothreonine (**2**), Reid *et al.*

This suggests that interconversion *per se* does not happen, but the 4-fluorothreonine (**2**) production can be rationalised by defluorination. If *Streptomyces cattleya* has the ability to defluorinate fluoroacetate (**1**) the liberated fluoride will be utilised in *de novo* biosynthesis of both fluoroacetate (**1**) and 4-fluorothreonine (**2**). Evidence for this was provided by incubating *S. cattleya* with [3-<sup>2</sup>H]-4-fluorothreonine (**2a**), which indeed generated unlabelled fluoroacetate (**1**) and 4-fluorothreonine (**2**) from fluoride, as well as retaining some labelled [3-<sup>2</sup>H]-4-fluorothreonine (**2a**).

#### 1.6.5 Incorporation of stable isotope enriched glycolate (**50**), glycine (**86**) and pyruvate (**10**)

Reid *et al.* demonstrated that glycolate (**50**) could act as an effective carbon source for fluorometabolite production. The development in Belfast and Durham of GC-MS and <sup>19</sup>F NMR analysis of the fluorometabolites has allowed for a more detailed study of their biosynthesis.<sup>102,103</sup> <sup>19</sup>F NMR analysis of fluoroacetate (**1**) and 4-fluorothreonine (**2**) was refined so that proton decoupled <sup>19</sup>F{<sup>1</sup>H}-NMR spectra could give positional information on the incorporation into fluoroacetate (**1**) and positions 3 and 4 of 4-fluorothreonine (**2**). GC-MS analysis of derivatives of fluoroacetate (**1**) and 4-fluorothreonine (**2**) (*para*-phenylphenacyl and *N*-methyl-*N*-trimethylsilyltrifluoroacetamide (MSTFA) derivatives respectively) enabled the determination of absolute levels of stable isotope incorporation. For a more detailed discussion of these techniques see **sections 2.2.2 & 2.2.3**.

Initial feeding experiments have traced <sup>13</sup>C-labelled glycolate (**50**) and, the metabolically related, glycine (**86**), through to fluoroacetate (**1**) and 4-fluorothreonine (**2**). [1-<sup>13</sup>C]-, [2-<sup>13</sup>C]- & [1,2-<sup>13</sup>C<sub>2</sub>]-Glycine (**90**), (**91**) & (**92**) were each fed to resting cells of *Streptomyces cattleya*. This series of experiments revealed that both C-1 and C-2 of fluoroacetate (**1**) and both C-3 and C-4 of 4-fluorothreonine (**2**) are derived from

[2-<sup>13</sup>C]-glycine (91). [1-<sup>13</sup>C]-Glycine (90) did not label the fluorometabolites, and [1,2-<sup>13</sup>C<sub>2</sub>]-glycine (92) gave a labelling pattern similar to that of [2-<sup>13</sup>C]-glycine (91) alone.

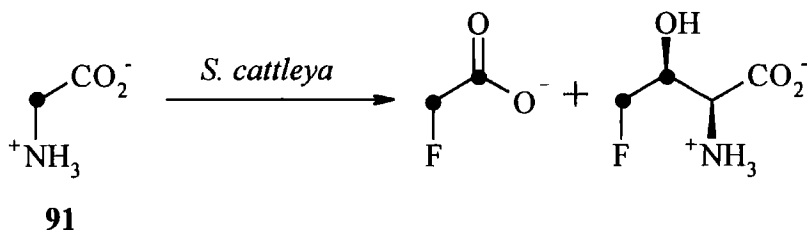


**Fig. 1.32:** Recombination of label from [2-<sup>13</sup>C]-glycine (91) into both fluoroacetate (1c) and 4-fluorothreonine (2b).

[2-<sup>13</sup>C]-Glycine (91) was incorporated at a level of 32 %, whereas [2-<sup>13</sup>C]-glycolate gave a similar labelling pattern, but at a level of 9 %. This apparently contradicts the results obtained by Reid *et al.* who noted that glycolate (50) was a better precursor than glycine (86). However, further studies in the light of this anomaly have shown that the level of incorporation into the fluorometabolites was particularly sensitive to both substrate concentration and cell density in these resting cells experiments. This also explains why Sanada *et al.* found that glycolate (50) was a poor precursor in their experiments.

The incorporation of double label from [2-<sup>13</sup>C]-glycine (91) can be explained in terms of serine (54) metabolism. Serine hydroxymethyltransferase catalyses the combination of two molecules of glycine (86) to generate serine (54). The conversion utilises *N*<sup>5</sup>,*N*<sup>10</sup>-methylenetetrahydrofolate (THF), and can account for the observed labelling pattern from glycolate (50) and glycine (86).

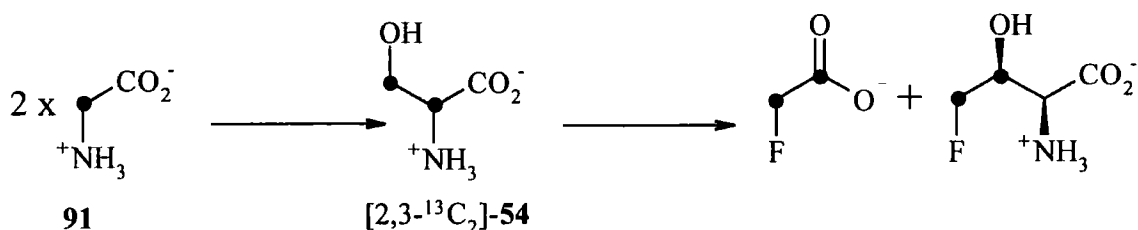


**Fig. 1.33:** Glycine (86) recombination *via* serine (54).

Clearly following this hypothesis serine and related metabolites should become readily incorporated into both fluoroacetate (1) and 4-fluorothreonine (2). This is indeed the case with <sup>13</sup>C labelled serine (54) and pyruvate (10) labelling the fluorometabolites in a

manner consistent with this hypothesis. Pyruvate (**10**) is metabolically related to serine by way of serine dehydratase. [2-<sup>13</sup>C]- & [3-<sup>13</sup>C]-Pyruvate (**93**) & (**94**) labelled C-1 and C-2 of fluoroacetate (**1**) and C-3 and C-4 of 4-fluorothreonine (**2**) respectively, by analogy and [1-<sup>13</sup>C]-pyruvate did not result in any significant labelling.

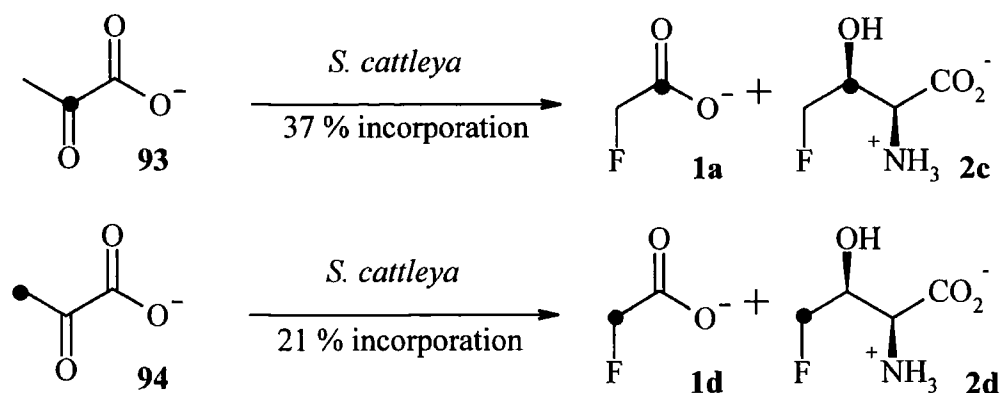


**Fig. 1.34:** Incorporation of [2-<sup>13</sup>C]- & [3-<sup>13</sup>C]-pyruvate (**93**) & (**94**) into fluoroacetate (**1a** & **1d**) and 4-fluorothreonine (**2c** & **2d**).

The similarity of the labelling patterns into each metabolite in given examples, both in terms of magnitude and regiochemistry in fluoroacetate (**1**) and positions 3 and 4 of 4-fluorothreonine (**2**) was observed to be a reproducible feature of these whole cell feeding experiments. Since they contain the same labelling pattern the biosynthesis of fluoroacetate (**1**) and 4-fluorothreonine (**2**) must follow, at least in part, a common pathway. This common pathway must include the fluorination step and as it is already known that the level of interconversion between the fluorometabolites is low. The current working hypothesis predicts at least one common fluorinated intermediate.

#### 1.6.6 The stereochemical processing of glycerol (**87**)

Sanada *et al.* fed [2-<sup>13</sup>C]-glycerol (**89**) and demonstrated that it effectively labelled position 1 of fluoroacetate (**1**). Glycerol (**87**) is prochiral, and can be rendered chiral when labelled with stable isotope. Nieschalk *et al.*<sup>104</sup> synthesised both (2*R*)-[1,1-<sup>2</sup>H<sub>2</sub>]-glycerol (**95**) and (2*S*)-[1,1-<sup>2</sup>H<sub>2</sub>]-glycerol (**96**), and fed these chiral glycerols to resting cells of *Streptomyces cattleya*. Analysis of the fluorometabolites demonstrated that label was incorporated only *via* the metabolism of (2*R*)-[1,1-<sup>2</sup>H<sub>2</sub>]-glycerol (**95**), which delivered both deuterium atoms into the fluoromethyl group.



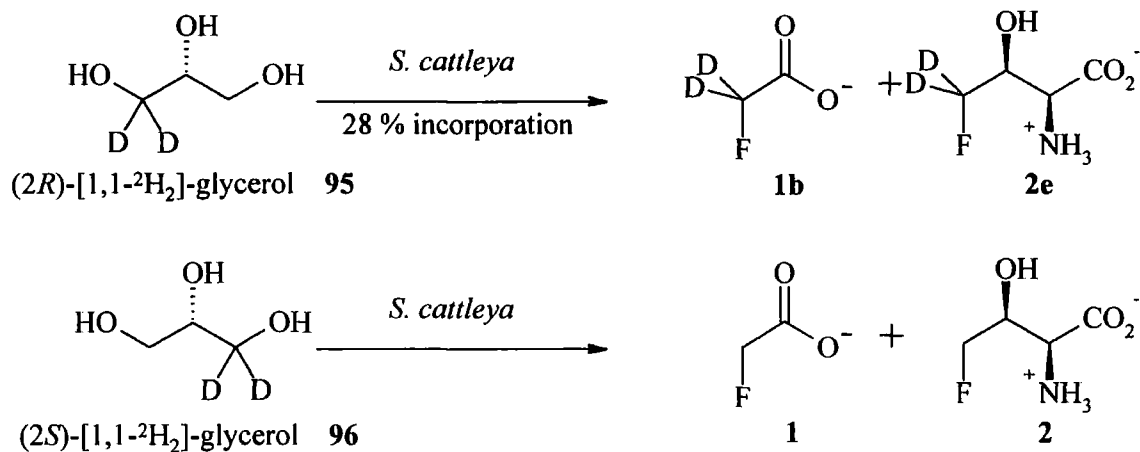


**Fig. 1.35:** The feeding of chiral glycerols (**95**) & (**96**) to *S. cattleya*, Nieschalk *et al.*

This key experiment highlighted the involvement of the glycolytic pathway in the biosynthesis of the fluorometabolites. The glycolytic pathway catabolises carbohydrates to yield pyruvate (**10**), which is then involved in further catabolism *via* the TCA cycle. Glycerol (**87**) can enter the glycolytic pathway as glycerol-3-phosphate (**97**) which is oxidised to form dihydroxyacetone phosphate (**98**), a key intermediate in the pathway. When glycerol (**87**) is used as a carbon source by a microorganism, the first step in its activation is phosphorylation by glycerol kinase. This phosphorylation is stereospecific operating on the *pro*-R hydroxymethyl group of glycerol (**87**).

In the event label was retained from the chiral glycerol (**95**) where the deuterium atoms were present on the *pro*-R arm. This indicated that the fluoromethyl group in the fluorometabolites is ultimately derived from C-1 of 1-phosphoglycerol (**97**), the carbon that is phosphorylated.

There is a low amount of single label (5 % compared with 28 % double label) which can be accounted for by wash out, possibly *via* enolisation on the glycolytic pathway. However retention of both deuteriums suggests that this carbon does not become oxidised between phosphorylation and fluorination and a plausible explanation could be that fluorination is effected by the displacement of a phosphate leaving group (section 1.5.2).

### 1.6.7 Overview

Previous studies have shown the assimilation of many different metabolites into fluoroacetate (1) and 4-fluorothreonine (2). The metabolic relationship between the primary metabolites that incorporate label into the fluorometabolites and the pattern in which they do so is consistent with the substrate for fluorination being delivered from the glycolytic pathway and is outlined below in Fig. 1.36.

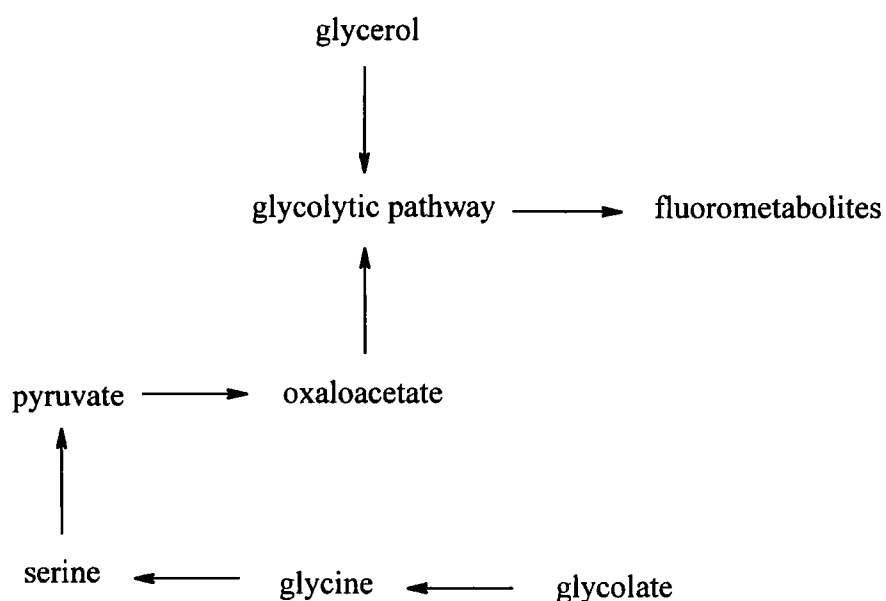


**Fig. 1.36:** The metabolic relationship between primary metabolites that contribute to fluorometabolite biosynthesis.

From the outset this project has focused on identifying the substrate for fluorination. Initially the role of the glycolytic pathway was investigated and this developed towards further biotransformation studies with putative initial products of fluorination.

*Chapter 2*

*Fluorometabolite biosynthesis and primary metabolism*

## 2.1 Maintenance and growth of *Streptomyces cattleya*

At the outset of this study it was necessary to reassess the production parameters of fluoroacetate (1) and 4-fluorothreonine (2) in *Streptomyces cattleya*. To this point, our collaborators at the Queen's University of Belfast had carried out the majority of the resting cell feeding experiments. It was important that resting cell experiments in Durham were conducted in an identical fashion in both laboratories so that results generated from the two groups could be directly compared.

Reid *et al.*<sup>98</sup> had conducted a detailed study of fluorometabolite production in batch cells. The onset of fluoroacetate (1) and 4-fluorothreonine (2) production was shown to be concurrent, starting just after day 4 of batch cell growth. Day 4 was also a maximum in terms of cell density in the culture and so fluorometabolite production could be considered to initiate with the onset of the idiophase.

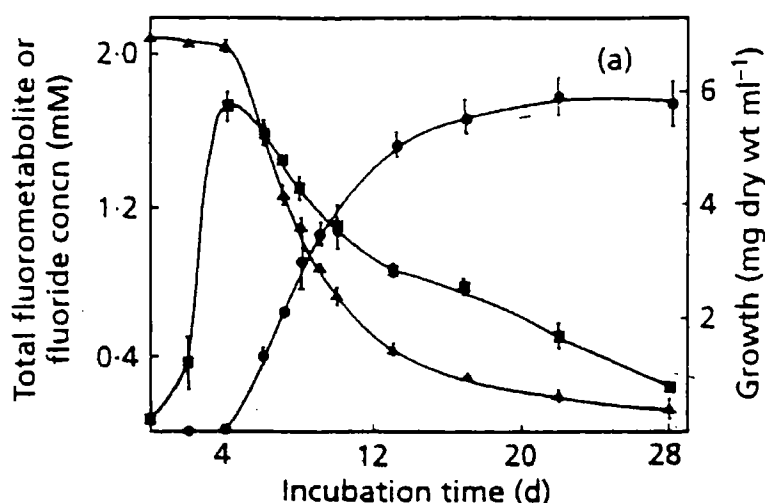


Fig. 2.1: Growth of *S. cattleya* and fluorometabolite production. ■ growth, ▲ fluoride, ● total fluorometabolites.

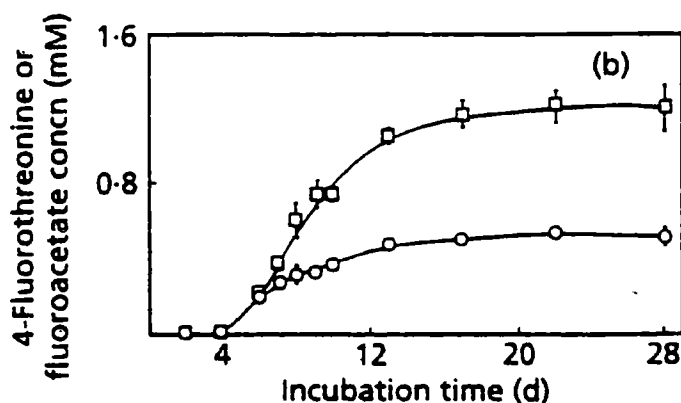


Fig. 2.2: □ Fluoroacetate (1) and ○ 4-fluorothreonine (2) production in *S. cattleya*.

However, these results were obtained over 4 years ago and in a different laboratory. It was therefore important to assess the onset of fluorometabolite production in the Durham laboratory.

### **2.1.1 Preparation of a starter culture of *Streptomyces cattleya***

*Streptomyces cattleya* NRRL 8057, obtained from the Belfast laboratory, was maintained on agar slopes on a complex media. The media contained soybean flour (2 % w/v), mannitol (2 % w/v), agar (1.5 % w/v) and tap water, and the culture was grown for 14 days at 28 °C. It was usual to observe growth within 2-3 days as small white colonies. By day 10 the thick vegetative mycelium that had formed began to colour, so that by day 14 the culture was pink / purple. These slants were then sealed and stored at 4 °C, and in general they remained viable for one year.

For biosynthetic studies on the fluorometabolites the bacterium was grown in a chemically defined (minimal) liquid media. The media was prepared as follows: Previously prepared solutions (ion solution 150 ml, carbon source solution 75 ml, phosphate buffer solution 75 ml, fluoride solution 3 ml) were added to 450 ml of water in a 1 l Erlenmeyer flask. For the exact composition of these solutions see **section 5.2.2**. After mixing, an aliquot (90 ml) was decanted into a sterilised 500 ml Erlenmeyer flask and was inoculated with a loop of mature mycelium from the agar slopes. This starter culture was then incubated for 4 days at 28 °C on an orbital shaker (175 rpm). It was necessary to subculture the bacterium once it had past the lag phase (4 days), when there was considerable cell mass, and the culture was starting to colour slightly (pink / purple).

### **2.1.2 Preparation of batch cultures of *Streptomyces cattleya***

The sterile defined media, prepared for the starter culture, was stored at 4 °C for 4 days. It was then transferred to 7 x 500 ml Erlenmeyer flasks (90 ml each), and inoculated from the starter culture (0.3 ml). The cultures were then incubated for 8 days at 28 °C. During this time the following observations were made. By day 4 the cell mass had coloured (pink-purple) and the cultures began to smell of the volatile, geosmin (79). By day 6-7 the cultures lost their pink-purple colour and become golden-brown.

### 2.1.3 Time course study on fluorometabolite biosynthesis

In order to monitor the ability of these batch cultures of *Streptomyces cattleya* to produce fluorometabolites a time course study was planned at the outset. In this experiment, batch cultures, prepared as described above had an aliquot removed every 12 hours for 14 days. For each aliquot the pH was measured and the fluoride concentration determined. The cells were removed from this aliquot (1 ml) by microcentrifugation (5000 rpm, 10 minutes) and the supernatant stored at -4 °C pending analysis.

#### 2.1.3.1 Results: pH analysis

The pH of all of the samples was recorded using a pH microelectrode. The mean average of 4 samples for each time point was determined and is plotted against time as shown below (Fig. 2.3).

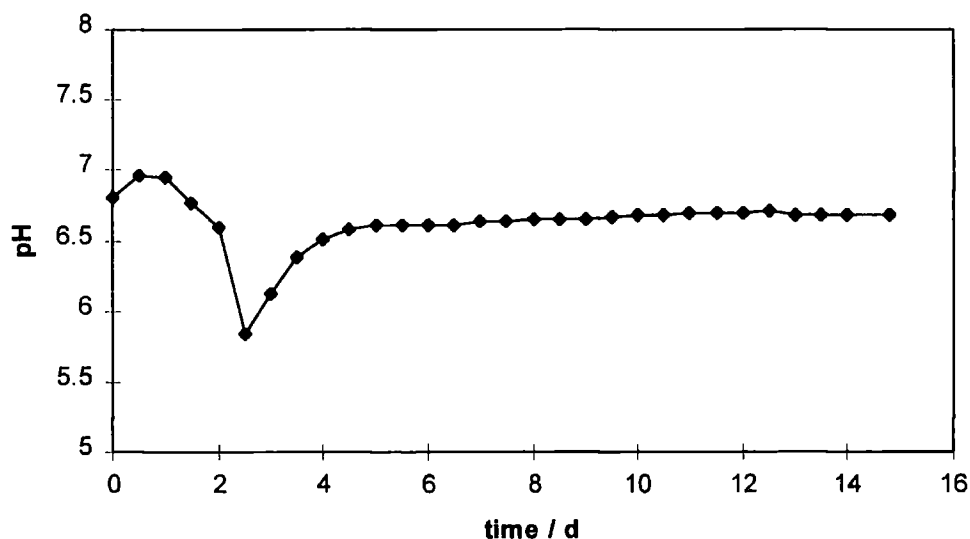


**Fig. 2.3:** The variation of pH with time in batch cells of *S. cattleya*.

The pH of the defined media is buffered to pH 7.0. Therefore the observed perturbations are effects greater than the buffering capacity of the phosphate buffer. On day 3 there is a clear drop in the pH value to 5.7 after which the pH rises again and remains relatively constant at pH = 6.5 for the remainder of the experiment.

### 2.1.3.2 Results: fluoride analysis

Fluoride concentrations were determined using a fluoride selective electrode. Each sample (0.5 ml) was mixed with 1.0 M  $\text{H}_2\text{SO}_4$  (0.5 ml) and 0.5 M  $\text{KNO}_3$  & 0.5 M trisodium citrate (4.0 ml). The potential difference of the sample was recorded and compared with a standard curve generated in the same way, with NaF solutions of 10.0 mM, 5.0 mM, 2.0 mM, 1.5 mM, 1.0 mM, 0.5 mM and 0.1 mM.

[NaF] / mM	10.0	5.0	2.0	1.5	1.0	0.5	0.1	0.0
PD / mV	-470	-453	-430	-420	-413	-392	-367	-309

Table 2.1: Calibration data for the fluoride selective electrode.

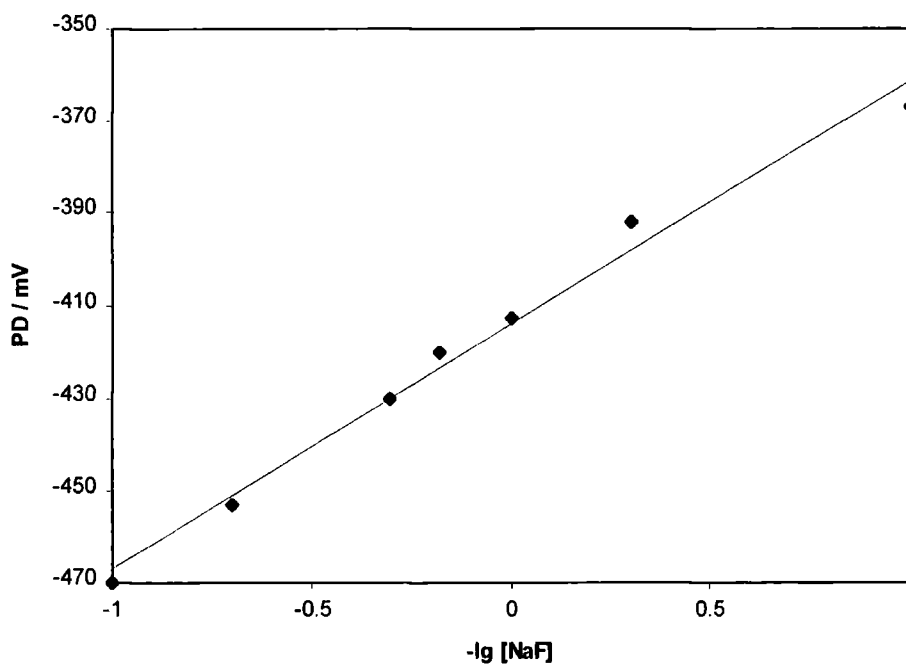
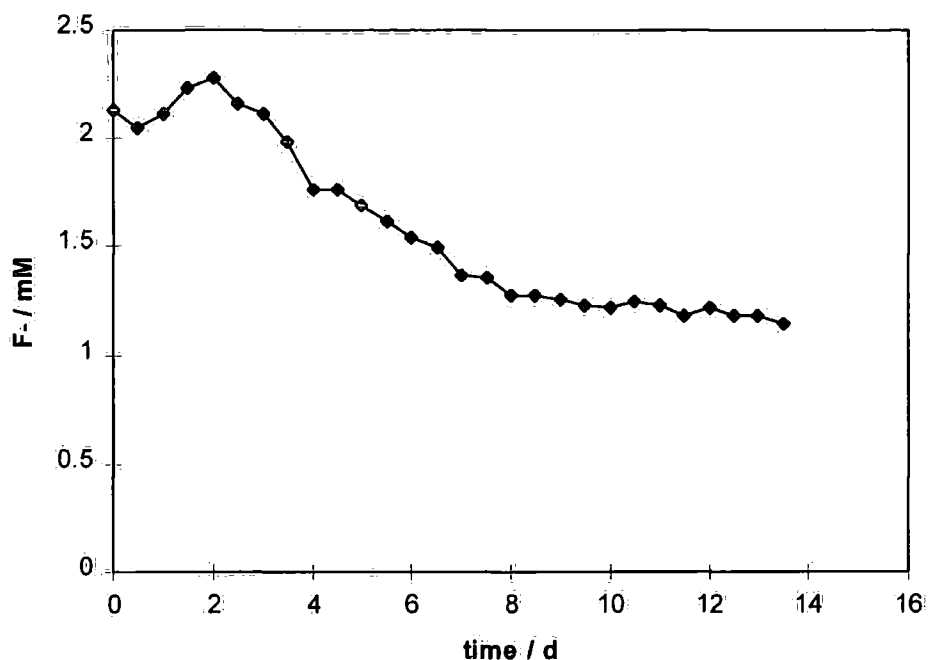


Fig. 2.4: Calibration curve for fluoride selective electrode.

The calibration curve was generated by plotting the  $-\lg [\text{F}^-]$  against the potential difference (PD). Using this calibration curve the fluoride concentration for any given sample could be measured. To that end the supernatant (0.5 ml) from each aliquot of batch cells was treated in a standard manner and the potential differences measured to deduce the fluoride concentration. Fig. 2.5 shows the mean average of 4 samples at each time point plotted against time of incubation



**Fig. 2.5:** Fluoride uptake by batch cells of *S. cattleya*.

Clearly, the fluoride concentration in the supernatant began to drop after day 3 and continued to do so until day 8. It then remained constant until the termination of the experiment.

### 2.1.3.3 Discussion

The drop in pH and the beginning of fluoride ion uptake into the cells are concurrent, on day 3. This also correlates visually with the maximum in cell growth, and therefore the end of the trophophase. Reid<sup>105</sup> showed that fluorometabolite biosynthesis begins when fluoride is taken up into the cells and therefore, the fluorometabolites are produced in a classical manner for microbial secondary metabolites. However it was noticed that not all of the fluoride (approximately 1 mM) was utilised by the bacterium in fluorometabolite biosynthesis, whereas Reid<sup>105</sup> found that essentially all of the free fluoride was utilised by the cells.



## 2.2 Studying fluorometabolite biosynthesis

### 2.2.1 Preparation of resting cells of *Streptomyces cattleya*

Resting cells have been used extensively in the study of fluorometabolite production in *Streptomyces cattleya*.<sup>101,102,103,105,106,107,108</sup> Sterilised MES buffer (50 mM) was used throughout this and the previous studies and the pH was adjusted to 6.5 using 1.0 M NaOH (aq.). The viability of the cells was assessed, prior to harvesting, by removing an aliquot from each flask. The cells were removed by centrifugation and the pH of the supernatant measured to assess if the pH was  $6.5 \pm 0.2$ . In cases of any doubt the fluoride uptake was also measured as discussed in **section 2.1.4**. Only 'healthy' cells were used in resting cell experiments. Cells were then prepared by harvesting mature cells of the bacterium (on day 8 of batch cell growth) by centrifugation. As the fluorometabolites are excreted extracellularly, the cells were washed three times in MES buffer, to remove any endogenous fluorometabolites and any other potential carbon sources excreted from the cells. Typically, batch cells were prepared by the method described in **section 2.1.2**, yielding between 10 and 12 g in wet weight. The bacterial pellet was then resuspended in buffer at a final concentration of  $0.176 \text{ g.ml}^{-1}$  wet wt.

Resting cell experiments were carried out by taking this cell suspension (5 ml) and adding putative precursors at a known concentration. If the precursor contained no organically bound fluorine then the cells were supplemented with NaF (final concentration 2 mM) and the total volume of the experiment taken to 23 ml with MES buffer. To maintain the aseptic conditions in the resting cell flask, putative precursors were added *via* filter sterilisation, through a presterilised 20  $\mu\text{m}$  nylon membrane.

Resting cell experiments were then incubated for 48 hours at 28 °C on an orbital shaker (180 rpm). The experiments were arrested by spinning down the cells by centrifugation (20,000 rpm, 20 minutes) and the supernatants were frozen pending analysis. Individual experiments were then analysed by  $^{19}\text{F}$   $\{^1\text{H}\}$  NMR (**section 2.2.2**) and / or GCMS (**section 2.2.3**).

### **2.2.1.1 Resting cell experiments: controls**

Resting cell experiments were conducted in duplicate (whenever possible) and the following controls were employed. Fluorometabolite production was assessed in the absence of any putative precursors, that is utilising only carbon sources present in the cells, by incubating cells (5 ml) with 40 mM NaF (1 ml, final concentration 2 mM) in MES buffer (17 ml). This was designed to demonstrate any anomalies from usual patterns of fluorometabolite production and allowed the natural isotopic abundance of the fluorometabolites to be calculated for referencing in GCMS analysis (see **section 2.2.3**).

The ability of a specific set of resting cell experiments to incorporate isotopically enriched precursors was evaluated by adding [2-<sup>13</sup>C]-glycine (**91**) to the medium as a control. Cells (5 ml) were incubated with 40 mM NaF (1 ml, final concentration 2 mM), and 200 mM [2-<sup>13</sup>C]-glycine (**91**) (1 ml, final concentration 10 mM) in MES buffer (16 ml). The labelling pattern resulting from this experiment is well established and the levels of isotope incorporation are used as a reference. The observations from feeding this precursor are described in greater depth in the subsequent sections.

### **2.2.2 Studying fluoroacetate and 4-fluorothreonine with <sup>19</sup>F NMR**

As discussed previously <sup>19</sup>F NMR has been used by both Soda *et al.*<sup>101</sup> and Reid *et al.*<sup>99</sup> to monitor and quantify fluorometabolite production. However, this technique is particularly powerful for determining incorporation of isotopes into both of the fluorometabolites. Using proton decoupled <sup>19</sup>F {<sup>1</sup>H} NMR regiochemical information on stable isotope incorporation (both <sup>2</sup>H and <sup>13</sup>C) into the fluorometabolites can be readily obtained. For example, in the case of 4-fluorothreonine (**2**), deuterium atoms can potentially label C-3 and C-4 once (in 2 combinations), twice (2 combinations) or three times (see Fig. 2.6).

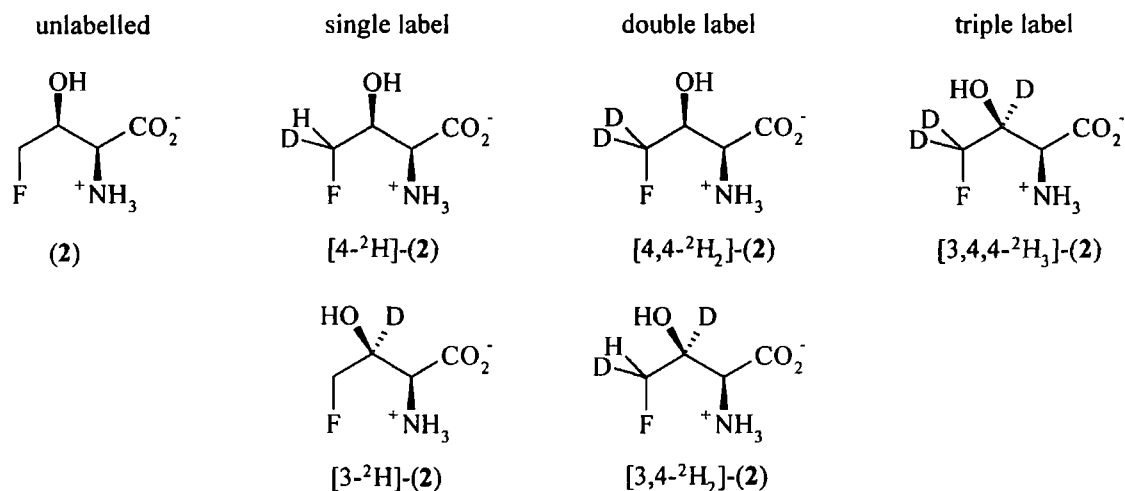


**Fig. 2.6:** Potential patterns of deuterium labelling in 4-FT (2).

The fluorine signal in the  $^{19}\text{F}\{^1\text{H}\}$  NMR spectrum in all of the labelled species illustrated in Fig. 2.6 is different, because the chemical shift is perturbed by the deuterium isotope, to a different extent in each case. This induced isotope shift is cumulative and decreases with the increased distance between the isotope and the fluorine atom. The effect is also observed with  $^{13}\text{C}$  isotope incorporation, although the magnitude of the upfield shift is not so great, because the ratio of the mass  $^{13}\text{C} / ^{12}\text{C}$  is much less than  $^2\text{H} / ^1\text{H}$ . The magnitude of the induced upfield shifts in  $^{19}\text{F}$  NMR are tabulated below (Table 2.2).

Stable Isotope	Shifts to the lower frequency / ppm		
	$\alpha$ -shift	$\beta$ -shift	$\gamma$ -shift
$^2\text{H}$		0.55	0.30
$^{13}\text{C}$	0.07	0.02	

**Table 2.2:** Upfield shifts observed in  $^{19}\text{F}\{^1\text{H}\}$  NMR due to  $^2\text{H}$  and  $^{13}\text{C}$  in both fluoroacetate (1) and 4-fluorothreonine (2).

Proton decoupling greatly enhances the signal to noise ratio as the signals collapse into singlets as coupling to protons is removed.

The following two examples from previous studies demonstrate the use of these upfield shifts in determining the regiochemical location of isotope incorporation. When resting

cells of *Streptomyces cattleya* were supplemented with [2,2,3,3- $^2\text{H}_4$ ]-succinate (**99**),<sup>103</sup> both fluoroacetate (**1**) and 4-fluorothreonine (**2**) were labelled with a single deuterium atom in the fluoromethyl group (**1e** & **2f**). Fig. 2.7 shows that both fluorometabolites have a large unlabelled peak and associated with each is the signal arising from the population of molecules carrying a deuterium atom.

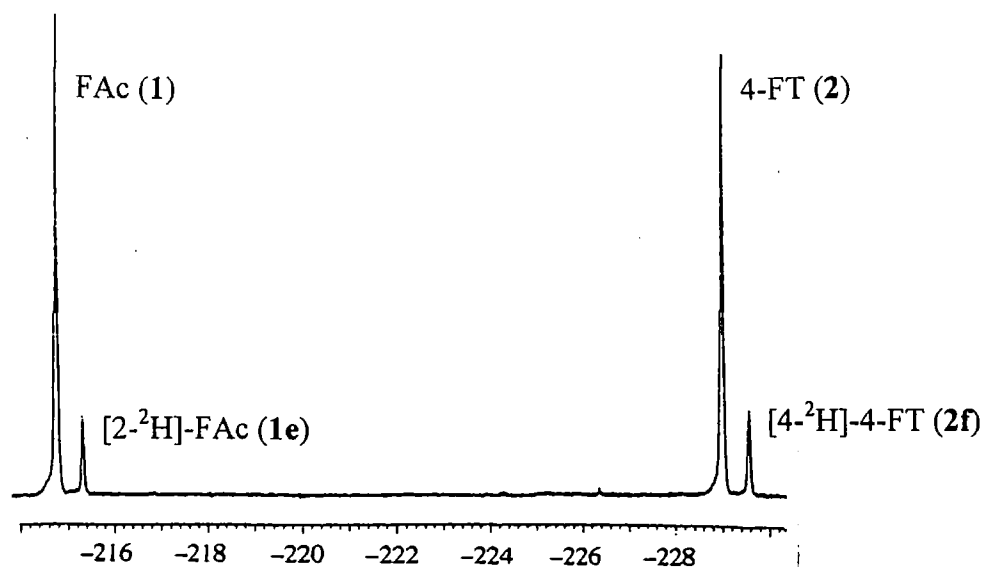


**Fig. 2.7:**  $^{19}\text{F}\{^1\text{H}\}$ NMR of FAc (**1** & **1e**) and 4-FT (**2** & **2f**) labelled via [2,2,3,3- $^2\text{H}_4$ ]-succinate (**99**) metabolism.

As  $^{13}\text{C}$  has  $I = \frac{1}{2}$  there is coupling between carbon-13 and the fluorine atom ( $I = \frac{1}{2}$ ), generating a doublet. [3- $^{13}\text{C}$ ]-Pyruvate (**100**) is metabolised to deliver isotope into the fluoromethyl groups of each fluorometabolite and accordingly Fig. 2.8 shows that the unlabelled signal for each fluorometabolite has an associated doublet (centred on an upfield shift of + 0.07 ppm and  $^1J_{\text{FC}} = 165$  Hz), arising from this coupling.

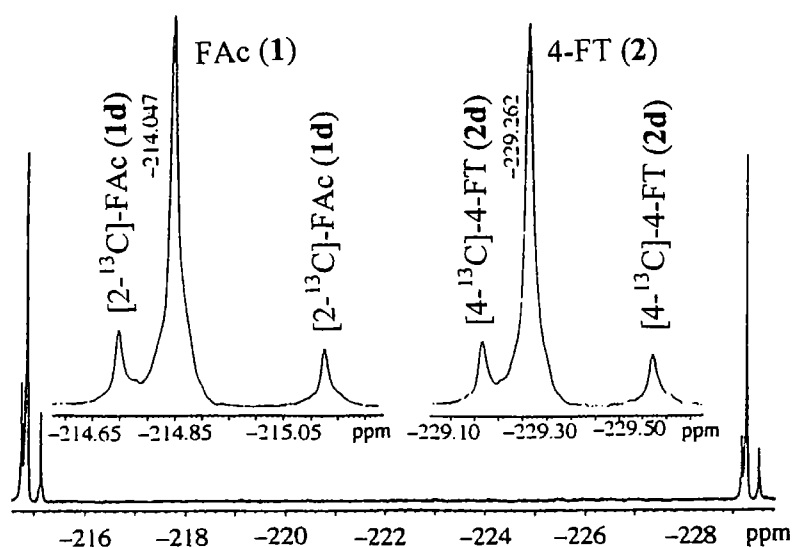
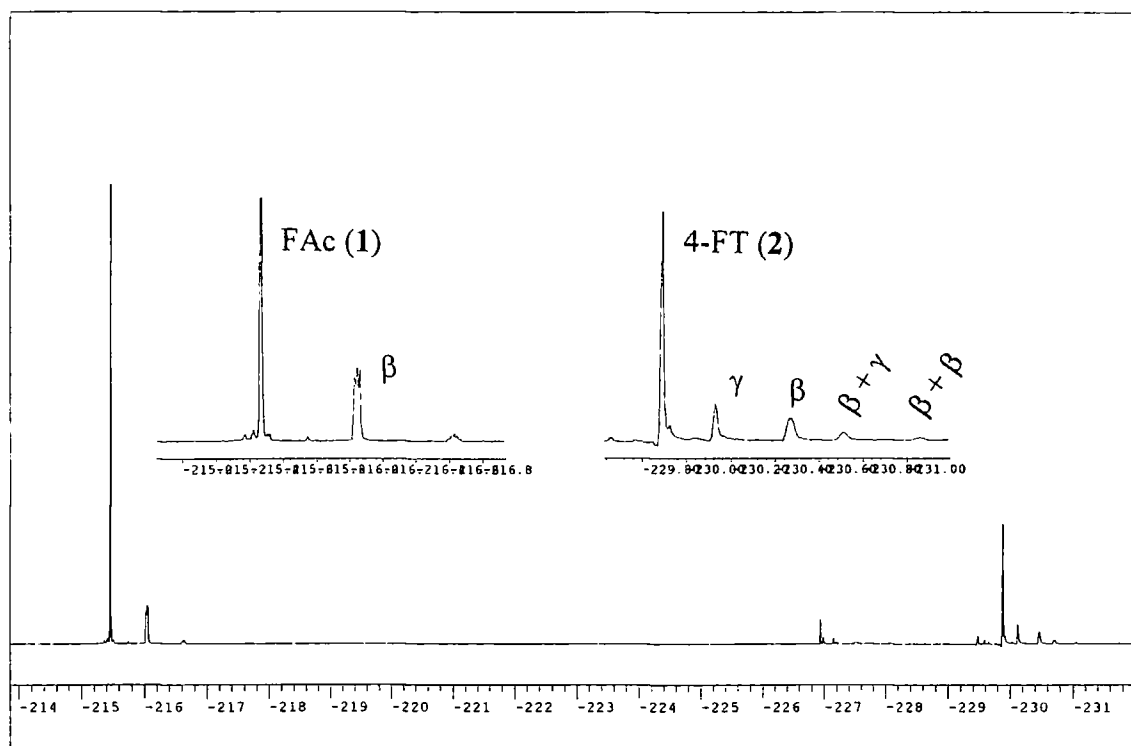


Fig. 2.8:  $^{19}\text{F}\{^1\text{H}\}$ NMR of FAc (1 & 1d) and 4-FT (2 & 2d) labelled via [3- $^{13}\text{C}$ ]-pyruvate (100) metabolism.

$^{19}\text{F}\{^1\text{H}\}$ NMR analysis cannot, however, yield any information on labelling in positions 1 & 2 of 4-fluorothreonine (2) as isotopes at these locations are too distant from the fluorine atom to perturb the chemical shift. For that information GC-MS analysis is used.

#### 2.2.2.1 Feeding $^2\text{H}_2\text{O}$

In order to demonstrate the effectiveness of the upfield shift originating from deuterium incorporation into the fluorometabolites an experiment was carried out in 20 %  $^2\text{H}_2\text{O}$ . Deuterium from the medium was expected to label the fluorometabolites in a rather indiscriminate manner. Accordingly, deuterium oxide (5 ml) was added to the cell suspension (5 ml) with 50 mM MES buffer (13 ml). After incubation for 48 hours, the resultant supernatant was analysed by  $^{19}\text{F}\{^1\text{H}\}$  NMR (Fig. 2.9).



**Fig. 2.9:**  $^{19}\text{F}$   $\{^1\text{H}\}$  NMR analysis of resting cells of *Streptomyces cattleya* incubated in the presence of  $^2\text{H}_2\text{O}$ .

The fluoroacetate (1) resonance ( $\delta_{\text{F}} = -215.47$  ppm) in the resultant  $^{19}\text{F}$   $\{^1\text{H}\}$  NMR spectrum has two associated upfield peaks ( $\delta_{\text{F}} = -216.05$  ppm and  $\delta_{\text{F}} = -216.63$  ppm), which corresponds to populations of to FDHC- and  $\text{FD}_2\text{C}$ - fluoroacetate (1). The deuterium nuclei also couples with the fluorine nuclei, although the resolution of the spectrum is not sufficient to obtain accurate information on those coupling constants. The 4-fluorothreonine (2) resonance ( $\delta_{\text{F}} = -229.89$  ppm) also has related upfield peaks, due to unlabelled populations of 4-fluorothreonine (2). These display quite elegantly the additive nature of the upfield shift. The first peak ( $\delta_{\text{F}} = -230.13$  ppm) results from a  $\gamma$ -shift (+ 0.24 ppm) due to a  $^2\text{H}$  at C-3 and the second peak ( $\delta_{\text{F}} = -230.47$  ppm) is also due to a single isotope incorporation, in this case a  $\beta$ -shift (+0.58 ppm), from a deuterium atom on the fluoromethyl group. Following this are two additional resolved peaks corresponding to double label incorporations. Label in both the C-3 and C-4 results in a  $\beta + \gamma$ -shift combination ( $\delta_{\text{F}} = -230.71$  ppm, +0.82 ppm). The peak to the highest field is due to a  $2\beta$ -shift ( $\delta_{\text{F}} = -231.05$  ppm, +1.16 ppm).

There are also other resonances in the fluoromethyl region shown in Fig. 2.9. These relate to as yet unidentified fluorinated metabolites of *Streptomyces cattleya*, the production of these metabolites is relatively rare but they do appear from time to time in low concentration and clearly could have some significance as biosynthetic intermediates or are metabolites of fluoroacetate (1) and 4-fluorothreonine (2).

#### 2.2.2.2 Incorporation of [2-<sup>13</sup>C]-glycine (91) into the fluorometabolites: <sup>19</sup>F NMR analysis

As stated previously (section 2.2.1.1) [2-<sup>13</sup>C]-glycine (91) is used as a control in feeding experiments on resting cells of *Streptomyces cattleya*. The label at C-2 of this amino acid has been shown to recombine (section 1.6.5) via serine hydroxymethyl transferase to contribute both C-1 and C-2 of fluoroacetate (1). Likewise [2-<sup>13</sup>C]-glycine (91) enriches C-3 and C-4 of 4-fluorothreonine (2) with carbon-13. This incorporation is readily observed by <sup>19</sup>F{<sup>1</sup>H}NMR (Fig. 2.10), where each fluorometabolite signal has an associated doublet of doublets (centred on an upfield shift of + 0.09 ppm <sup>1</sup>J<sub>FC</sub> = 165 Hz and <sup>2</sup>J<sub>FC</sub> = 18 Hz) due to coupling of fluorine with both isotopes.

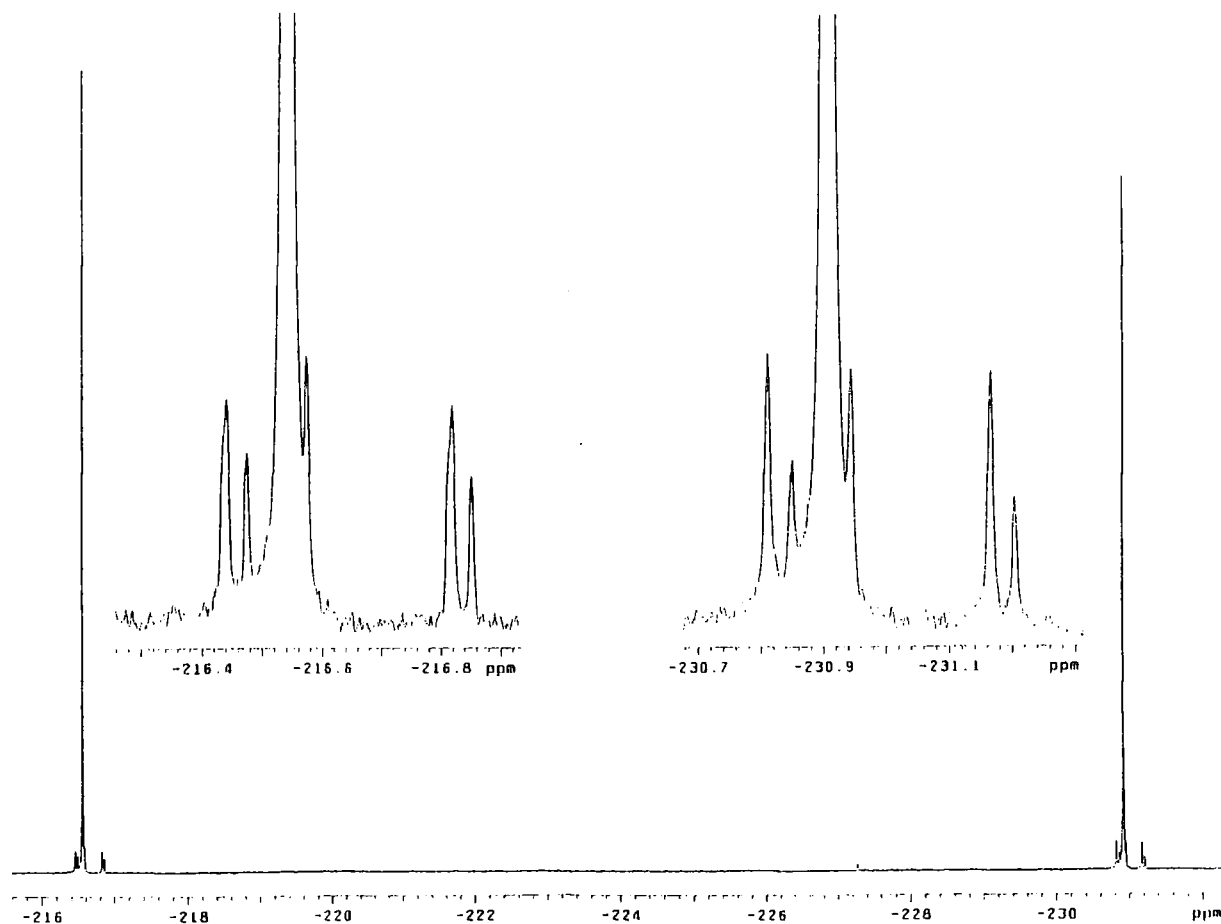


Fig. 2.10: <sup>19</sup>F {<sup>1</sup>H} NMR analysis of resting cells of *Streptomyces cattleya* incubated with [2-<sup>13</sup>C]-glycine (91).

### 2.2.3 GCMS analysis of fluoroacetate (1) and 4-fluorothreonine (2)

Gas chromatography - mass spectroscopy (GC-MS) is a powerful tool in biosynthetic studies. In this study it provides a limited amount of positional information, but more importantly accurate data on the levels of isotope incorporation, with a lower detection level than  $^{19}\text{F}$   $\{^1\text{H}\}$  NMR. GC-MS is also used for accurate quantification of fluoroacetate (1) levels in different experiments. This analysis was carried out by our collaborators at The Queen's University, Belfast and all of the GCMS data presented in this thesis was obtained from the Belfast laboratory.

#### 2.2.3.1 GCMS analysis of fluoroacetate (1)<sup>106</sup>

A method was developed whereby fluoroacetate (1) was analysed as its phenylphenacyl derivative (102), prepared *in situ* from the supernatant resulting from a resting cell experiment. The culture supernatant was lyophilised and the derivative was prepared by dissolving it in toluene / acetonitrile (1:1), with 2-bromo-4'-phenacetophenone (101), 18-crown-6, and heating the resultant solution at 75 °C for 12 hours.

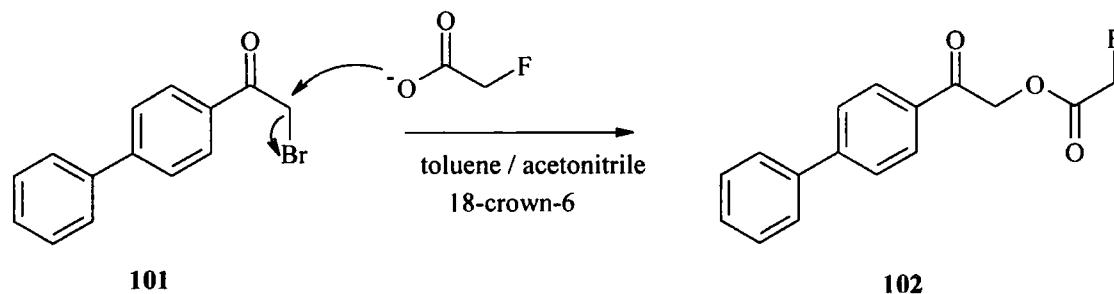


**Fig. 2.11:** Derivatisation of fluoroacetate (1) with 2-bromo-4'-phenacetophenone (101).

Prior to derivatisation the culture supernatant was mixed with a known quantity of sodium propionate, for accurate quantification by GCMS. The phenylphenacyl derivatives of fluoroacetate (102) and propionate (103) were then analysed by GCMS in selected ion monitoring (SIM) mode.

To detect levels of incorporation of stable isotope the ion current at  $m/z = 272$  (molecular ion) and the masses immediately above that ( $m/z = 273$ ,  $m/z = 274$ ) are observed. After correcting for natural isotope abundances the incorporation of label into both C-1 and C-2 of fluoroacetate is evaluated. Details on incorporation into C-2 of



fluoroacetate (**1**) were determined by monitoring the ion current  $m/z = 33$  and those immediately above that. This ion arises due to cleavage of the fluoromethyl group. The incorporation into C-1 is then deduced by subtracting the level of single label incorporation in both positions from that at C-2 only.

Quantification of fluoroacetate (**1**) levels was measured by monitoring the ion current  $m/z = 181$  of both the fluoroacetate (**102**) and the propionate (**103**) derivatives, relative to a standard response curve. This fragment arises due to cleavage of the phenylphenacyl derivative to yield  $C_6H_5C_6H_4CO^+$ . Fluoroacetate (**1**) can be detected at concentrations down to 0.01 mM using this method.

### 2.2.3.2 GCMS analysis of 4-fluorothreonine (**2**)<sup>106</sup>

GCMS can be used to detect isotope incorporation into 4-fluorothreonine (**2**). However attempts to quantify absolute levels of 4-fluorothreonine (**2**) by this method have proven unreliable.<sup>106</sup> 4-Fluorothreonine (**2**) was conveniently analysed as its per-trimethylsilylated derivative (**104**) prepared directly from a resting cell experiment. The culture supernatant was lyophilised and the derivative prepared by heating with *N*-methyl-*N*-(trimethylsilyl)-trifluoroacetamide (MSTFA) at 100 °C for 1 hour. The derivative (**104**) was then analysed by GCMS in selected ion monitoring (SIM) mode.

No mass ion is observed under the ionisation conditions for the per-trimethylsilylated derivative of 4-fluorothreonine (**104**) as it fragments  $\alpha$  to the amino group on either side. However this gives rise to two signature ions ( $m/z = 218$  and  $m/z = 272$ , see Fig. 2.12).

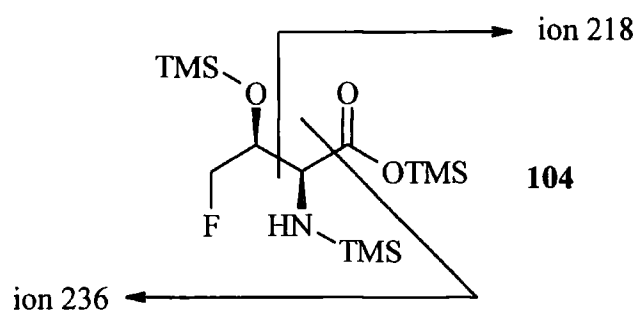


**Fig. 2.12:** Cleavage of per-trimethylsilylated derivative of 4-fluorothreonine (**104**).

Fragmentation allows the incorporation of isotope into these two fragments to be evaluated separately. Ion currents  $m/z = 218, 219$  and  $220$  show none, single and double label, respectively, into positions C-1 and C-2 of 4-fluorothreonine (2). Whereas, ion currents  $m/z = 236, 237, 238$  and  $239$  show none, single, double and triple label, respectively, into positions C-2, C-3 and C-4 of 4-fluorothreonine (2). In both cases the natural isotope abundances require to be corrected for.

## 2.3 Resting cell incorporation studies

### 2.3.1 [6,6-<sup>2</sup>H<sub>2</sub>]-Glucose (105)

#### 2.3.1.1 Background

Previous experiments have highlighted the involvement of the glycolytic pathway in fluorometabolite biosynthesis. Murphy<sup>107</sup> had shown that glycerol (87) is an efficient precursor to the fluorometabolites after feeding [2-<sup>13</sup>C]-glycerol (89) to resting cells of *S. cattleya*. This confirmed the findings of Soda *et al.*,<sup>101</sup> with both groups reporting a level of incorporation of ~ 40 %. Furthermore, Nieschalk *et al.*<sup>104</sup> have shown that when (2*R*)-[1-<sup>2</sup>H<sub>2</sub>]- and (2*S*)-[1-<sup>2</sup>H<sub>2</sub>]-glycerol (95) & (96) were fed only label from the *pro*-R hydroxymethyl group of glycerol (87) became incorporated into the fluorometabolites. These findings are consistent with the assimilation of glycerol (87) into the fluorometabolites *via* the glycolytic pathway (section 1.6.6). Hamilton *et al.*<sup>103</sup> showed a high level of incorporation from <sup>13</sup>C labelled pyruvates. Fig. 2.13 illustrates the glycolytic pathway, and demonstrates the metabolic relationship between glycerol (87) and pyruvate (10). The labelling in Fig. 2.13 does not refer to specific feeding experiments, but serves to highlight the equivalence of positions 1 and 2 of glycerol (87) with positions 2 and 3 of pyruvate (10). It is these positions that have been shown to account for C-1 and C-2 of fluoroacetate (1) and C-3 and C-4 of 4-fluorothreonine (2).

The glycolytic pathway converts glucose (9) to pyruvate (10), *via* the fission of fructose-1,6-bisphosphate (108) to deliver the triose phosphates, dihydroxyacetone phosphate (DHAP) (98) and glyceraldehyde-3-phosphate (G-3-P) (11). These trioses are interconvertible and G-3-P (11) is further metabolised to pyruvate (10), where it may enter the TCA cycle. Notably the conversion of phosphoenolpyruvate (12) to pyruvate (10), mediated by pyruvate kinase, is irreversible. For pyruvate (10) to enter the glycolytic pathway it is converted to oxaloacetate (42) and then phosphoenolpyruvate (12) by intercepting gluconeogenesis.

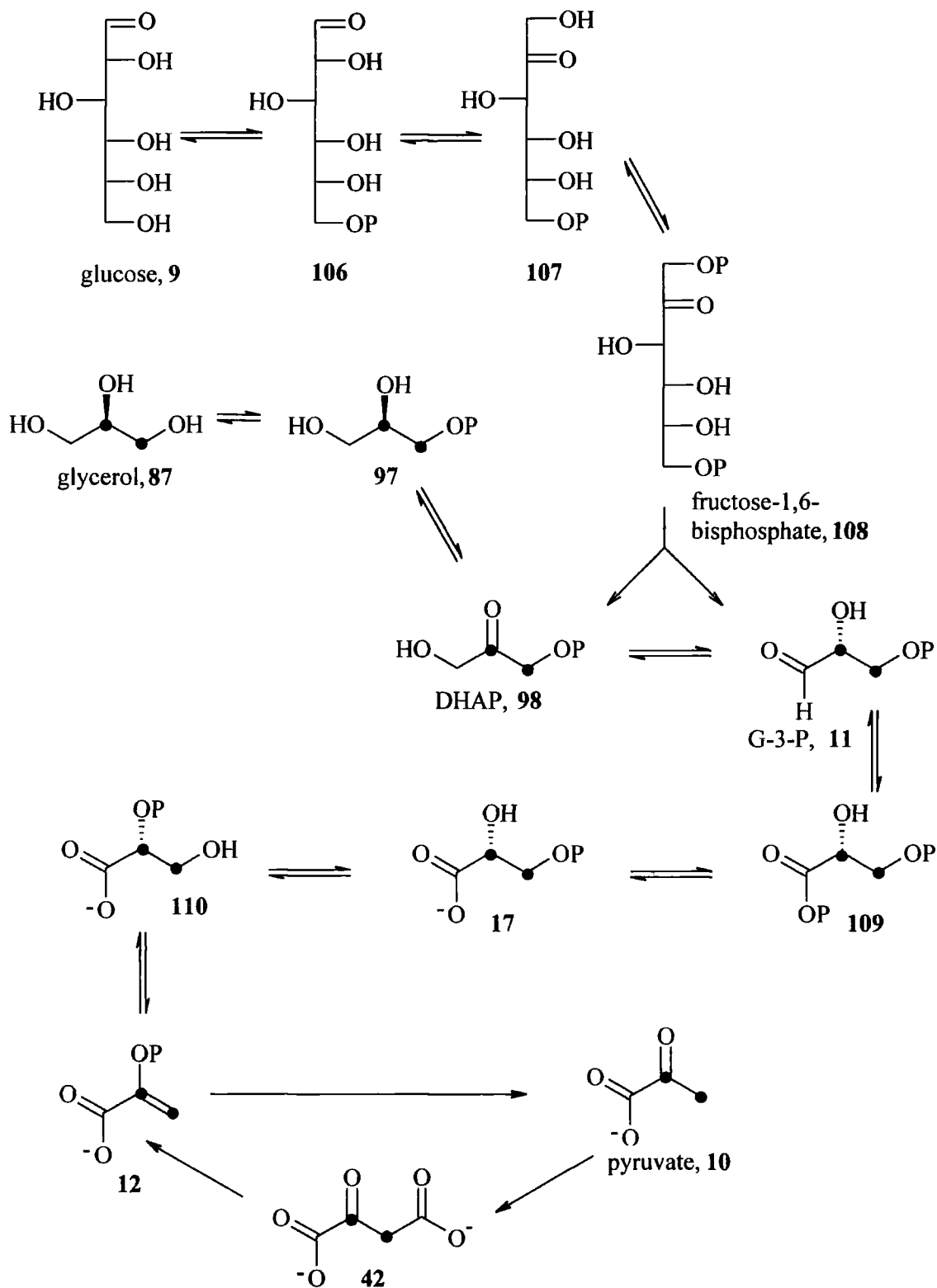


**Fig. 2.13:** The glycolytic pathway, P = phosphate.

As incorporation into the fluorometabolites had been demonstrated from glycerol (87) and pyruvate (10) it appeared appropriate to study the incorporation of labelled glucose, to provide further information on fluorometabolite biosynthesis *via* the glycolytic pathway.

### 2.3.1.2 Results and discussion

[6,6-<sup>2</sup>H<sub>2</sub>]-Glucose (105) was fed at a final concentration of 5 mM to resting cells of *Streptomyces cattleya*, with the medium supplemented with 2 mM fluoride. Glucose (9) is a good carbon source for microorganisms and if fed at a sufficiently high level then secondary metabolism may be suppressed as primary metabolism is reactivated, thus the relatively low concentration of 5 mM was judged to be an appropriate concentration. [2-<sup>13</sup>C]-Glycine (91) was also fed as a control.

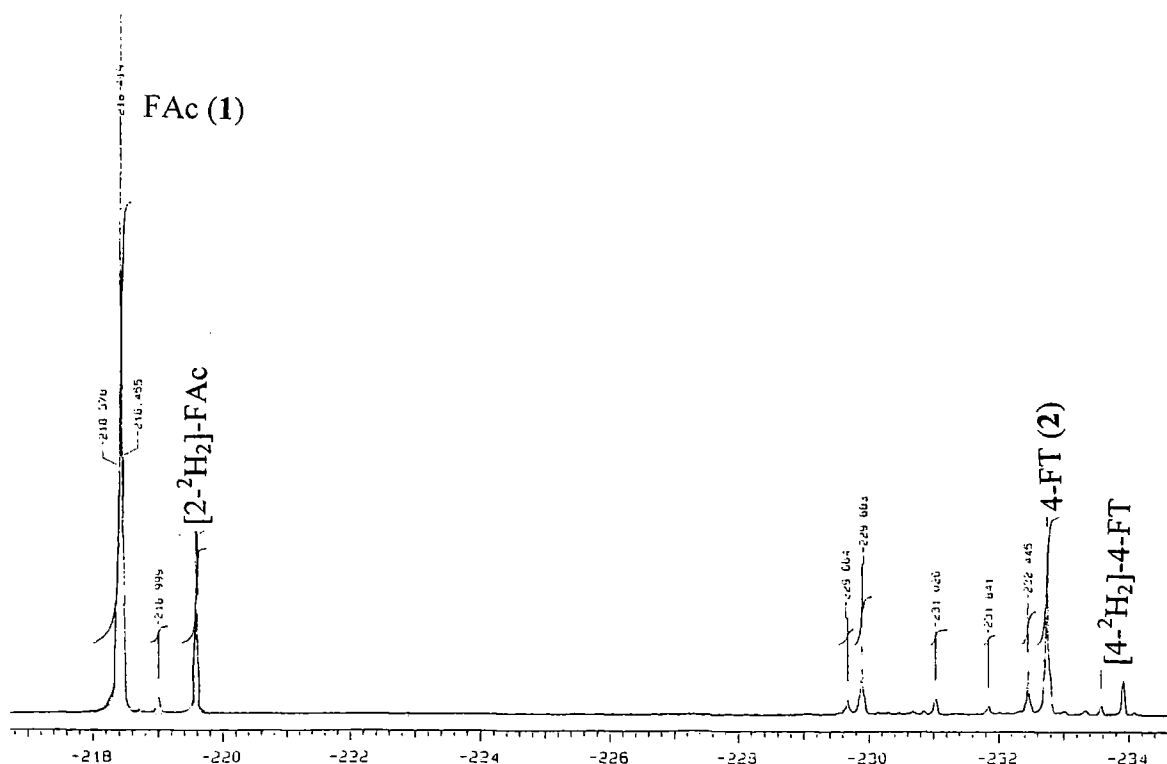


**Fig. 2.14:** <sup>19</sup>F {<sup>1</sup>H} NMR of fluoroacetate (1) and 4-fluorothreonine (2), following incubation of resting cells of *S. cattleya* with 5 mM [6,6-<sup>2</sup>H<sub>2</sub>]-glucose (105).

precursor	Incorporation into positions 2, 3 and 4 of 4-fluorothreonine (2) (%)			
	none	single	double	triple
10 mM [2- <sup>13</sup> C]-glycine (91)	53.6	14.7	25.5	6.3
5 mM [6,6- <sup>2</sup> H <sub>2</sub> ]-glucose (105)	74.6	2.9	22.6	0.0

**Table 2.3:** GCMS analysis of 4-fluorothreonine (2), following incubation of resting cells of *S. cattleya* with 5 mM [6,6-<sup>2</sup>H<sub>2</sub>]-glucose (105).

Precursor	Incorporation into fluoroacetate (1) (%)			
	None	Single (C-1)	Single (C-2)	Double
10 mM [2- <sup>13</sup> C]-glycine (91)	55.6	6.3	4.7	33.4
5 mM [6,6- <sup>2</sup> H <sub>2</sub> ]-glucose (105)	74.0	< 0.5	3.0	23.0

**Table 2.4:** GCMS analysis of fluoroacetate (1), following incubation of resting cells of *S. cattleya* with 5 mM [6,6-<sup>2</sup>H<sub>2</sub>]-glucose (105).

Both <sup>19</sup>F NMR and GCMS analyses indicated that [6,6-<sup>2</sup>H<sub>2</sub>]-glucose (105) has labelled the fluoromethyl position of both fluorometabolites, with a substantial population of the molecules retaining both deuterium atoms.

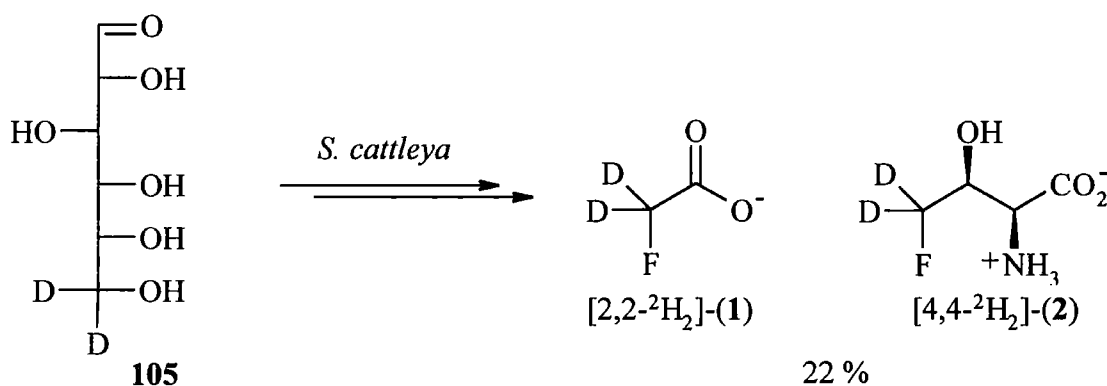


**Fig. 2.15:** Labelling pattern in the fluorometabolites from [6,6-<sup>2</sup>H<sub>2</sub>]-glucose (105).

This result highlights two important issues. Firstly it confirms the role of the glycolytic pathway in fluorometabolite biosynthesis, as the three most efficient precursors are now demonstrated to be glycerol (87), glucose (9) and pyruvate (10). Secondly, both deuterium atoms are retained, in a similar result to the (2R)-[1-<sup>2</sup>H<sub>2</sub>]-glycerol (95) experiment.<sup>104</sup> This confirms that the process of fluorination does not alter the oxidation state of the carbon atom that becomes the fluoromethyl group, from the glycolytic intermediates to the fluorometabolites.

These observations together support the proposed minimal mechanism (section 1.6.6) for fluorination that envisages displacement of a phosphate group by nucleophilic attack

by fluoride. Many of the glycolytic intermediates are phosphorylated in the position that would map through to the fluorination site, these include 3-phosphoglycerol (97), DHAP (98), G-3-P (11) and 3-phosphoglycerate (17), and all emerge as candidate substrates for the fluorination.

Concurrent with this experiment was a study by Murphy<sup>107</sup> who fed [1-<sup>13</sup>C]-, [2-<sup>13</sup>C]- and [6-<sup>13</sup>C]-glucose, (112), (113) & (114) all at 5 mM. These results support those generated above and highlight some further issues. Of particular interest was the difference in levels of incorporation from the three isotopomers. To briefly review Murphy's results, [6-<sup>13</sup>C]-glucose (114) labelled the fluoromethyl position by 30 %, whereas [1-<sup>13</sup>C]-glucose (112) labelled the same position by only 15 %. The glycolytic pathway renders these positions equivalent through the fission of fructose-1,6-bisphosphate (108) to the triose phosphates. Murphy<sup>107</sup> rationalised this observation by partitioning of glucose metabolism through glycolysis, and also the pentose phosphate pathway.

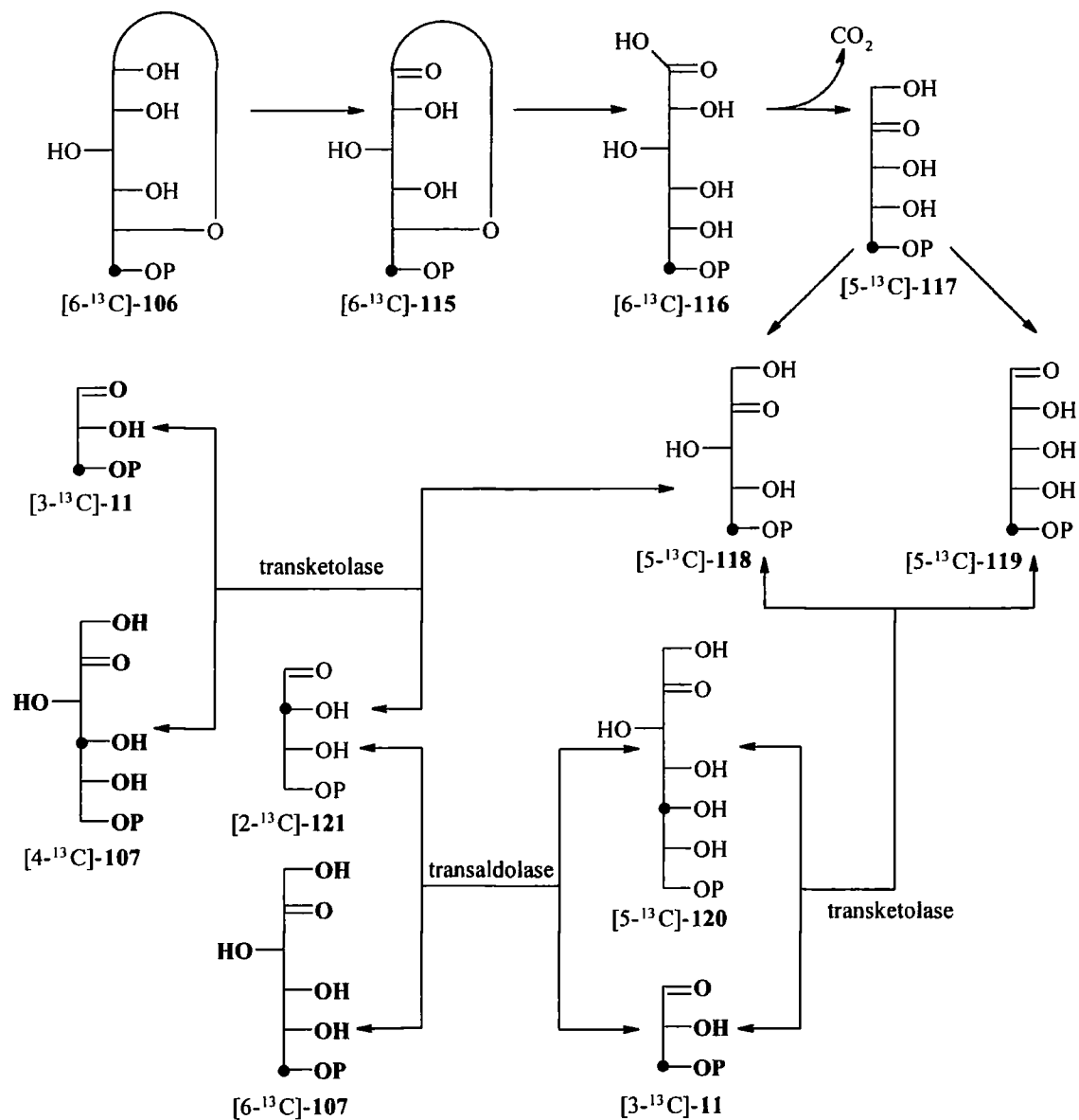


**Fig. 2.16:** The pentose phosphate pathway, P = phosphate. Compounds in bold are glycolytic pathway intermediates and the label refers to that derived from **[6-<sup>13</sup>C]-glucose (114)**.

Glucose (**9**) enters the pentose phosphate pathway as glucose-6-phosphate (**106**) and is converted to ribulose-6-phosphate (**117**), with the concomitant loss of CO<sub>2</sub>. This CO<sub>2</sub> originates from C-1 of glucose (**9**), which explains the relatively low level of incorporation from **[1-<sup>13</sup>C]-glucose (112)**. Isotope from C-6 of **[6-<sup>13</sup>C]-glucose (114)** however, is wholly converted to **[3-<sup>13</sup>C]-G-3-P (11)** by the pentose phosphate pathway, both directly and *via* fructose-6-phosphate (**107**), where it may re-enter the glycolytic pathway. The labelling pattern resulting from the **[2-<sup>13</sup>C]-glucose (113)** experiment (C-1 of fluoroacetate (**1a**), 16 %; C-2 of fluoroacetate (**1d**), 8 %; likewise in 4-



fluorothreonine (**2c** & **2d**)) is more complex, though can be rationalised also by the same arguments of glycolytic / pentose phosphate pathway partitioning.<sup>107</sup>

### 2.3.2 Isotopically labelled acetates

#### 2.3.2.1 Background

Acetate (**6**) is central to primary metabolism. It becomes involved in the TCA cycle by condensation with oxaloacetate (**42**) to generate citrate (**43**). It appeared appropriate to feed isotopically labelled acetates to map their label through to the fluorometabolites. [1-<sup>13</sup>C]-, [1,2-<sup>13</sup>C]- & [2,2,2-<sup>2</sup>H<sub>3</sub>]-Acetate (**20**), (**21**) & (**122**) were each fed at a final concentration of 10 mM to resting cells of *Streptomyces cattleya* which were also supplemented with 2 mM fluoride. Again [2-<sup>13</sup>C]-glycine (**91**) was fed at 10 mM in a control experiment.

#### 2.3.2.2 Results and discussion

The resting cell experiments were analysed by <sup>19</sup>F {<sup>1</sup>H} NMR (see Fig. 2.17, Fig. 2.18 and Fig. 2.19) and GCMS was used to analyse of the resultant fluoroacetate (Table 2.5).

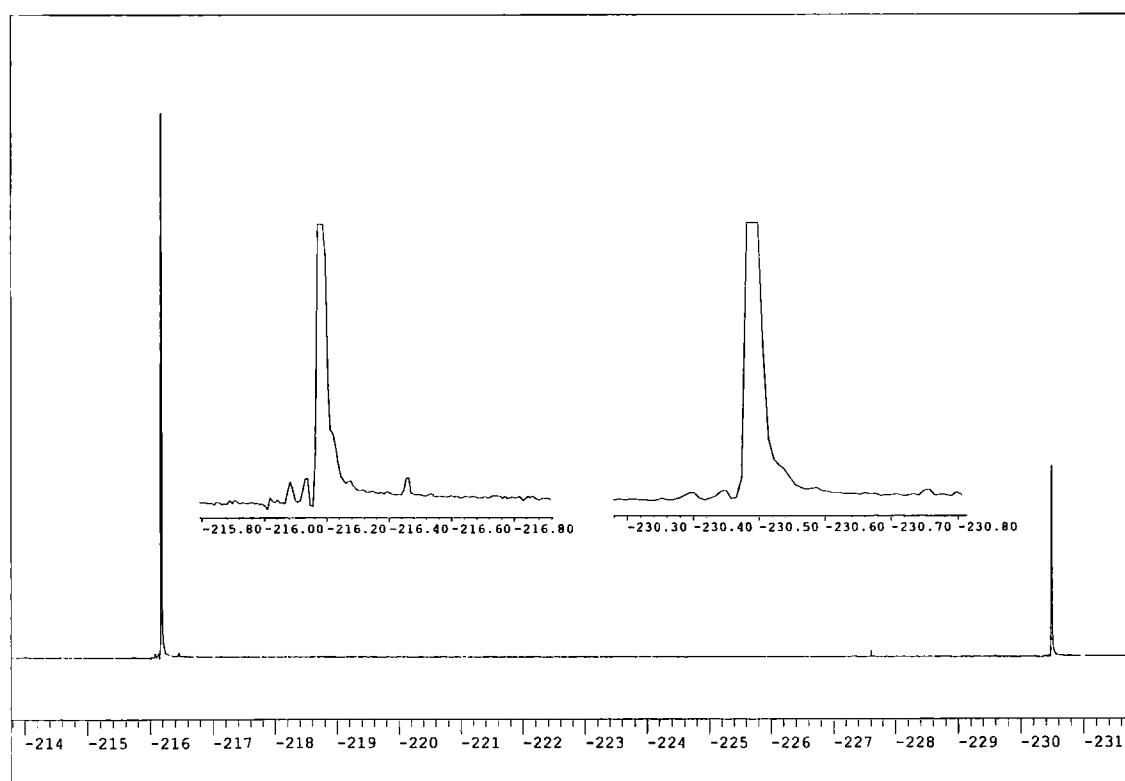


**Fig. 2.17:** <sup>19</sup>F {<sup>1</sup>H} NMR analysis of resting cells of *S. cattleya* fed with [1-<sup>13</sup>C]-acetate (**20**).

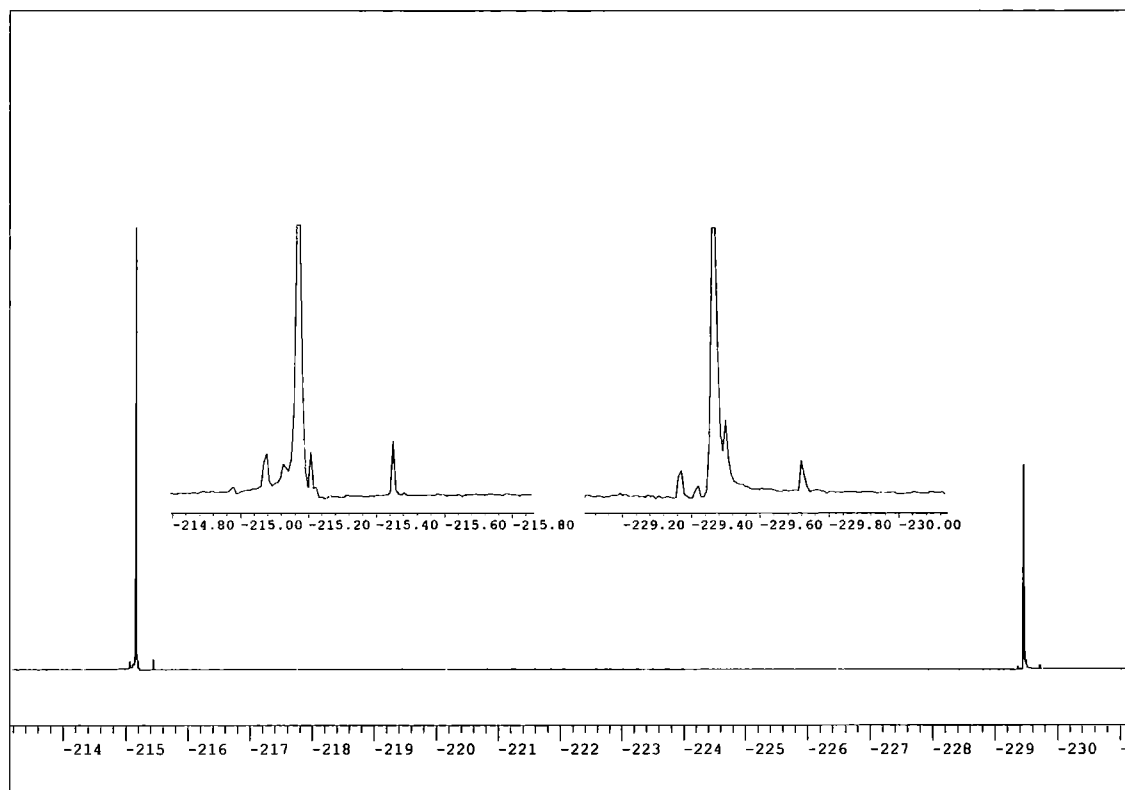


**Fig. 2.18:**  $^{19}\text{F}$   $\{^1\text{H}\}$  NMR analysis of resting cells of *S. cattleya* fed with  $[1,2\text{-}^{13}\text{C}_2]$ -acetate (**21**).

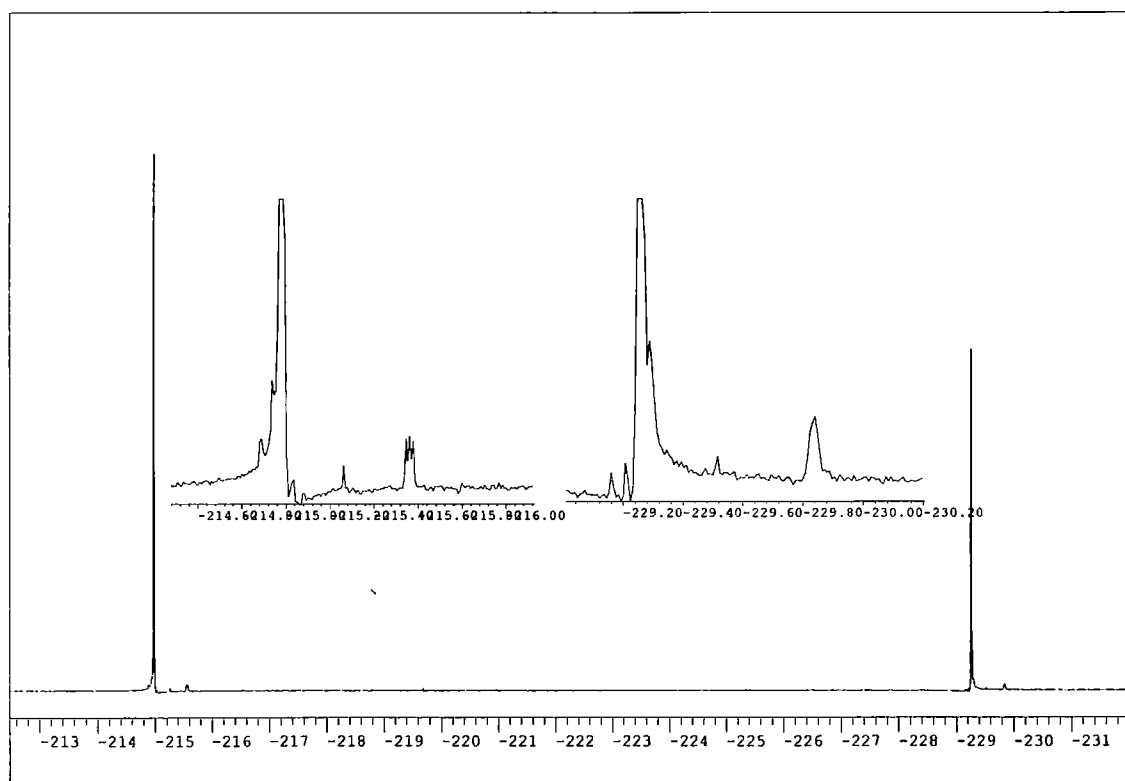


**Fig. 2.19:**  $^{19}\text{F}$   $\{^1\text{H}\}$  NMR analysis of resting cells of *S. cattleya* fed with  $[2,2,2\text{-}^2\text{H}_3]$ -acetate (**122**).

Precursor	Incorporation into fluoroacetate (1) (%)			
	None	Single (C1)	Single (C2)	Double
10 mM [2- <sup>13</sup> C]-glycine (91)	64.7	8.0	2.4	24.9
10 mM [1- <sup>13</sup> C]-acetate (20)	94.0	3.4	2.6	0.1
10 mM [1,2- <sup>13</sup> C <sub>2</sub> ]-acetate (21)	73.4	8.1	3.5	15.0
10 mM [2- <sup>2</sup> H <sub>3</sub> ]-acetate (122)	97.4	< 0.1	2.6	0.1

**Table 2.5:** GCMS analysis of fluoroacetate (1), following incubation of resting cells of *S. cattleya* with isotopically enriched acetates.

It is clear from this series of experiments that acetate (6) is not incorporated into the fluorometabolites as an intact unit. There is a high level of double label resulting from [1,2-<sup>13</sup>C<sub>2</sub>]-acetate (21), but notably [1-<sup>13</sup>C]-acetate (20) does not label the fluorometabolites significantly. Therefore the incorporation from [1,2-<sup>13</sup>C<sub>2</sub>]-acetate (21) originates wholly from C-2 of acetate (6). It is interesting to note that deuterium is only incorporated poorly from C-2 of acetate (6). There was less than a 3 % incorporation of single deuterium into the fluoromethyl groups. This pattern of labelling from acetate (6) can be rationalised by considering acetate (6) metabolism around the TCA cycle and into the glycolytic pathway.

Acetate (6) enters the TCA cycle, as acetyl-S-CoA (13), by condensation with oxaloacetate (42) to form citrate (43). Oxaloacetate (42) is also the intermediate at which gluconeogenesis branches from the TCA cycle to enter the glycolytic pathway. Fig. 2.20 shows the TCA cycle and traces the fate of C-2 of acetate (6) through one revolution of the cycle. Positions C-2 and C-3 of oxaloacetate (42) label positions C-1 and C-2 of fluoroacetate (1) respectively (and likewise in 4-fluorothreonine (2)). Therefore the single label from [1,2-<sup>13</sup>C<sub>2</sub>]-acetate (21) can be explained in terms of biosynthesis of labelled oxaloacetate (42) which enters the glycolytic pathway and eventually contributes to fluorometabolite biosynthesis. Single label is observed in both C-1 and C-2 of fluoroacetate (1), and this most probably arises as succinate (124) and fumarate (125) are symmetrical molecules, and thus the label is scrambled to synthesise [2-<sup>13</sup>C]-oxaloacetate ([2-<sup>13</sup>C]-42) and [2-<sup>13</sup>C]-oxaloacetate ([2-<sup>13</sup>C]-42). The lower level

of label at C-2 of fluoroacetate (1) must be attributed to incomplete scrambling, or perhaps some other ill defined pathway.

The incomplete scrambling of label in fumarate (125) explains the low level of deuterium incorporation from [2,2,2-<sup>2</sup>H<sub>3</sub>]-acetate (122). The assimilation of label from this metabolite can only occur *via* C-3 of oxaloacetate (42) and thus must arise after scrambling at succinate (124) or fumarate (125). Half of this label is necessarily lost through oxidation of C-2 of oxaloacetate (42) (see Fig. 2.20). The level of incorporation of deuterium from [2,2,2-<sup>2</sup>H<sub>3</sub>]-acetate (122) is only slightly lower than that of single label incorporation into C-2 of fluoroacetate (1) from [1,2-<sup>13</sup>C<sub>2</sub>]-acetate (21) (2.6 % vs 3.5 %). It is usual for deuterium to label at a lower level than the equivalent <sup>13</sup>C experiment (*e.g.* [6,6-<sup>2</sup>H<sub>2</sub>]-glucose (105), 22 %, *c.f.* [6-<sup>13</sup>C]-glucose (114), 30 %) and this can be rationalised as label being lost through process exchange with the media. In this case the deuterium atom passes through a highly enolisable position in [3-<sup>2</sup>H]-oxaloacetate ([3-<sup>2</sup>H]-42).

The high level of double label in the fluorometabolites after feeding [1,2-<sup>13</sup>C<sub>2</sub>]-acetate (21) is rationalised by considering multiple revolutions of the TCA cycle. A single revolution produces [2-<sup>13</sup>C]-oxaloacetate ([2-<sup>13</sup>C]-42), which may go on to fluorometabolite biosynthesis to label C-1 of fluoroacetate (1) and C-3 of 4-fluorothreonine (2). Alternately, it may condense with a second molecule of [1,2-<sup>13</sup>C<sub>2</sub>]-acetate (21) and continue around the TCA cycle. This will eventually produce [2,3-<sup>13</sup>C<sub>2</sub>]-oxaloacetate ([2,3-<sup>13</sup>C<sub>2</sub>]-42) and thus deliver label into both C-1 & C-2 of fluoroacetate (1) and likewise in C-3 & C-4 of 4-fluorothreonine (2).

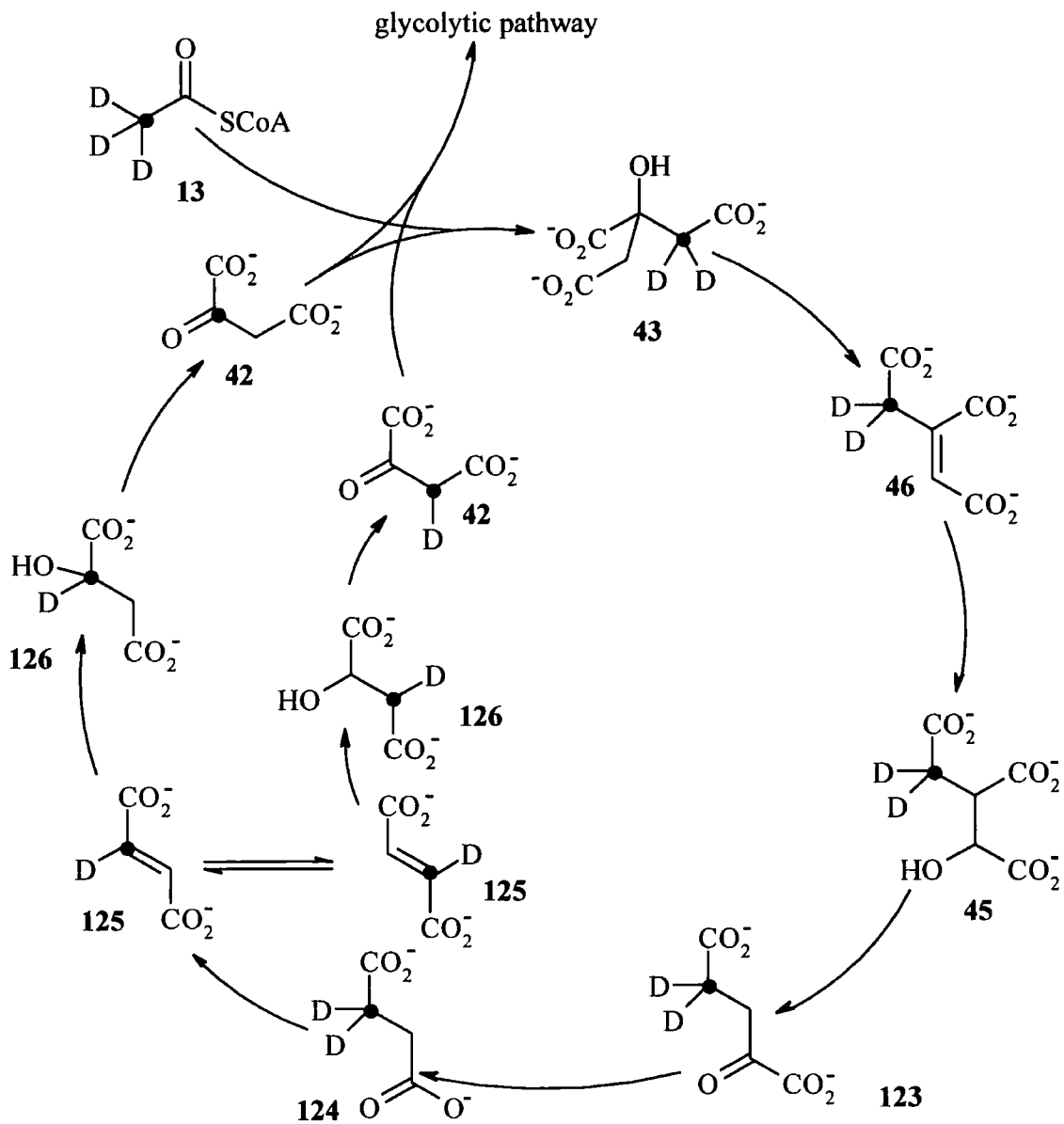
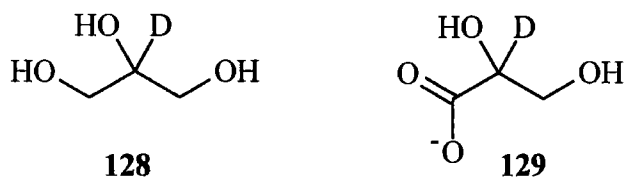


**Fig. 2.20:** The TCA cycle, demonstrating both the fate of  $[2-^{13}\text{C}]$ -acetate (**127**) and  $[2-^3\text{H}]$ -acetate (**122**), including the scrambling of label through fumarate (**125**).

Fig. 2.20 also demonstrates why only one deuterium atom is retained in the fluorometabolites from  $[2-^3\text{H}]$ -acetate (**122**). The oxidation from succinate (**124**) to fumarate (**125**) removes one deuterium atom, thus only one is retained.

### 2.3.3 [2-<sup>2</sup>H]-Glycerol (128) and [2-<sup>2</sup>H]-glycerate (129)



#### 2.3.3.1 Background

In order to understand where fluorometabolite biosynthesis branches from the glycolytic pathway it appeared appropriate to study deuterium incorporation into position 3 of 4-fluorothreonine (2). Previously, labelling studies have shown incorporation of <sup>13</sup>C and <sup>2</sup>H into all positions of fluoroacetate (1) and 4-fluorothreonine (2) except for C-3.

In the context of delineating the branch point to fluorometabolite biosynthesis from the glycolytic pathway the origin of the C-3 hydrogen is clearly important. DHAP (98) is a significant metabolite in this respect, as metabolism passing through this intermediate will lose the proton that may account for C-3 in 4-fluorothreonine (2) (Fig. 2.21).

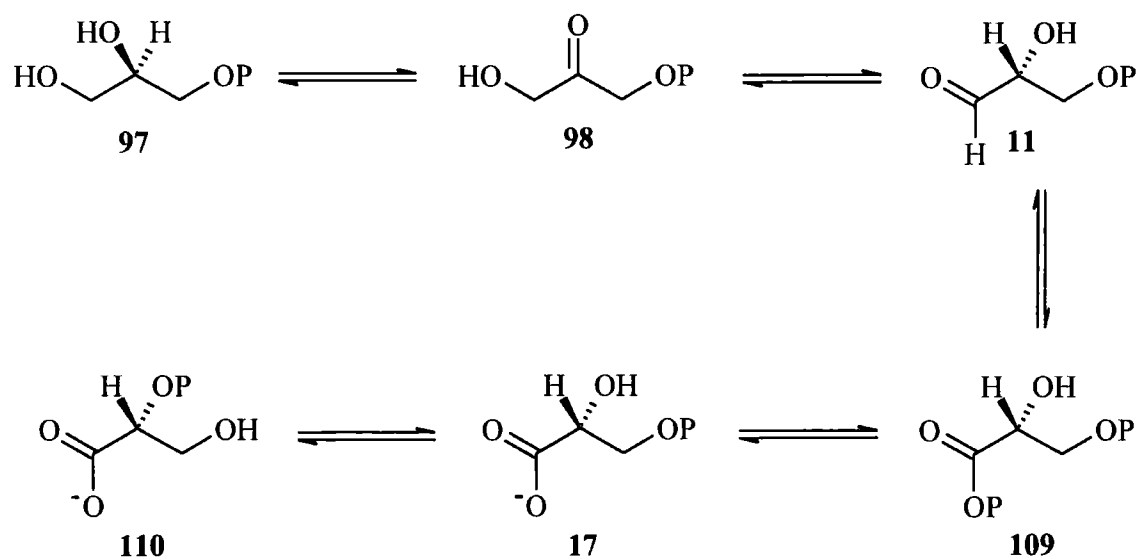


**Fig. 2.21:** Oxidation state at C-2 of the glycolytic intermediates on either side of DHAP (98), P = phosphate.

Feeding a glycolytic intermediate labelled with a deuterium atom at C-2 could delineate which side of DHAP (98) fluorometabolite biosynthesis leaves the glycolytic pathway. Accordingly, [2-<sup>2</sup>H]-glycerol (128) and [2-<sup>2</sup>H]-glycerate (129) were prepared by a co-

worker (Dr D. Bouvet) at the University of Durham, by sodium borodeuteride reduction of dihydroxyacetone and  $\beta$ -hydroxypruvate respectively.

### 2.3.3.2 Results and discussion

[2-<sup>2</sup>H]-Glycerol (**128**) was fed at a final concentration of 5 mM to resting cells of *S. cattleya* supplemented with 2 mM NaF and incubated for 48 hours. <sup>19</sup>F {<sup>1</sup>H} NMR analysis did not reveal any incorporation into C-3 of 4-fluorothreonine (**2**). Previous studies with isotope enriched glycerols demonstrated high levels of incorporation into the fluorometabolites, and glycerol (**87**) is a good carbon source for the fluorometabolites. This experiment perhaps suggests that fluorometabolite biosynthesis does not derive from a glycolytic pathway metabolite upstream of DHAP (**98**).

[2-<sup>2</sup>H]-Glycerate (**129**) was then fed to resting cells of *S. cattleya* supplemented with 2 mM NaF and incubated for 48 hours. As glycerate (**130**) had not previously been fed to *S. cattleya*, nothing is known on its efficiency as a carbon source to the fluorometabolites and so **129** was fed separately at two concentrations, 2.5 mM and 10 mM. <sup>19</sup>F {<sup>1</sup>H} NMR analysis did not reveal any incorporation into C-3 of 4-fluorothreonine (**2**). This was also confirmed by GCMS analysis of the resultant 4-fluorothreonine (**2**).

Precursor	Incorporation into 4-fluorothreonine ( <b>2</b> ) (%)					
	Ion 218 (positions 1 and 2)			Ion 236 (positions 2, 3 and 4)		
	M	M + 1	M + 2	M	M + 1	M + 2
10 mM [2- <sup>2</sup> H]-glycerate ( <b>129</b> )	96.1	1.3	2.6	97.9	1.4	0.7
2.5 mM [2- <sup>2</sup> H]-glycerate ( <b>129</b> )	100.8	1.4	-2.3	98.2	0.9	0.8

**Table 2.6:** GCMS analysis of 4-fluorothreonine (**2**), following incubation of resting cells of *S. cattleya* with [2-<sup>2</sup>H]-glycerate (**129**).

The data (Table 2.6) does not indicate any significant incorporation into positions 2, 3 and 4 of 4-fluorothreonine (**2**).

The absence of incorporation from [2-<sup>2</sup>H]-glycerate (129) may be due to a number of reasons. Perhaps deuterium is lost in the glycolytic pathway or during fluorometabolite biosynthesis itself. However, glycerate (130) itself is not a *bone fide* glycolytic intermediate, although phosphorylated analogues of it are. In feeding other non-phosphorylated glycolytic intermediates (*viz.* glycerol (87) and glucose (9)) phosphate kinases have acted and allowed these to enter the glycolytic pathway. It may be that there is no phosphate kinase in *Streptomyces cattleya* capable of utilising glycerate (130) as a substrate. A further possibility is that glycerate (130) is phosphorylated but is not involved in fluorometabolite biosynthesis. The glycolytic pathway may be active in the direction from glucose (9) to pyruvate (10), which may channel the glycerate (130) downstream and thus remove it from possible involvement in fluorometabolite biosynthesis.

Three additional experiments were designed to probe the incorporation of label from [2-<sup>2</sup>H]-glycerate (129) further.

**Experiment 1:** [2-<sup>2</sup>H]-Glycerate (129) was fed at 10 mM to resting cells of *S. cattleya* one hour after they were supplemented with 2 mM NaF. The rationale for this experiment was that after this time fluorometabolite biosynthesis will proceed efficiently and [2-<sup>2</sup>H]-glycerate (129) can then be channelled into that biosynthesis.

**Experiment 2:** [2-<sup>2</sup>H]-Glycerate (129) at a final concentration of 10 mM and NaF at 2 mM were fed to resting cells of *S. cattleya* one hour after they had been supplemented with 10 mM glycolate (50). Glycolate (50) is known to be an efficient carbon source, and may serve to channel the glycerate (130) into fluorometabolite biosynthesis.

**Experiment 3:** [2-<sup>2</sup>H]-Glycerate (129) at a final concentration of 10 mM and 2 mM NaF were fed to resting cells of *S. cattleya* one hour after they had been supplemented with 10 mM glycerol (87). This may remove the possibility that label is lost through enolisation between G-3-P (11) and DHAP (98). Triose phosphate isomerase mediates this conversion and under normal conditions the equilibrium is in favour of production of DHAP (98).<sup>109</sup> This equilibrium would clearly result in loss of deuterium label from G-3-P (11) to produce unlabelled G-3-P (11).



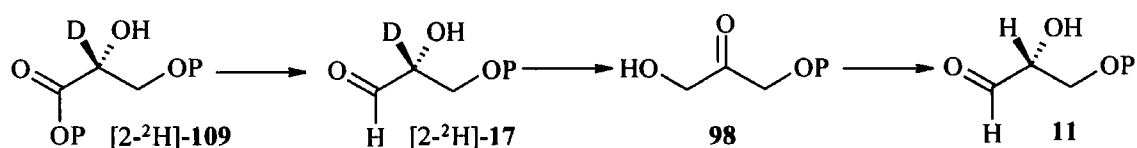


**Fig. 2.22:** The removal of deuterium from glyceraldehyde *via* triose phosphate isomerase.

In all three of these experiments <sup>19</sup>F {<sup>1</sup>H} NMR analysis did not indicate any incorporation of deuterium into C-3 of 4-fluorothreonine (**2**), and this was also confirmed by GCMS analysis.

	Incorporation into 4-fluorothreonine ( <b>2</b> ) (%)					
	Ion 218 (positions 1 and 2)			Ion 236 (positions 2, 3 and 4)		
	M	M + 1	M + 2	M	M + 1	M + 2
<b>Experiment 1</b>	96.0	1.3	2.7	97.9	1.4	0.7
<b>Experiment 2</b>	95.7	1.4	3.0	98.5	0.7	0.8
<b>Experiment 3</b>	96.0	1.4	2.7	97.8	1.3	0.9

**Table 2.7:** GCMS analysis of 4-fluorothreonine (**2**), following incubation of resting cells of *S. cattleya* with [2-<sup>2</sup>H]-glycerate (**129**).

It appears that the deuterium from C-2 of the glycolytic intermediates, both upstream and downstream of dihydroxyacetone phosphate (**98**), was not carried through to label C-3 of 4-fluorothreonine (**2**). This result may be interpreted in one of two ways. Either DHAP (**98**) is the substrate for the first committed step of fluorometabolite biosynthesis, or the deuterium atom is lost during at a later stage in fluorometabolite biosynthesis itself.

## 2.4 Synthesis and feeding of 3-fluoro-1-hydroxypropanone

### 2.4.1 Background

Two events must occur between the glycolytic pathway and fluorometabolite biosynthesis; the fluorination event and a C-C bond cleavage. The bond cleavage is necessary as glycolytic intermediates are C<sub>3</sub> entities and the final stages of fluorometabolite biosynthesis must involve a C<sub>2</sub> moiety. Further, the labelling patterns from isotope feeding experiments have shown that a common fluorinated intermediate must be involved, as the labelling patterns in C-1 and C-2 of fluoroacetate (1) are identical to that in C-3 and C-4 of 4-fluorothreonine (2) (section 1.6.5).

The direct fluorination of a glycolytic intermediate, by nucleophilic substitution of a phosphate group would yield a C<sub>3</sub> fluorinated intermediate. This could then lie at a branch point to both of the fluorometabolites or it could be cleaved to a fluorinated C<sub>2</sub> intermediate, as shown schematically in Fig. 2.23.

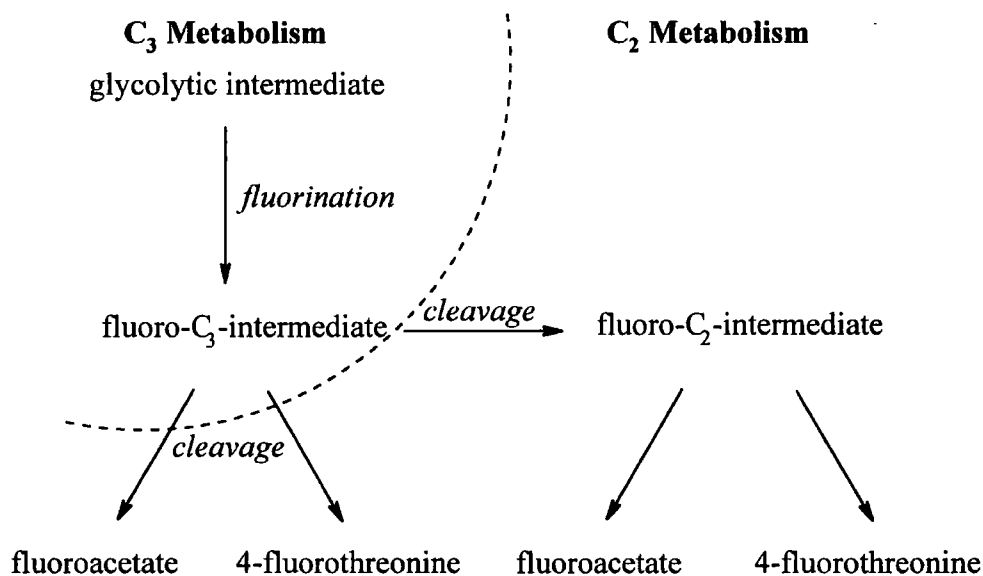


**Fig. 2.24:** Working hypothesis for fluorometabolite biosynthesis via a fluorinated C<sub>3</sub> unit.

Putative initial products of fluorination were fed to resting cells of the bacterium to assess their bio-conversion to the fluorometabolites. In previous studies<sup>107,108</sup> β-fluoropyruvate (65), 3-fluorolactate (131) and 3-fluoropropan-1,2-diol (132) have been synthesised in this respect and were administered to *Streptomyces cattleya*. Deuterium was substituted into these putative intermediates such that their fluoromethyl groups were labelled (c.f. 'bond labelling' in double labelled feeding experiments,

**section 1.2.2.4).** For these compounds to be implicated as *bona fide* intermediates in fluorometabolite biosynthesis, the fluoromethyl group must become incorporated intact into the fluorometabolites.

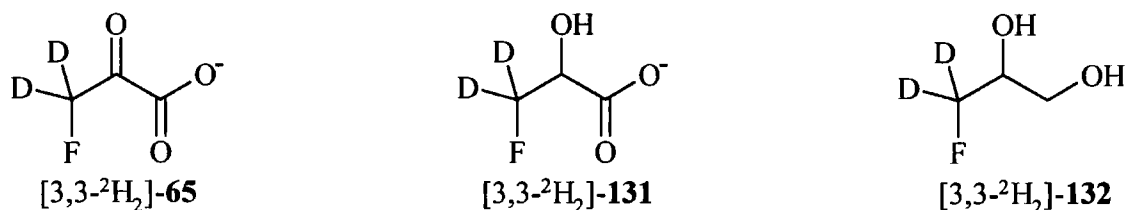


**Fig. 2.25:** Putative post fluorination products synthesised and fed by Amin<sup>108</sup> and Murphy,<sup>107</sup> respectively.

In the event none of these intermediates proved to be directly involved in fluorometabolite biosynthesis. The experiments with  $\beta$ -fluoropyruvate (**65**) and 3-fluorolactate (**131**) did lead to the production of fluoroacetate (**1**), although this was attributed to non-enzymatic oxidative cleavage. Also small amounts of unlabelled fluorometabolites were observed due to defluorination, of  $\beta$ -fluoropyruvate (**65**) and 3-fluorolactate (**131**), followed by assimilation of that fluoride into fluorometabolite biosynthesis.<sup>108</sup> 3-Fluoropropan-1,2-diol (**132**) was stable to both oxidative cleavage and defluorination in resting cells of *S. cattleya* and proved resistant to metabolism.<sup>107</sup>

These observations appear to rule out the direct fluorination 3-phosphoglycerate (**17**), 1,3-bisphosphoglycerate (**109**) and 1-phosphoglycerol (**97**). However, stable isotope feeding experiments have highlighted the importance of the triose phosphates in fluorometabolite biosynthesis and so it appeared appropriate to extend this study further and to prepare and feed the fluorinated analogue of DHAP (**98**).

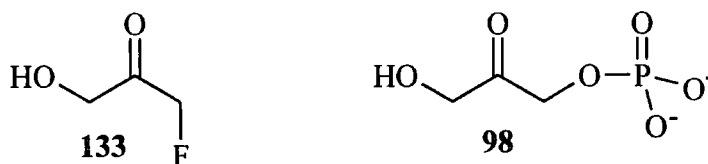


**Fig. 2.26:** 3-Fluoro-1-hydroxypropanone (**133**) and DHAP (**98**).

As in previous studies it is advantageous to have deuterium atoms geminal to the fluorine atom in the prepared precursor and a strategy towards such labelling was pursued.

#### 2.4.2 3-Fluoro-1-hydroxypropanone (133)

3-Fluoro-1-hydroxypropan-2-one (133) was prepared in 1982 by Kozarich.<sup>110</sup> In this study on halohydroxyacetones and halomethylglyoxals,  $\beta$ -fluoropyruvate (65) was converted to 3-fluoro-1-hydroxypropan-2-one (133) by protecting the ketone and reducing the carboxyl group to a primary alcohol (see Fig. 2.27).

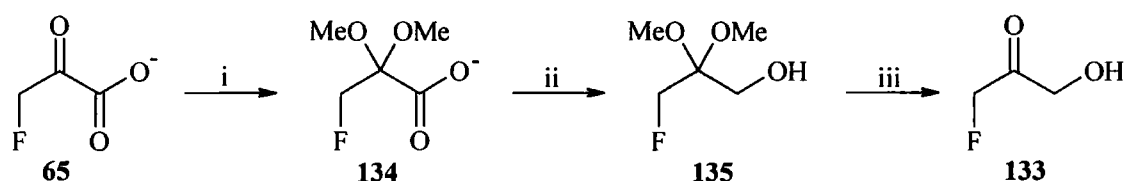


**Fig. 2.27:** Synthesis of 3-fluoro-1-hydroxypropan-2-one (133) by Kozarich.<sup>110</sup> i) (MeO)<sub>3</sub>CH, MeOH, H<sub>2</sub>SO<sub>4</sub>, 59 %; ii) LiAlH<sub>4</sub>, Et<sub>2</sub>O, 89 %; iii) H<sub>2</sub>O<sup>+</sup>.

In the event this literature method was not followed because the route did not facilitate the introduction of deuterium atoms geminal to the fluorine. Deuterium can be introduced into the required position *via* enolisation in a deuterium enriched solvent, and so synthetic schemes amenable to solvent exchange were investigated.

Van Hijfte<sup>111</sup> has described the synthesis of  $\alpha$ -(monofluoromethyl) amino acids *via* 3-fluoro-1-hydroxypropanone benzyl ether (136). It was envisaged that this compound could undergo enolisation to introduce deuterium geminal to the fluorine atom, and then removal of the protecting group would yield the target compound (133).

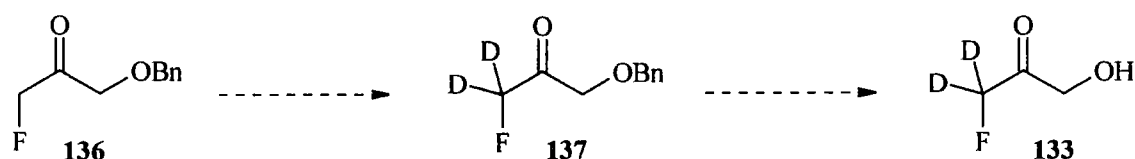


**Fig. 2.28:** Putative synthesis of [3-<sup>2</sup>H<sub>2</sub>]-3-fluoro-1-hydroxypropanone ([3,3-<sup>2</sup>H<sub>2</sub>]-133) from 3-fluoro-1-hydroxypropanone benzyl ether (136).

Accordingly 3-fluoro-1-hydroxypropanone benzyl ether (**136**) was prepared by the method of Van Hijfte<sup>111</sup>.

### 2.4.3 Synthesis of 3-fluoro-1-hydroxypropanone (133)

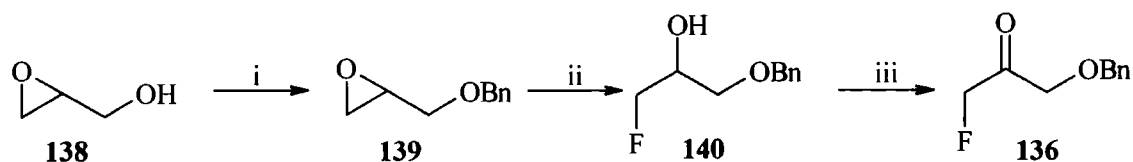


**Fig. 2.29:** Synthesis of 3-fluoro-1-hydroxypropan-2-one benzyl ether (**140**); i) NaH, THF, 0 °C then BnBr, 16 hours, 20 °C, 22 %; ii) KHF<sub>2</sub>, diethylene glycol, 170 °C, 4 hours, 40 %; iii) (COCl)<sub>2</sub>, DMSO, DCM, -60 °C, then Et<sub>3</sub>N, 93 %.

The first step in the route involved the protection of glycidol (**138**) as its benzyl ether (**139**). The Van Hijfte<sup>111</sup> publication is a communication and so experimental details are scant. More detailed experimental description of the synthesis of glycidol benzyl ether (**139**) was given by Liu<sup>112</sup> in the total synthesis of [(methylene)cyclopropyl]acetyl]-SCoA and their method was followed here. Therefore glycidol benzyl ether (**139**) was prepared from racemic glycidol (**138**) in THF treated with freshly distilled benzyl bromide and using sodium hydride as the base. The resultant oil was purified by high vacuum distillation. The yield was significantly lower than that published (22 % vs 84 %), although this can be rationalised because of impurities in the starting material. The commercial sample of glycidol (**138**) was discovered to be only 70 % pure by <sup>1</sup>H NMR and the remainder appeared to be glycerol (**87**). However, sufficient material was purified for the synthesis to proceed.

The epoxide (**139**) was then ring-opened to form the corresponding fluorohydrin (**140**). This reaction was mediated by heating **139** in the presence of potassium hydrogen fluoride. The epoxide (**139**) can open both ways to form either the benzyl ether of 3-fluoro-2-hydroxypropan-1-ol (**140**) or 2-fluoro-3-hydroxypropan-1-ol (**141**) (see Fig. 2.30), although literature precedents suggest predominant ring opening to the desired regioisomer (**140**).<sup>113,114,115</sup>

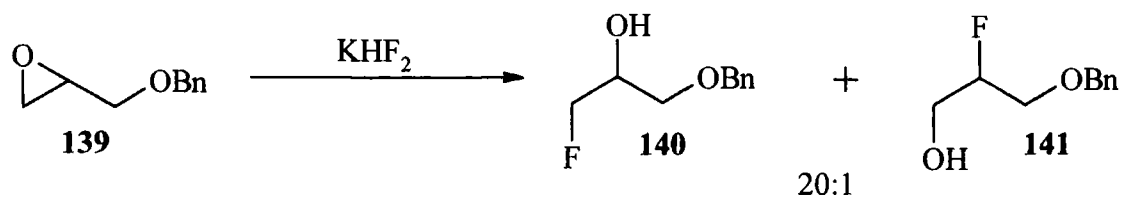


**Fig. 2.30:** Ring opening of glycidol benzyl ether (139) with  $\text{KHF}_2$ .

In the event both regiomers were produced although the reaction conditions strongly favoured the production of the desired fluorohydrin (140). The reaction was carried out in a high boiling solvent (diethylene glycol) at 170 °C. After 4 hours TLC analysis demonstrated complete consumption of the starting material (139), and the production of two products.  $^{19}\text{F}$  NMR analysis showed that the desired fluorohydrin (140) and its regioisomer (141) had formed ( $\delta_{\text{F}} = -232$  and  $-196$  ppm respectively, in a ratio of 20:1, by  $^{19}\text{F}$  NMR). The regioisomers were easily separated by dry flash chromatography as 140 was less polar and overall the reaction proceeded in a modest yield of 40 %.

Oxidation of the fluorohydrin (140) to yield the  $\alpha$ -fluoroketone (136) was performed using Swern methodology,<sup>116</sup> and proceeded in good yield, 93 %. The synthesis so far is summarised in Fig. 2.29.

Deuterium exchange into the  $\alpha$ -fluoromethyl group was followed by  $^{19}\text{F}$  NMR. At the outset it was envisaged that acid catalysed enolisation would be the most suitable method, however studies using  $\text{D}_2\text{SO}_4$  showed that the  $\alpha$ -fluoroketone (140) was unstable under these conditions, even at relatively low acid concentrations. Therefore base catalysed exchange of deuterium was then investigated. Small amounts of Na metal were dissolved in  $\text{CH}_3\text{OD}$  and the subsequent exchange monitored by  $^{19}\text{F}$  NMR, observing the isotope induced shift associated with the fluorine signal. There was a limited level of exchange producing both the monodeutero- (~ 20 %) and dideutero-labelled (~ 5 %)  $\alpha$ -fluoroketones (140).

The hydrogenation of the  $\alpha$ -fluoroketone (140) to deliver the target compound (133) was studied in the first instance on unlabelled material. Firstly a transfer hydrogenation was explored by stirring the  $\alpha$ -fluoroketone (140), with cyclohexene in MeOH using palladium supported on carbon as the catalyst. The reaction was monitored by tlc and

$^{19}\text{F}$  NMR, but failed to proceed and the starting material (**140**) was reisolated. In a second attempt, the reaction was carried out under a positive pressure of hydrogen using the same catalyst. This time the reaction was successful and all of the starting material was consumed within 16 hours as monitored by tlc.

To isolate the deprotected  $\alpha$ -fluoroketone (**133**) the catalyst was removed by filtration through a Celite plug. Care had to be taken in removing the methanol, as the boiling point of 3-fluoro-1-hydroxypropanone (**133**) was not envisaged to be very high. The boiling point of a fluorinated compound is generally only a few degrees Celsius above that for the non-fluorinated species. The boiling point of acetol is 145-146  $^{\circ}\text{C}$ , so that of 3-fluoro-1-hydroxypropanone (**133**) will clearly be similar. Therefore the solvent was removed under reduced pressure ensuring that the temperature did not exceed 40  $^{\circ}\text{C}$ .  $^{19}\text{F}$  NMR analysis of the resultant oil demonstrated the presence of a number of fluoromethyl groups.

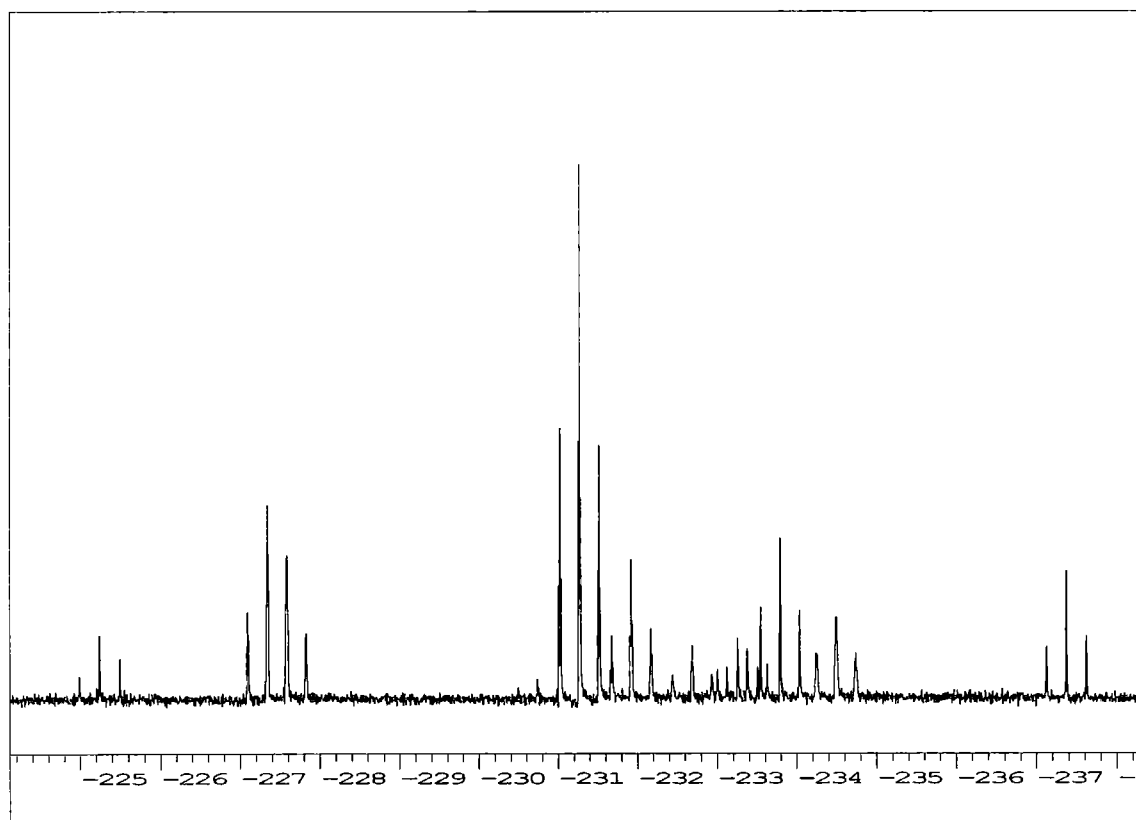


**Fig. 2.31:**  $^{19}\text{F}$  NMR of 3-fluoro-1-hydroxypropanone (**133**).

Attempts to derivatise this product further for characterisation were not successful. DNP-derivatisation resulted in a precipitate that was dried and analysed by  $^{19}\text{F}$  NMR, however there were no resonances in the fluoromethyl region. Further analysis showed

that in forming the DNP derivative of 3-fluoro-1-hydroxypropanone (133) the compound was efficiently defluorinated. A putative mechanism for this facile defluorination is given in Fig. 2.32.

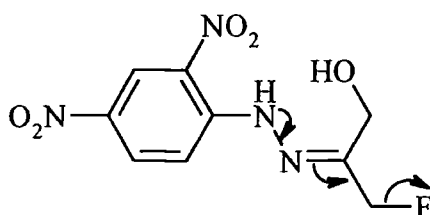


**Fig. 2.32:** Putative mechanism for 3-fluoro-1-hydroxypropanone DNP defluorination.

In the published synthesis of 3-fluoro-1-hydroxypropanone (133) by Kozarich<sup>110</sup> the final step involved an aqueous acetal hydrolysis. The product of this reaction was not isolated but observed only by NMR analysis. In our case <sup>19</sup>F and <sup>1</sup>H NMR analyses of the debenzoylation product was consistent with the reported data. Also the authors described how 3-fluoro-1-hydroxypropanone (133) exists as both the ketone and the hydrate. The equilibrium between these species was observed by <sup>19</sup>F NMR. As such it is not unreasonable to suggest the presence of the acetal, hemiacetal, hydrate and ketone after the debenzoylation. In the feeding experiment the compound was administered as a dilute aqueous solution and as such the acetal and hemiacetal should convert back to either the ketone or the hydrate.

In summary, 3-fluoro-1-hydroxypropanone (133) had been synthesised, in equilibrium with a complex mixture of other species. This material was then used in a feeding experiment.

#### **2.4.4 Biotransformation of 3-fluoro-1-hydroxypropanone (133)**

Accordingly 3-fluoro-1-hydroxypropanone (133) was administered to resting cells of *Streptomyces cattleya* and incubated for 48 hours. As the synthesised material was known not to be pure the final concentration could not be accurately determined, although it is estimated to be approximately 1 mM (**experiment 1**). In a separate experiment 3-fluoro-1-hydroxypropanone (133) was also fed at half of that concentration (**experiment 2**). No free fluoride was present in these samples at the beginning of the feeding experiments.



After 18 hours an aliquot was removed from each experiment and analysed by  $^{19}\text{F}$  NMR and then the fluoride concentration was measured. Fluoride analysis showed that inorganic fluoride had been liberated to the level of 0.25 mM in the medium in **experiment 1**.

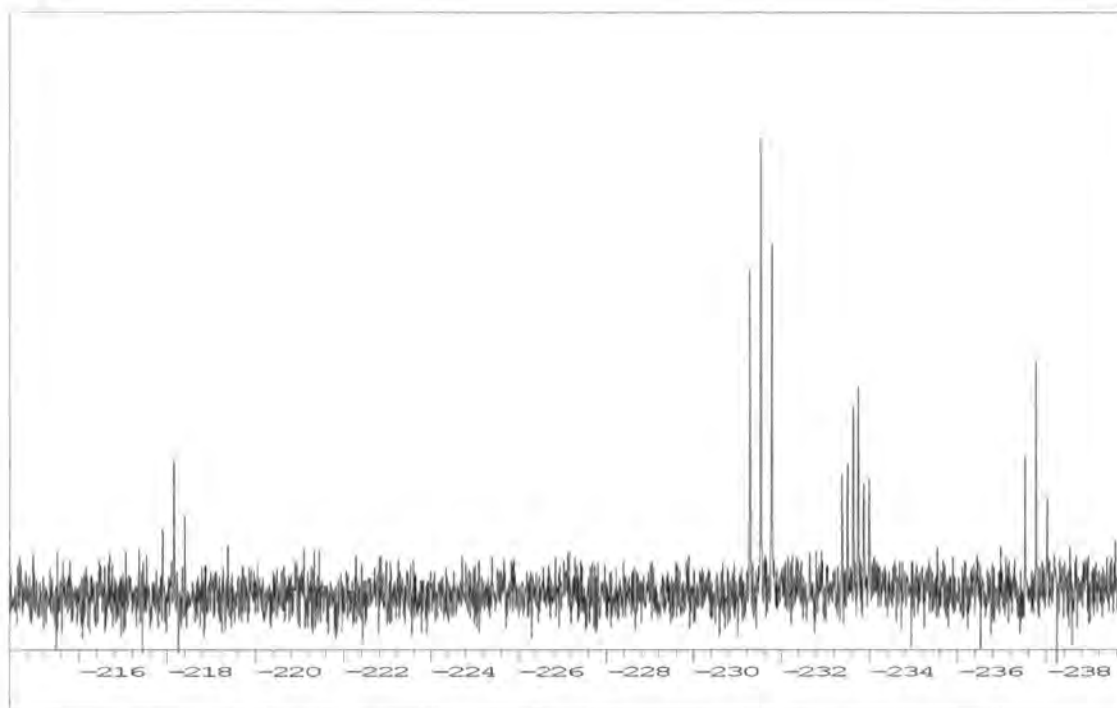


**Fig. 2.33:**  $^{19}\text{F}$  NMR spectrum of the resultant supernatant from incubating resting cells of *S. cattleya* for 18 hours with 3-fluoro-1-hydroxypropanone (**133**) (**experiment 1**).

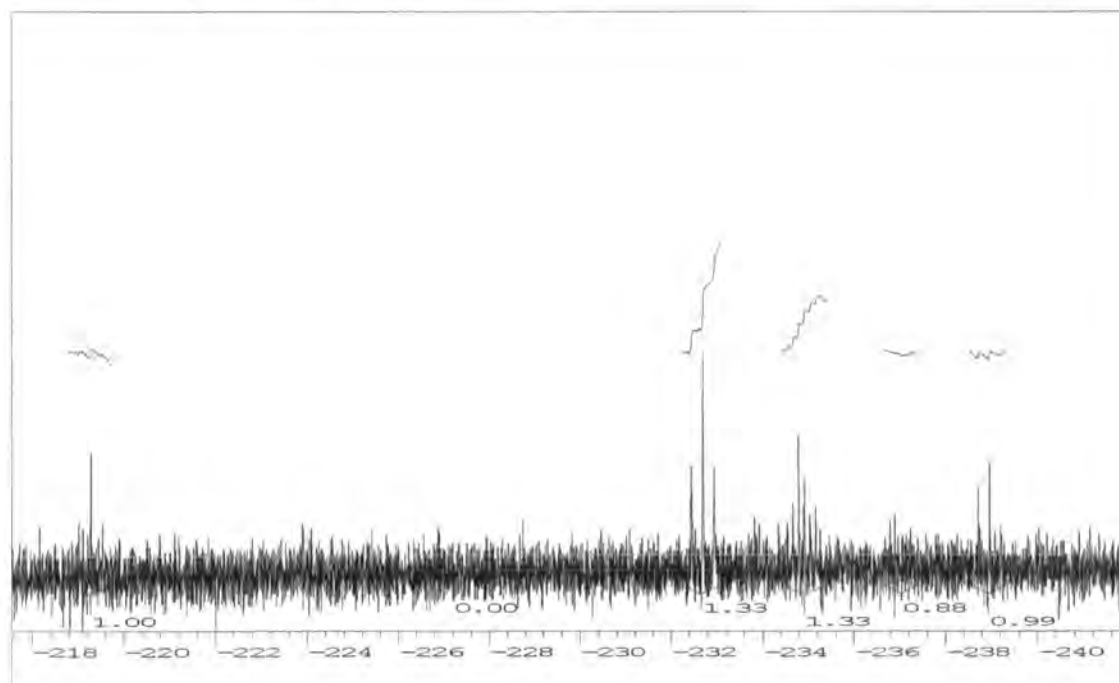


**Fig. 2.34:**  $^{19}\text{F}$  NMR spectrum of the resultant supernatant from incubating resting cells of *S. cattleya* for 18 hours with 3-fluoro-1-hydroxypropanone (**133**) (**experiment 2**).

After 48 hours the experiments were terminated in the usual way and the supernatants analysed by  $^{19}\text{F}$  NMR.

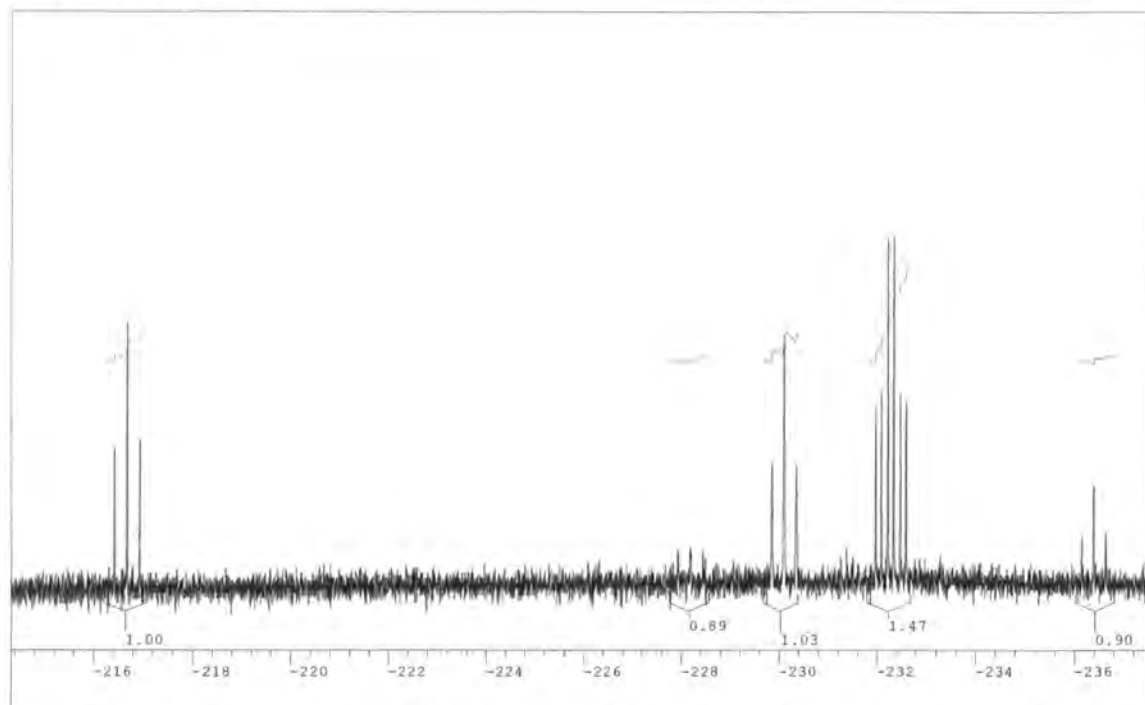


**Fig. 2.35:**  $^{19}\text{F}$  NMR spectrum of the resultant supernatant from incubating resting cells of *S. cattleya* for 48 hours with 3-fluoro-1-hydroxypropanone (133) (experiment 1).

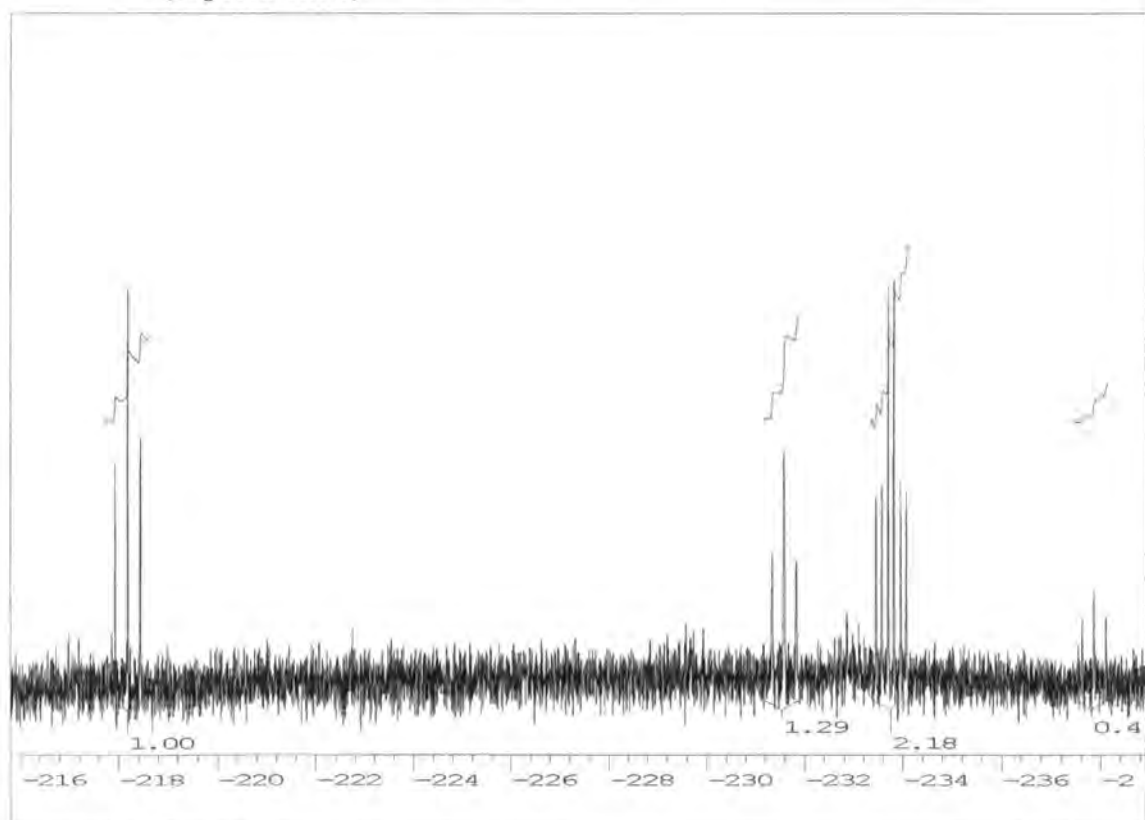


**Fig. 2.36:**  $^{19}\text{F}$  NMR spectrum of the resultant supernatant from incubating resting cells of *S. cattleya* for 48 hours with 3-fluoro-1-hydroxypropanone (133) (experiment 2).

If 3-fluoro-1-hydroxypropanone (**133**) is the initial product of fluorination, then it was anticipated that upon addition to resting cells that the fluorometabolites would readily accumulate. In the event fluoroacetate (**1**) and 4-fluorothreonine (**2**) were only produced in low concentration. The presence, at all, of the fluorometabolites in these experiments can be rationalised in terms of defluorination of 3-fluoro-1-hydroxypropanone (**133**), or a metabolite of it, followed by a *de novo* biosynthesis of the fluorometabolites from the liberated fluoride.

An interesting feature of the  $^{19}\text{F}$  NMR analysis of these feeding experiments is the appearance of a new fluoromethyl resonance that was not in the administered sample. Fig 2.31 shows the  $^{19}\text{F}$  NMR spectrum of the solution that was fed to the bacterium. This is compared to the  $^{19}\text{F}$  NMR spectrum resulting after **experiment 1**, both at 18 and 48 hours (Fig. 2.33 and Fig. 2.35 respectively). In each case the spectra simplify and a new resonance appears at  $\delta_{\text{F}} = -232$  ppm. This resonance is also visible in the spectrum relating to **experiment 2**. The resonance is not, as all the others are, a simple triplet resulting from a fluoromethylacyl moiety. In this case a doublet of triplets is observed ( $^2J_{\text{FH}} = 47.0$  Hz,  $^3J_{\text{FH}} = 22.3$  Hz), clearly resulting from a fluoromethyl group with a proton on the vicinal carbon. This resonance is similar in pattern (but not chemical shift) to 4-fluorothreonine (**2**) and there are a number of explanations for this observation.

Clearly, 3-fluoro-1-hydroxypropanone (**133**) may be reduced by an alcohol dehydrogenase to 3-fluoropropan-1,2-diol (**132**) a compound which has previously been shown not to be involved in fluorometabolite biosynthesis. However, the resonance that corresponds to  $[3,3\text{-}^2\text{H}_2]$ -3-fluoropropan-1,2-diol (**132**) in  $^{19}\text{F}$  NMR is at  $-236.0$  ppm,<sup>107</sup> therefore the unlabelled resonance would be approximately  $-234.8$  ppm. The signal resultant from feeding 3-fluoropropan-2-one (**133**) appears at  $-232$  ppm, so this hypothesis cannot account for the appearance of this new resonance.

Alternatively, 3-fluoro-1-hydroxypropanone (**133**) was metabolised by triose phosphate isomerase to yield the fluorinated analogue of G-3-P, 3-fluoroglyceraldehyde (**142**).

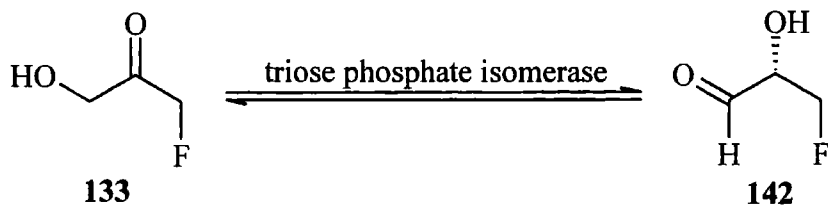


**Fig. 2.37:** Putative conversion of 3-fluoro-1-hydroxypropanone (**133**) to 3-fluoroglyceraldehyde (**142**).

3-Fluoroglyceraldehyde (**142**) has been synthesised by Wong,<sup>117,118,119</sup> to study its role in asymmetric aldol condensations. This compound is obviously difficult to handle and so spectroscopic data is only reported on the diethoxyacetal of 3-fluoroglyceraldehyde. Effenberger<sup>120</sup> published a chemoenzymatic synthesis of 3-fluoroglyceraldehyde (**142**). Neither group published <sup>19</sup>F NMR data of 3-fluoroglyceraldehyde (**142**), however Effenberger<sup>120</sup> did publish a complete <sup>1</sup>H NMR analysis. Using the coupling constants quoted from this analysis the <sup>19</sup>F NMR resonance of 3-fluoroglyceraldehyde (**142**) should be a triplet of doublets, with the coupling constants given in Fig. 2.38.

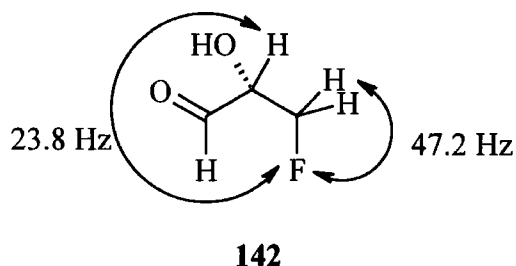


**Fig. 2.38:** Coupling constants in 3-fluoroglyceraldehyde (**142**), taken from Effenberger.<sup>120</sup>

These values are in agreement with the observed resonance in the feeding experiment with 3-fluoro-1-hydroxypropanone (**133**).

Clearly 3-fluoro-1-hydroxypropanone (**133**) is not directly involved in fluorometabolite biosynthesis. Instead, it appears that 3-fluoro-1-hydroxypropanone (**133**) was converted to, another species which may be 3-fluoroglyceraldehyde (**142**). Fluoride was then liberated from one of the fluorinated species present, which generated the fluorometabolites *via a de novo* biosynthesis.

It was decided not to repeat the experiment with deuterium labelled 3-fluoro-1-hydroxypropanone (133), as the absence of rapid conversion to either fluorometabolites rules out the direct involvement of this  $\alpha$ -fluoroketone (133).

## 2.5 Conclusions

The involvement of the glycolytic pathway in fluorometabolite biosynthesis in *S. cattleya* has been unambiguously confirmed by feeding isotopically enriched glucose and acetates. Glucose (9) enters fluorometabolite biosynthesis *via* both the glycolytic and pentose phosphate pathways. Acetate (6) was shown to become incorporated into the fluorometabolites *via* the glycolytic pathway after first being metabolised by the TCA cycle. This evidence and data collected by Murphy<sup>107</sup> demonstrate that the glycolytic pathway is the metabolic pathway that delivers substrates for fluorometabolite biosynthesis.

Feeding experiments with [2-<sup>2</sup>H]-glycerol (128) and [2-<sup>2</sup>H]-glycerate (129) attempted to trace this deuterium atom through from the glycolytic pathway to position 3 of 4-fluorothreonine (2). However, in none of these feeding experiments did this position become labelled. This implies that either dihydroxyacetone phosphate (98) is the substrate for the first committed step towards fluorometabolite biosynthesis from the glycolytic pathway, or that this deuterium is lost in subsequent steps in fluorometabolite biosynthesis.

3-Fluoro-1-hydroxypropanone (133) was successfully synthesised and the difficulties in handling this compound were addressed. Feeding experiments appear to have ruled out its involvement as an intermediate in fluorometabolite biosynthesis. <sup>19</sup>F NMR analysis suggested that 3-fluoro-1-hydroxypropanone (133) was converted to either 3-fluoropropan-1,2-diol (132) or 3-fluoroglyceraldehyde (142).

Fluorinated analogues of all of the glycolytic intermediates have now been administered to resting cells of *Streptomyces cattleya*. None of these substrates are converted to either fluoroacetate (1) or 4-fluorothreonine (2) and together these experiments appear to rule out a fluorination event on a *bona fide* glycolytic intermediate.

*Chapter 3*

*A role for fluoroacetaldehyde*

### 3.1 Fluoroacetaldehyde

None of the glycolytic intermediates appear to be a substrate for the fluorination process. As discussed previously (section 2.4.1), the final stages of fluorometabolite biosynthesis may involve C<sub>2</sub> units. Fluoroacetaldehyde (40) meets this criterion, as oxidation will directly generate fluoroacetate (1). Also condensation of fluoroacetaldehyde with a *pseudo*-C<sub>2</sub> unit (section 3.5) in an aldol type process could generate 4-fluorothreonine (2). In order to assess the role of fluoroacetaldehyde a synthesis, amenable to isotopic labelling was required.

#### 3.1.1 Synthesis of fluoroacetaldehyde (40)

Fluoroacetaldehyde (40) was first synthesised by Saunders *et al*<sup>121</sup> in a series of papers studying the toxicity of fluoroacetate (1) derivatives on behalf of the Ministry of Supply during World War II. In that case 2-fluoroethanol (71) was oxidised with manganese dioxide and produced a 6 % solution of fluoroacetaldehyde (40) in water. The LD<sub>50</sub> of fluoroacetaldehyde (40) was measured and it was found to be identical to that of fluoroacetate (1), so it was surmised that fluoroacetaldehyde (40) is efficiently converted to fluoroacetate (1) *in vivo*. Recently fluoroacetaldehyde has been implicated as a toxic impurity in the chemotherapy drug 5-fluorouracil (143).<sup>122</sup> <sup>19</sup>F NMR studies have shown its presence in the drug formulation and the presence of fluoroacetate (1) in the urine of patients that have been exposed to the drug suggests that fluoroacetaldehyde (40) is indeed oxidised *in vivo*. Therefore during this project great care was taken in the handling and manipulation of fluoroacetaldehyde (40), which is hazardous both due to its toxicity and volatile nature.

Studies into the synthesis of fluoroacetaldehyde (40) were initiated in Durham by a former member of the group, Dr J. Fuchser. The oxidation of 2-fluoroethanol (71) was investigated by enzymatic methods and with a variety of chemical oxidants. It emerged that the most efficient oxidant was pyridinium dichromate and this was adopted for these subsequent studies.

Fluoroacetaldehyde (40) was synthesised by oxidation of 2-fluoroethanol (71) with pyridinium dichromate (PDC). PDC was suspended in dichloromethane, 2-fluoroethanol (71) was added and the solution was heated to reflux for 16 hours. After



this time the solution was allowed to cool and the reflux condenser replaced with a vigreux distillation apparatus. The solution was then distilled to dryness, leaving PDC as a solid residue. Efforts to separate fluoroacetaldehyde (**40**) from 2-fluoroethanol (**71**) and DCM by distillation proved to be unsuccessful. Due to its toxic and volatile nature, the DCM solution containing both fluoroacetaldehyde (**40**) and 2-fluoroethanol (**71**) was extracted into water to form the less volatile hydrate. This generated an aqueous solution of 2-fluoroethanol (**71**) and the hydrate of fluoroacetaldehyde (**40**). PDC oxidation did not prove efficient under these conditions stopping at about a 20 % conversion. Efforts were made to optimise this by increasing the amount of oxidant and the reaction time, however the conversion remained at 20 %. Confirmation that fluoroacetaldehyde (**40**) was indeed prepared by this method was provided by analysis of its 2,4-dinitrophenylhydrazine (DNP) derivative (**144**).

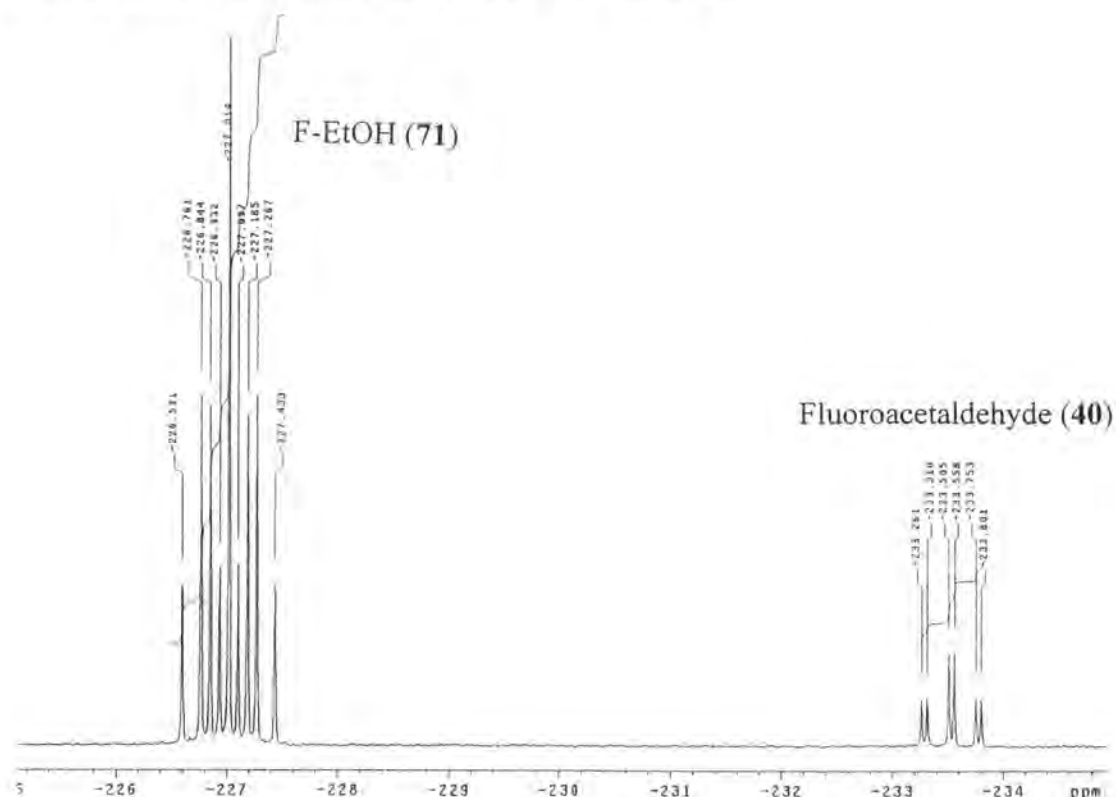


**Fig. 3.1:**  $^{19}\text{F}$  NMR spectrum of fluoroacetaldehyde (**40**) and 2-fluoroethanol (**71**).

Aqueous solutions of fluoroacetaldehyde hydrate (**40**) were routinely prepared, at a final concentration of 40 mM. These samples also contained 2-fluoroethanol (**71**) (160 mM) as a by-product of the synthesis as discussed above. The concentrations were deduced by  $^{19}\text{F}$  NMR analysis, based on complete recovery of all fluorinated species. This appeared reasonable as the PDC and aqueous layer were routinely checked by  $^{19}\text{F}$  NMR and contained no fluorine resonances.

2-Fluoroethanol (71) was confirmed as the contaminant by spiking the solution with commercial 2-fluoroethanol (71) and subsequent  $^{19}\text{F}$  NMR analysis. Likewise the concentration of fluoroacetaldehyde (40) and 2-fluoroethanol (71) was confirmed by adding a known quantity of fluoroacetone (39) to the sample and comparing the integrals of the resonances in the  $^{19}\text{F}$  NMR spectrum. Gravimetric analysis of the DNP derivative of fluoroacetaldehyde (144) did not prove to be a reliable method for determining fluoroacetaldehyde (40) concentration

Studies by Reid<sup>105</sup> have already shown that 2-fluoroethanol (71) is not involved in fluorometabolite biosynthesis, either directly or through defluorination. Therefore, this solution of fluoroacetaldehyde (40) and 2-fluoroethanol (71) was used in the following whole cell and cell free experiments.

## 3.2 Whole cell feeding studies with fluoroacetaldehyde

### 3.2.1 Preliminary studies

#### 3.2.1.1 Introduction

To assess whether fluoroacetaldehyde (**40**) has a role in fluorometabolite biosynthesis, the fluoroacetaldehyde solution was administered to resting cells of *Streptomyces cattleya*. Immediately prior to this study, fluoroacetaldehyde (**40**) (as an aqueous solution, **section 3.1.1**) was fed to the bacterium by co-workers in Belfast.<sup>107</sup> Those resting cell experiments suggested that there was a rapid metabolism of fluoroacetaldehyde (**40**) to fluoroacetate (**1**). Importantly, those studies also demonstrated that 2-fluoroethanol (**71**) is not involved in fluorometabolite biosynthesis, either directly or through defluorination and *de novo* biosynthesis from fluoride.

It was decided to develop these experiments in Durham and follow any metabolism of fluoroacetaldehyde (**40**) by <sup>19</sup>F NMR in real time.

#### 3.2.1.2 Results and discussion

Fluoroacetaldehyde (**40**) (2.0 mM) was administered to resting cells of *Streptomyces cattleya*. As this study utilised the fluoroacetaldehyde (**40**) solution prepared in **section 3.1.1** it contained 2-fluoroethanol (**71**), and under these conditions the final concentration of **71** was 10 mM.

An aliquot was removed every 10 minutes and the cells were removed by microcentrifugation. The sample was then immediately analysed by <sup>19</sup>F NMR. Samples were stored at 4 °C prior to a high field <sup>19</sup>F NMR analysis that was compared with the original spectra, to ensure that there had been no subsequent metabolism.

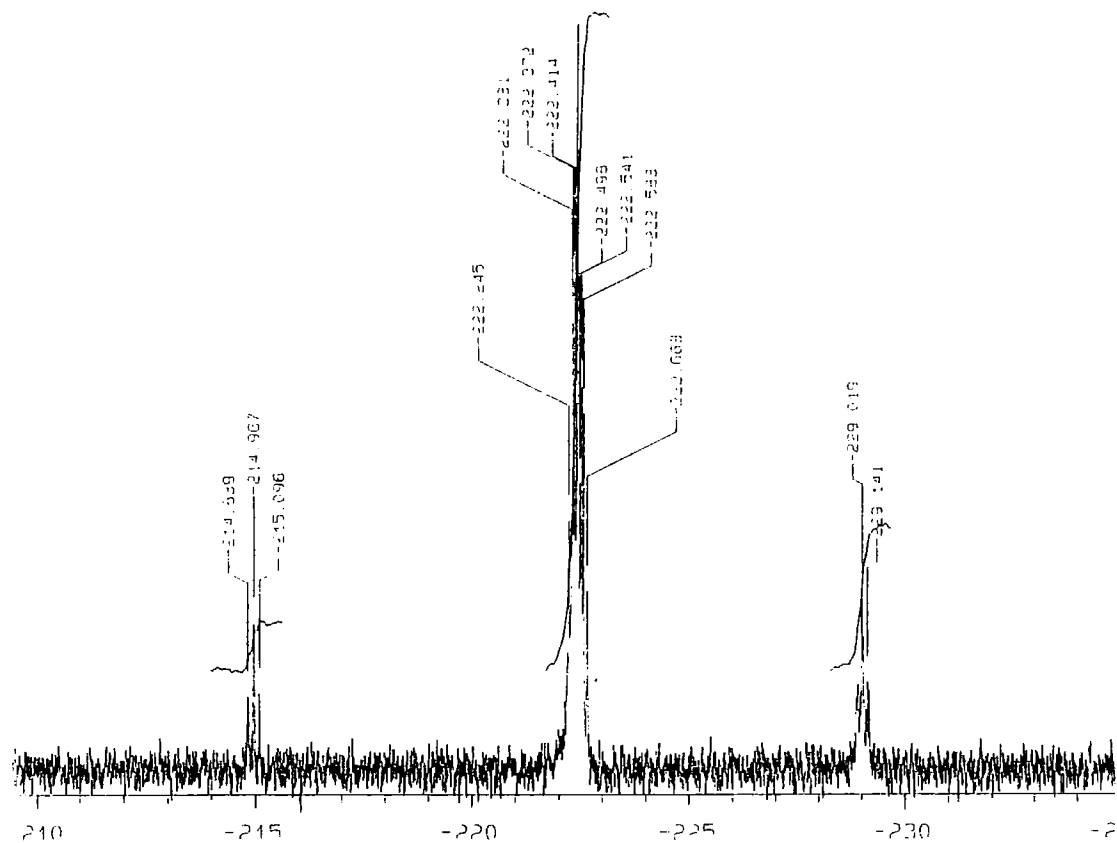


**Fig. 3.2:**  $^{19}\text{F}$  NMR, fluoroacetaldehyde (40) (2.0 mM) fed to *Streptomyces cattleya*, Time = 0 minutes

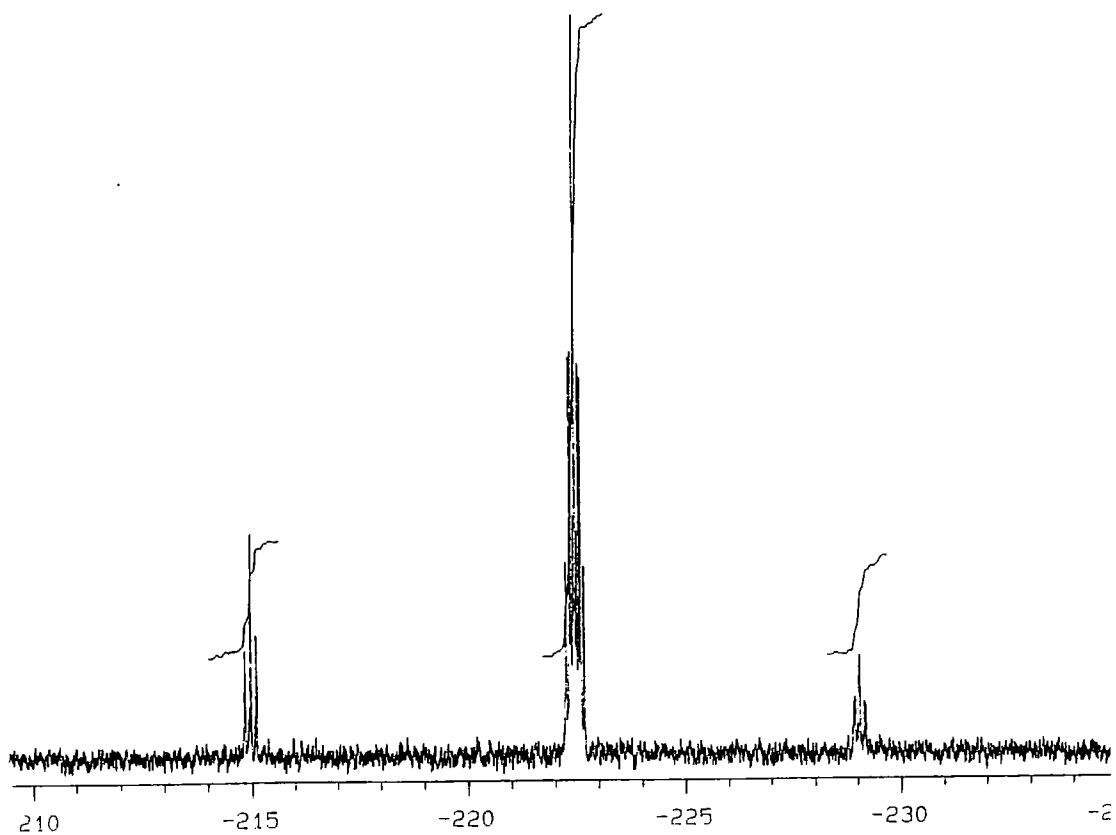


**Fig. 3.3:**  $^{19}\text{F}$  NMR, fluoroacetaldehyde (40) (2.0 mM) fed to *Streptomyces cattleya*, Time = 10 minutes

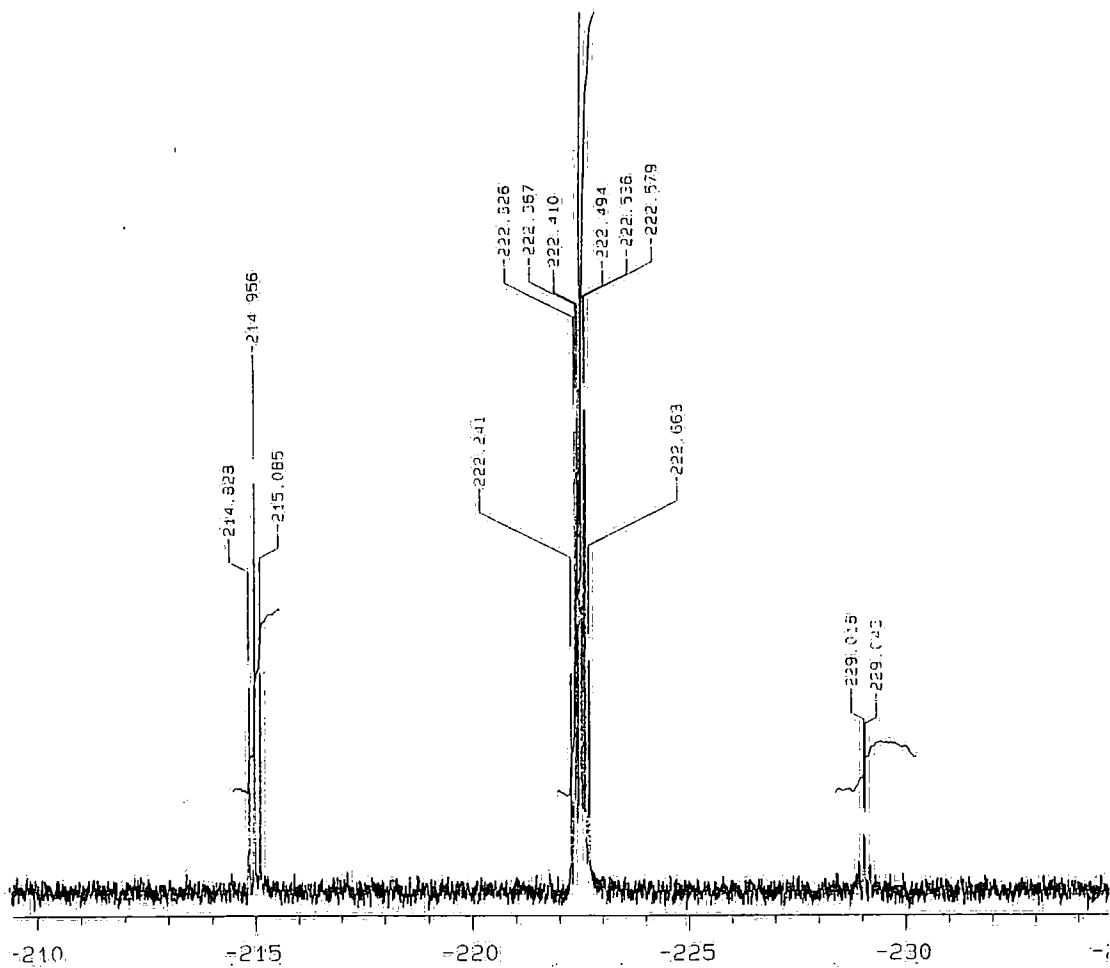


Fig. 3.4:  $^{19}\text{F}$  NMR, fluoroacetaldehyde (40) (2.0 mM) fed to *Streptomyces cattleya*, Time = 30 minutes

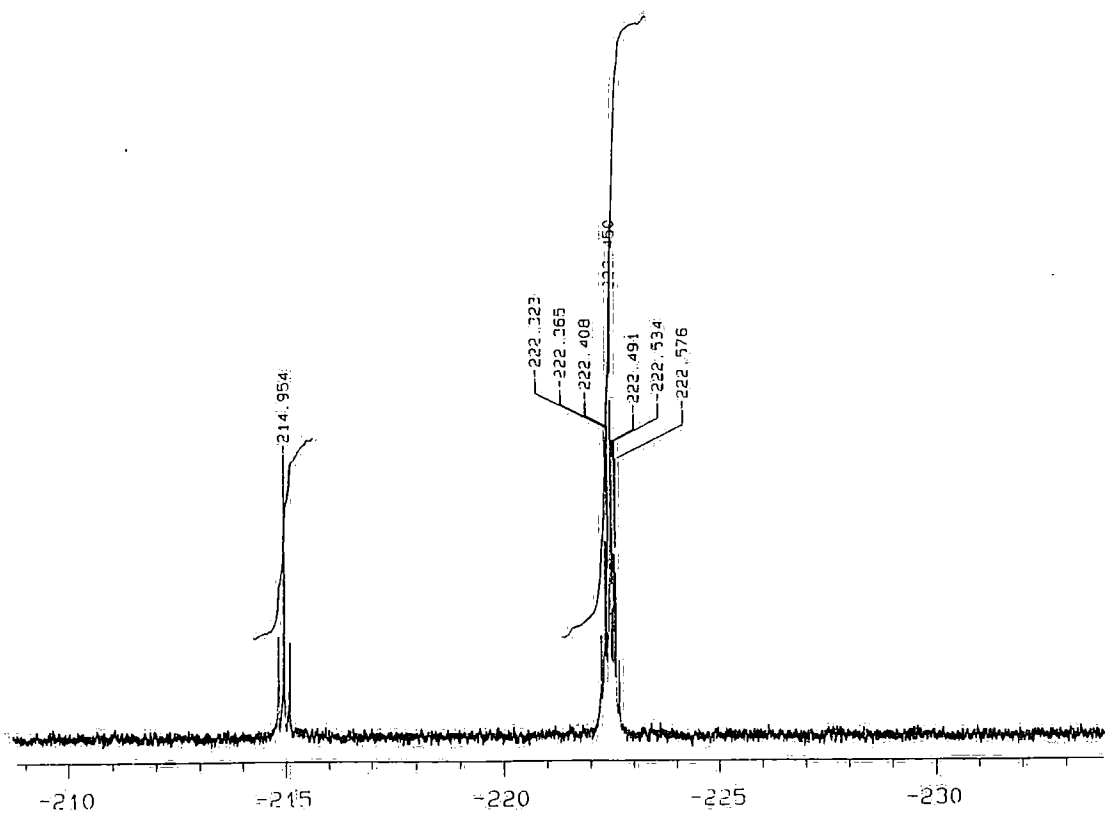
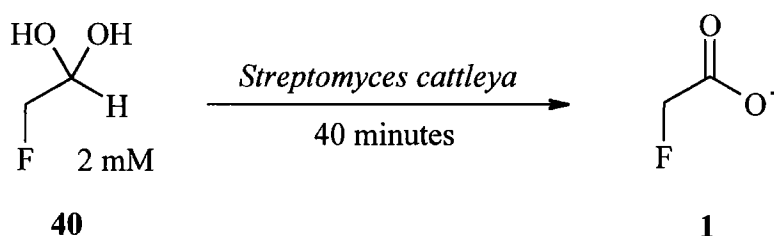


Fig. 3.5:  $^{19}\text{F}$  NMR, fluoroacetaldehyde (40) (2.0 mM) fed to *Streptomyces cattleya*, Time = 40 minutes

It appears that resting cells of the bacterium are capable of rapidly metabolising fluoroacetaldehyde (**40**) to fluoroacetate (**1**), as monitored by  $^{19}\text{F}$  NMR (see Fig 3.2 to Fig. 3.5). At the first time point ( $T = 0$  minutes), there is a significant level of conversion (25 %). It is worth noting that there is no fluoroacetate (**1**) in the fluoroacetaldehyde (**40**) solution added to the bacterium at the outset, and there is no conversion when the fluoroacetaldehyde (**40**) solution was added to MES buffer without cells in a control experiment. Therefore this metabolism is mediated by the bacterium. The conversion continues quite rapidly and utilises all of the 2 mM fluoroacetaldehyde (**40**) within 40 minutes under these conditions.

Fluoroacetaldehyde (**40**) is the first organofluorine compound that has been shown to be converted to either of the fluorometabolites by *Streptomyces cattleya*.



**Fig. 3.6:** Conversion of fluoroacetaldehyde (**40**) to fluoroacetate (**1**), by resting cells of *S. cattleya*.

### 3.2.2 Oxygen requirements of fluoroacetaldehyde (**40**) metabolism

The conversion of fluoroacetaldehyde (**40**) to fluoroacetate (**1**) is formally an oxidation process. Enzymatically this could be mediated by either an aldehyde dehydrogenase, aldehyde oxidase or aldehyde mono-oxygenase.<sup>123</sup> It appeared appropriate to study the dependence of this biotransformation on molecular oxygen, as this can be suggestive of the process that is occurring. To do this the conversion was studied both under a nitrogen atmosphere and in an  $^{18}\text{O}_2$  enriched atmosphere (section 3.2.2.1 & 3.2.2.2)

#### 3.2.2.1 Fluoroacetaldehyde (**40**) metabolism under nitrogen

Flavin mediated oxidase and mono-oxygenase and also  $\text{P}_{450}$  oxidative processes require molecular oxygen, whereas dehydrogenase mediated reactions do not as in the latter case molecular oxygen is not required for co-factor regeneration.

Fluoroacetaldehyde (**40**) was incubated in resting cells of the bacterium under a nitrogen atmosphere. This was done by taking the cell suspension and purging it with a stream of N<sub>2</sub> gas before it was stoppered with a rubber septum. Prior to this the MES buffer used in the experiment was degassed by three subsequent freeze-thaw cycles under a high vacuum. Fluoroacetaldehyde (**40**), again at a final concentration of 2 mM (i.e. with 10 mM 2-fluoroethanol (**71**) present), was added and aliquots were removed every 10 minutes as before.

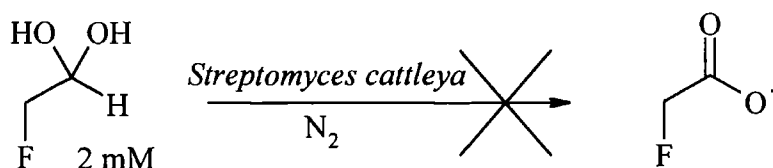


**Fig. 3.7:** Fluoroacetaldehyde (**40**) under a N<sub>2</sub> atmosphere, in resting cells of *S. cattleya*.

Subsequent <sup>19</sup>F NMR analysis demonstrated that there was absolutely no conversion of fluoroacetaldehyde (**40**) to fluoroacetate (**1**) when oxygen was excluded. Simultaneous control experiments demonstrated that these cells did convert fluoroacetaldehyde (**40**) to fluoroacetate (**1**) when exposed to the air.

### 3.2.2.2 Fluoroacetaldehyde (**40**) metabolism under <sup>18</sup>O<sub>2</sub>

When an oxidative biotransformation is conducted under an atmosphere of <sup>18</sup>O<sub>2</sub> then the assimilation of label into the substrate can be studied. Both mono-oxygenase and oxidase flavin catalysed processes would be expected to introduce label from <sup>18</sup>O<sub>2</sub> into the species that is being oxidised.<sup>123</sup>

To incubate the bacterium in an <sup>18</sup>O<sub>2</sub> atmosphere a specialist apparatus had to be designed and assembled. Essentially the glassware set up was the same as that for an atmospheric pressure hydrogenation. This involved a measuring cylinder, closed at both ends, which drains below to a reservoir of water and which has three taps at the top, for vacuum, gas inlet and gas outlet. The resting cell experiment itself was conducted in a 100 ml Erlenmeyer flask with a tapped side arm. Before the bacterium was incubated under the <sup>18</sup>O<sub>2</sub> atmosphere, a trial run was conducted in which <sup>16</sup>O<sub>2</sub> was used. The cell suspension, in previously degassed buffer, was subjected to a light vacuum and the

headspace above the cells filled with  $N_2 / {}^{16}O_2$  (1:1) gas, from the measuring cylinder described above. Fluoroacetaldehyde (**40**) solution (1 ml, 2 mM final concentration) was added by injection through the septum that seals the Erlenmeyer flask. The tap on the side arm was closed and the flask placed on the orbital shaker. After one hour the experiment was terminated and  ${}^{19}F$  NMR analysis of the resultant supernatant demonstrated that all of the fluoroacetaldehyde (**40**) had been converted to fluoroacetate (**1**).

The experiment was then repeated, this time using  ${}^{18}O_2$  gas again mixed with  $N_2$  in a 1:1 ratio, and incubated for one hour.  ${}^{19}F$  NMR analysis confirmed that conversion had occurred and the resultant fluoroacetate (**1**) was analysed by GCMS. That analysis showed that there was no incorporation at all of oxygen-18 into fluoroacetate (**1**).

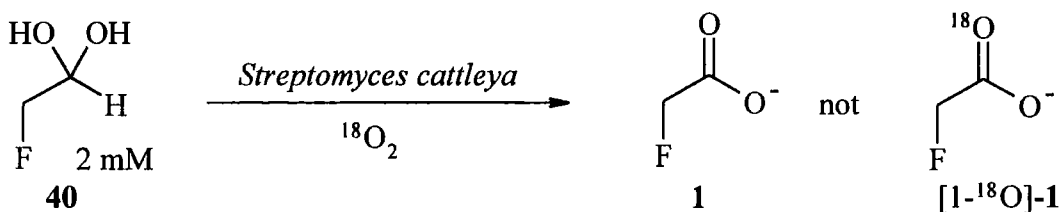


**Fig. 3.8:** Incubation of fluoroacetaldehyde (**40**) in an  ${}^{18}O_2$  atmosphere, with resting cells of *S. cattleya*.

### 3.2.2.3 Conclusions

The inability of *Streptomyces cattleya* to convert fluoroacetaldehyde (**40**) in the absence of molecular oxygen suggests that oxygen is required for the biotransformation. This would appear to rule out a process mediated by an aldehyde dehydrogenase. Flavin mediated enzymatic processes require molecular oxygen, however  ${}^{18}O_2$  labelling studies show that label is not assimilated into the carboxylate group of fluoroacetate (**1**) and this appears to rule out the involvement of a flavin mediated oxidase or mono-oxygenase process. Superficially these results are contradictory. Further experimentation was required to delineate the reaction type and this was done in cell free experiments, which are discussed in detail later in this chapter.



### 3.3 Fluoroacetaldehyde in fluorometabolite biosynthesis

It has been demonstrated that fluoroacetaldehyde (40) is biotransformed to fluoroacetate (1) by *Streptomyces cattleya*, although whether this biotransformation has a role in the biosynthesis of fluoroacetate (1) is unclear. Therefore the biotransformation of fluoroacetaldehyde (40) to fluoroacetate (1) has been studied in other *Streptomyces* spp.

#### 3.3.1 Fluoroacetaldehyde (40) metabolism by other *Streptomyces* spp.

The oxidation of fluoroacetaldehyde (40) to fluoroacetate (1) observed in *S. cattleya* may not be an integral part of fluorometabolite biosynthesis, but merely a peripheral activity mediated by an indiscriminate enzyme on an unusual substrate. It was therefore decided to incubate fluoroacetaldehyde (40) with different *Streptomyces* spp. to observe any conversion to fluoroacetate (1). The strain that produces the ionophoric antibiotic monensin (145),<sup>124</sup> *Streptomyces cinnamonensis*, was available in the laboratory and so it was decided to study fluoroacetaldehyde (40) metabolism in that organism.

##### 3.3.1.1 Growth of *Streptomyces cinnamonensis*

*Streptomyces cinnamonensis* was grown from spores that had been stored at -15 °C, suspended in a glycerol matrix. Once thawed, these spores were used to inoculate petri dishes containing a complex media (yeast and malt extract based, section 5.2.3), and were grown at 29.5 °C for 10 days. The resultant vegetative mycelium was then used to inoculate liquid complex media and the cultures were incubated for 14 days at 32 °C on an orbital shaker. The liquid complex media used was the same as that used for the biosynthetic studies carried out to evaluate monensin (145) biosynthesis.<sup>124,125</sup> This medium contains both a high level of iron ( $\text{FeSO}_4 \cdot 7\text{H}_2\text{O}$ , 5.5 g.l<sup>-1</sup>) and soybean flour (15.0 g.l<sup>-1</sup>). The latter did not dissolve completely, even after autoclaving, but was finely dispersed in the media. However, the bacterium grew as described in the previous publications<sup>125</sup> and these cells were satisfactory for assessing the biotransformation.

### 3.3.1.2 Administering fluoroacetaldehyde (40) to resting cells of *Streptomyces cinnamomensis*

The cells were harvested, then washed with MES buffer as for *Streptomyces cattleya*, and they were suspended in buffer to the same cell density (0.176 g wet wt. / ml). Two experiments were carried out, one at a high density and the other at a low density of cells. The high-density cell experiment was set up by adding an aqueous solution of fluoroacetaldehyde (40) (1 ml, final concentration 2 mM) to the cell suspension (22 ml) and the resting cells were incubated on an orbital shaker. The low-density experiment was conducted at the same cell density as in the whole cell studies with *S. cattleya*. MES buffer (17 ml) and fluoroacetaldehyde (40) (1 ml) were added to the cell suspension of *S. cinnamomensis* (5 ml). An aliquot (1 ml) was removed every 20 minutes over one hour and the cells were then removed by microcentrifugation and the supernatants were analysed by  $^{19}\text{F}$  NMR.

Time / minutes	20	40	60
low density cells	0	0	0
high density cells	0	0	12

**Table 3.1:** Percentage conversion of fluoroacetaldehyde (40) to fluoroacetate (1) by resting cells of *Streptomyces cinnamomensis*.

The results of the conversion, as measured by  $^{19}\text{F}$  NMR are tabulated above (Table 3.1). Fluoroacetaldehyde is not metabolised by *Streptomyces cinnamomensis* as efficiently as that observed in *Streptomyces cattleya*. In the aliquots removed after 20 minutes and 40 minutes there was no conversion at all to fluoroacetate (1) in either experiment. In the aliquots removed after 60 minutes there is a low level of conversion (12 %) to fluoroacetate (1) in the high-density experiment but no conversion in the low-density experiment.

Although only one additional strain had been studied, this experiment suggests that it is unlikely that the enzyme responsible for fluoroacetaldehyde (40) oxidation is ubiquitous in the Streptomycetes. Although there was a small level of conversion to fluoroacetate (1) at high cell density, this represents a very low level of activity compared with that observed in *S. cattleya*.

### 3.3.2 Fluoroacetaldehyde (40): incubation with alanine (146) and serine (54)

The purpose of this experiment was to probe the role of fluoroacetaldehyde (40) in 4-fluorothreonine (2) biosynthesis. It was anticipated that fluoroacetaldehyde (40) may undergo a condensation reaction with an as yet unidentified species, to produce 4-fluorothreonine (2). This obviously mirrors the suggestion of Sanada *et al.*<sup>72</sup> that 4-fluorothreonine (2) could originate from a condensation between fluoroacetaldehyde (40) and glycine (86). However, it has been shown in previous studies that positions C-1 and C-2 of 4-fluorothreonine (2) are readily labelled by C<sub>3</sub> primary metabolites, such as serine (54), alanine (146) and pyruvate (10), but not directly from glycine (86).<sup>107,106</sup>

The oxidation of fluoroacetaldehyde (40) to fluoroacetate (1) is rapid in whole cells of *S. cattleya*. Clearly, if the concentration of the substrate for the condensation to 4-fluorothreonine (2) is low, then only fluoroacetate (1) will be apparent.

As it appears that fluoroacetaldehyde (40) is not oxidised in the absence of molecular oxygen, it appeared appropriate to repeat those experiments, in degassed buffer supplemented with alanine (146) and serine (54), as these are known carbon sources for C-1 and C-2 of 4-fluorothreonine (2). This was anticipated to suppress oxidation and promote the putative condensation reaction.

#### 3.3.2.1 Experimental considerations

For each amino acid two experiments were conducted. In the first experiment, cell suspension (5 ml), buffer and amino acid (final concentration 10 mM) were purged with N<sub>2</sub> (5 minutes) and sealed before the addition of fluoroacetaldehyde (40) (2 mM). Aliquots were removed for analysis at 1 hour, 3 hours and 48 hours. The cells were removed at each time point by microcentrifugation. In the second experiment the amino acid (10 mM) was incubated in the cell suspension (5 ml) and buffer for 2 hours, whilst exposed to air. This was anticipated to allow metabolism for the synthesis the putative condensation adduct. After 2 hours the cell suspensions were purged in a stream of N<sub>2</sub> (5 minutes), and the flasks were sealed and fluoroacetaldehyde (40) (2 mM) added. Aliquots were collected 1 hour, 3 hours and 48 hours after this time point and the cells were removed by microcentrifugation. The resultant supernatants were then analysed by <sup>19</sup>F NMR as discussed below.

### ***3.3.2.2 Results and discussion***

In none of the 4 experiments (alanine (146) and serine (54), with and without pre-incubation of the amino acid) was any 4-fluorothreonine (2) observed by  $^{19}\text{F}$  NMR. In the samples that had been incubated for 48 hours there was an observable level of conversion of fluoroacetaldehyde (40) to fluoroacetate (1), although this is most likely a consequence of molecular oxygen leaking through the septum, perhaps when aliquots were removed from these experiments. The fact that 4-fluorothreonine (2) production was not observed in this set of experiments may be because fluoroacetaldehyde (40) does not have a role in 4-fluorothreonine (2) biosynthesis. Alternatively incubating resting cells of the bacterium under  $\text{N}_2$  may adversely affect peripheral metabolism to such an extent that the adduct for condensation is not produced.

### ***3.3.3 The synthesis and feeding of [1- $^2\text{H}$ ]-fluoroacetaldehyde (147)***

Studies in Durham had concentrated on following fluoroacetaldehyde (40) metabolism by  $^{19}\text{F}$  NMR and as such the whole cell conversion of fluoroacetaldehyde (40) to fluoroacetate (1) has been studied in detail (section 3.2). The biosynthesis of 4-fluorothreonine (2) from fluoroacetaldehyde (40) had not however been demonstrated by  $^{19}\text{F}$  NMR. As well as conducting feeding experiments in Durham, aqueous solutions of fluoroacetaldehyde (40) were sent to our collaborators in Belfast. Murphy<sup>107</sup> studied the metabolism of fluoroacetaldehyde (40) and quantified production of fluoroacetate (1) and 4-fluorothreonine (2) by GCMS and HPLC respectively. In a key experiment the production of 4-fluorothreonine (2) by resting cells of the bacterium incubated with fluoroacetaldehyde (40) was demonstrated, as summarised in Table 3.2.



Treatment Resting cells +	Incubation time / hours	4-fluorothreonine (2) / mM	fluoroacetate (1) / mM
NaF (2 mM)	0	< 0.01	< 0.01
	1	0.02	0.01
	3	0.03	0.05
Resting cells alone	0	< 0.01	< 0.01
	1	< 0.01	< 0.01
	3	0.02	0.01
Fluoroacetaldehyde (40) (1.9 mM) <sup>1</sup>	0	< 0.01	0.16
	1	0.01	1.74
	3	0.03	1.88
Fluoroacetaldehyde (40) (3.8 mM) <sup>2</sup>	0	< 0.02	0.27
	1	0.02	1.46
	3	0.04	3.71

**Table 3.2:** Fluorometabolite production resultant from feeding fluoroacetaldehyde (40) to resting cells of *Streptomyces cattleya*, Murphy.<sup>107</sup>

The level of 4-fluorothreonine (2) production in this system is low. However, control experiments and monitoring the production of 4-fluorothreonine (2) by HPLC demonstrated that the amino acid production is increased on addition of fluoroacetaldehyde (40). Previous studies have demonstrated that the bacterium can defluorinate both fluorometabolites and the resultant fluoride is then involved in *de novo* fluorometabolite biosynthesis. However, the levels of 4-fluorothreonine (2) after 1 hour (Table 3.2) were above such background levels and suggest that this is not due to defluorination of fluoroacetate (1) to liberate fluoride, but is a direct response to fluoroacetaldehyde additions.

It was necessary to demonstrate unambiguously whether fluoroacetaldehyde (40) is involved in 4-fluorothreonine (2) biosynthesis. To study that [1-<sup>2</sup>H]-fluoroacetaldehyde

<sup>1</sup> contains 18 mM 2-fluoroethanol <sup>2</sup> contains 36 mM 2-fluoroethanol

(147) was synthesised and incubated with resting cells of *Streptomyces cattleya*. Clearly if [1-<sup>2</sup>H]-fluoroacetaldehyde (147) is involved directly in 4-fluorothreonine (2) biosynthesis then [3-<sup>2</sup>H]-4-fluorothreonine (2) will be generated by the experiment.

### 3.3.3.1 Synthesis of [1-<sup>2</sup>H]-fluoroacetaldehyde (147)

[1,1-<sup>2</sup>H<sub>2</sub>]-2-Fluoroethanol (148) can be envisaged as the product of reduction of an ester of fluoroacetate (149) using a deuterium labelled reducing agent (see Fig. 3.9). [1-<sup>2</sup>H]-Fluoroacetaldehyde (147) could then be prepared by oxidation of the resultant [1,1-<sup>2</sup>H<sub>2</sub>]-2-fluoroethanol (148).

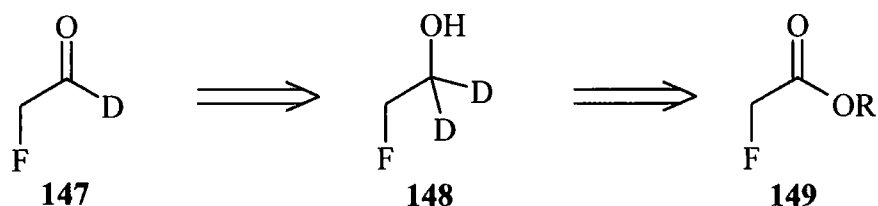


**Fig. 3.9:** Retrosynthetic analysis of [1-<sup>2</sup>H]-fluoroacetaldehyde (147).

A potential problem in the synthesis of [1,1-<sup>2</sup>H<sub>2</sub>]-2-fluoroethanol (148) is the isolation of 2-fluoroethanol (71), which is a polar species of low molecular mass. A previous study in the group had approached the synthesis of [1-<sup>13</sup>C, 1,1-<sup>2</sup>H<sub>2</sub>]-ethanol (151) by the reduction of the phenylphenacyl derivative of [1-<sup>13</sup>C]-acetate (150) using LiAlD<sub>4</sub>,<sup>126</sup> following a method from Cane *et al.*<sup>127</sup> Therefore it was decided to adapt this methodology in our approach to [1,1-<sup>2</sup>H<sub>2</sub>]-2-fluoroethanol (148).

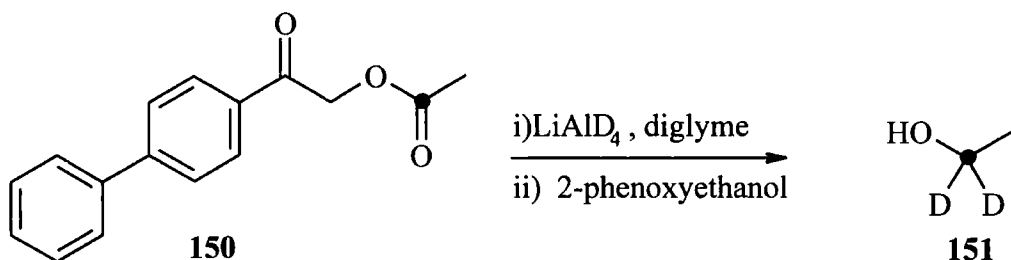


**Fig. 3.10:** Synthesis of [1-<sup>13</sup>C, 1,1-<sup>2</sup>H<sub>2</sub>]-ethanol (151), Rogers.<sup>126</sup>

The key feature of this method is that the resultant ethanol (151) is the lowest boiling component of the solvent and product mixture. The reaction was carried out in a high boiling solvent (in this case diglyme) and the reaction was quenched with 2-phenoxyethanol (152). This enables 151 to be collected by heating the solution to

50 °C, and collecting the vapour. In that case the labelled [1-<sup>13</sup>C,1,1-<sup>2</sup>H<sub>2</sub>]-ethanol (**151**) was not isolated but its tosylate was generated immediately *in situ*, and the yield over these two steps was 27 %.

*para*-Phenylphenacyl fluoroacetate (**102**) is the derivative already used for the GCMS analysis of fluoroacetate (**1**), and in previous <sup>14</sup>C labelling studies.<sup>99</sup> Therefore a method of synthesis was already optimised. The adduct was formed by dissolving *para*-phenylphenacyl bromide (**101**) in a 1:1 mixture of acetonitrile and benzene and then suspending sodium fluoroacetate (**1**) in the resultant solution. A catalytic amount of 18-crown-6 was added and the solution was heated at reflux for 16 hours. The resultant solution was washed with water and the solvent removed to yield the product (**102**) in 89 % as a yellow solid.

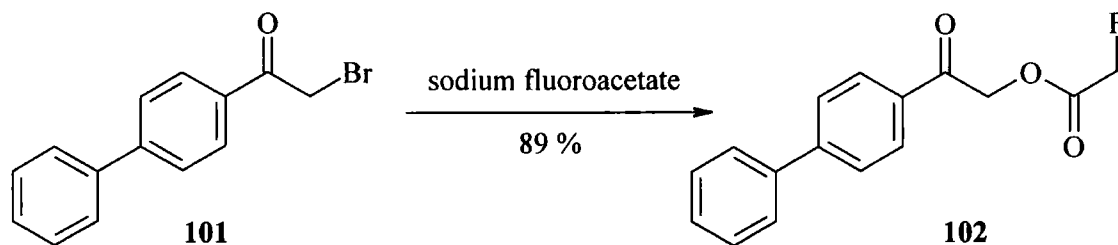


**Fig. 3.11:** Synthesis of *para*-phenylphenacyl fluoroacetate (**102**); in acetonitrile / benzene, 1:1, 18-crown-6, reflux, 16 hours.

Studies then concentrated on the reduction of this adduct (**102**) using LiAlH<sub>4</sub>. Initially the method of Rogers<sup>126</sup> was adapted, whereby *para*-phenylphenacyl fluoroacetate (**102**) was suspended in diglyme and was added slowly to a suspension of LiAlH<sub>4</sub> in diglyme that had been cooled to -10 °C. The solution was then stirred at room temperature and then cooled in an ice bath such that the reaction could be quenched using 2-phenoxyethanol (**152**). Attempts then to distil the 2-fluoroethanol (**71**) out of the resultant solution proved to be difficult. As 2-fluoroethanol (**71**) boils at 103 °C, an attempt was made to distil this product from the reaction solution through a vigreux column. A small quantity (90 mg) was collected that proved to be a mixture of 2-fluoroethanol (**71**) and diglyme. <sup>1</sup>H NMR analysis indicated that the sample was 62 % 2-fluoroethanol (**71**), which in this reaction gave a yield of 9.8 %. The sample contained diglyme and so the next step was conducted to establish if the PDC oxidation from 2-fluoroethanol (**71**) to fluoroacetaldehyde (**40**) could proceed in the presence of

this contaminant. The reaction proceeded smoothly and the diglyme did not inhibit the transformation. Fluoroacetaldehyde (**40**) was recovered in 12.5 % yield (as judged by  $^{19}\text{F}$  NMR).

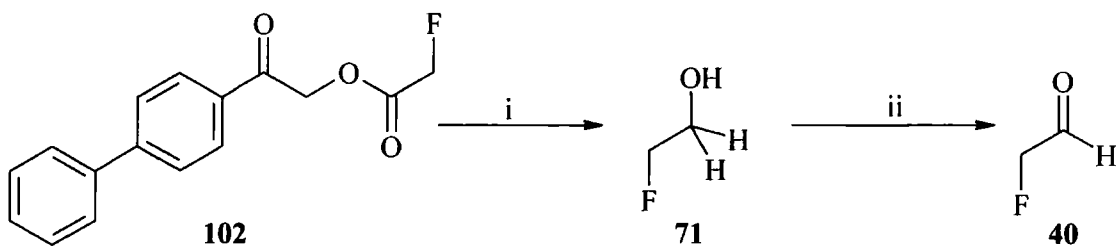


**Fig. 3.12:** Synthesis of fluoroacetaldehyde (**40**) from phenylphenacyl fluoroacetate (**102**); i)  $\text{LiAlH}_4$ , diglyme, 4 hours then phenoxyethanol (**152**), 9.8 %; ii) PDC, DCM, 16 hours, 12.5 %

This initial investigation was promising, however the yields required optimisation. As the  $\text{LiAlH}_4$  reduction did not proceed in good yield it was decided to try to improve this step and investigate alternate methods for the preparation of  $[1,1\text{-}^2\text{H}_2]$ -2-fluoroethanol (**148**). Different methods of collecting the 2-fluoroethanol (**71**) were explored. Rogers<sup>126</sup> synthesis of labelled ethanol (**151**) was adapted, whereby the quenched reaction was heated to below the boiling point of fluoroethanol (**71**) and a stream of  $\text{N}_2$  passed the vapours through into a cold trap. However this method failed to improve the recovery of 2-fluoroethanol (**71**), even when heated to 80 °C for 22 hours. The reaction solvent was also changed from diglyme to tetraglyme (boiling points: 162 °C vs. 276 °C) as this boils at a higher temperature and should ensure that less solvent was distilled over with the 2-fluoroethanol (**71**). However, in the event the resultant 2-fluoroethanol (**71**) was still contaminated with the tetraglyme.

Samples of  $[1\text{-}^2\text{H}]$ -fluoroacetaldehyde (**147**) were prepared for feeding experiments as follows. *para*-Phenylphenacyl fluoroacetate (**102**) was reduced by  $\text{LiAlD}_4$  in tetraglyme and the reaction was quenched with 2-phenoxyethanol (**152**). The resultant  $[1,1\text{-}^2\text{H}_2]$ -2-fluoroethanol (**148**) was distilled out of the reaction mixture. The reaction mixture was cooled and DCM (5 ml) added to the residual. The resultant solution was distilled and  $^{19}\text{F}$  NMR demonstrated that more  $[1,1\text{-}^2\text{H}_2]$ -2-fluoroethanol (**148**) was carried over. This procedure was repeated a further two times, until no more fluorine signals were observed in  $^{19}\text{F}$  NMR of the distillate. This method maximised the



[1,1-<sup>2</sup>H<sub>2</sub>]-2-fluoroethanol (**148**) recovery, although an accurate yield could not be calculated as the final mass was now unknown.

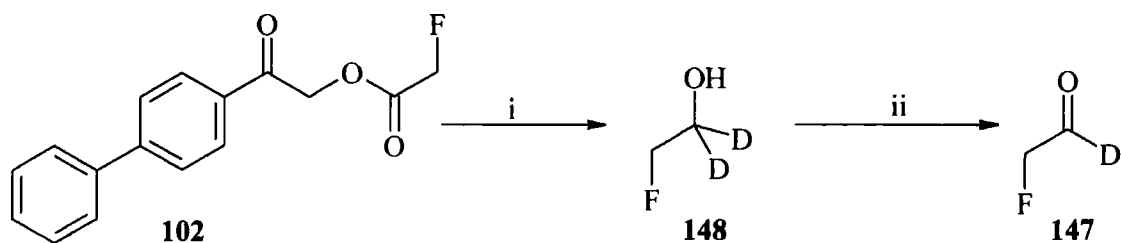


**Fig. 3.13:** Synthesis of [1-<sup>2</sup>H]-fluoroacetaldehyde (**147**) from *para*-phenylphenacyl fluoroacetate (**102**); i) LiAlD<sub>4</sub>, tetraglyme, then 2-phenoxyethanol (**152**); ii) PDC, DCM, 20 %.

PDC was added to the DCM that had been distilled from the reaction solution, to oxidise [1,1-<sup>2</sup>H<sub>2</sub>]-2-fluoroethanol (**148**) to [1-<sup>2</sup>H]-fluoroacetaldehyde (**147**). After heating under reflux for 16 hours the reaction mixture was distilled over a vigreux column and dropped into water (2 ml). The reaction mixture was also extracted with a further volume (2 ml) of water. The synthesis of [1-<sup>2</sup>H]-fluoroacetaldehyde (**147**) was confirmed by <sup>19</sup>F NMR. This method provided samples suitable for a feeding experiment with resting cells of *Streptomyces cattleya*.

**Fig. 3.14:** <sup>19</sup>F NMR of [1-<sup>2</sup>H]-fluoroacetaldehyde (**147**) and [1,1-<sup>2</sup>H<sub>2</sub>]-2-fluoroethanol (**148**).

[1,1-<sup>2</sup>H<sub>2</sub>]-2-fluoroethanol (**148**) recovery, although an accurate yield could not be calculated as the final mass was now unknown.

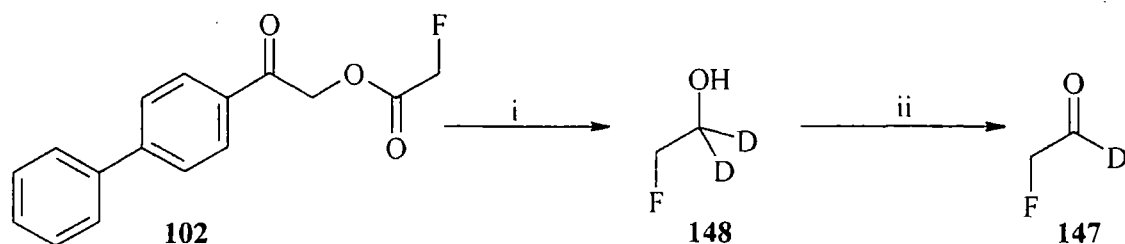


**Fig. 3.13:** Synthesis of [1-<sup>2</sup>H]-fluoroacetaldehyde (**147**) from *para*-phenylphenacyl fluoroacetate (**102**); i) LiAlD<sub>4</sub>, tetraglyme, then 2-phenoxyethanol (**152**); ii) PDC, DCM, 20 %.

PDC was added to the DCM that had been distilled from the reaction solution, to oxidise [1,1-<sup>2</sup>H<sub>2</sub>]-2-fluoroethanol (**148**) to [1-<sup>2</sup>H]-fluoroacetaldehyde (**147**). After heating under reflux for 16 hours the reaction mixture was distilled over a vigreux column and dropped into water (2 ml). The reaction mixture was also extracted with a further volume (2 ml) of water. The synthesis of [1-<sup>2</sup>H]-fluoroacetaldehyde (**147**) was confirmed by <sup>19</sup>F NMR. This method provided samples suitable for a feeding experiment with resting cells of *Streptomyces cattleya*.

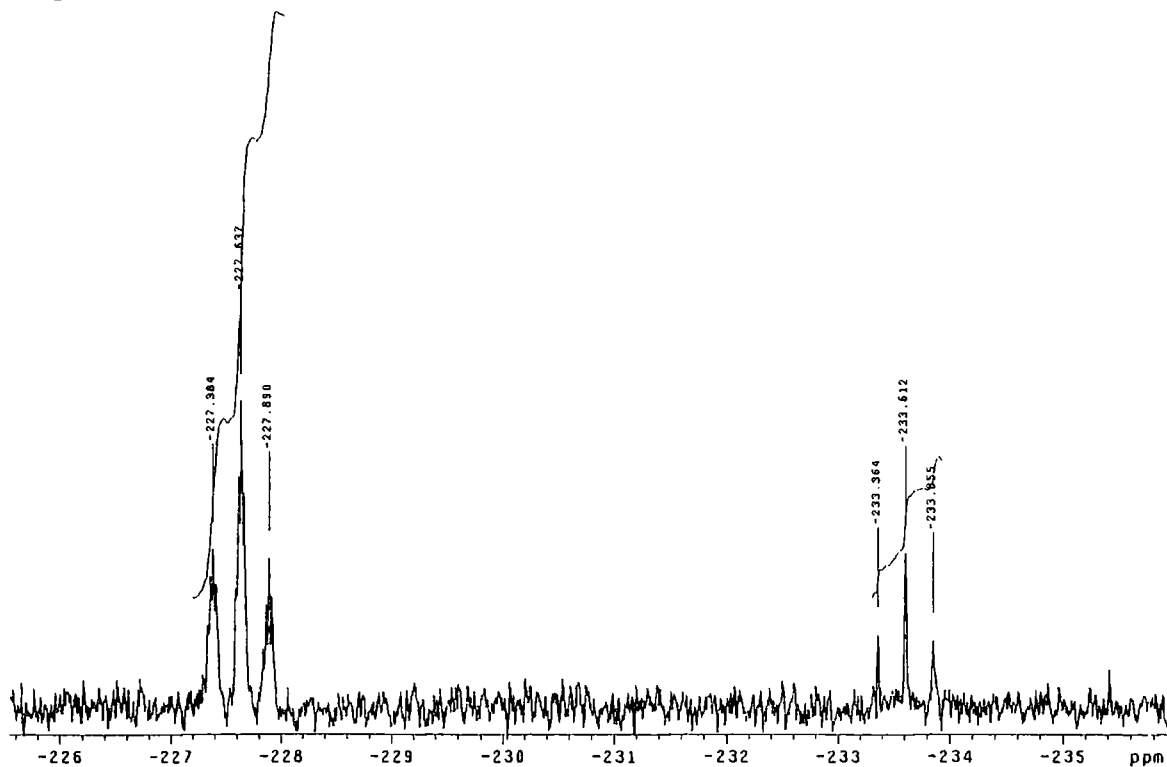


**Fig. 3.14:** <sup>19</sup>F NMR of [1-<sup>2</sup>H]-fluoroacetaldehyde (**147**) and [1,1-<sup>2</sup>H<sub>2</sub>]-2-fluoroethanol (**148**).

The method described above exploits the fact that 2-fluoroethanol (**71**) is the lowest boiling component of the product mixture after the  $\text{LiAlD}_4$  reaction is quenched. In an attempt to explore an alternative method a set of conditions was designed with 2-fluoroethanol (**71**) as the highest boiling component of the product mixture. This could be achieved by reducing ethyl fluoroacetate (**153**) in diethyl ether and quenching the reaction with ethanol (**154**).

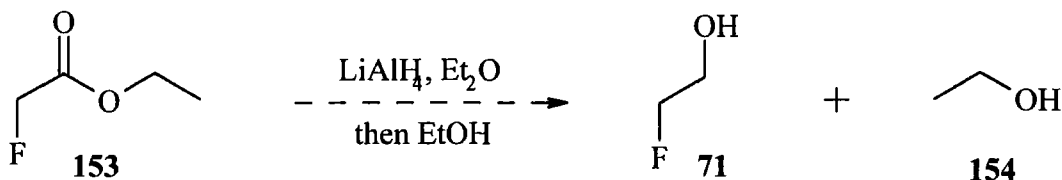


**Fig. 3.15:** Putative reduction of ethyl fluoroacetate (**153**) with  $\text{LiAlH}_4$

As the boiling point of 2-fluoroethanol (**71**) is 25 °C above that of ethanol (**154**) (103 °C vs. 78 °C), an attempt was made to separate the two alcohols by distillation. Ethyl fluoroacetate (**153**) was added slowly to a cooled suspension of  $\text{LiAlH}_4$  in ether. It was allowed to warm and stir for 4 hours before the reaction was quenched by the addition of ethanol (**154**). The solid  $\text{LiAlH}_4$  residues were removed by filtration and the solvent removed by distillation at atmospheric pressure.  $^{19}\text{F}$  NMR of the product mixture indicated that there were no fluoromethyl resonances. Treatment of  $\text{LiAlH}_4$  residues with water liberated 2-fluoroethanol (**71**) and fluoride (ratio 35:65). This indicated that during the reduction 2-fluoroethanol (**71**) is bound to the  $\text{LiAlH}_4$  residue, probably as an aluminium oxide. Further studies on this system allowed for an optimal release of 2-fluoroethanol (**71**) from the reduction. However, this route was not developed further as it proved difficult to separate ethanol (**154**) from 2-fluoroethanol (**71**). Oxidation of ethanol (**154**) generates acetaldehyde (**155**), which is known to be toxic to bacterial cells. Therefore it was judged that the sample would be unsuitable for feeding experiments as it is significantly contaminated with acetaldehyde (**155**).

### 3.3.3.2 Feeding [1-<sup>2</sup>H]-fluoroacetaldehyde (147)

[1-<sup>2</sup>H]-Fluoroacetaldehyde (147) (4 ml) was fed to resting cells of *Streptomyces cattleya* (5 ml) in MES buffer (14 ml). Aliquots were removed 0, 1, 2, 3, 4, 7.5 and 18.5 hours into the experiment. <sup>19</sup>F NMR analysis demonstrated that [1-<sup>2</sup>H]-fluoroacetaldehyde (147) was converted to fluoroacetate (1) as previously observed. The 4-fluorothreonine (2) content of each sample was then assessed by GCMS, to assess the presence of [3-<sup>2</sup>H]-4-fluorothreonine (2) and the data is presented below (Table 3.3).

time / hours	Incorporation into positions 2, 3 & 4 of 4-fluorothreonine (2) (%)		
	none (M)	single (M+1)	double (M+2)
0	nd	nd	nd
1	nd	nd	nd
2	74.8	39.7	-14.5
3	63.5	52.7	-16.4
5	51.6	51.8	-3.2
7.5	41.8	59.5	-1.3
21	86.6	13.8	-0.3
48	87.7	12.6	-0.3

**Table 3.3:** % Incorporation into positions 2, 3 & 4 of 4-fluorothreonine (2), resulting from feeding [1-<sup>2</sup>H]-fluoroacetaldehyde (147), to resting cells of *S. cattleya*.

Table 3.3 shows that the 4-fluorothreonine (2) resulting from feeding [1-<sup>2</sup>H]-fluoroacetaldehyde (147) does indeed incorporate deuterium at C-3. However the levels of 4-fluorothreonine (2) are very low. At 0 and 1 hours they were below the level that could be detected by GCMS. At 2 and 3 hours the level of 4-fluorothreonine (2) reaches the detectable threshold, and approximately half of the 4-fluorothreonine (2) contains isotopic label. After 7.5 hours the level of single label in 4-fluorothreonine (2) decreases. This is readily explained by dilution with unlabelled 4-fluorothreonine (2) arising from *de novo* biosynthesis. Early in the experiment, before all the [1-<sup>2</sup>H]-fluoroacetaldehyde (147) was consumed, [3-<sup>2</sup>H]-4-fluorothreonine (2) production accounted for the origin of a significant amount of the 4-fluorothreonine (2).

Fluoroacetate (**2**) is biosynthesised concurrently and in time becomes defluorinated liberating fluoride ions. The fluorometabolites are then biosynthesised *de novo* from fluoride and the unlabelled 4-fluorothreonine (**2**) dilutes the pool of labelled 4-fluorothreonine (**2**).

This experiment clearly supports a role for fluoroacetaldehyde (**40**) as an intermediate in 4-fluorothreonine (**2**) biosynthesis. However there is an important caveat, as the generation of low concentrations of labelled 4-fluorothreonine (**2**) could perhaps arise by the presence of an indiscriminate aldolase, acting to condense fluoroacetaldehyde (**40**) with *e.g.* glycine (**86**). In view of this a feeding experiment with [1-<sup>2</sup>H]-fluoroacetaldehyde (**147**) and [2-<sup>13</sup>C]-glycine (**91**) was conducted, in an attempt to explore the issue.

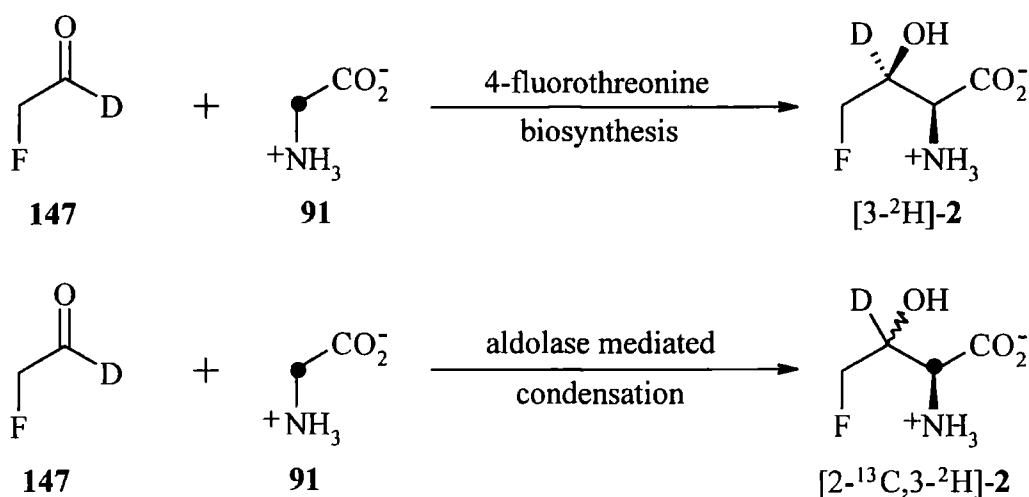


**Fig. 3.16:** Potential labelling patterns in 4-fluorothreonine (**2**) from feeding both [1-<sup>2</sup>H]-fluoroacetaldehyde (**147**) and [2-<sup>13</sup>C]-glycine (**91**), to resting cells of *S. cattleya*.

Fig. 3.16 shows the two possible outcomes that could result from feeding both [1-<sup>2</sup>H]-fluoroacetaldehyde (**147**) and [2-<sup>13</sup>C]-glycine (**91**) together. Therefore in feeding the labelled compounds together a high level of double label in 4-fluorothreonine (**2**) would indicate that fluoroacetaldehyde (**40**) condensed directly with glycine (**86**), whereas a low level of double label will lead to the opposite conclusion.

Accordingly [1-<sup>2</sup>H]-fluoroacetaldehyde (**147**) was fed to resting cells of *Streptomyces cattleya* in two separate experiments, one supplemented with 10 mM [2-<sup>13</sup>C]-glycine (**91**) and the other with 1.0 mM [2-<sup>13</sup>C]-glycine (**91**).

**Experiment 1:** Resting cells of *S. cattleya* (2.5 ml) were supplemented with [1-<sup>2</sup>H]-fluoroacetaldehyde (147) (2 ml) and 10 mM [2-<sup>13</sup>C]-glycine (91), total volume (11.5 ml).

**Experiment 2:** Resting cells of *S. cattleya* (2.5 ml) were supplemented with [1-<sup>2</sup>H]-fluoroacetaldehyde (147) (2 ml) and 1.0 mM [2-<sup>13</sup>C]-glycine (91), total volume (11.5 ml).

**Experiment 3:** Resting cells of *S. cattleya* (5 ml) were supplemented with 2 mM fluoride and 10 mM [2-<sup>13</sup>C]-glycine (91), total volume (23 ml).

Aliquots were removed at the times indicated in Table 3.4 and the cells were removed by microcentrifugation. The 4-fluorothreonine (2) content of the samples was then analysed by GCMS (4-fluorothreonine (2) production between 0 and 3 hours was too low to be determined by GCMS).

Treatment	time / hours	Incorporation into positions 2, 3 & 4 of 4-fluorothreonine (2) / %			
		none	single	double	triple
<b>Experiment 1</b>	6	46.8	29.4	22.5	1.3
<b>Experiment 2</b>	6	57.2	39.0	3.4	0.3
<b>Experiment 1</b>	9	63.5	18.4	17.3	0.8
<b>Experiment 2</b>	9	72.0	24.9	2.5	0.6
<b>Experiment 1</b>	24	58.7	15.9	24.6	0.8
<b>Experiment 2</b>	24	87.2	11.1	1.4	0.3
<b>Experiment 3</b>	24	69.3	9.3	21.3	0.3

**Table 3.4:** Incorporation of <sup>13</sup>C & <sup>2</sup>H into positions 2, 3 & 4 of 4-fluorothreonine (2), resulting from incubating [1-<sup>2</sup>H]-fluoroacetaldehyde (147) and [2-<sup>13</sup>C]-glycine (91) with resting cells of *S. cattleya*.

In analysing these results it is helpful to reduce the problem down to the individual reactions that can take place. There is the condensation of [1-<sup>2</sup>H]-fluoroacetaldehyde

(147) with either  $[2-^{13}\text{C}]$ -glycine (91) or a dedicated biosynthetic intermediate (see Fig. 3.16). It is assumed that whichever of these is happening, the process has ceased 6 hours into the experiment, as all of the  $[1-^2\text{H}]$ -fluoroacetaldehyde (147) will have been consumed. Therefore all changes in labelling patterns from that point onwards are due to  $[2-^{13}\text{C}]$ -glycine (91) and its assimilation into the fluorometabolites *via* a *de novo* biosynthesis involving fluoride. This biosynthesis from  $[2-^{13}\text{C}]$ -glycine (91) and fluoride will deliver a high level of double, and some triple label, as  $[2-^{13}\text{C}]$ -glycine (91) is known to recombine in positions C-4 and C-3 of 4-fluorothreonine (2) and assimilates separately into position C-2. Within 6 hours the label from  $[2-^{13}\text{C}]$ -glycine (91) will have incorporated into the biosynthetic intermediate responsible for positions C-1 and C-2 of 4-fluorothreonine (2) and this makes it difficult to delineate between direct condensation with  $[2-^{13}\text{C}]$ -glycine (91) and the direct biosynthetic intermediate.

**Experiment 1:** The most significant observation of this experiment is the dilution of labelled 4-fluorothreonine (2) at 9 hours. Fig. 3.17 shows the variation of the populations of labelled 4-fluorothreonine (2) with time. At 9 hours 63.5 % of the 4-fluorothreonine (2) is unlabelled, compared to 46.8 % at 6 hours and 58.7 % at 24 hours.

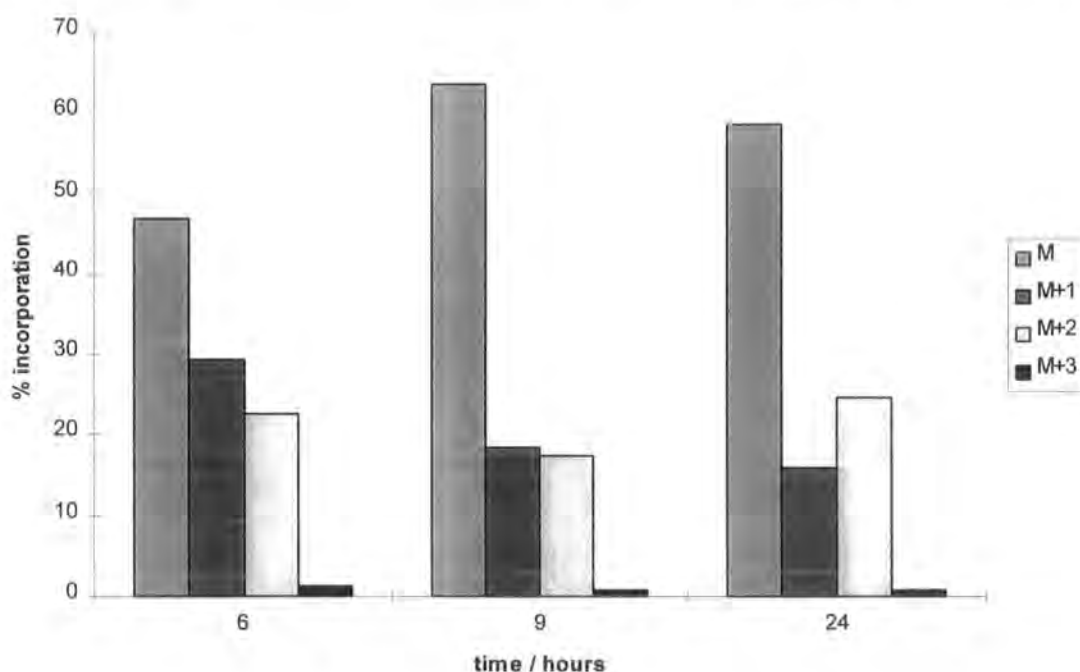


**Fig. 3.17:** Comparison of populations of none (M), single (M+1), double (M+2) and triple (M+3) label in positions 2, 3 & 4 of fluorothreonine (2) resultant from incubating  $[1-^2\text{H}]$ -fluoroacetaldehyde (147) and 10 mM  $[2-^{13}\text{C}]$ -glycine (91) with resting cells of *S. cattleya*, **Experiment 1**.

Between 6 & 9 hours the amount of both single and double label decreases. Between 9 and 24 hours the amount of single label decreases, but the amount of double label increases. This represents labelling from the *de novo* biosynthesis of 4-fluorothreonine (2) from [2-<sup>13</sup>C]-glycine that is additive on the labelled 4-fluorothreonine (2) already present. Considering the label in 4-fluorothreonine (2) at 6 hours, the single label originates either from <sup>2</sup>H in C-3 or <sup>13</sup>C in C-2. However, the majority of this single label must originate from [1-<sup>2</sup>H]-fluoroacetaldehyde (147) in the early stages of this experiment, before fluoride is liberated. This high level of single label suggests incorporation of [1-<sup>2</sup>H]-fluoroacetaldehyde (147) and from not glycine (86). [2-<sup>13</sup>C]-Glycine (91) was fed at 10 mM, which would clearly label the glycine (86) pool. Double label (22 %) at 6 hours can be accounted for by the coupling of [1-<sup>2</sup>H]-fluoroacetaldehyde (147) and a <sup>13</sup>C labelled species. If that species were [2-<sup>13</sup>C]-glycine (91), there should be a general increase in the M+2 in going from 6 to 9 hours and this is not observed. It is concluded therefore that [1-<sup>2</sup>H]-fluoroacetaldehyde (147) does not couple directly with glycine (86). In summary the single and double labelled 4-fluorothreonine (2) present after 6 hours must originate directly from the biosynthesis of 4-fluorothreonine (2) *via* fluoroacetaldehyde (40) and not an aldolase mediated biotransformation.

**Experiment 2:** [2-<sup>13</sup>C]-Glycine (91) was fed at the lower concentration of 1.0 mM.

If [1-<sup>2</sup>H]-fluoroacetaldehyde (147) is condensing directly with [2-<sup>13</sup>C]-glycine (91) then again the proportion of double label after 6 hours would be expected to be higher compared to the single label.



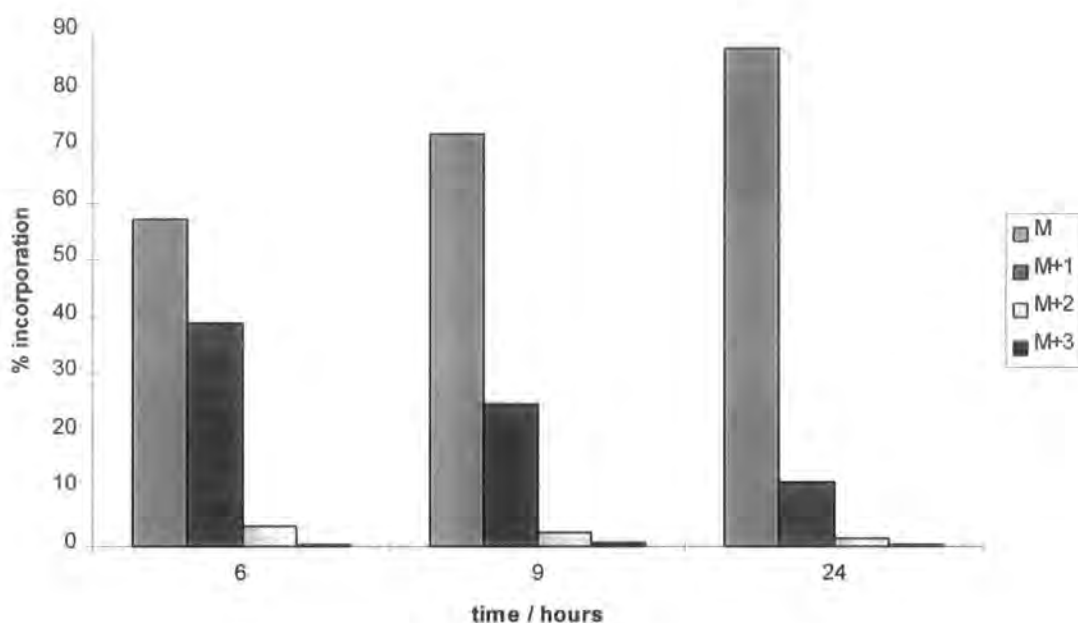


**Fig. 3.18:** Comparison of populations of none (M), single (M+1), double (M+2) and triple (M+3) label in positions 2, 3 & 4 of fluorothreonine (**2**) resultant from incubating [1-<sup>2</sup>H]-fluoroacetaldehyde (**147**) and 1.0 mM [2-<sup>13</sup>C]-glycine (**91**) with resting cells of *S. cattleya*, **Experiment 2**.

The level of double label in 4-fluorothreonine (**2**) remains low even at 24 hours (c.f. **Experiment 1**) as the label in the [2-<sup>13</sup>C]-glycine (**91**) pool is diluted by endogenous glycine (**86**). Thus recombination of label is less in this experiment than the higher concentration fed in **experiment 1**. This experiment confirms that [1-<sup>2</sup>H]-fluoroacetaldehyde (**147**) is involved in the biosynthesis of 4-fluorothreonine (**2**). It is noteworthy that in both experiments the level of unlabelled (M) 4-fluorothreonine (**2**) is high. That is clearly because the labelled 4-fluorothreonine (**2**) is additional to that generated by the cells by *de novo* biosynthesis (Table 3.2).

### 3.3.3.3 Conclusions

These experiments demonstrate that 4-fluorothreonine (**2**) is biosynthesised when resting cells of *Streptomyces cattleya* are incubated with fluoroacetaldehyde (**40**). The 4-fluorothreonine (**2**) is not accounted for by a direct condensation with glycine (**86**), but with some other intermediate. The results presented in this chapter suggest that fluoroacetaldehyde (**40**) has a pivotal role both in fluoroacetate (**1**) and 4-fluorothreonine (**2**) biosynthesis. Fluoroacetaldehyde emerges as a common intermediate in the biosynthesis of the fluormetabolites.

### 3.4 Cell free studies on fluoroacetaldehyde (40) metabolism

It was necessary to develop cell free methodologies for further study of fluorometabolite biosynthesis. Fluoroacetaldehyde (40) is readily converted to fluoroacetate (1) by whole cells of *Streptomyces cattleya*, and this activity provides a useful starting point to study cell free metabolism to the fluorometabolites. Methods for disrupting the cells and measuring the subsequent protein concentration were explored.

#### 3.4.1 Protein determination

Throughout these cell free studies protein concentrations were determined using the Bradford assay.<sup>128</sup> Coomassie Brilliant Blue G changes colour from red to blue when bound to protein, the blue form absorbs at  $\lambda = 590$  nm. Using this chromophore the concentration of protein in a given sample can be quantified. A reagent solution containing (0.01 % (w/v) Coomassie Blue G, 4.7 % (w/v) ethanol and 8.5 % (w/v) phosphoric acid) was prepared and mixed (1.0 ml) with a test sample (20  $\mu$ l). The absorbance at  $\lambda = 590$  nm was measured between 5 and 15 minutes later. Standard curves were generated using bovine serum albumin (BSA) solutions and a typical standard curve is presented below (Fig. 3.19). The protein concentration in the test sample can then be determined directly from the standard curve.

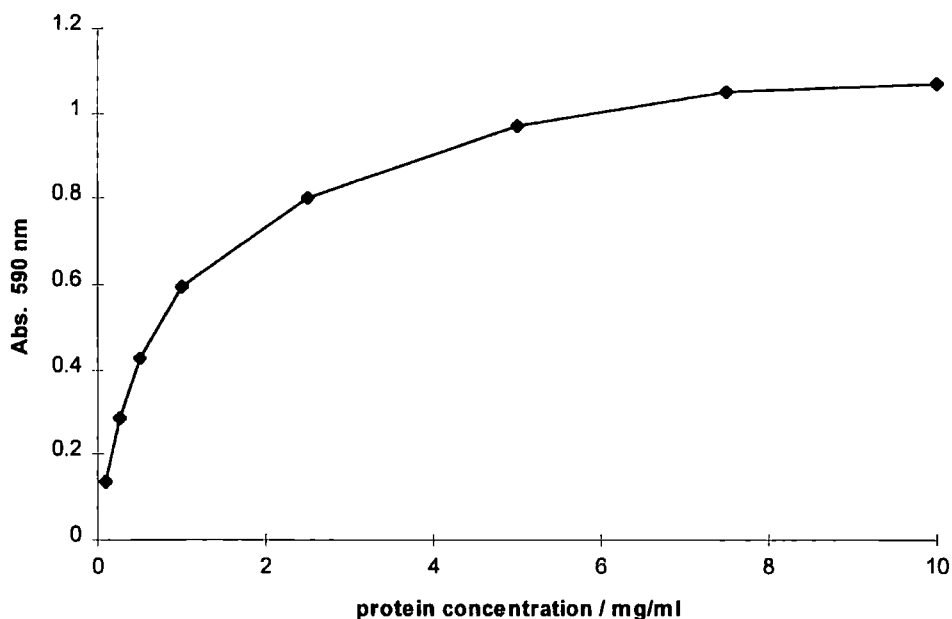


Fig. 3.19: Standard curve for protein (BSA) determination using the Bradford assay.

### **3.4.2 Disruption of the cells by sonication**

Our collaborators at The Queen's University of Belfast had studied defluorination activity in *S. cattleya*. A partial purification of a defluorination activity was performed in this study after cell disruption by sonication.<sup>107</sup> Disrupting cells with ultra sound has been used extensively in *Streptomyces* Spp., therefore it was decided to prepare cell free extracts by sonication and study the conversion of fluoroacetaldehyde (**40**) to fluoroacetate (**1**).

#### **3.4.2.1 Maximising the protein yield**

Preliminary studies focused on maximising the yield of protein from the cells using a sonic probe. Cells were harvested and suspended in ice cold MES buffer (50 mM) at 1.0 g wet wt. / ml. The slurry was placed in a thick test tube supported in ice water and was exposed to repeated pulses from the sonic probe, ensuring that the internal temperature did not rise above 7 °C. It emerged that the yield of protein fell off with prolonged exposure to sonication and the optimum conditions were 3 pulses, each of 10 seconds on 60 % power (the maximum power for that probe), allowing the solution to cool between pulses. The cell debris was then removed by centrifugation (20,000 rpm, 40 minutes, 4 °C) in a pre-chilled centrifuge. Typically this method yielded between 4 mg /ml and 8 mg /ml of protein in the resultant cell free extract.

#### **3.4.2.2 Fluoroacetaldehyde metabolism**

The conversion of fluoroacetaldehyde (**40**) to fluoroacetate (**1**) was studied using cell free extracts obtained in this manner. The cell free extract (0.625 ml, 4 mg / ml protein) was incubated with fluoroacetaldehyde (**40**) (2 mM), at 29 °C in 50 mM MES buffer containing dithiothreitol (DTT) (2 mM) and a variety of co-factors; NAD<sup>+</sup> (2 mM), NADP<sup>+</sup> (1 mM), FAD (2 mM), FMN (2 mM), ATP (5 mM) and CoASH (2 mM). The experiments were stopped after 0, 2 and 4 hours by placing the test tube in hot water (> 85 °C) for 5 minutes and the resultant protein precipitate was removed by centrifugation. The supernatants were analysed by <sup>19</sup>F NMR, however in none of the experiments was the presence of fluoroacetate (**1**) observed.

### 3.4.3 Disruption of the cells with a French Press

In view of the lack of success with cell free extracts prepared by sonication an alternate method of cell disruption was explored by using a French press (Biological Sciences Department, University of Durham). This method involves pumping a cellular slurry through a small aperture (0.25 mm), onto a metal target and the resultant solution is drained into a collection vessel. The whole unit can be refrigerated, and was generally cooled to 4 °C. Harvested cells were suspended in ice cold 50 mM MES buffer that contained DTT (2 mM). A thin cell slurry (0.1 g wet wt. / ml) was passed through the French press, at an operating pressure of 26,000 psi (1700 bar) and collected into pre-chilled glassware. The French press was then washed with ice cold 50 mM MES (containing 2 mM DTT) buffer, with a volume equal to half that of the cell slurry and the washings combined with the extract. The cellular debris was removed by centrifugation (20,000 rpm, 40 minutes, 4 °C) and the supernatant collected. The protein concentration of the resultant cell free extract was then determined using the method described in section 3.4.1. The protein concentration was routinely found to be between 1 and 2 mg / ml. Importantly this generated a far greater volume of crude cell free extract than the sonication method and consequently a far greater amount of protein could be used in each experiment. This method of disrupting the cells was used in all of the subsequent cell free experiments.

#### 3.4.3.1 Fluoroacetaldehyde metabolism

The following experiment was used to study fluoroacetaldehyde (40) metabolism in cell free extracts (2.5 mg/ml protein) of *S. cattleya*.

	<b>A</b>	<b>B</b>	<b>C</b>	<b>D</b>	<b>E</b>	<b>F</b>
<b>cell free extract</b>	5		5		5	
<b>50 mM MES + 2 mM DTT</b>		5		5		5
<b>co-factor 'soup'</b>	1	1	1	1	1	1
<b>40 mM fluoroacetaldehyde (40)</b>	1	1	1	1	1	1
<b>incubation time / hours</b>	<b>0</b>	<b>0</b>	<b>7</b>	<b>7</b>	<b>24</b>	<b>24</b>

**Table 3.5:** The experimental protocol for studies into fluoroacetaldehyde metabolism by cell free extracts of *S. cattleya*. Numbers refer to volume (ml).

The co-factor 'soup' contained (final concentration upon adding 1 ml to cell free experiment): NAD<sup>+</sup> (2 mM), NADP<sup>+</sup> (1.33 mM), FAD (2 mM), FMN (2 mM), CoASH (0.5 mM) and ATP (5 mM). The experiments were terminated by immersing the test tube into hot water (>85 °C) for 5 minutes and the resultant protein precipitate removed by centrifugation (20,000 rpm, 10 minutes).

### 3.4.3.2 Results and discussion

<sup>19</sup>F NMR analysis of the resultant supernatants A → F revealed that there was no conversion in the samples in the controls without cell free extract (B, D & F). Conversion of fluoroacetaldehyde (40) to fluoroacetate (1) was observed only in those samples (A, C & E) containing the cell free extract (Table 3.6).

A	time = 0 hours	3.1 % conversion
C	time = 7 hours	10.6 % conversion
E	time = 24 hours	35.9 % conversion

**Table 3.6:** Conversion of fluoroacetaldehyde (40) to fluoroacetate (1) by cell free extracts of *S. cattleya*. % Conversion determined from integrals of <sup>19</sup>F NMR analysis.

These results demonstrate that cell free extracts of *S. cattleya*, with the co-factor 'soup', are capable of converting fluoroacetaldehyde (40) to fluoroacetate (1). The concentration of fluoroacetaldehyde (40) that was administered to the resting cells was high (5.7 mM) compared with that for each co-factor (2 mM). In sample E (24 hours), a 36 % conversion was observed which represents a final concentration of fluoroacetate (1) of approximately 2 mM. Therefore this may represent the complete consumption of one of the co-factors (2 mM).

### 3.4.3.3 Conclusions

The conversion of fluoroacetaldehyde (40) to fluoroacetate (1) has been demonstrated in cell free extracts of *S. cattleya*. The final concentration was approximately 2 mM, which equates with the amount of NAD<sup>+</sup>, FAD and FMN that was added to the buffer.

It may be that one or more of these co-factors has a direct role in the oxidation of fluoroacetaldehyde (40) to fluoroacetate (1).

### 3.4.4 Co-factor dependence

In order to establish the co-factor dependence for the oxidation of fluoroacetaldehyde (40) to fluoroacetate (1) a set of experiments were conducted where one co-factor was removed each time from the co-factor cocktail.

#### 3.4.4.1 Experimental protocol

Cell free extracts were prepared as described previously and the protein concentration measured as 1.4 mg /ml. In this series of experiments fluoroacetaldehyde (40) was supplied at a final concentration of 2 mM.

	A	B	C	D	E	F	G	H	I
<b>cell free extract</b>		5	5	5	5	5	5	5	5
<b>50 mM MES &amp; 2 mM DTT</b>	5								
<b>fluoroacetaldehyde (40) (14 mM)</b>	1	1	1	1	1	1	1	1	1
<b>co-factor 'soup'</b>	1	1	1						
<b>NAD<sup>+</sup> (70 mM)</b>					0.2	0.2	0.2	0.2	0.2
<b>NADP<sup>+</sup> (35 mM)</b>				0.2		0.2	0.2	0.2	0.2
<b>FAD (54 mM)</b>				0.2	0.2		0.2	0.2	0.2
<b>FMN (70 mM)</b>				0.2	0.2	0.2		0.2	0.2
<b>CoASH (17.5 mM)</b>				0.2	0.2	0.2	0.2		0.2
<b>ATP (175 mM)</b>				0.2	0.2	0.2	0.2	0.2	
<b>time / hours</b>	<b>24</b>	<b>0</b>	<b>24</b>	<b>24</b>	<b>24</b>	<b>24</b>	<b>24</b>	<b>24</b>	<b>24</b>

**Table 3.7:** Experimental protocol for co-factor dependence studies. Numbers refer to volume (ml).

The co-factor 'soup' contained (final concentration upon adding 1 ml to cell free experiment): NAD<sup>+</sup> (2 mM), NADP<sup>+</sup> (1.33 mM), FAD (2 mM), FMN (2 mM), CoASH

(0.5 mM) and ATP (5 mM). The experiments were terminated by immersing the test tube into hot water (> 85 °C) for 5 minutes and the resultant protein precipitate was removed by centrifugation.

#### 3.4.4.2 Results and discussion

The results of the  $^{19}\text{F}$  NMR analysis are summarised below in Table 3.8. The numbers refer to the percentage conversion of fluoroacetaldehyde (**40**) to fluoroacetate (**1**) observed after 24 hours.

Expt C (none)	Expt D ( $\text{NAD}^+$ )	Expt E ( $\text{NADP}^+$ )	Expt F (FAD)	Expt G (FMN)	Expt H (CoASH)	Expt I (ATP)
100	0	100	100	100	100	100

**Table 3.8:** Percentage conversion of fluoroacetaldehyde (**40**) to fluoroacetate (**1**) as determined from integrals of  $^{19}\text{F}$  NMR analysis. The bracketed abbreviations refer to the co-factor that was absent in that experiment.

The data is very clear and reveals that the conversion of fluoroacetaldehyde (**40**) to fluoroacetate (**1**) proceeds only when  $\text{NAD}^+$  is present. The transformation does not require any other co-factors. Interestingly it was noted that after 4 hours of incubation in all of the experiments, except **D**, a fine dark precipitate formed, suggesting that fluoroacetate (**1**) production may account for this colouring.

The conversion of fluoroacetaldehyde (**40**) to fluoroacetate (**1**) requires  $\text{NAD}^+$  and is therefore mediated by an aldehyde dehydrogenase. A minimal mechanism is presented in Fig. 3.20.

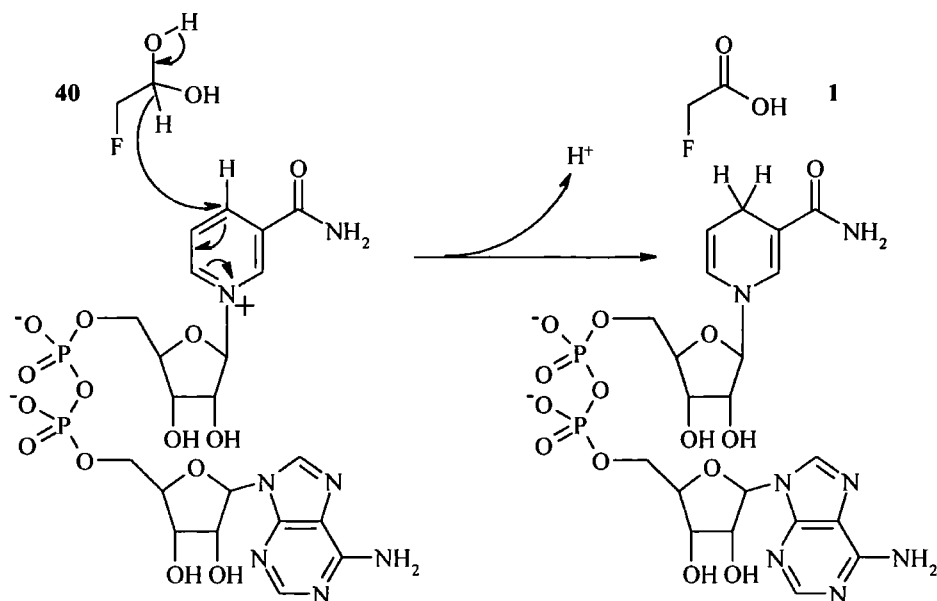


**Fig. 3.20:** Action of NAD<sup>+</sup> on the fluoroacetaldehyde dehydrogenase.

The concomitantly produced NADH contains a chromophore that absorbs in the ultra-violet region. Therefore the reaction could be followed spectrophotometrically. An experiment was set up as outlined in Table 3.9 to assess the production of fluoroacetate (1) from fluoroacetaldehyde (40) with time in the cell free extract.

	A	B	C	D	E	F	G
<b>cell free extract</b>	5	5	5	5	5	5	5
<b>50 mM MES &amp; 2 mM DTT</b>	1						
<b>fluoroacetaldehyde (40) (14 mM)</b>		1	1	1	1	1	1
<b>NAD<sup>+</sup> (14 mM)</b>	1	1	1	1	1	1	1
<b>time / hours</b>	<b>0</b>	<b>0</b>	<b>2</b>	<b>4</b>	<b>8</b>	<b>16</b>	<b>24</b>

**Table 3.9:** Experimental protocol for spectrophotometric analysis of fluoroacetate (1) production in cell free extracts of *S. cattleya* incubated with fluoroacetaldehyde (40) and NAD<sup>+</sup>. Numbers refer to volume (ml).

The protein concentration was determined as 2.1 mg /ml and the experiments were terminated by immersing the test tube into hot water (> 85 °C) for 5 minutes and the resultant protein precipitate removed by centrifugation. The results of the <sup>19</sup>F NMR and spectrophotometric analysis are tabulated below. UV measurements were taken by



comparing samples with a reference (**sample A**). Absorbance was measured at 340 nm, in a quartz curvette.

Time / hours	0 (B)	2 (C)	4 (D)	8 (E)	16 (F)	24 (G)
% Conversion ( $^{19}\text{F}$ NMR)	29.0	70.0	83.2	98.5	100	100
% Absorbance ( $\lambda = 340 \text{ nm}$ )	0.079	0.165	0.993	0.302	-0.107	-0.235

**Table 3.10:** % conversion and % absorbance of experiments to determine fluoroacetate (1) and NADH production in cell free extracts of *S. cattleya*.

Fluoroacetate (1) production was concomitantly monitored by  $^{19}\text{F}$  NMR analysis and is shown below (Fig. 3.21) with the variation in the spectrophotometric analysis.

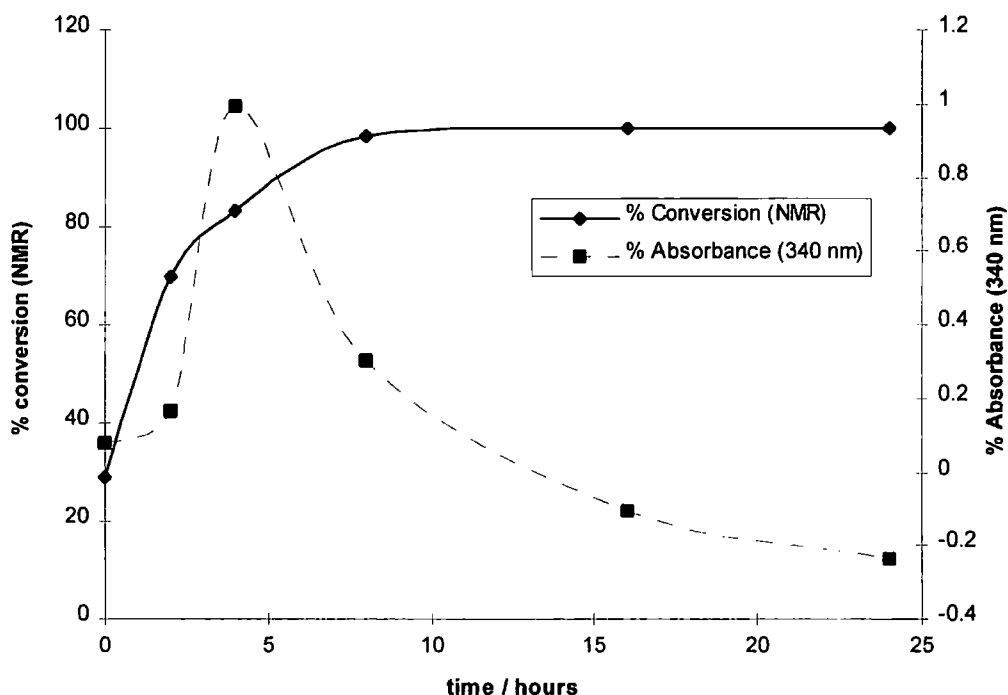


**Fig. 3.21:** Graphical representation of conversion of fluoroacetaldehyde (40) to fluoroacetate (1) and the variation of absorbance, measured at  $\lambda = 310 \text{ nm}$ .

The change in absorbance increases initially as a result of reduction of  $\text{NAD}^+$  to NADH, however it reaches a maximum before the complete consumption of fluoroacetaldehyde (40) and then falls off to a value below that in the reference cell. This may be due to the NADH produced by the oxidation of fluoroacetaldehyde (40) being used in another enzymatic reaction, for which there is sufficient substrate in the cell free extract. It is

noticeable that the rates of  $\text{NAD}^+$  reduction by the cell free extract when incubated with fluoroacetaldehyde diminished significantly with the age of the cell free extract. This is shown in Fig. 3.22, where the gradient of the initial slope decreases with time.

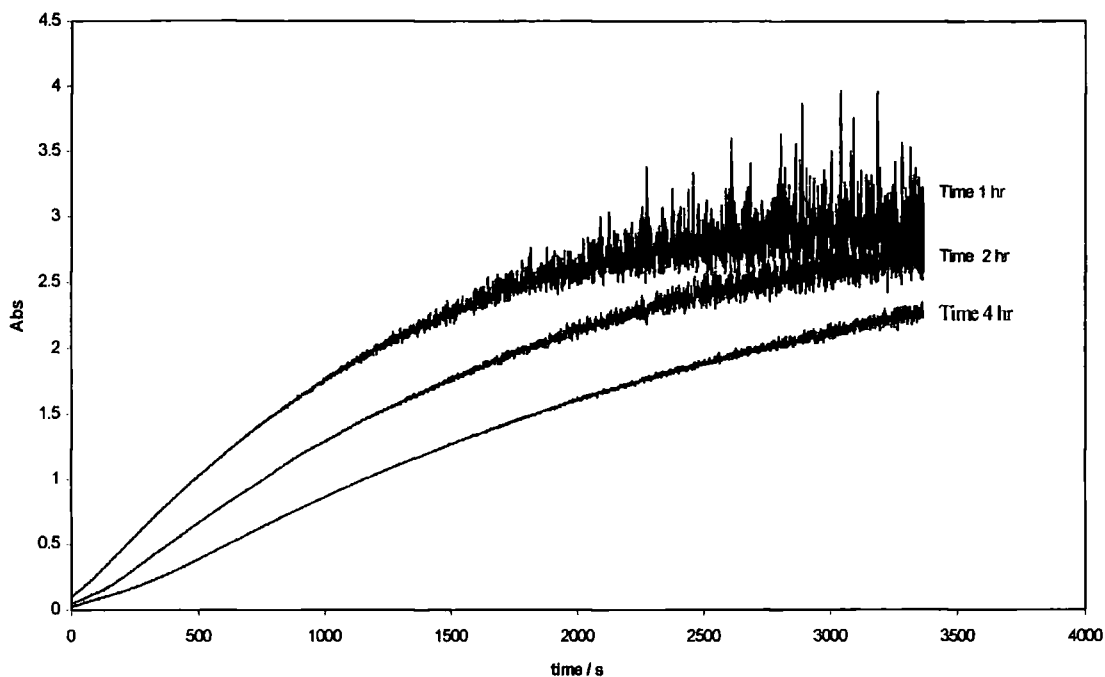


**Fig. 3.22:** Decrease in rate of NADH production with time. All samples are cell free extract, 2 mM fluoroacetaldehyde (40) and 2 mM  $\text{NAD}^+$

This data demonstrates that the crude cell free extract is not stable, either due to the inherent instability of the aldehyde dehydrogenase, or perhaps that proteases gradually diminish the activity.

### 3.4.5 Substrate specificity

In order to test the substrate specificity of fluoroacetaldehyde dehydrogenase a variety of commercially available aldehydes were incubated with the cell free extract and the rate of oxidation measured spectrophotometrically. It was particularly interesting at the outset to assess the efficiency of acetaldehyde as a substrate, as acetaldehyde (155) is the substrate for mammalian and yeast acetaldehyde dehydrogenase. As this was a crude cell free extract only the relative rates of NADH production could be assessed for the different aldehydes, with respect to that of fluoroacetaldehyde (40).

### 3.4.5.1 *Experimental protocol*

The assay was conducted simultaneously on two spectrophotometers kept in a room at constant temperature (26 °C). Crude cell free extracts were prepared as previously described and each experiment was conducted as follows:

Sample A: cell free extract (5 ml) and 14 mM fluoroacetaldehyde (1 ml)

Sample B: cell free extract (5 ml) and 14 mM aldehyde (1 ml)

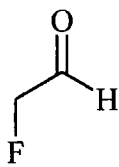
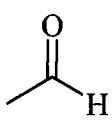
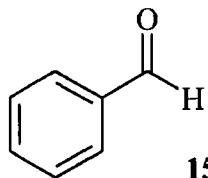
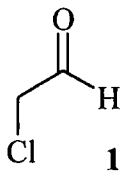
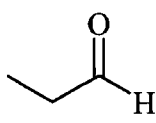
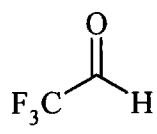
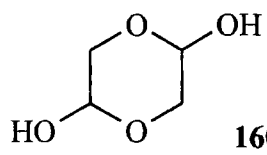
Sample C: cell free extract (5 ml) and 50 mM MES with 2 mM DTT (1 ml)

All three samples were incubated for 5 minutes at 28 °C before 14 mM NAD<sup>+</sup> (1 ml) was added and mixed by vortex. The final concentration of both aldehyde and NAD<sup>+</sup> was 2 mM. The absorbance of samples A and B were measured at  $\lambda = 340$  nm with respect to time in separate spectrophotometers using sample C as an *in situ* reference. Data was collected for a sufficient time to compare the initial rate of NADH production in both A and B.

Acetaldehyde (155), benzaldehyde (156), chloroacetaldehyde (157), propionaldehyde (158), trifluoroacetaldehyde (159) and glycolaldehyde dimer (160) were all assessed as substrates for the aldehyde dehydrogenase.

### 3.4.5.2 *Results and discussion*

The relative rate of oxidation of the various aldehydes was calculated relative to fluoroacetaldehyde (40) (i.e. by comparing the initial rate in sample B with that in sample A). This is expressed as a percentage and tabulated (Table 3.11) with the structures below.

Aldehyde	Relative rate of NAPH production	Aldehyde	Relative rate of NAPH production
 40	100 %	 155	40 %
 156	31 %	 157	24 %
 158	2 %	 159	0 %
 160	140 %		

**Table 3.11:** Relative rate of aldehyde oxidation by the crude cell free extract of *S. cattleya* and  $\text{NAD}^+$ .

All of the aldehydes, except trifluoroacetaldehyde (159) emerged as substrates for the aldehyde dehydrogenase. The rates were all slower than that of fluoroacetaldehyde (40) which appears to be the optimal substrate for the aldehyde dehydrogenase. Acetaldehyde (155), which is the substrate for a yeast and mammalian acetaldehyde dehydrogenase, is the most efficient substrate after fluoroacetaldehyde, but is oxidised at only 40 % of the rate of fluoroacetaldehyde.

Benzaldehyde (156) and chloroacetaldehyde (157) both had similar activities as substrates (31 % & 24 %), whereas that of propionaldehyde (158) was far lower (2 %). This suggests that electronic considerations are more significant than steric factors in determining the efficiency of a substrate for this enzyme.

It would appear that the enzyme prefers a hydrate to an aldehyde as a substrate. This was demonstrated by the effective metabolism of glycolaldehyde dimer (160). When crude cell free extract and  $\text{NAD}^+$  were incubated with glycolaldehyde dimer (160) oxidation occurred more rapidly (140 %) than in the case of fluoroacetaldehyde (40). As there are two centres on the glycolaldehyde dimer (160) that are potential sites for oxidation it was incubated at half the concentration of the other aldehydes (that is 1 mM instead of 2 mM).

### **3.4.5.3 Conclusions**

The aldehyde dehydrogenase that is responsible for the oxidation of fluoroacetaldehyde (40) to fluoroacetate (1) is capable of oxidising a variety of different aldehydes to their respective carboxylic acids. It appears that the ability to generate a hydrate in solution is significant in determining whether an aldehyde will act as a substrate.

### **3.4.6 Fluoroacetaldehyde dehydrogenase: membrane bound or soluble?**

An enzyme that is membrane bound is more difficult to purify than if it is soluble. However, membrane bound enzymes tend to be more stable in cell free extracts as they can be supported *in situ* by fragments of membrane. It appeared appropriate to conduct a preliminary investigation into whether the putative fluoroacetaldehyde dehydrogenase is membrane bound or soluble.

#### **3.4.6.1 Experimental protocol**

Crude cell free extract was prepared as previously described and divided into two portions. The first was stored in ice until required and the second was subjected to ultracentrifugation (50,000 rpm, 4 °C, 1 hour, equivalent to 200,000 g). This provided a centrifugal force sufficient to remove all particulate matter from solution. The supernatant was then decanted and stored in ice. The pellet was resuspended in its original volume of 50 mM MES and 2 mM DTT. The three fractions were then examined for fluoroacetaldehyde dehydrogenase activity by the method that is outlined below (Table 3.11).

	<b>A</b>	<b>B</b>	<b>C</b>
<b>crude cell free extract</b>	5		
<b>supernatant (solubles)</b>		5	
<b>resuspended pellet (particulate)</b>			5
<b>14 mM fluoroacetaldehyde (40)</b>	1	1	1
<b>14 mM NAD<sup>+</sup></b>	1	1	1

**Table 3.12:** Experimental protocol for membrane bound study. Number refer to volume (ml).

Each experiment was incubated at 29 °C and aliquots were removed at 0, 1, 3 and 24 hours. The aliquots were immersed in hot water (> 85 °C) for 5 minutes and the resultant precipitate removed by microcentrifugation.

#### 3.4.6.2 Results and discussion

The supernatants were analysed by <sup>19</sup>F NMR and the results are tabulated below (Table 3.13).

<b>Time / hours</b>	<b>1</b>	<b>3</b>	<b>24</b>
<b>A crude cell free extract</b>	40.5 %	91.7 %	100 %
<b>B supernatant (solubles)</b>	21.8 %	100 %	100 %
<b>C resuspended pellet (particulate)</b>	0 %	0 %	0 %

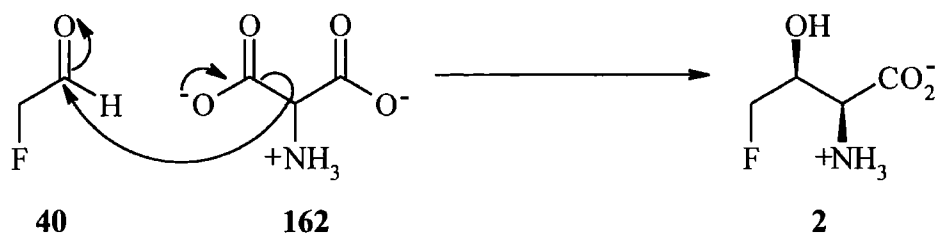
**Table 3.13:** <sup>19</sup>F NMR analysis of membrane bound study for fluoroacetaldehyde dehydrogenase in *S. cattleya*, the figures refer to % conversion of a 2 mM fluoroacetaldehyde (40) solution.

Table 3.13 clearly demonstrates that fluoroacetaldehyde dehydrogenase activity is located in the soluble fraction of the cell free extract and that the enzyme is not membrane bound

### 3.5 Cell free studies on 4-fluorothreonine (2) biosynthesis

Whole cell studies on fluoroacetaldehyde (40) metabolism have demonstrated its involvement in fluorometabolite biosynthesis in *Streptomyces cattleya*. It has been demonstrated that fluoroacetaldehyde (40) is rapidly oxidised to fluoroacetate (1) and that it also undergoes a condensation to form 4-fluorothreonine (2). Initial studies on cell free extracts of *Streptomyces cattleya* have focused on the identification of a fluoroacetaldehyde dehydrogenase activity. It appeared appropriate to initiate studies into cell free biosynthesis of 4-fluorothreonine (2) from fluoroacetaldehyde (40). In an attempt to study 4-fluorothreonine (2) biosynthesis in a cell free system fluoroacetaldehyde (40) was incubated, in the absence of  $\text{NAD}^+$ , with putative intermediates that may contribute C-1 and C-2 of 4-fluorothreonine (2).

Hamilton *et al.*<sup>103</sup> have already studied the incorporation of labelled pyruvate into 4-fluorothreonine (2). It was noted that both  $[1-^{13}\text{C}]$ - and  $[3-^{13}\text{C}]$ -pyruvate (161), (100) label positions C-1 and C-2 of 4-fluorothreonine (2) at approximately the same level (4.4 % vs. 4.6 % respectively). Also  $[2-^{13}\text{C}]$ -pyruvate (93) labelled those same positions at approximately twice that level (11.6 %). This would suggest that pyruvate (10) is metabolised through to C-1 and C-2 of 4-fluorothreonine (2) *via* a symmetrical  $\text{C}_3$  intermediate. A possible candidate for this role would be 2-aminomalonate (162). Such a compound could undergo a decarboxylative condensation with fluoroacetaldehyde (40) to produce 4-fluorothreonine (2) (Fig. 3.23), providing a rationale for all of the labelling studies carried out to date.



**Fig. 3.23:** Putative biosynthesis of 4-fluorothreonine (2) from fluoroacetaldehyde (40) and 2-aminomalonate (162).

With this hypothesis in mind, it was decided to prepare a sample of 2-aminomalonate (162), for incubation with cell free extracts of *Streptomyces cattleya*.

### 3.5.1 Synthesis of 2-aminomalonate (162)

2-Aminomalonate (**162**) was prepared by the hydrolysis of diethyl 2-aminomalonate hydrochloride (**163**), which is commercially available.<sup>129</sup> Ester hydrolysis in potassium hydroxide generated the zwitterionic potassium salt of 2-aminomalonate (**162**).

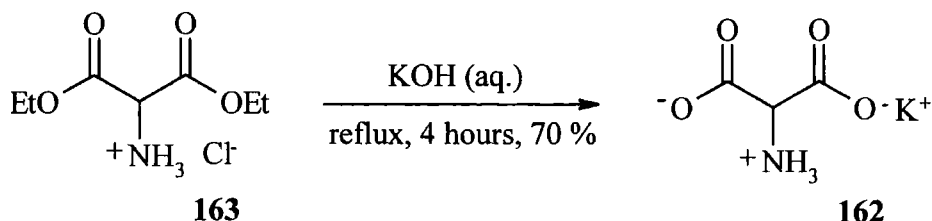


Fig. 3.24: Synthesis of potassium 2-aminomalonate (**162**).

### 3.5.2 Cell free studies with 2-aminomalonate (162)

Pyridoxal phosphate (PLP) is a co-factor involved in amino acid decarboxylation.<sup>123</sup> Therefore it was decided to involve PLP in this study as this co-factor may have a role in a decarboxylative condensation type reaction. In order to delineate between 4-fluorothreonine (**2**) biosynthesis and adventitious condensation with fluoroacetaldehyde (**40**), control experiments involving glycine (**86**) and boiled cell free extract were run simultaneously.

Crude cell free extracts of *Streptomyces cattleya* were prepared as previously described using the French press and the protein concentration was determined to be 1.8 mg /ml. The experiment was then set up as outlined below (Table 3.14).

After 2 hours a further 0.5 ml of 28 mM 2-aminomalonate (**162**) was added to experiments **B** and **D**. Likewise, a further 0.5 ml of 28 mM glycine (**86**) was added to **C** and **E**. All of the experiments (**A**  $\rightarrow$  **E**) were incubated at 29 °C for 16 hours, and were then terminated by immersing the test tube in hot water ( $> 85$  °C) for 5 minutes and the resultant precipitate was removed by centrifugation. The supernatants were then analysed by  $^{19}\text{F}$  NMR and 4-fluorothreonine (**2**) assessed by HPLC.



	A	B	C	D	E
<b>cell free extract</b>	5	5	5		
<b>14 mM fluoroacetaldehyde (40)</b>	1	1	1	1	1
<b>28 mM NAD<sup>+</sup></b>	0.5				
<b>28 mM aminomalonate (162)</b>		0.5		0.5	
<b>28 mM glycine (86)</b>			0.5		0.5
<b>28 mM PLP</b>		0.5	0.5	0.5	0.5
<b>boiled cell free extract</b>				5	5
<b>50 mM MES &amp; 2 mM DTT</b>	0.5				

**Table 3.14:** Experimental protocol for 2-aminomalonate (**162**) incubations in cell free extracts of *S. cattleya*.

In the control (experiment **A**), complete conversion to fluoroacetate (**1**) was observed indicating active fluoroacetaldehyde dehydrogenase in the cell free extract. <sup>19</sup>F NMR analysis of experiments **B** → **E** demonstrated only the presence of fluoroacetaldehyde (**40**) and the associated 2-fluoroethanol (**71**). In none of these experiments was 4-fluorothreonine (**2**) production observed and this was confirmed by HPLC, which failed to identify any 4-fluorothreonine (**2**) in these samples.

### 3.5.3 Conclusions

The failure to identify any 4-fluorothreonine (**2**) does not rule out the involvement of 2-aminomalonate (**162**) in 4-fluorothreonine (**2**) biosynthesis. It may be that a co-factor is required that was not included in this experiment or that the necessary condensing enzyme was deactivated during preparation of the cell free extract. However, in the absence of a positive result this experiment yields little information on the role of 2-aminomalonate (**162**) in the biosynthesis of 4-fluorothreonine (**2**).

### 3.6 Conclusions

The role of fluoroacetaldehyde (**40**) in fluorometabolite biosynthesis has been addressed. The rapid oxidation of fluoroacetaldehyde (**40**) to fluoroacetate (**1**) has been observed in both whole cell and cell free systems of *Streptomyces cattleya*. Co-factor studies have shown a dependence on NAD<sup>+</sup> and therefore the conversion is mediated by an aldehyde dehydrogenase. This is in agreement with the <sup>18</sup>O<sub>2</sub> study too, where oxygen-18 was not incorporated into the product.

In the absence of molecular oxygen the oxidation of fluoroacetaldehyde (**40**) to fluoroacetate (**1**) is arrested in whole cells. The flavin, FAD can convert NADH to NAD<sup>+</sup> and the flavins, in turn, are recycled by molecular oxygen.<sup>123</sup> It may be that in this case the conversion of fluoroacetaldehyde (**40**) to fluoroacetate (**1**) stops in the absence of O<sub>2</sub> as this cycle is arrested.

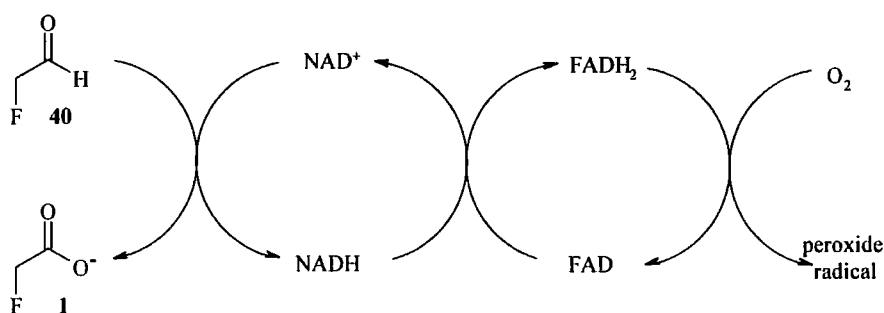


**Fig. 3.25:** Putative relationship between molecular oxygen and fluoroacetaldehyde (**40**) oxidation in *S. cattleya*.

Murphy<sup>107</sup> observed very low levels of 4-fluorothreonine (**2**) production from resting cells of *Streptomyces cattleya* incubated with fluoroacetaldehyde (**40**). To study the biosynthesis of 4-fluorothreonine (**2**) in more detail [1-<sup>2</sup>H]-fluoroacetaldehyde (**141**) was synthesised for incubation studies. The synthesis of this labelled species (**141**) proved to be problematic at the outset, although sufficient material was prepared in solution for feeding experiments. The label was converted through into 4-fluorothreonine (**2**). To rule out an adventitious condensation between fluoroacetaldehyde (**40**) and glycine (**86**) a feeding study using both of these species in labelled form was conducted. The analysis of those experiments indicated that glycine (**86**) does not contribute directly to 4-fluorothreonine (**2**), an observation in agreement with previous labelling studies. The results imply that fluoroacetaldehyde (**40**) is directly involved in 4-fluorothreonine (**2**) biosynthesis.

It can now be stated with some confidence that fluoroacetaldehyde (**40**) is a common fluorinated intermediate to both of the fluorometabolites elaborated by *Streptomyces cattleya*.

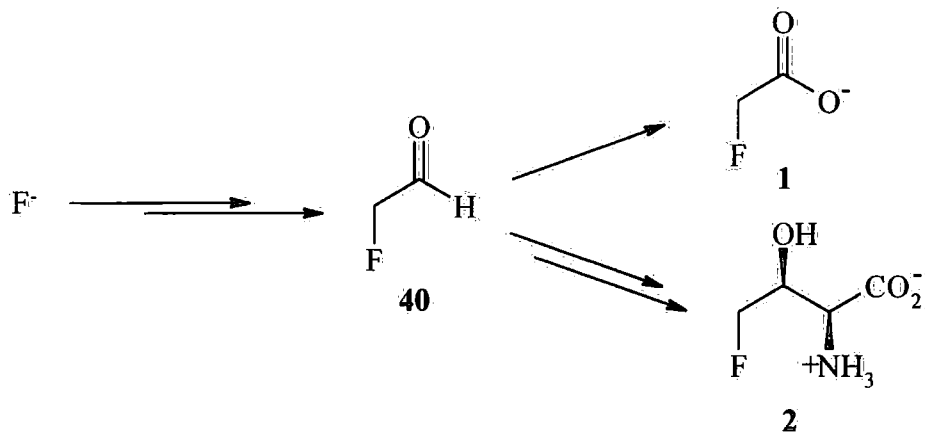


**Fig. 3.26:** The pivotal role of fluoroacetaldehyde in fluorometabolite biosynthesis in *S. cattleya*.

When resting cells of *S. cattleya* are incubated with fluoride, fluoroacetate (**1**) and 4-fluorothreonine (**2**) are biosynthesised in a 2:1 ratio.<sup>99</sup> Conversely, when resting cells are incubated with fluoroacetaldehyde (**40**) the ratio is now approximately 100:1 (Table 3.2). This change in ratio may hint at mechanistic aspects of 4-fluorothreonine (**2**) biosynthesis. Fluoroacetaldehyde (**40**) could be biosynthesised, and reacts on to form 4-fluorothreonine (**2**), whilst bound to an enzyme or co-factor, potentially as an imine. Fluoroacetaldehyde (**40**) is potentially toxic to bacterial cells, so *S. cattleya* may have evolved an efficient fluoroacetaldehyde dehydrogenase so as to oxidise this toxin and expel it extracellularly.

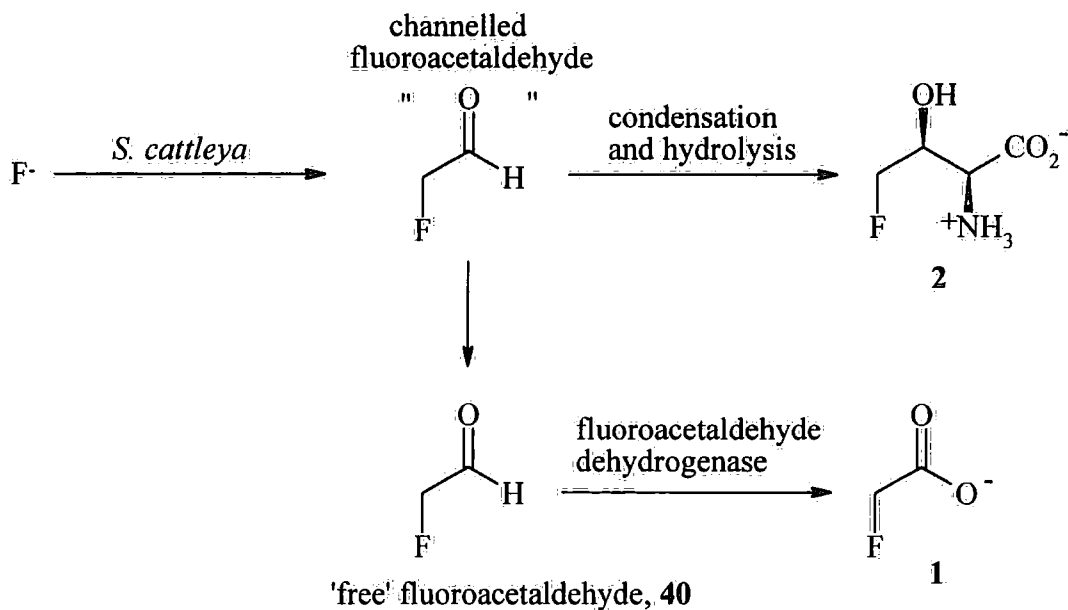


**Fig. 3. 27:** Hypothetical role of channelled fluoroacetaldehyde in fluorometabolite biosynthesis, in *S. cattleya*.

This would suggest that 4-fluorothreonine (**2**) is the secondary metabolite that *Streptomyces cattleya* is attempting to produce, whereas fluoroacetate (**1**) is a shunt metabolite liberated by a toxic intermediate from that biosynthesis.

*Chapter 4*

*Cell free investigation of the fluorination event*

## Chapter 4: Cell free investigation of the fluorination event

Fluoroacetaldehyde (**40**) has been identified as a common fluorinated intermediate in the biosynthesis of fluoroacetate (**1**) and 4-fluorothreonine (**2**) in *Streptomyces cattleya*. The project now aimed to investigate the biosynthetic origin of fluoroacetaldehyde (**40**). Clearly, to produce fluoroacetaldehyde (**40**) from a C<sub>3</sub>-glycolytic intermediate two events must occur; fluorination and bond cleavage.

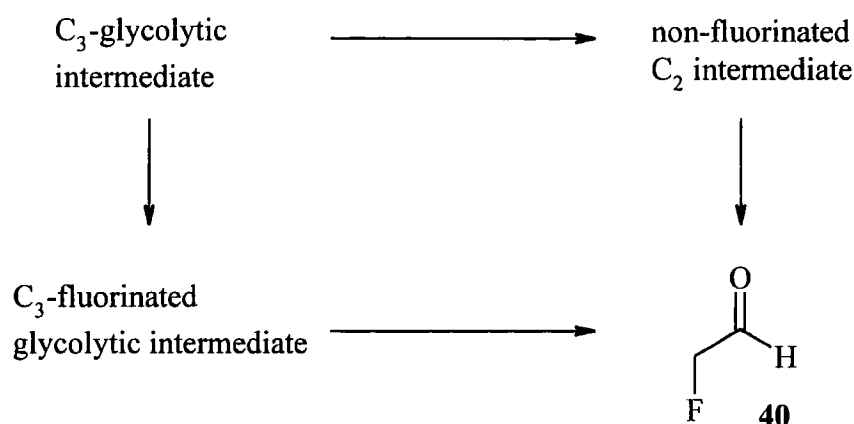


**Fig. 4.1:** Oxidative bond cleavage and fluorination are required to synthesis fluoroacetaldehyde (**40**) from a glycolytic intermediate.

Fluorination of a glycolytic intermediate will generate a fluorinated C<sub>3</sub> intermediate (Fig. 4.1), as explored in **section 2.4** and in previous studies.<sup>100</sup> There are however unanswered questions in the direct fluorination of glycolytic intermediates, such as the role for 3-fluoroglyceraldehyde (**142**), that have not been satisfactorily addressed. Also, if a glycolytic intermediate were to undergo bond cleavage prior to fluorination there would have to be a non-fluorinated C<sub>2</sub> intermediate, acting as the substrate for fluorination. Clearly, this role could be fulfilled by glycolaldehyde phosphate (**164**).

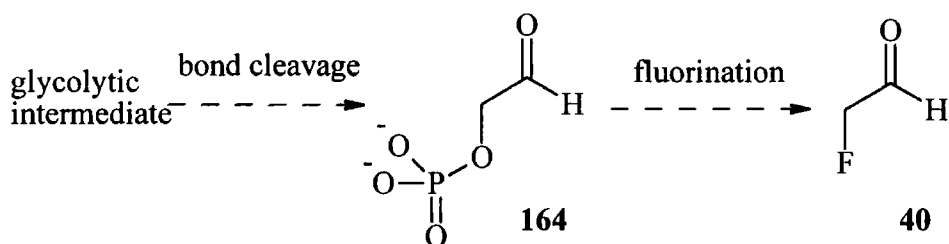


**Fig. 4.2:** Putative role of glycolaldehyde phosphate (**164**) in fluoroacetaldehyde (**40**) biosynthesis.

Fluorination of glycolaldehyde phosphate (**164**), *via* substitution of the phosphate group, would provide a route to fluoroacetaldehyde (**40**).

The cell free methodologies developed in studying the fluoroacetaldehyde dehydrogenase (section 3.4) were employed to explore the fluorination event. The general approach was to incubate cell free extracts of *S. cattleya* with fluoride and putative substrates for fluorination. In addition to studying glycolaldehyde phosphate (**164**) as a substrate, various glycolytic intermediates were explored as additional candidates. The putative initial product of fluorination for DL- $\alpha$ -glycerophosphate (**97**), dihydroxyacetone phosphate (**98**) and 3-phosphoglycerate (**17**) have all been synthesised and fed to resting cells of *S. cattleya* with no apparent fluorometabolite biosynthesis (section 2.4). However, it appeared appropriate to include them in this study as a matter of rigour.

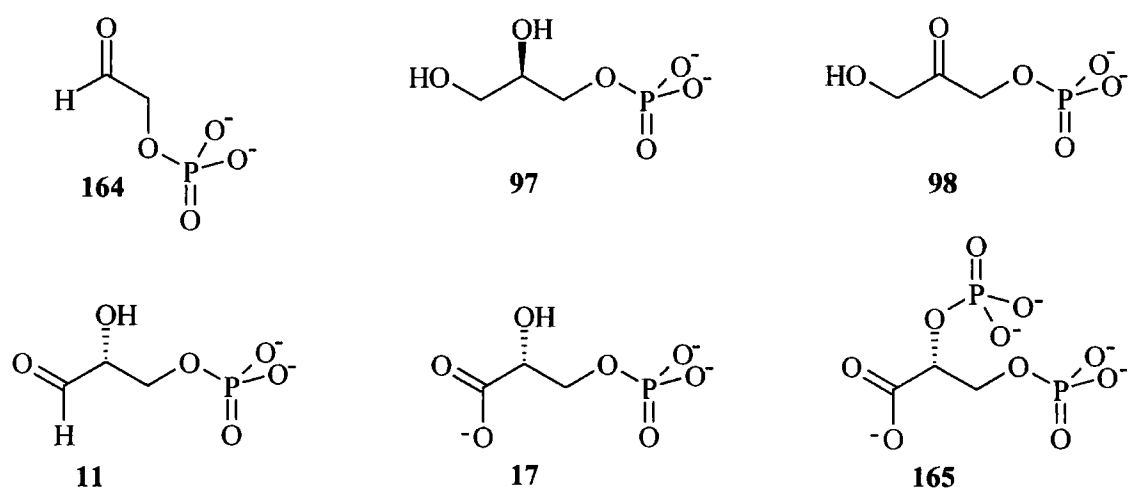


**Fig. 4.3:** Putative substrates for the fluorination event in *S. cattleya*.

## 4.1 Cell free studies with phosphorylated intermediates

Several of the phosphorylated glycolytic intermediates are commercially available. However, glycolaldehyde phosphate (**164**) is not and therefore it was prepared following the method of Eschenmoser *et al.*<sup>130</sup>

### 4.1.1 Synthesis of glycolaldehyde phosphate (164)

Glycolaldehyde phosphate (**164**) has been implicated in the prebiotic synthesis of ribonucleic acids, in a variation of the formose reaction.<sup>131</sup> Eschenmoser *et al.*<sup>130</sup> have developed a convenient synthesis of this phosphate (**164**) and explored its base catalysed aldol condensations to generate higher sugars.

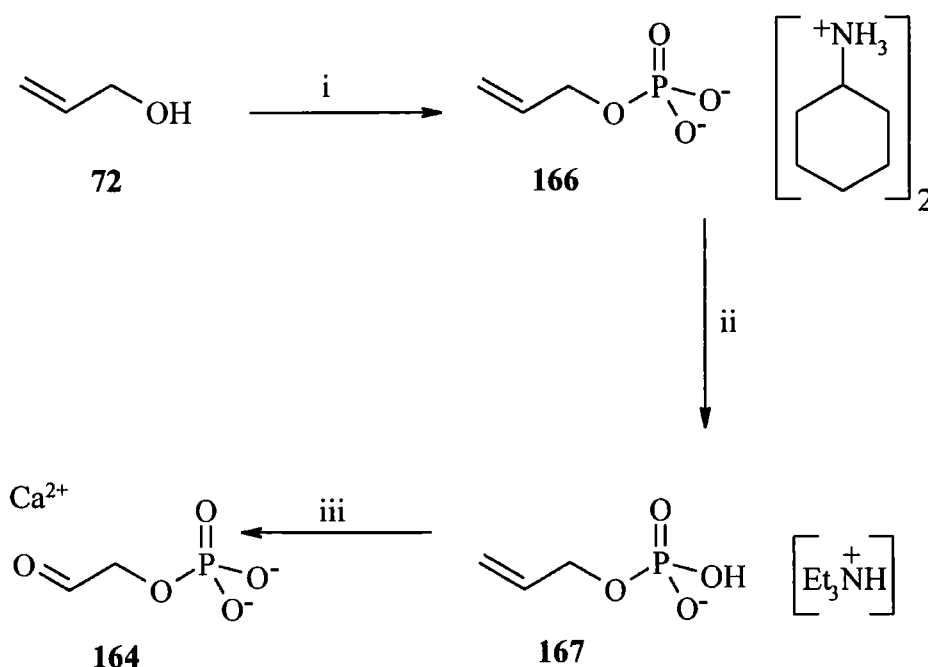


**Fig. 4.4:** Synthetic scheme to glycolaldehyde phosphate (**164**), Eschenmoser *et al.*<sup>130</sup> i) H<sub>3</sub>PO<sub>4</sub>, Et<sub>3</sub>N, CCl<sub>3</sub>CN, 75 °C, then cyclohexylamine, 76 %; ii) IR 120 (H<sup>+</sup> form), Et<sub>3</sub>N; iii) O<sub>3</sub> / MeOH, -78 °C → Me<sub>2</sub>S, -20 °C, then IR 120 (H<sup>+</sup> form), then Ca(OAc)<sub>2</sub>, 74 % from **167**.

Glycolaldehyde phosphate (**164**) was thus synthesised following the method outlined in Fig. 4.4. The first step involved activating allyl alcohol (**72**) with trichloroacetonitrile before nucleophilic attack by phosphoric acid. The cyclohexylamine salt of allyl phosphate (**166**) was then isolated in good yield (74 %). The key step in the synthesis



of glycolaldehyde phosphate (**164**) is the ozonolysis of allylphosphate. The authors reported that the ozonolysis is more successful on the mono(triethylamine) (**167**) salt rather than the bis(cyclohexylamine) (**166**). Therefore allylphosphate mono(triethylamine) (**167**) was prepared using acidic ion exchange resin to generate allylphosphoric acid and addition of triethylamine resulted in a modest recovery of allylphosphate mono(triethylamine) (**167**) (44 %). The ozonolysis was carried out according to the literature preparation. Accordingly, allylphosphate mono(triethylamine) (**167**) was dissolved in methanol and cooled to -78 °C. A stream of O<sub>3</sub> was passed through this solution until it turned light blue, indicating ozone saturation and complete formation of the ozonide. The ozonide was reduced by adding DMS and the reaction was stirred for 24 hours at -20 °C. Glycolaldehyde phosphoric acid was generated using acidic DOWEX ion exchange resin and the calcium salt (**164**) isolated by adding Ca(OAc)<sub>2</sub>. The salt precipitated out on treatment with acetone, to form a white amorphous solid (74 % from allylphosphate mono(triethylamine) (**167**)).

#### ***4.1.2 Preliminary cell free experiments***

All of the candidate substrates were used in the cell free experiments. The glycolytic intermediates were all soluble in MES buffer, however glycolaldehyde phosphate (**164**) required a drop of 1 M HCl (aq.) to help it dissolve. The cell free extract was incubated with the relevant substrate (2 mM for a single stereoisomer, 4 mM if racemic), fluoride (2 mM as NaF) and a mixture of co-factors (Co-factors administered were at the following final concentrations; thiamine pyrophosphate, 2 mM; ATP, 5 mM; MgSO<sub>4</sub>·7H<sub>2</sub>O, 2 mM; NAD<sup>+</sup>, 2 mM; NADP<sup>+</sup>, 1 mM; NADH, 2 mM; NADPH, 0.5 mM; CoASH, 0.5 mM; pyridoxal phosphate, 1 mM). The experimental protocol is outlined below in Table 4.1.

	A	B	C	D	E	F	G	H
<b>cell free extract</b>	5	5	5	5	5	5	5	5
<b>50 mM MES and 2 mM DTT</b>	1							
<b>14 mM fluoroacetaldehyde (40)</b>		1						
<b>co-factor 'soup' and 14 mM F<sup>-</sup></b>	1	1	1	1	1	1	1	1
<b>28 mM DL-<math>\alpha</math>-glycerophosphate (97)</b>			1					
<b>14 mM dihydroxyacetone phosphate (98)</b>				1				
<b>28 mM DL-glyceraldehyde-3-phosphate (11)</b>					1			
<b>14 mM 3-phosphoglycerate (17)</b>						1		
<b>14 mM 2,3-diphosphoglycerate (165)</b>							1	
<b>14 mM glycolaldehyde phosphate (164)</b>								1
<b>time / hours</b>	<b>24</b>	<b>24</b>	<b>24</b>	<b>24</b>	<b>24</b>	<b>24</b>	<b>24</b>	<b>24</b>

**Table 4.1:** Experimental protocol for preliminary fluorination event studies in cell free extracts of *S. cattleya*. Numbers refer to volume (ml).

The experiment was then incubated for 24 hours at 29 °C and terminated by immersing in hot water (> 85 °C) for 5 minutes and the resultant precipitate removed by centrifugation. The supernatants were then analysed by <sup>19</sup>F NMR and subsequently by GCMS quantification of fluoroacetate (1). Control A contained no fluorometabolites, which demonstrated that there was no endogenous fluorometabolites in the cell free extract. Control B showed a 70 % conversion from fluoroacetaldehyde (40) to fluoroacetate (1), demonstrating that the cell free extract contained active fluoroacetaldehyde dehydrogenase.

<sup>19</sup>F NMR demonstrated that samples C → H contained no resonances equivalent to fluoromethyl groups, and fluoride remained in all of the samples. GCMS confirmed that there was no fluoroacetate (1) in samples C → H.

The experiment was repeated with the same result. Therefore, it is concluded that the cell free extract of *S. cattleya*, with those co-factors and substrates was not capable of generating fluorinated organic intermediates. To explore this further the investigation was extended to an analysis of further co-factors.

#### 4.1.3 Cell free experiments with SAM (168), methionine (169), cysteine (55) and glutathione (170)

Microorganisms that are symbionts on plants that biosynthesise fluoroacetate (1) have developed a defluorination strategy based on nucleophilic attack of a free thiol residue of the dehalogenase (section 1.4.5). Glutathione (170) has also been implicated as having a role in fluoroacetate defluorination. Therefore it was deemed appropriate to investigate the putative involvement of sulphur-containing bio-molecules. A thiol, for example, could displace phosphate to generate a thio ether (172), which in turn could be subject to nucleophilic attack, by fluoride (see Fig. 4.5).

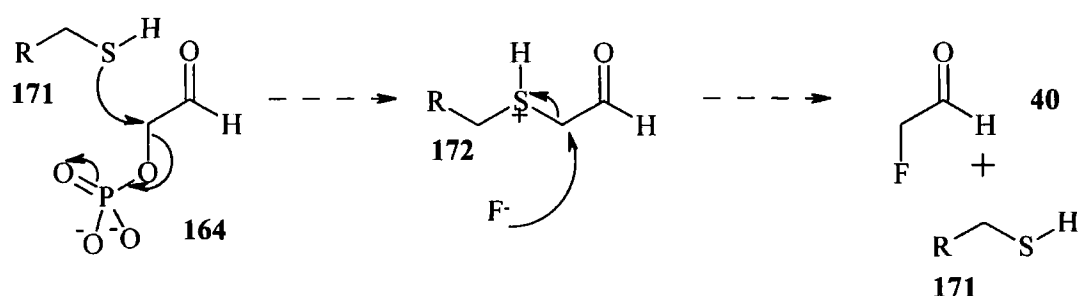


**Fig. 4.5:** Putative mechanism for fluorination *via* nucleophilic displacement of phosphate by a thiol (171), followed by nucleophilic attack by fluoride. Glycolaldehyde phosphate (164) is used as the substrate by way of example.

Cell free extracts were prepared as previously described using a French press and were incubated with fluoride (2 mM as NaF) and the co-factor 'soup'. The co-factor soup contained NAD<sup>+</sup> (2 mM), NADP<sup>+</sup> (2 mM), ATP (5 mM) and thiamine pyrophosphate (2 mM), MgSO<sub>4</sub>·7H<sub>2</sub>O (2 mM). Two sets of experiments were conducted. In the first the co-factor 'soup' was supplemented with both 2 mM *S*-adenosine methionine (SAM) (168) and 2 mM methionine (169) (**experiment 1**). In the second it was supplemented with both 2 mM cysteine (55) and 2 mM glutathione (170) (**experiment 2**).

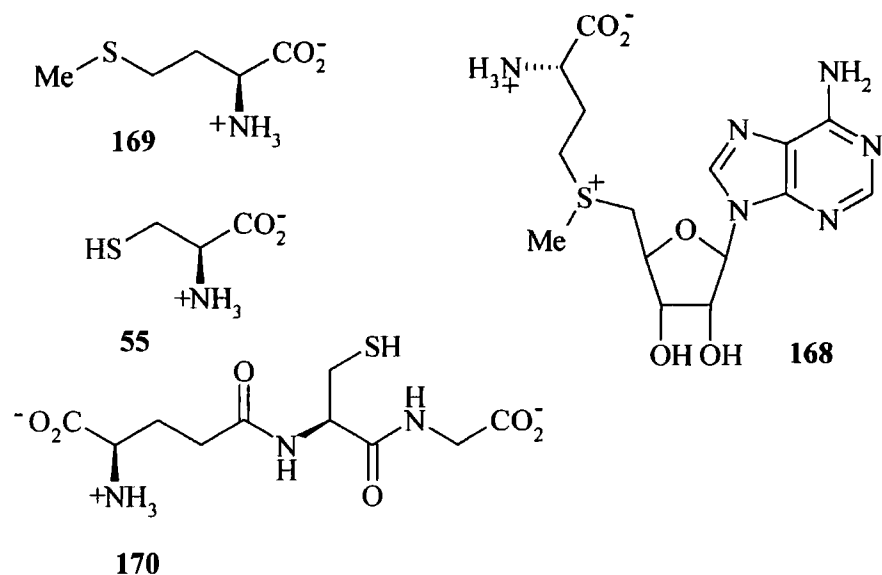


Fig. 4.6: SAM (168), methionine (169), cysteine (55) and glutathione (170).

	A	B	C	D	E	F	G	H
cell free extract	5	5	5	5	5	5	5	5
50 mM MES and 2 mM DTT	1							
14 mM fluoroacetaldehyde (40)		1						1
co-factor 'soup' and 14 mM F <sup>-</sup>	1		1	1	1	1	1	1
14 mM NAD <sup>+</sup>		1						
14 mM glycolaldehyde phosphate (164)			1					
14 mM dihydroxyacetone phosphate (98)				1				
28 mM DL-glyceraldehyde-3-phosphate (11)					1			
14 mM 3-phosphoglycerate (17)						1		
14 mM 2,3-diphosphoglycerate (165)							1	
time / hours	24	24	24	24	24	24	24	24

Table 4.2: Experimental protocol for cell free study. **Experiment 1:** Co-factor soup was supplemented with 2 mM SAM (168) and 2 mM methionine (169). **Experiment 2:** Co-factor soup was supplemented with 2 mM cysteine (55) and 2 mM glutathione (170). Numbers refer to volume (ml).

The experiments (1 & 2) were set up as outlined in the protocol (Table 4.2), and were then incubated for 24 hours at 29 °C and the experiments were terminated by immersing in hot water (> 85 °C) for 5 minutes and the resultant precipitate removed by centrifugation. The supernatants were then analysed by <sup>19</sup>F NMR. In neither experiment were any fluoromethyl resonances observed in samples incubated with substrate and fluoride (C → G), demonstrating that the presence of SAM (168), methionine (169), cysteine (55) or glutathione (170) did not act to mediate the fluorination. No fluoroacetate was detected by GCMS analysis in any of the samples (C → G).

In **experiment 1** (SAM (168) and methionine (169)) the controls were as expected, with the cell free extract capable of converting fluoroacetaldehyde (40) to fluoroacetate (1) in the presence of both NAD<sup>+</sup> alone and with the co-factor 'soup' (which included NAD<sup>+</sup>, SAM (168) and methionine (169)). However, in **experiment 2** (cysteine (55) and glutathione (170)), an anomalous result was revealed in the control. When incubated with NAD<sup>+</sup> alone fluoroacetaldehyde (40) was converted to fluoroacetate (1), but when it was incubated with the co-factor 'soup' (which included NAD<sup>+</sup>, cysteine (55) and glutathione (170)) no fluoromethyl resonances were observed and the fluoride signal was enhanced. This demonstrated that cysteine (55) or glutathione (170) could act to *defluorinate* either fluoroacetate (1) or fluoroacetaldehyde (40).

It was decided to study this defluorination activity further particularly as it may emerge that either cysteine (55) or glutathione (170) are co-factors in fluorometabolite biosynthesis, and that they were also acting to defluorinate fluoroacetate (1) in a reversible manner. Accordingly, cell free extracts were prepared as previously described and an experiment was conducted, as outlined in the protocol below (Table 4.3).

	<b>A</b>	<b>B</b>	<b>C</b>	<b>D</b>	<b>E</b>	<b>F</b>	<b>G</b>	<b>H</b>
<b>cell free extract</b>	5	5	5	5				
<b>denatured cell free extract</b>					5	5		
<b>50 mM MES &amp; 2 mM DTT</b>			0.5	0.5	0.5	0.5	5.5	5.5
<b>14 mM fluoroacetaldehyde (40)</b>	1	1	1	1	1	1	1	1
<b>28 mM NAD<sup>+</sup></b>	0.5	0.5						
<b>28 mM cysteine (55)</b>	0.5		0.5		0.5		0.5	
<b>28 mM glutathione (170)</b>		0.5		0.5		0.5		0.5
<b>time / hours</b>	<b>16</b>	<b>16</b>	<b>16</b>	<b>16</b>	<b>19</b>	<b>19</b>	<b>19</b>	<b>19</b>

**Table 4.3:** Experimental protocol for defluorination studies with cysteine (55) and glutathione (170).

The cell free extract was denatured for experiments **E** & **F** by immersion in hot water (> 85 °C) for 5 minutes and the resultant precipitate removed by centrifugation. The experiment was incubated at 29 °C for the times indicated and terminated by immersion in hot water (> 85 °C) for 5 minutes and the precipitate removed by centrifugation. The supernatants were then analysed by <sup>19</sup>F NMR.

Samples **A** & **B** contained predominantly fluoroacetate (**1**) and a small quantity of fluoride. This suggested that fluoroacetaldehyde (**40**) and not fluoroacetate (**1**) was defluorinated. It also demonstrated that both cysteine (**55**) and glutathione (**170**) are capable of defluorinating fluoroacetaldehyde (**40**). This was confirmed by studying samples **C** & **D**, which contained only fluoride and no fluoroacetaldehyde (**40**) at the end of the reaction. Samples **E** → **G** contained fluoride only, demonstrating that the defluorination of fluoroacetaldehyde (**40**) by cysteine (**55**) or glutathione (**170**) is non-enzymatic. In sample **H** approximately half of the fluoroacetaldehyde (**40**) had been defluorinated, suggesting that cysteine (**55**) is a better defluorinating agent than glutathione (**170**).

A plausible explanation for this non-enzymatic defluorination is nucleophilic attack of the free thiol at the  $\alpha$ -position of fluoroacetaldehyde (**40**), liberating fluoride and generating a thioether. Cysteine (**55**) may be more efficient than glutathione (**170**) as fluoroacetaldehyde (**40**) could form an imine (**173**) with cysteine (**55**) followed by an intramolecular displacement of fluoride to generate the thiapiperidine **174** (Fig. 4.7).

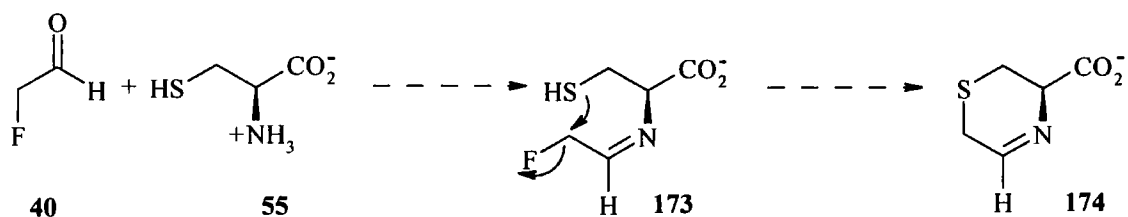


**Fig. 4.7:** Putative mechanism for fluoroacetaldehyde (**40**) defluorination by cysteine (**55**).

Although the observation is clear, these mechanistic conclusions remain tentative. The focus of this study was on the enzymatic fluorination and isolation of reaction products was not pursued.

#### 4.1.4 Cell free studies with pyridoxamine (175)

Pyridoxamine phosphate (PMP) (**175**) bonds, as an imine, with aldehydes and ketones to facilitate biotransformations such as transaminase reactions, thus it appeared appropriate to study the involvement for PMP (**175**) in the fluorination event. The role of PMP on  $\alpha$ -phosphocarbonyl compounds was studied as they may be activated to nucleophilic attack (Fig. 4.8) by this cofactor.

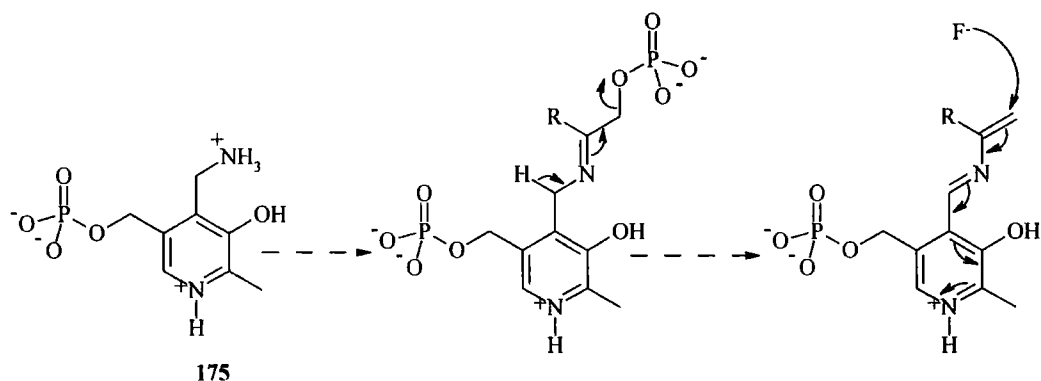


**Fig. 4.8:** Putative mechanism involving pyridoxamine phosphate (PMP) (**175**).

Cell free extracts were prepared as previously described and the experiment was conducted as outlined below (Table 4.4). Dihydroxyacetone phosphate (**98**) and glycolaldehyde phosphate (**164**) were selected as potential substrates, with the putative site for fluorination  $\alpha$  to the carbonyl.

	A	B	C
cell free extract	5	5	5
14 mM fluoroacetaldehyde ( <b>40</b> )	1		
14 mM NAD <sup>+</sup>	1		
28 mM glycolaldehyde phosphate ( <b>164</b> )		0.5	
28 mM dihydroxyacetone phosphate ( <b>98</b> )			0.5
co-factor 'soup', contains 28 mM PMP ( <b>175</b> )		0.5	0.5
14 mM NaF		1	1

**Table 4.4:** Experimental protocol on pyridoxamine (**175**) co-factor study. Numbers refer to volume (ml).

The co-factor 'soup' contained (as final concentrations); 2 mM PMP (**175**) and 2 mM NAD<sup>+</sup>. After the experiment had been incubated for 19 hours at 29 °C it was terminated by immersing the samples in hot water (> 85 °C) for 5 minutes and the resultant precipitate removed by centrifugation. The supernatants were analysed by <sup>19</sup>F NMR. Sample A was capable of catalysing the conversion from fluoroacetaldehyde (**40**) to fluoroacetate (**1**), demonstrating that the cell free extract contained an active fluoroacetaldehyde dehydrogenase. There were no fluoromethyl resonances in either sample B or C, and GCMS analysis did not reveal any evidence for fluoroacetate (**1**) in the samples. This indicates that the PMP (**175**) did not act to facilitate the fluorination of either glycolaldehyde phosphate (**164**) or dihydroxyacetone phosphate (**98**).

#### 4.1.5 Conclusions

Incubating potential substrates with fluoride and a plethora of co-factors in the cell free extract of *S. cattleya* did not result in any demonstrable fluorination activity. In each experiment the cell free extract has been shown to be active by monitoring



fluoroacetaldehyde dehydrogenase activity, although it may be that the fluorination enzyme is more susceptible to degradation, resulting in ready loss of activity. Alternatively, the experiments may be deficient in one or more co-factors or in the correct substrate. As this series of experiments has explored potential co-factor requirement in some depth, but without success, an alternate strategy was pursued. It was considered more fruitful to study the degradation or further metabolism of the candidate substrates. Some of the issues surrounding the substrates are addressed in the next section.

## ***4.2 Assessing phosphatase activity in the cell free extract***

Cell free studies were designed based on the putative mechanistic hypothesis, whereby phosphate is displaced in a nucleophilic attack by fluoride. The glycolytic intermediates and glycolaldehyde phosphate (**164**) have all been studied as potential substrates in cell free experiments (**section 4.1**), however these experiments did not demonstrate any fluorinating capability.

In the crude cell free extract of *S. cattleya* there will clearly be other enzymes displaying activities other than fluorination and fluoroacetaldehyde dehydrogenase. It is possible that phosphatase activities are acting on the substrates to dephosphorylate them, and lead to deactivation. It appeared appropriate therefore to study phosphatase activity in cell free extracts of *Streptomyces cattleya*.

### ***4.2.1 Phosphate assay***

Traditionally malachite green assays are used to determine inorganic phosphate ( $P_i$ ) concentration.<sup>132</sup> However it was decided to use the method of Jenkins and Marshall,<sup>133</sup> because the method does not require deproteinisation of the sample and MES buffer is known not to interfere with the assay.

To determine the phosphate concentration in a sample, an aliquot (1.0 ml) was mixed with 1.0 M perchloric acid (0.2 ml), which acts to denature the protein. To the resultant solution 0.25 M pH 5.0 imidazole (0.1 ml) and 1.5 % sodium molybdate were added and mixed by vortexing. Butyl acetate (2.0 ml) was added to the solution and then the reaction was mixed by vortexing for 10 seconds. Phase separation was achieved by centrifugation (5,000 rpm, 2 minutes) and 1.0 ml of the sample was removed from the organic layer. The absorbance of this sample was then measured at  $\lambda = 310$  nm and correlated to a standard curve (Fig. 4.9).

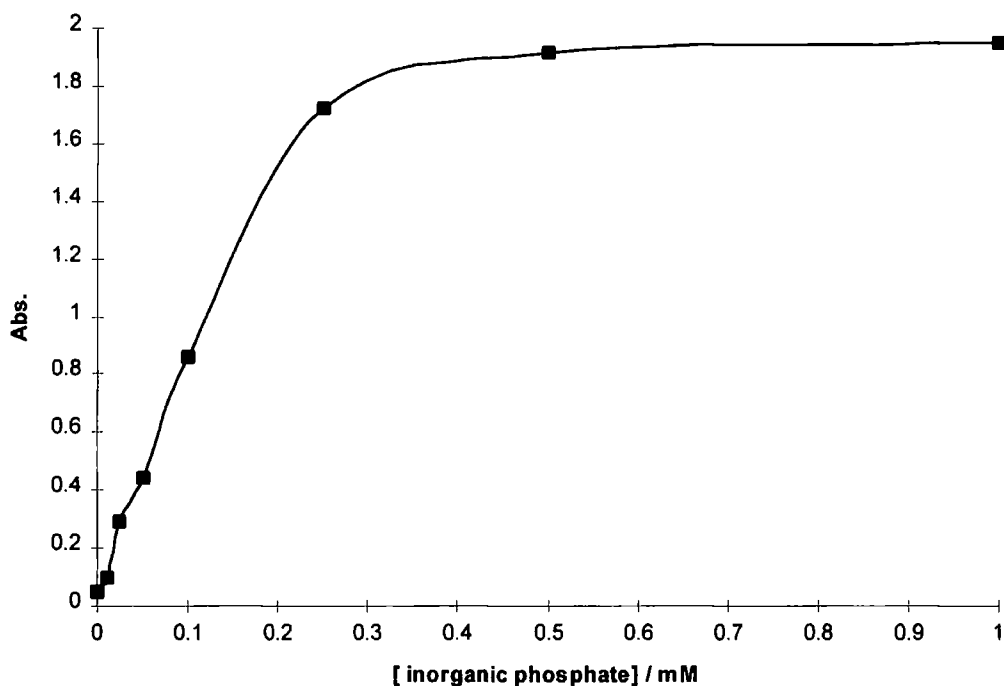


**Fig. 4.9:** Standard curve for phosphate assay, absorbance @  $\lambda = 310$  nm.

The assay can detect levels of phosphate between 0.02 mM and 0.5 mM, at which concentration the response reaches a plateau.

#### ***4.2.2 Preliminary dephosphorylation studies***

Cell free extracts were prepared as previously described and the experiment was set up following the protocol outlined below (Table 4.5). The co-factor soup contained (final concentration);  $\text{NAD}^+$  (2 mM), NaF (2 mM), ATP (5 mM) and  $\text{MgSO}_4 \cdot 7\text{H}_2\text{O}$  (2 mM). Therefore, it is important to note that all the samples contain ATP, which if acted on by an appropriate phosphatase, could result in phosphate release.

	A	B	C	D	E	F	G	H	I
cell free extract	5		5	5	5	5	5	4.6	5
50 mM MES & 2 mM DTT		5							
10 mM NaH <sub>2</sub> PO <sub>4</sub>								1.4	
14 mM fluoroacetaldehyde (40)	1	1							1
14 mM NAD <sup>+</sup>	1	1							
14 mM DHAP (98)			1						
28 mM G-3-P (11)				1					
14 mM 3-phosphoglycerate (17)					1				
14 mM 2,3-diphosphoglycerate (165)						1			
14 mM glycolaldehyde phosphate (164)							1		
co-factor 'soup'			1	1	1	1	1	1	1

**Table 4.5:** Experimental protocol for preliminary dephosphorylation studies. Numbers refer to volume (ml).

The experiments were incubated at 29 °C and the phosphate concentration of each sample determined after 0 and 4 hours by the method previously described (section 4.2.1). The results are tabulated below (Table 4.6). <sup>19</sup>F NMR of the supernatant of **sample I** demonstrated complete conversion from fluoroacetaldehyde (40) to fluoroacetate (1).

Time / hours	A	B	C	D	E	F	G	H
0	0.02	<0.02	0.02	0.03	0.02	0.02	0.02	>0.5
4	0.05	<0.02	>0.5	>0.5	>0.5	>0.5	>0.5	>0.5

**Table 4.6:** Phosphate release (mM) from glycolytic intermediates and glycolaldehyde phosphate (164) incubated with crude cell free extract of *S. cattleya*.

After 4 hours of incubation all of the samples contained greater than 0.5 mM phosphate. This clearly indicates that there was a release of phosphate from the substrate and/or ATP. There was also a moderate release (< 10 %) from the cell free extract in the absence of endogenous phosphate sources, sample A.

It was deemed necessary to study this dephosphorylation further. To that end cell free extracts were prepared as previously described and a series of experiments set up as outlined in the protocol below (Table 4.7). It was decided to focus on phosphate release from glyceraldehyde-3-phosphate (11) and glycolaldehyde phosphate (164) only, as all of the substrates in the previous study demonstrated the same response.

	A	B	C	D	E	F	G	H	I
<b>cell free extract</b>	5	5		5		5		5	5
<b>50 mM MES &amp; 2 mM DTT</b>		1	6	1	6	1	6	1	2
<b>14 mM fluoroacetaldehyde (40)</b>	1								
<b>ATP</b>		1	1						
<b>14 mM glyceraldehyde-3-phosphate (11)</b>				1	1				
<b>14 mM glycolaldehyde phosphate (164)</b>						1	1		
<b>14 mM NaH<sub>2</sub>PO<sub>4</sub></b>								1	
<b>NAD<sup>+</sup></b>	1								

**Table 4.7:** Experimental protocol for dephosphorylation studies on glycolaldehyde phosphate (164) and glyceraldehyde-3-phosphate (11). Numbers refer to volume (ml).

The experiments were incubated at 29 °C and aliquots removed at 0, 0.75, 1.5, 6.5 and 18 hours. The aliquots were then treated as previously described to determine the phosphate concentration and the results are tabulated below (Table 4.8).

	<b>[P<sub>i</sub>] / mM in sample</b>							
<b>time / hours</b>	<b>B</b>	<b>C</b>	<b>D</b>	<b>E</b>	<b>F</b>	<b>G</b>	<b>H</b>	<b>I</b>
<b>0</b>	<0.02	0.05	0.07	>0.5	<0.02	0.02	>0.5	<0.02
<b>0.75</b>	0.10	0.05	>0.5	>0.5	<0.02	0.02	>0.5	n.d.
<b>1.5</b>	0.12	0.05	>0.5	>0.5	0.03	0.02	>0.5	0.02
<b>6.5</b>	0.15	0.06	>0.5	>0.5	>0.5	0.04	>0.5	0.08
<b>18</b>	>0.5	0.06	>0.5	>0.5	>0.5	0.03	>0.5	n.d.

**Table 4.8:** Phosphate release (mM) from glyceraldehyde-3-phosphate (11) and glycolaldehyde phosphate (164).

Samples **B** & **C** demonstrate the dephosphorylation of ATP when incubated in cell free extracts or MES buffer, respectively. This experiment demonstrated that ATP was slowly dephosphorylated in the cell free extract, or during the phosphate assay. The first step of the assay involved the addition of dilute perchloric acid to denature the protein. It may be that this process hydrolyses ATP. However, the release of phosphate from ATP was different in the control (buffer only, 0.06 mM after 18 hours) from that in cell free extract (>0.5 mM after 18 hours). The experiments revealed that phosphate release from ATP by the cell free extract does not become significant until after 6 hours of incubation.

Samples **F** & **G** (glycolaldehyde phosphate (164) with and without CFE, respectively) demonstrate that glycolaldehyde phosphate (164) was dephosphorylated by the cell free extract of *S. cattleya*. Phosphate release from glycolaldehyde phosphate (164) was minimal in the presence of buffer only. However samples **D** & **E** (glyceraldehyde-3-phosphate (11) with and without CFE, respectively) are ambiguous. In the presence of the cell free extract glyceraldehyde-3-phosphate (11) was dephosphorylated, but the control contained a high level of phosphate (>0.5 mM), even at time = 0 hours. This anomaly is difficult to rationalise as glyceraldehyde-3-phosphate (11) was added at the same concentration to the cell free extract (**D**) and to the buffer (**E**). It would be expected that the concentration of phosphate in the t = 0 samples should be identical.

It is concluded from these experiments that glycolaldehyde phosphate (164) can be dephosphorylated and that glyceraldehyde-3-phosphate (11) may be dephosphorylated by cell free extracts of *S. cattleya*. The cell free extract itself also releases a small amount of phosphate with time, as demonstrated by sample I.

With this initial survey of dephosphorylation completed, it was decided to attempt a partial purification of the cell free extract to determine if dephosphorylation and the putative fluorination activities could be separated.

#### **4.2.3 Partial purification of the cell free extract**

A partial purification of the cell free extract was facilitated by precipitation of protein from solution by adding ammonium sulphate. Ammonium sulphate is routinely used to salt out protein from solution, as the density of a saturated solution (4 M, 761 g.l<sup>-1</sup>) is less than that of most aggregate proteins (1.235 g.cm<sup>-3</sup> vs. 1.33 g.cm<sup>-3</sup>). Therefore precipitated protein can be removed from the solution by centrifugation.<sup>134</sup>

Cell free extracts were prepared as previously described and ammonium sulphate was slowly added to it, whilst stirred at 4 °C. The amount of ammonium sulphate required to achieve the desired saturation was calculated using published precipitation tables.<sup>135</sup> Once the correct amount of ammonium sulphate had dissolved in the extract it was left to stir for 10 minutes, before the protein precipitate was removed by centrifugation (20,000 rpm, 4 °C, 10 minutes). By this method protein in the cell free extract was separated into that which salted out between 0 - 40 %, 40 - 65 %, 65 - 100 % and 0 - 100 % saturation (fractions a, b, c & d respectively). The protein was resuspended in 50 mM MES with 2 mM DTT, to one fifth the original volume. The experiment was then set up as outlined in the protocol below (Table 4.9).

	A	B	C	D	E	F	G	H
<b>0 - 40 % saturation, fraction a</b>	1				1			
<b>40 - 65 % saturation, fraction b</b>		1				1		
<b>65 - 100 % saturation, fraction c</b>			1				1	
<b>0 - 100 % saturation, fraction d</b>				1				1
<b>14 mM fluoroacetaldehyde (40)</b>	1	1	1	1				
<b>14 mM NAD<sup>+</sup></b>	1	1	1	1				
<b>14 mM G-3-P (11)</b>					1	1	1	1
<b>50 mM MES &amp; 2 mM DTT</b>	4	4	4	4	5	5	5	5

**Table 4.9:** Experimental protocol for assay of partially purified CFE. Numbers refer to volume (ml).

The experiment was incubated at 29 °C and aliquots removed at various time points for <sup>19</sup>F NMR studies (A → D) or phosphate (P<sub>i</sub>) concentration determination (E → H). The phosphate release (Table 4.10) and fluoroacetaldehyde (40) to fluoroacetate (1) conversion results (Table 4.11) are tabulated below.

Fraction of cell free extract, as % saturation with ammonium sulphate	0 - 40 %	40 - 65 %	65 - 100 %	0 - 100 %
time / hours	E	F	G	H
<b>0</b>	<0.02	0.02	<0.02	0.03
<b>4</b>	>0.5	>0.5	>0.5	>0.5

**Table 4.10:** Phosphate release (mM) from glyceraldehyde-3-phosphate (11) when incubated with fractions a → d of the CFE of *S. cattleya*.

Clearly the data presented in Table 4.10 demonstrate that the phosphatase activity is spread across all three fractions of the cell free extract. Ammonium sulphate cuts will not therefore be an effective method for separating phosphatase activity from the putative fluorination activity. These results also imply that more than one phosphatase



is active in the cell free extract as the efficiency of the fractionation process is demonstrated by monitoring the conversion from fluoroacetaldehyde (40) to fluoroacetate (1) (Table 4.11).

fraction of cell free extract, as % saturation with ammonium sulphate	0 - 40 %	40 - 65 %	65 - 100 %	0 - 100 %
time / hours	A	B	C	D
0.5	0 %	5.0 %	0 %	0 %
2	0 %	62.4 %	0 %	65.7 %
8	12.9 %	100 %	0 %	100 %

**Table 4.11:** Conversion from fluoroacetaldehyde (40) to fluoroacetate (1) by fractions a → d of the CFE of *S. cattleya*. Estimated from integrals of <sup>19</sup>F NMR.

The fluoroacetaldehyde dehydrogenase activity was partially purified after ammonium sulphate treatment. The activity is predominately in the fraction of protein that salted out between 40 and 65 % saturation. It appeared appropriate to treat the crude cell free extract further so as to establish where in this ammonium sulphate precipitate fraction the fluoroacetaldehyde dehydrogenase activity was located.

#### 4.2.4 Partial purification of fluoroacetaldehyde dehydrogenase

Cell free extracts were prepared as previously described and treated with ammonium sulphate (as described in section 4.2.3). By this method protein was separated into that which salted out between 0 - 65 % saturation, 40 - 53 % saturation and 53 - 65 % saturation (fractions a, b & c respectively). The amount of ammonium sulphate required to achieve the desired saturation was again calculated using published precipitation tables.<sup>135</sup> The protein was resuspended in 50 mM MES with 2 mM DTT to one fifth the original volume. The experiment was then set up as outlined in the protocol below (Table 4.12).

	A	B	C	D
<b>0 - 65 % saturation, fraction a</b>	1			
<b>40 - 52.5 % saturation, fraction b</b>		1		
<b>52.5 - 65 % saturation, fraction c</b>			1	
<b>crude cell free extract</b>				5
<b>14 mM fluoroacetaldehyde (40)</b>	1	1	1	1
<b>14 mM NAD<sup>+</sup></b>	1	1	1	1
<b>50 mM MES &amp; 2 mM DTT</b>	4	4	4	

**Table 4.12:** Experimental protocol for partial purification of fluoroacetaldehyde dehydrogenase. Numbers refer to volume (ml).

These experiments were incubated at 29 °C and aliquots were removed at 1, 2.75 and 5.5 hours and terminated by immersing in hot water (> 85 °C) for 5 minutes and the protein removed by centrifugation. The supernatants were then analysed by <sup>19</sup>F NMR to calculate the conversion from fluoroacetaldehyde (40) to fluoroacetate (1) (Table 4.13).

fraction of CFE, as % saturation with ammonium sulphate	0 - 65 %	40 - 53 %	53 - 65 %	CFE
time / hours	A	B	C	D
<b>1</b>	54.6 %	49.8 %	0 %	38.8 %
<b>2.75</b>	100 %	82.2 %	28.3 %	100 %
<b>5.5</b>	100 %	100 %	40.8 %	100 %

**Table 4.13:** Conversion from fluoroacetaldehyde (40) to fluoroacetate (1) by fractions a → c of the CFE of *S. cattleya*. Estimated from integrals of <sup>19</sup>F NMR.

Clearly the majority of the fluoroacetaldehyde dehydrogenase activity was salted out between 40 % and 53 % saturation of ammonium sulphate. A further experiment demonstrated that the actual level of purification of the cell free extract was poor. Crude cell free extracts were prepared as usual and the fraction equivalent to 40 -55 %

saturation with ammonium sulphate was precipitated out. The protein was resuspended in one fifth of the original volume with 50 mM MES and 2 mM DTT and desalted by passage through a sephadex slurry. The crude cell free extract and partially purified protein were then compared by SDS-PAGE electrophoresis. Both samples were denatured in SDS buffer heated to 95 °C for 5 minutes and loaded onto a stacking gel. A potential difference of 150 mV was applied across the gel, which was standing in SDS buffer, for 1 hour. The gel was washed and developed in Coomassie blue dye solution.

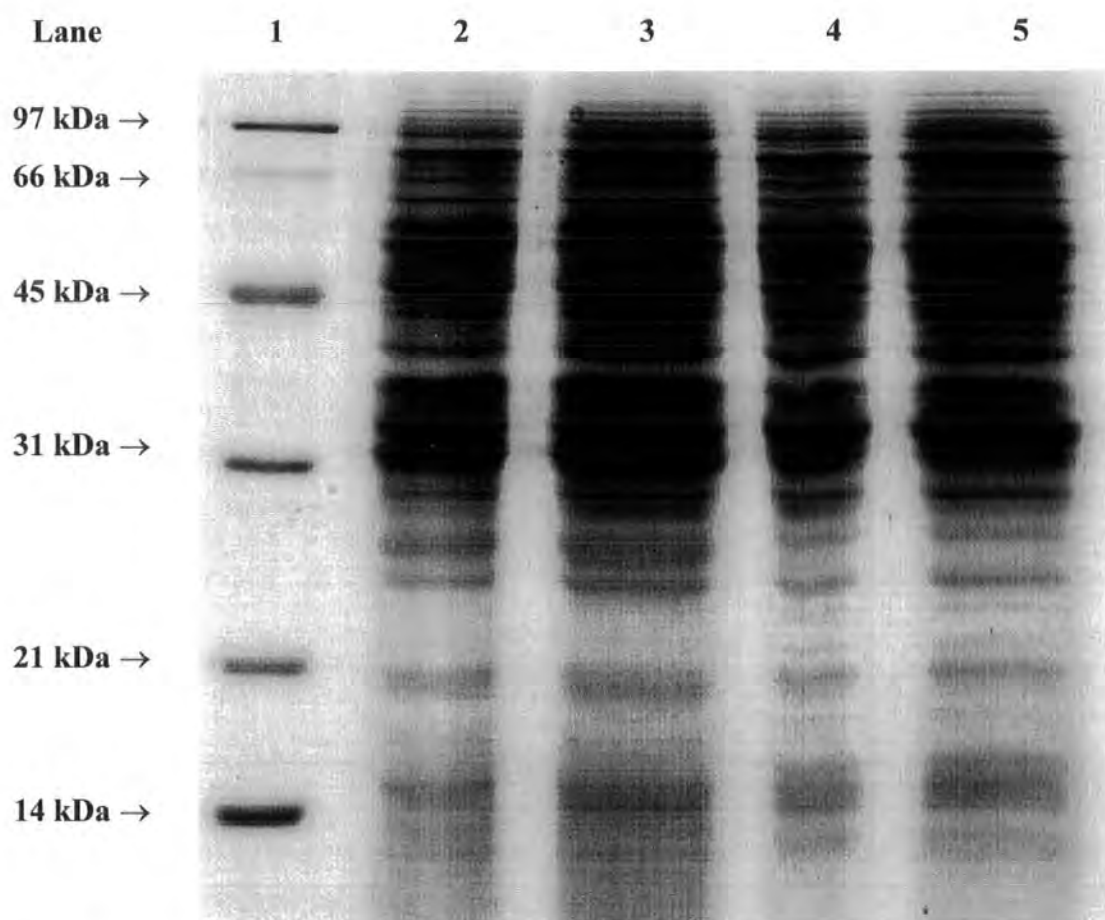


**Fig. 4.10:** SDS-PAGE electrophoresis analysis of crude and partially purified cell free extract of *S. cattleya*. **Lane 1**, molecular weight markers; **Lane 2**, 10 µl crude CFE; **Lane 3**, 17 µl crude CFE; **Lane 4**, 10 µl partially purified CFE; **Lane 5**, 17 µl partially purified CFE.

Clearly the difference between lanes 2 & 4 or 3 & 5 is not dramatic. In the partially purified cell free extract two bands with a molecular mass just over 31 kDa (present in crude CFE) have been removed. Other than that there is no significant increase in purification.

#### **4.2.5 Conclusions**

The phosphate assay has demonstrated that phosphate is released from all of the glycolytic intermediates and glycolaldehyde phosphate (164) when they are incubated with cell free extracts of *S. cattleya*. Fluorination activity is yet to be demonstrated in cell free experiments and the rate of phosphate release could perhaps account for the degradation of the glycolytic phosphates at a faster rate than fluorination.

Ammonium sulphate precipitate cuts of the cell free extract of *S. cattleya* facilitated a partial purification of the fluoroacetaldehyde dehydrogenase, albeit with little visual purification of the CFE (when studying the SDS-PAGE gel of the CFE and the partially purified fraction). Purification of the phosphatase activity could not be achieved in this way.

### 4.3 Synthesis and evaluation of isotope enriched glycolaldehydes

Glycolaldehyde phosphate (164) has been implicated as a putative substrate for fluorination and significant attempts have been made to study this in a cell free system. In the absence of any observed fluorination activity in those experiments it was decided to synthesise and feed stable isotopically labelled glycolaldehyde (176) to resting cells of *Streptomyces cattleya* and evaluate incorporation into the fluorometabolites. This would provide an alternative strategy to investigate the direct fluorination of glycolaldehyde phosphate (164) to generate fluoroacetaldehyde (40).

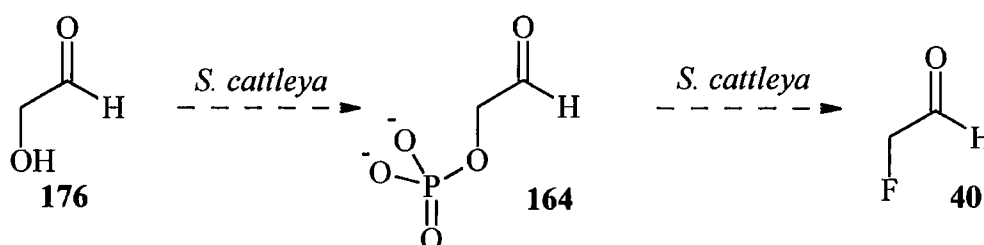


Fig. 4.11: Putative conversion of glycolaldehyde (176) to fluoroacetaldehyde (40) via glycolaldehyde phosphate (164).

#### 4.3.1 Synthesis of isotope enriched glycolaldehydes

In this study it was envisaged that a double labelled feeding experiment would be required. This would ensure that glycolaldehyde (176) was incorporated as an intact unit, if isotope became incorporated into the fluorometabolites. Routes were explored that were amenable to the synthesis of this desired labelling pattern.

Glycolaldehyde (176) is a C<sub>2</sub> carbohydrate. Therefore it could be prepared by a Kiliani-Fischer type synthesis involving attack of cyanide onto formaldehyde (177).

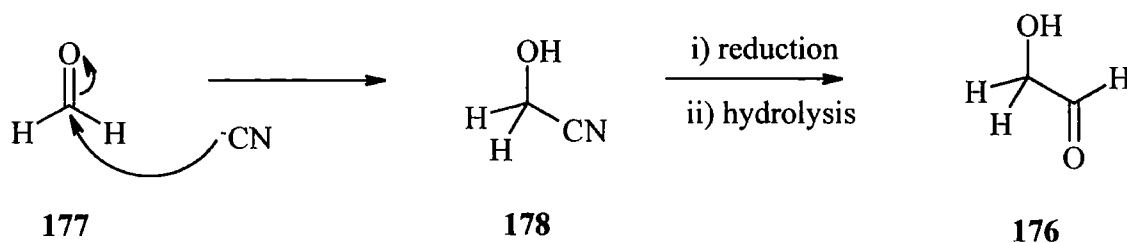


Fig. 4.12: Kiliani-Fischer type synthesis to prepare glycolaldehyde (176).

This method has been used to prepare  $^{13}\text{C}$  enriched carbohydrates, including  $[1-^{13}\text{C}]$ -glycolaldehyde (**179**),<sup>136</sup> starting with  $[^{13}\text{C}]$ -KCN. The method was modified by Thirkettle for the preparation of  $[1-^{13}\text{C}, 1,2,2-^2\text{H}_3]$ -glycolaldehyde (**180**) by using  $[^2\text{H}_2]$ -formaldehyde (**181**),  $[^{13}\text{C}]$ -KCN and conducting the reduction in a  $\text{D}_2$  atmosphere.<sup>137,138</sup>

It was decided to attempt the synthesis of  $[1-^{13}\text{C}, 2,2-^2\text{H}_2]$ -glycolaldehyde (**182**) using  $[^2\text{H}_2]$ -formaldehyde (**181**) and  $[^{13}\text{C}]$ -KCN. The intact incorporation of both isotopes would secure its role in fluoroacetaldehyde biosynthesis. Additionally, it would be desirable to synthesise  $[1-^2\text{H}]$ -glycolaldehyde (**183**) to establish if the isotope is retained at C-3 of 4-fluorothreonine (**2**), in a similar manner to that observed with  $[1-^2\text{H}]$ -fluoroacetaldehyde (**147**).

$[1-^{13}\text{C}, 2,2-^2\text{H}_2]$ -Glycolaldehyde (**182**) was prepared by dissolving  $[^{13}\text{C}]$ -KCN in  $\text{D}_2\text{O}$  and adjusting the pD to 8.5 with  $[1-^2\text{H}]$ -acetic acid. The pD of solution was measured using a pH probe calibrated to protic buffers and using the formula,  $\text{pD} = \text{pH} + 0.4$ . An equimolar quantity of  $[^2\text{H}_2]$ -formaldehyde (**181**), as an aqueous solution in  $\text{D}_2\text{O}$ , was added dropwise and the resultant solution stirred at room temperature. The pD was maintained at 8.5 with aqueous solutions (in  $\text{D}_2\text{O}$ ) of  $[1-^2\text{H}]$ -acetic acid and NaOD. Formation of  $[1-^{13}\text{C}, 2,2-^2\text{H}_2]$ -glycolonitrile (**184**) was observed by tlc ( $\text{CH}_3\text{CN} : \text{H}_2\text{O} : \text{AcOH}, 40 : 10 : 0.5$ ,  $R_f = 0.9$ , compared against commercial glycolonitrile (**178**)) and a negative result in a cyanide precipitation test. The reaction was quenched by lowering the pD to 4.2 with  $[1-^2\text{H}]$ -acetic acid. Glycolonitrile (**178**) is known to be unstable to the elimination of cyanide and to polymerisation, therefore the solution was reacted directly without isolation of  $[1-^{13}\text{C}, 2,2-^2\text{H}_2]$ -glycolonitrile (**184**). The pD was lowered to 1.7 (with  $\text{D}_2\text{SO}_4$ ) and was reduced at atmospheric pressure with hydrogen, using Pd-C as a catalyst (60 mg per mmol of nitrile). Complete conversion was confirmed by tlc after 16 hours and the catalyst was removed by filtration through a hyflo plug. The solution was then treated to remove sulphate, by lowering the pD with DOWEX ( $\text{H}^+$ ) resin and adding  $\text{BaCO}_3$  to precipitate  $\text{BaSO}_4$ . The precipitate was removed by centrifugation, as a sticky white solid. The solution was then treated with subsequent additions of DOWEX ( $\text{AcO}^-$ ) and DOWEX ( $\text{H}^+$ ) such that the final pD was 0.9. The solvent and acetic acid was partially removed *in vacuo* to yield  $[1-^{13}\text{C}, 2,2-^2\text{H}_2]$ -glycolaldehyde (**184**).  $^{13}\text{C}$  NMR analysis revealed that  $[1-^{13}\text{C}, 2,2-^2\text{H}_2]$ -aminoethan-2-ol (**185**) (resulting from the further reduction of the imine of glycolaldehyde under the

reaction conditions) was also present along with acetic acid. The solution contained approximately 65 % [1-<sup>13</sup>C, 2,2-<sup>2</sup>H<sub>2</sub>]-glycolaldehyde (**184**) compared with 5 % [1-<sup>13</sup>C, 2,2-<sup>2</sup>H<sub>2</sub>]-aminoethan-2-ol, (**185**) the remainder comprising of acetic acid (unlabelled). The volume of this solution was not reduced further due to the relative instability of glycolaldehyde, and was used directly in feeding studies, after neutralisation to pH 7.

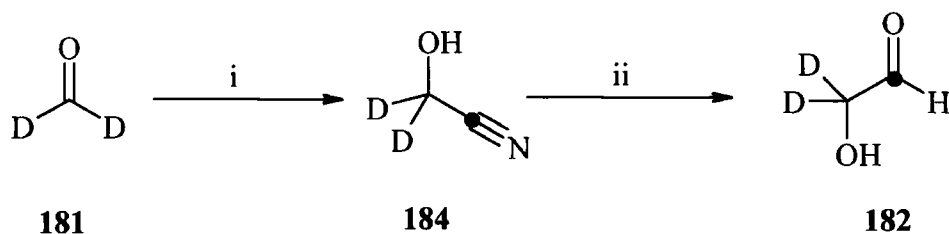


**Fig. 4.13:** Synthesis of [1-<sup>13</sup>C, 2,2-<sup>2</sup>H<sub>2</sub>]-glycolaldehyde (**182**). i) K<sup>13</sup>CN, D<sub>2</sub>O, pD = 8.5 ; ii) H<sub>2</sub>, Pd-C, pD = 1.7 (D<sub>2</sub>SO<sub>4</sub>).

A sample of [1-<sup>13</sup>C]-glycolaldehyde (**179**) was also prepared by this synthetic method, but without a deuterium labelled solvent. In this case the sample was free of any [1-<sup>13</sup>C]-aminoethan-2-ol (**186**), but did contain acetic acid.

#### 4.3.2 Feeding isotope enriched glycolaldehydes

The prepared solutions of [1-<sup>13</sup>C, 2,2-<sup>2</sup>H<sub>2</sub>]-glycolaldehyde (**182**) and [1-<sup>13</sup>C]-glycolaldehyde (**179**) were fed to resting cells of *Streptomyces cattleya* and incubated with 2 mM fluoride. Resting cells were prepared as previously described and the experimental set-up was as detailed below in Table 4.14.

	A	B	C	D	E
cells	5	5	5	5	5
50 mM MES	16	16	15	16	15
40 mM fluoride	1	1	1	1	1
200 mM [2- <sup>13</sup> C]-glycine (91)	1				
[1- <sup>13</sup> C, 2,2- <sup>2</sup> H <sub>2</sub> ]-glycolaldehyde (182)		1	2		
[1- <sup>13</sup> C]-glycolaldehyde (179)				1	2

**Table 4.14:** Experimental protocol for feeding isotope enriched glycolaldehydes to resting cells of *S. cattleya*. Numbers refer to volume (ml). The concentration of both glycolaldehydes was estimated to be 200 mM, therefore their final concentration was approximately 10 mM and 20 mM (from 1 ml and 2 ml respectively).

Each experiment was incubated at 28 °C for 48 hours on an orbital shaker and terminated by centrifugation to remove the cells. <sup>19</sup>F NMR analysis demonstrated that in sample A, fluorometabolite production followed a normal profile. Samples B → E all showed the same result, that of low incorporation of <sup>13</sup>C label into C-1 of fluoroacetate (1) and C-3 of 4-fluorothreonine (2). There was, however, no detectable incorporation from the deuterium atoms in either metabolite (by <sup>19</sup>F NMR and GCMS).

precursor	Incorporation into positions 2, 3 & 4 of 4-fluorothreonine (2) (%)		
	none	single	double
10 mM [1- <sup>13</sup> C, 2,2- <sup>2</sup> H <sub>2</sub> ]-glycolaldehyde (182)	96.8	3.2	0.0
20 mM [1- <sup>13</sup> C, 2,2- <sup>2</sup> H <sub>2</sub> ]-glycolaldehyde (182)	96.5	3.2	0.3
10 mM [1- <sup>13</sup> C]-glycolaldehyde (179)	96.5	3.2	0.3
20 mM [1- <sup>13</sup> C]-glycolaldehyde (179)	95.0	4.9	0.1

**Table 4.15:** GCMS analysis of 4-fluorothreonine (2) (positions 2, 3 & 4) resulting from incubation of resting cells of *S. cattleya* with isotopically labelled glycolaldehydes.



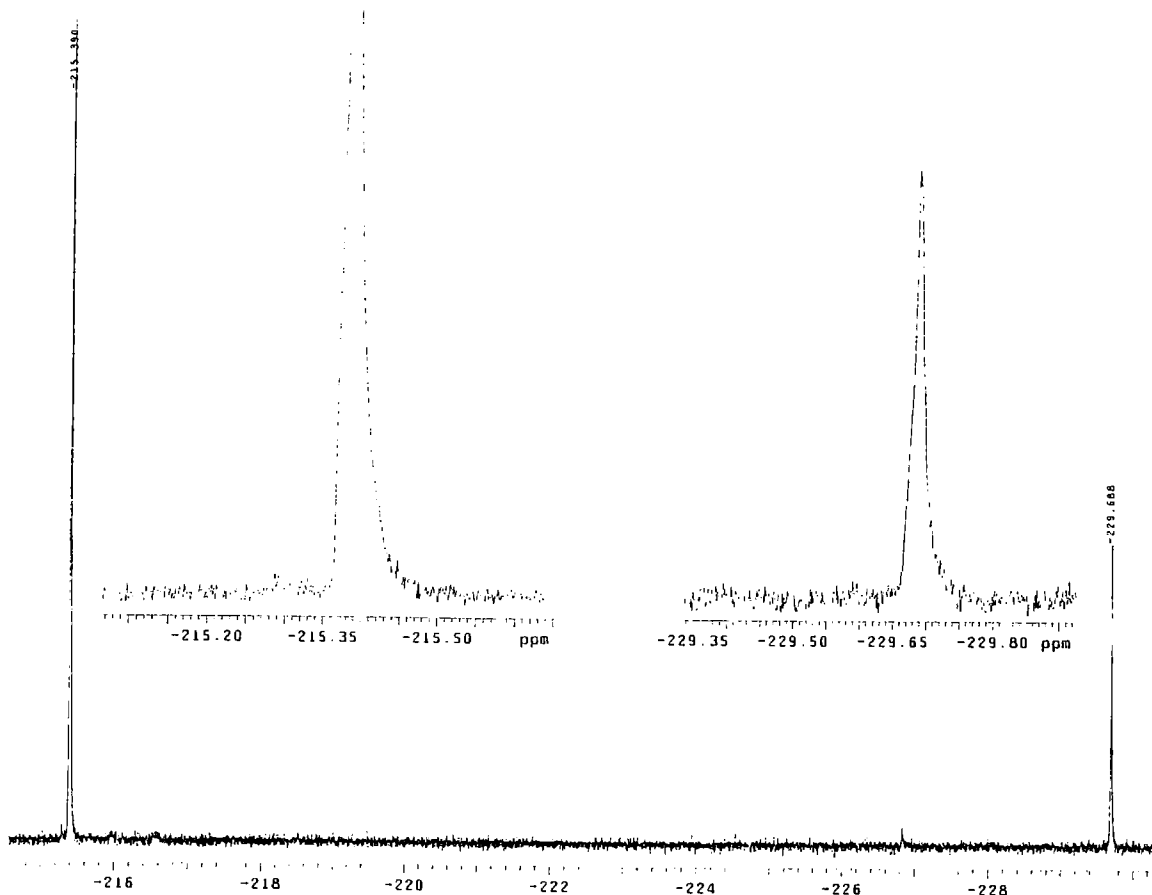


**Fig. 4.14:**  $^{19}\text{F}$   $\{^1\text{H}\}$  NMR of fluoroacetate (**1**) and 4-fluorothreonine (**2**), following incubation of resting cells of *S. cattleya* with 10 mM  $[1\text{-}^{13}\text{C}, 2,2\text{-}^2\text{H}_2]$ -glycolaldehyde (**182**).

These results demonstrate that glycolaldehyde (**176**) was not incorporated as an intact unit into the fluorometabolites. Carbon-13 from C-1 of glycolaldehyde (**176**) does label C-1 of fluoroacetate (**1**) and C-3 of 4-fluorothreonine (**2**). For that label to be assimilated directly into the fluorometabolites then the deuterium atoms should also be retained at C-2 of fluoroacetate (**1**), however this was not the case.

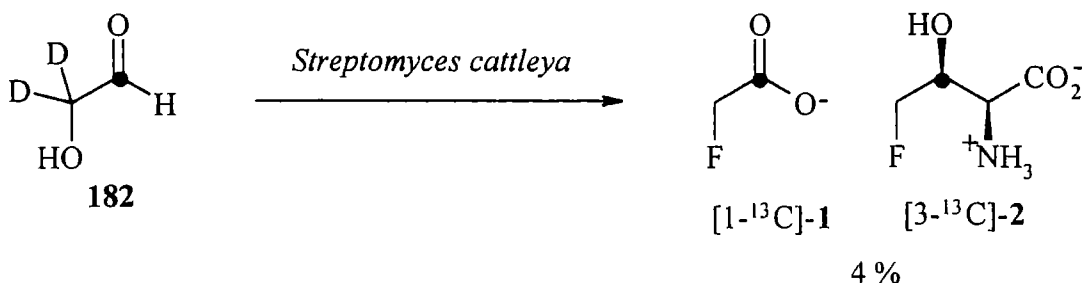


**Fig. 4.15:** Labelling observed in fluoroacetate (**1**) and 4-fluorothreonine (**2**) resulting from incubation of resting cells of *S. cattleya* with  $[1\text{-}^{13}\text{C}, 2,2\text{-}^2\text{H}_2]$ -glycolaldehyde (**182**).

Glycolaldehyde (176) does not appear to be directly involved in fluorometabolite biosynthesis. Perhaps it is also possible that it is a precursor and the bacterium does not have the capacity to phosphorylate glycolaldehyde (176), however its role must be considered tentative after these experiments.

Interestingly, glycolaldehyde (176) has not entered fluorometabolite biosynthesis *via* oxidation to glycolate (50) or by transamination to glycine (86), as the labelling patterns that result from these species are well established and would have resulted in double label in C-1 and C-2 of fluoroacetate (1) and C-3 & C-4 of 4-fluorothreonine (2). An explanation for the observed labelling pattern resultant feeding  $[1-^{13}\text{C}, 2,2-^2\text{H}_2]$ -glycolaldehyde (182) may involve the pentose phosphate pathway. This pathway was discussed in terms of rationalising the incorporation of  $^{13}\text{C}$  enriched glucoses in **section 2.3.1**. The pathway is mediated by a series of transketolase reactions that transfer an activated glycolaldehyde (176) unit. The glycolaldehyde (176) unit is resonance stabilised, bound to thiamine pyrophosphate (190 & 191), as represented in Fig. 4.16.

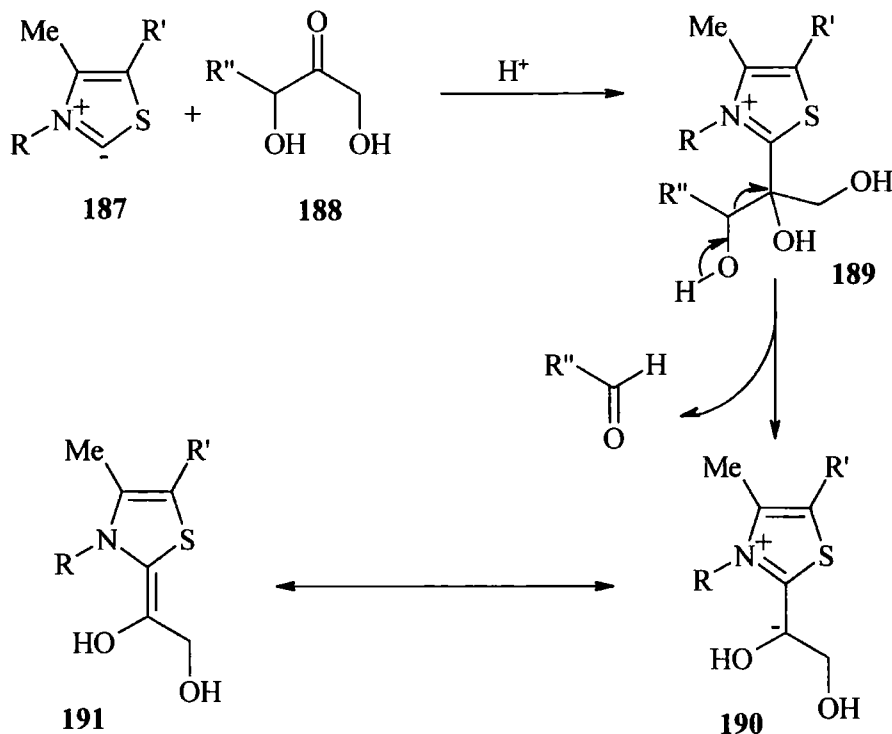


**Fig. 4.16:** The biosynthesis of activated glycolaldehyde by thiamine pyrophosphate and transketolase.

Perhaps the glycolaldehyde (176) that was administered to the bacterium condensed with TPP (187) on transketolase. If  $[1-^{13}\text{C}, 2,2-^2\text{H}_2]$ -glycolaldehyde (182) was then assimilated into the pentose phosphate pathway it would deliver  $[2-^{13}\text{C}, 1,1-^2\text{H}_2]$ -fructose-6-phosphate (194), as outlined in Fig. 4.17.

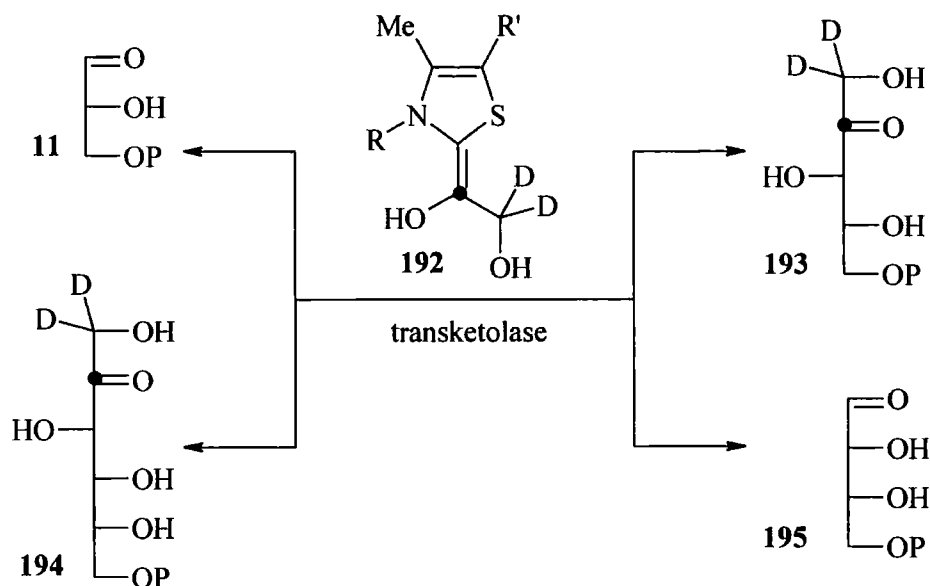


**Fig. 4.17:** Putative assimilation of  $[1-^{13}\text{C}, 2,2-^2\text{H}_2]$ -glycolaldehyde (182) into  $[2-^{13}\text{C}, 1,1-^2\text{H}_2]$ -fructose-6-phosphate (194) and  $[2-^{13}\text{C}, 1,1-^2\text{H}_2]$ -xylulose-5-phosphate (193).

$[2-^{13}\text{C}, 1,1-^2\text{H}_2]$ -Fructose-6-phosphate (194) would then enter the glycolytic pathway *via* phosphorylation and fission to  $[2-^{13}\text{C}, 1,1-^2\text{H}_2]$ -dihydroxyacetone phosphate (196) and glyceraldehyde-3-phosphate (11). The deuterium atoms may be removed from  $[2-^{13}\text{C}, 1,1-^2\text{H}_2]$ -fructose-6-phosphate (194), as their position is highly susceptible to enolisation, and would thus exchange with the media.

#### 4.4 Conclusions

To date fluorination activity has not been observed in cell free extracts of *Streptomyces cattleya*. Phosphorylated glycolytic intermediates and glycolaldehyde phosphate (**164**) were selected as candidate substrates on the basis of the minimal mechanism whereby phosphate is displaced by fluoride. Studies with different co-factors did not reveal any fluorination activity.

The cell free extract displayed significant phosphatase activity, which may deactivate candidate substrates with respect to nucleophilic attack by fluoride. Attempts to segregate phosphatase and fluorination activity using ammonium sulphate precipitation to partition the protein content of the cell free extract did not prove successful. Although the dephosphorylation of the candidate intermediates (glycolytic and glycolaldehyde phosphates) proceeds efficiently, the complete absence of any fluorination activity perhaps suggests that these were not substrates. Fluoroacetaldehyde dehydrogenase activity is high in the cell free extract and if any fluoroacetaldehyde (**40**) formed it would have been rapidly converted to fluoroacetate (**1**). The absence of any fluoroacetate (**1**) in these cell free incubations suggests that either the correct substrate or co-factors were absent from the assays.

The putative role of glycolaldehyde phosphate (**164**) as a substrate for fluorination was probed in whole cell experiments with  $[1-^{13}\text{C}, 2,2-^2\text{H}_2]$ -glycolaldehyde (**182**). Upon incubation of resting cells of *S. cattleya*, **182** did not label the fluorometabolites in a manner consistent with direct assimilation into fluoroacetaldehyde (**40**). Clearly a phosphate kinase would have to activate glycolaldehyde (**176**) to its phosphate (**164**), so that it could undergo nucleophilic attack by fluoride.

Overall the pivotal role of fluoroacetaldehyde in the biosynthesis of fluoroacetate and 4-fluorothreonine has been established. Further to that the glycolytic pathway was confirmed as the primary metabolic pathway that delivers a substrate for either direct fluorination, or bond cleavage followed by fluorination. This chapter has described a series of experiments that attempted to demonstrate fluorination activity in cell free extracts of *S. cattleya* that used these facts as starting points for the study. That

fluorination activity has not been demonstrated in cell free extracts may suggest that a more complex mechanism is operating, other than nucleophilic displacement of phosphate by fluoride.

*Chapter 5*

*Experimental*

## 5.1 Chemical Syntheses

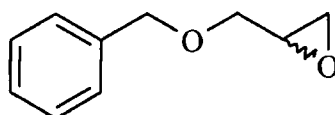
### 5.1.1 General Details

NMR spectra were recorded on Bruker AC-250 (250.133 MHz) and Varian VXR-400S (399.958 MHz), Unity (299.908 MHz) and Mercury (199.991 MHz) spectrometers in deuteriochloroform solution unless stated otherwise, using the deuterated solvent as a lock. Melting points were measured on a Gallenkamp variable heater and are uncorrected. IR spectra were recorded with absorption values in  $\text{cm}^{-1}$  on a Perkin-Elmer 257 Spectrometer as a neat film between NaCl plates unless stated otherwise. GCMS analysis was performed on a VG TRIO 1000 mass spectrometer equipped with a HP1 capillary column (25 m long, 0.22 mm i.d., 0.2  $\mu\text{m}$  film thickness) connected to a H.P. 5890 series II oven.

Reaction glassware was dried in an oven at 120 °C and cooled in a dry atmosphere of nitrogen. Reaction solvents were dried and freshly distilled prior to use. Petrol refers to the 40-60 °C boiling fraction of petroleum ether. Reactions requiring anhydrous conditions were conducted under an atmosphere of dry nitrogen and thin layer chromatography was carried out on Merck, Kieselgel 60, F<sub>254</sub> aluminium and glass backed plates. Visualisation of plates was achieved by use of a UV lamp or by use of permanganate or phosphomolybdic acid stains. Column chromatography was carried out over silica gel Merck, Kieselgel 60, 230-400 mesh.

### 5.1.2 Preparation of 3-fluoro-1-hydroxypropanone (133)

#### Glycidyl benzyl ether (139)<sup>139</sup>



139

Glycidol (**138**) (20 ml, 0.3 mol) was dissolved in THF (50 ml) and added dropwise to a suspension of NaH (7.6 g, 0.32 mol) in THF (300 ml), that had been cooled to 0 °C. The rate of addition was controlled such that the temperature did not rise above 10 °C, and the resultant solution was stirred until no further effervescence was observed. A solution of benzyl bromide (34 ml, 0.3 mol) in THF (50 ml) was added over one hour to

the reaction and left to stir for 16 hours. The resultant precipitate was filtered through a hyflo plug and the solvent removed under reduced pressure. The crude product (**139**) was suspended in ether (100 ml), washed with water (3 x 100 ml), and the combined aqueous layers were extracted into ether (2 x 100 ml). The organic layers were combined, dried and the solvent removed under reduced pressure. Glycidol benzyl ether (**139**) was purified by high vacuum distillation (bp 65 - 69 °C at 0.25 mmHg) to yield a colourless oil (11.2 g, 0.07 mol, 22 %).

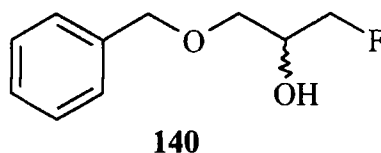
$R_f$  (1:3, ethyl acetate : petrol ether): 0.5.

IR (NaCl): 3087 $m$ , 3061 $s$ , 3030 $s$ , 2999 $s$ , 2922 $m$  (shoulder), 2861 $s$ , 2756 $w$ , 1957 $w$ , 1879 $w$ , 1815 $w$ , 1604 $w$ , 1586 $w$ , 1496 $m$ , 1453 $s$ , 1386 $m$ , 1365 $m$ , 1345 $m$ , 1337 $m$ , 1253 $m$ , 1207 $m$ , 1160 $m$ , 1133 $m$  (sh.), 1096 $s$ , 1028 $m$ , 910 $m$ , 899 $m$ , 857 $m$ , 847 $m$ , 739 $s$ , 699 $s$ , 608 $m$ .

NMR (CDCl<sub>3</sub>)  $\delta_H$  (400 MHz) (ppm): 7.3 (5H, m, Ph), 4.59 (2H, dd,  $J = 24.8$  Hz & 11.6 Hz, PhCH<sub>2</sub>O), 3.77 (1H, dd,  $J = 8.39$  Hz & 2.80 Hz, side chain-OCH<sub>a</sub>H<sub>b</sub>), 3.44 (1H, dd,  $J = 11.6$  Hz,  $J = 6.0$  Hz, side chain-OCH<sub>a</sub>H<sub>b</sub>), 3.20 (1H, m, OCH<sub>2</sub>CH), 2.80 (1H, dd,  $J = 4.40$  Hz,  $J = 4.80$  Hz, terminal-CH<sub>a</sub>H<sub>b</sub>), 2.62 (1H, dd,  $J = 4.80$  Hz,  $J = 2.40$  Hz, terminal-CH<sub>a</sub>H<sub>b</sub>).  $\delta_C$  (100 MHz) (ppm): 137.8 (Ph), 128.4 (Ph), 127.7 (Ph), 73.2 (PhCH<sub>2</sub>O), 70.7 (side chain-OCH<sub>2</sub>), 50.8 (ring-OCH), 44.2 (terminal-OCH<sub>2</sub>).

MS (EI<sup>+</sup>): 164 (M, 1.4 %), 163 (0.9 %), 108 (PhCH<sub>2</sub>O + 1, 3.4 %), 107 (PhCH<sub>2</sub>O, 39.1 %), 106 (4.2 %), 105 (29.3%), 92 (PhCH<sub>2</sub> + 1, 10.6 %), 91 (PhCH<sub>2</sub>, 100 %), 89 (6.5 %), 79 (24.8), 78 (6.6), 77 (18.6).

### 3-Fluoro-2-hydroxypropanol benzyl ether (**140**)<sup>111</sup>



Potassium hydrogen difluoride (38.0 g, 15 mol eq.) was added to a solution of glycidyl benzyl ether (**139**) (11.2 g, 0.07 mmol) in diethylene glycol (200 ml). The resultant suspension was heated at 170 °C for 4 hours under N<sub>2</sub>. Water (200 ml) was added to the cooled solution and the reaction extracted with diethyl ether (3 x 200 ml) and then with ethyl acetate (4 x 100 ml). The organic extracts were combined and concentrated to



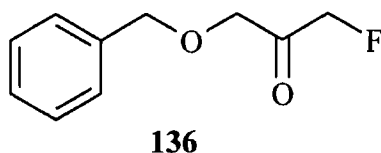
~ 300 ml under reduced pressure. The organics were then dried (over  $\text{MgSO}_4$ ) and the remainder of the solvent removed under reduced pressure to yield a yellow oil. Purification over silica (ethyl acetate : petrol) yielded **140** as a colourless oil (5.0 g, 0.03 mol, 40 %).

IR (NaCl): 3550*m* (sh.), 3416*s* (br.), 3088*w*, 3063*w*, 3031*m*, 2953*s*, 2867*s*, 1721*m*, 1603*w*, 1496*m*, 1454*s*, 1364*m*, 1328*m*, 1275*m*, 1098*s*, 1019*s*, 969*m*, 931*m*, 740*s*, 699*s*.

NMR  $\delta_{\text{H}}$  (200 MHz,  $\text{CDCl}_3$ ) (ppm): 7.40 - 7.28 (5H, m, Ph), 4.57 (2H, s,  $\text{PhCH}_2\text{OCH}_2\text{CH}(\text{OH})\text{CH}_2\text{F}$ ), 4.48 (2H, dm,  $^2J_{\text{HF}} = 47.1$  Hz,  $\text{PhCH}_2\text{OCH}_2\text{CH}(\text{OH})\text{CH}_2\text{F}$ ), 4.05 (1H, dm,  $^3J_{\text{HF}} = 18.6$  Hz,  $\text{PhCH}_2\text{OCH}_2\text{CH}(\text{OH})\text{CH}_2\text{F}$ ), 3.62 - 3.50 (2H, m,  $\text{PhCH}_2\text{OCH}_2\text{CH}(\text{OH})\text{CH}_2\text{F}$ ), 2.60 (1H, d,  $^3J_{\text{HH}} = 5.40$  Hz,  $\text{PhCH}_2\text{OCH}_2\text{CH}(\text{OH})\text{CH}_2\text{F}$ ).  $\delta_{\text{C}}$  (50 MHz,  $\text{CDCl}_3$ ): 137.56 (Ph), 128.45 (Ph), 127.87 (Ph), 127.72 (Ph), 83.88 (d,  $^1J_{\text{CF}} = 169.2$  Hz,  $\text{PhCH}_2\text{OCH}_2\text{CH}(\text{OH})\text{CH}_2\text{F}$ ), 73.53 ( $\text{PhCH}_2\text{OCH}_2\text{CH}(\text{OH})\text{CH}_2\text{F}$ ), 69.99 (d,  $^3J_{\text{CF}} = 6.99$  Hz,  $\text{PhCH}_2\text{OCH}_2\text{CH}(\text{OH})\text{CH}_2\text{F}$ ), 69.27 (d,  $^2J_{\text{CF}} = 20.17$  Hz,  $\text{PhCH}_2\text{OCH}_2\text{CH}(\text{OH})\text{CH}_2\text{F}$ ).  $\delta_{\text{F}}$  (235.34 MHz,  $\text{CDCl}_3$ ): -232.5 (td,  $^2J_{\text{HF}} = 46.4$  Hz,  $^3J_{\text{HF}} = 17.9$  Hz).

MS ( $\text{EI}^+$ ): 184 (M, 7.9 %), 107 ( $\text{PhCH}_2\text{O}$ , 8.2 %), 105 (3.2 %), 92 ( $\text{PhCH}_2 + 1$ , 25.6 %), 91 ( $\text{PhCH}_2$ , 00 %), 89 (4.7 %), 79 (5.2 %), 78 (2.3 %), 77 (8.5 %).

### 3-Fluoropropan-2-one benzyl ether (**136**)<sup>111</sup>



A solution of DMSO (0.5 ml, 6.9 mmol) in DCM (10 ml) was added to a solution of oxalyl chloride (0.3 ml, 3.3 mmol) in DCM (40 ml) at  $-60$  °C (solid  $\text{CO}_2$  / acetone bath). Addition was limited to ensure that the temperature did not exceed  $-55$  °C and the resultant solution was stirred for 10 minutes. A solution of 3-fluoro-2-hydroxypropanol benzyl ether (**140**) (0.6 g, 3.02 mmol) in DCM (10 ml) was added dropwise to the activated DMSO solution and the reaction was stirred for 15 minutes. Triethylamine (2.1 ml, 15.1 mmol) was added and the solution was allowed to warm to ambient temperature. After a further 15 minutes the reaction was quenched by the addition of water (60 ml). The organic layer was separated and the aqueous layer was extracted into

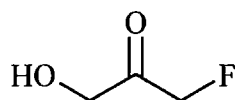
DCM (2 x 60 ml). The organics were combined and dried (over MgSO<sub>4</sub>) and the solvent was removed under reduced pressure to afford a crude oil. Purification by column chromatography over silica gel (ethyl acetate : petrol, 1:3) gave a colourless oil (**136**) (0.55 g, 2.8 mmol, 93 %).

IR (golden gate, cm<sup>-1</sup>): 2870*m*, 1742*s*, 1605*w*, 1496*m*, 1454*m*, 1426*m*, 1100*s*, 1040*s*.

NMR δ<sub>H</sub> (CDCl<sub>3</sub>, 400 MHz) (ppm): 7.27 - 7.28 (5H, m, aromatic), 4.99 (2H, d, <sup>2</sup>J<sub>HF</sub> = 47.2 Hz, OCH<sub>2</sub>COCH<sub>2</sub>F), 4.53 (2H, s, ArCH<sub>2</sub>O), 4.20 (2H, d, <sup>4</sup>J<sub>HF</sub> = 1.6 Hz, OCH<sub>2</sub>COCH<sub>2</sub>F). δ<sub>C</sub> (100.6 MHz, CDCl<sub>3</sub>) (ppm): 73.1 (ArCH<sub>2</sub>O), 73.6 (OCH<sub>2</sub>COCH<sub>2</sub>F), 84.5 (d, <sup>1</sup>J<sub>CF</sub> = 182.0 Hz, OCH<sub>2</sub>COCH<sub>2</sub>F), 127.9 (*o*-Ph), 128.2 (*p*-Ph), 128.6 (*m*-Ph), 136.6 (Ph), 203.3 (d, <sup>2</sup>J<sub>CF</sub> = 17.2 Hz, OCH<sub>2</sub>COCH<sub>2</sub>F). δ<sub>F</sub> (188 MHz, CDCl<sub>3</sub>): -236.11 (t, <sup>2</sup>J<sub>FH</sub> = 47.1 Hz).

MS (CI<sup>+</sup>, NH<sub>3</sub>): 201 (M + NH<sub>4</sub><sup>+</sup> +1, 5.0 %), 200 (M + NH<sub>4</sub><sup>+</sup>, 75.7 %), 183 (M + 1, 9.1 %), 182 (M, 100 %), 166 (8.6 %), 108 (55.7 %), 91 (22.9 %).

### 3-Fluoro-1-hydroxypropan-2-one (**133**)



**133**

A suspension Pd on carbon (50 mg) in a solution of 3-fluoropropan-2-one benzyl ether (**136**) (0.26 g, 1.4 mmol) in methanol (10 ml) was stirred vigorously under a hydrogen atmosphere for 16 hours. The catalyst was filtered through a hyflo plug and the solvent removed under reduced pressure, to yield the product (**133**) as a crude oil (0.15 g).

<sup>19</sup>F NMR (188 MHz, D<sub>2</sub>O): -225.20 (2 % of F signal, t, J = 47 Hz), -227.30 (13 % of F signal, t, J = 47 Hz), -227.53 (10 % of F signal, t, J = 47 Hz), -231.23 (28 % of F signal, t, J = 47 Hz), -231.87 (13 % of F signal, t, J = 47 Hz), -232.2 → -234.8 (28 % of F signal, many unresolved triplets, J = 47 Hz), -237.33 (5 % of F signal, t, J = 47 Hz).

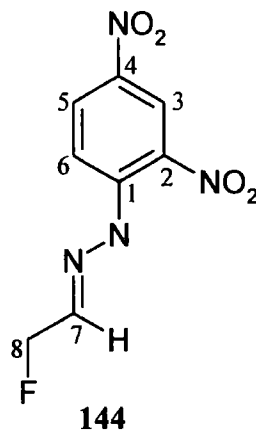
### 5.1.3 Preparation of fluoroacetaldehyde (40)

#### Fluoroacetaldehyde (40)

2-Fluoroethanol (71) (1 ml, 17.0 mmol) was added to suspension of pyridinium dichromate (PDC) (2.00 g, 5.3 mmol) in dichloromethane (30 ml) and the reaction was mixture heated under reflux for 16 hours. The reaction vessel was allowed to cool and the condenser changed for a vigereux distillation apparatus. The reaction solution was distilled into a separating funnel containing water (5 ml). After mixing, the organic layer was separated and extracted with a further volume of water (5 ml). The aqueous layers were combined and both the organic and aqueous layers analysed by  $^{19}\text{F}$  NMR analysis. Fluoroacetaldehyde hydrate (40) was present in the aqueous layer at a final concentration of 40 mM (~ 20 %) The sample also contained residual 2-fluoroethanol (71).

NMR ( $\text{D}_2\text{O}$ )  $\delta_{\text{F}}$  (376 MHz): -224.5 (80 % of total signal, tt,  $^2J_{\text{HF}} = 47.6$  Hz,  $^3J_{\text{HF}} = 31.8$  Hz, F-EtOH (71)), 233.5 (20 % of total signal, td,  $^2J_{\text{HF}} = 46.2$  Hz,  $^3J_{\text{HF}} = 9.4$  Hz, fluoroacetaldehyde (40)).

#### DNP derivative of fluoroacetaldehyde (144)



A DNP solution was prepared by dissolving 2,4-dinitrophenylhydrazone (0.4 g) in concentrated sulphuric acid (2 ml), followed by the slow addition of water (3 ml) and then 95 % aqueous ethanol (10 ml).

The DNP derivative of fluoroacetaldehyde (**144**) was prepared by adding the aqueous solution of fluoroacetaldehyde (**40**) to the DNP solution and the resultant precipitate filtered and recrystallised from ethanol.

Melting point: 143-144 °C

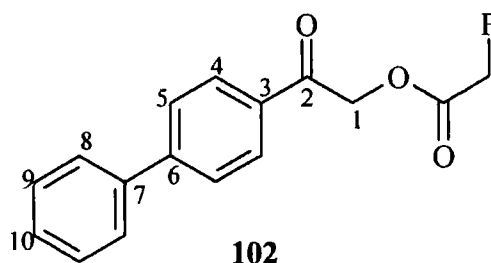
IR (KBr): 3296 $m$ , 3107 $w$ , 3091 $w$ , 2361 $w$ , 2343 $w$ , 1617 $s$ , 1590 $m$ , 1511 $s$ , 1418 $m$ , 1323 $s$ , 1305 $s$ , 1266 $s$ , 1140 $m$ , 1124 $m$ , 1086 $m$ , 924 $m$ , 854 $w$ , 842 $w$ , 831 $m$ , 744 $m$ , 724 $m$ , 606 $m$ .

NMR  $\delta_{\text{H}}$  (400 MHz,  $\text{CDCl}_3$ ): 11.17 (1H, s,  $\text{NH}$ ), 9.14 (1H, s, (C-3)- $\text{H}$ ), 8.36 (1H, m (C-5)- $\text{H}$ ), 7.98 (1H, m, (C-6)- $\text{H}$ ), 7.64 (1H, dd,  $^3J_{\text{HH}} = 5.2$  Hz,  $^3J_{\text{HF}} = 10.4$  Hz, (C-7)- $\text{H}$ ), 5.17 (2H, dd,  $^2J_{\text{HF}} = 46.4$  Hz,  $^3J_{\text{HH}} = 5.2$  Hz, (C-8)- $\text{H}$ ).  $\delta_{\text{C}}$  (100 MHz,  $\text{CDCl}_3$ ) (ppm): 80.92 (C-8, d,  $^1J_{\text{CF}} = 166.4$  Hz), 114.6 (C-6), 123.2 (C-3), 130.1 (C-5), 138.9 (C-7), 143.5 (C- $\text{NO}_2$ ), 143.7 (C- $\text{NO}_2$ ), 144.7 (C-1).  $\delta_{\text{F}}$  (376 MHz,  $\text{CDCl}_3$ ): -222.61 (dt,  $^2J_{\text{FH}} = 46.4$  Hz,  $^3J_{\text{FH}} = 6.4$  Hz).

HRMS (EI)  $\text{C}_8\text{H}_7\text{FN}_4\text{O}_4$ : Calculated ( $\text{M}^+$ ) 242.04513, found 242.0451

#### 5.1.4 Preparation of [1-<sup>2</sup>H]-fluoroacetaldehyde (147)

##### *para*-phenylphenacyl fluoroacetate (102)<sup>100</sup>



Sodium fluoroacetate (**1**) (7.27 g, 72.7 mmol) and a catalytic quantity of 18-crown-6 (0.3 g, 1.1 mmol) were added to a solution of *para*-phenylphenacyl bromide (**101**) (20.0 g, 72.7 mmol) in a 1:1 mixture of acetonitrile and benzene (280 ml) and the reaction was heated under reflux for 16 hours. When the reaction vessel had cooled to room temperature the organics were washed with water (2 x 100 ml) and then the solvent removed under reduced pressure to yield a yellow solid (16.0 g, 88.7 %). A small quantity was recrystallised from dichloromethane for analytical purposes.

Melting point: 140 - 142 °C (lit. 138 °C)<sup>100</sup>

IR (KBr, cm<sup>-1</sup>): 2930<sub>m</sub>, 1775<sub>s</sub>, 1693<sub>s</sub>, 1601<sub>s</sub>, 1558<sub>m</sub>, 1486<sub>m</sub>, 1440<sub>m</sub>, 1423<sub>s</sub>, 1403<sub>m</sub>, 1369<sub>m</sub>, 1284<sub>w</sub>, 1241<sub>m</sub>, 1212<sub>s</sub>, 1187<sub>s</sub>, 1117<sub>m</sub>, 1089<sub>s</sub>, 1046<sub>m</sub>, 1007<sub>m</sub>, 965<sub>s</sub>, 856<sub>m</sub>, 834<sub>m</sub>, 767<sub>s</sub>, 748<sub>m</sub>, 730<sub>m</sub>, 701<sub>m</sub>.

NMR δ<sub>H</sub> (200 MHz, CDCl<sub>3</sub>): 7.99 (2H, d, <sup>3</sup>J<sub>HH</sub> = 8.20 Hz, C4-H), 7.72 (2H, d, <sup>3</sup>J<sub>HH</sub> = 8.20 Hz, C5-H), 7.66 - 7.58 (2H, m, C9-H), 7.54 - 7.38 (3H, m, C8-H & C10-H), 5.52 (2H, s, C1-H), 5.08 (2H, d, <sup>2</sup>J<sub>HF</sub> = 46.8 Hz). δ<sub>C</sub> (50 MHz, CDCl<sub>3</sub>): 190.42 (s, C2), 167.35 (d, <sup>2</sup>J<sub>CF</sub> = 22.3 Hz, OCOCH<sub>2</sub>F), 146.87 (s, C6), 139.47 (s, C7), 132.44 (s, C3), 129.00 (s, Ar), 128.50 (s, Ar), 128.32 (s, Ar), 127.54 (s, Ar), 127.35 (s, Ar), 77.39 (d, <sup>1</sup>J<sub>CF</sub> = 182.3 Hz, OCOCH<sub>2</sub>F), 66.41 (s, C1). δ<sub>F</sub> (188 MHz, CDCl<sub>3</sub>): -230.63 (t, <sup>2</sup>J<sub>FH</sub> = 46.7 Hz).

MS (EI<sup>+</sup>): 272 (M, 2.6 %), 196 (M - FH<sub>2</sub>CCO<sub>2</sub> + 1, 17.5 %), 182 (PhPhCO + 1, 13.7 %), 181 (PhPhCO, 100 %), 154 (5.3 %), 153 (28.3 %), 152 (59.8 %), 150 (6.4 %).

##### [1,1-<sup>2</sup>H<sub>2</sub>]-2-Fluoroethanol (148)

*para*-Phenylphenacyl fluoroacetate (**102**) (6.8 g, 25.0 mmol) was suspended in tetraglyme (20 ml) and added over 20 minutes to a suspension of LiAlD<sub>4</sub> (1.4 g, 33.3

mmol) in tetraglyme (60 ml) at -10 °C (ice / acetone slush bath). The resultant suspension was allowed to warm to room temperature and was stirred for a further 4 hours before the reaction vessel was cooled in ice water. The reaction was quenched by the addition of 2-phenoxyethanol (**152**) (20 ml) and left to stir overnight. [1,1-<sup>2</sup>H<sub>2</sub>]-2-Fluoroethanol (**148**) was then distilled out of the reaction vessel over a vigreux column at atmospheric pressure. The reaction vessel was heated to 140 °C and the vigreux column heated with a hair dryer to distil over the colourless liquid. The vessel was cooled again and DCM (5 ml) was added this was solution distilled along with any residual [1,1-<sup>2</sup>H<sub>2</sub>]-2-fluoroethanol. This process was repeated with two further volumes of DCM (5 ml), and all the distillates combined.

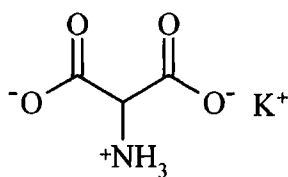
NMR  $\delta_{\text{H}}$  (200 MHz, CDCl<sub>3</sub>): 4.43 (d,  $^2J_{\text{HF}} = 47.7$  Hz, HOCD<sub>2</sub>CH<sub>2</sub>F), 4.0 - 2.8 (tetraglyme), 1.11 (s, AcOH).  $\delta_{\text{F}}$  (188 MHz, CDCl<sub>3</sub>): -227.4 (tp,  $^2J_{\text{FH}} = 47.6$  Hz,  $^3J_{\text{FD}} = 4.37$  Hz)

#### *[1-<sup>2</sup>H]-Fluoroacetaldehyde (147)*

Pyridinium dichromate (PDC) (1.0 g, 2.7 mmol) was added to a solution of [1,1-<sup>2</sup>H<sub>2</sub>]-2-fluoroethanol (**148**) in DCM (15 ml) and the reaction was heated under reflux for 18 hours. After cooling, the condenser was exchanged for a vigreux column and the [1-<sup>2</sup>H]-fluoroacetaldehyde (**147**) and DCM mixture was distilled over into water (2 ml). The phases were separated and the organics were extracted with a further volume of water (2 ml) and the aqueous layers combined.

NMR (D<sub>2</sub>O)  $\delta_{\text{F}}$  (188 MHz): -227.6 (80 % of total signal, tm,  $^2J_{\text{HF}} = 47.6$  Hz, HOCD<sub>2</sub>CH<sub>2</sub>F), 233.6 (20 % of total signal, t,  $^2J_{\text{HF}} = 46.1$  Hz, ).

### 5.1.5 Preparation of potassium aminomalonate (162)<sup>129</sup>



**162**

Potassium hydroxide (4.63 g, 0.0825 mol) was added to an aqueous solution (30 ml) of diethyl aminomalonate hydrochloride salt (163) (5.00 g, 0.024 mol) and the reaction was heated under reflux for 4 hours. When the reaction mixture had cooled to room temperature it was adjusted to pH 4.1 using concentrated aqueous hydrochloric acid and stored at 4 °C for 16 hours. The resultant white precipitate was filtered off and washed with ice cold water (50 ml) and then ethanol (50 ml), to yield a white amorphous solid (2.63 g, 69.7 %).

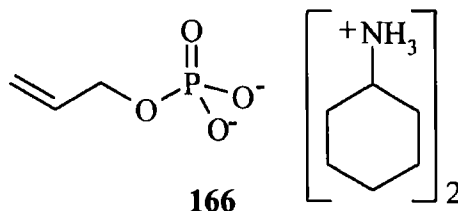
Melting point: 245 °C (decomposes) (lit. not quoted)<sup>129</sup>

IR (KBr): 3067<sub>s</sub>, 2749<sub>s</sub>, 2641<sub>s</sub>, 2168<sub>w</sub>, 2120<sub>w</sub>, 1625<sub>s</sub>, 1531<sub>s</sub>, 1424<sub>s</sub>, 1152<sub>m</sub>, 1081<sub>m</sub>, 937<sub>m</sub>, 929<sub>m</sub>, 913<sub>m</sub>, 836<sub>m</sub>

NMR  $\delta_{\text{H}}$  (200 MHz, D<sub>2</sub>O): 4.03 (1H, s,  $\text{O}_2\text{CCH}(\text{NH}_3^+)\text{CO}_2\text{K}^+$ );  $\delta_{\text{C}}$  (50.3 MHz, D<sub>2</sub>O): 59.32 (s,  $\text{O}_2\text{CCH}(\text{NH}_3^+)\text{CO}_2\text{K}^+$ ), 170.30 (s,  $\text{O}_2\text{CCH}(\text{NH}_3^+)\text{CO}_2\text{K}^+$ ).

### 5.1.6 Preparation of glycolaldehyde phosphate (164)

#### Allylphosphate bis(cyclohexylamine) salt (166)<sup>130</sup>



Trichloroacetonitrile (14.40 g, 100 mmol) was added to a solution of (crystalline) phosphoric acid (1.90 g, 19.4 mmol) and triethylamine (4.00 g, 39.6 mmol) in allyl alcohol (72) (35 ml, 517 mmol), and the solution became turbid. The mixture was heated at 75 °C for 4 hours and the volume then reduced under reduced pressure to approximately 15 ml. Water (200 ml) was added to this oily solution and the mixture

was extracted into diethyl ether (2 x 150 ml). Cyclohexylamine (15 ml, 130 mmol) was added to the resultant aqueous fraction and the solvent was removed under reduced pressure. The resultant turbid oil was resuspended in water (50 ml) and acetone was added dropwise until the solution became turbid, at which point the solution was stored in ice for 3 hours. A white amorphous powder was collected by filtration and washed with ice cold acetone (20 ml). The mother liquor was treated with a further volume of acetone (20 ml) and the resultant white solid was filtered and washed with acetone. The solids were combined to produce a white amorphous solid of **166** (4.8 g, 74 % based on phosphoric acid)

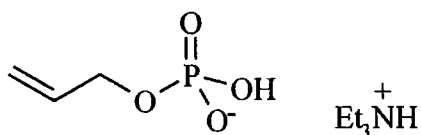
Melting point: 213 - 218 °C (lit. 217-219 °C)<sup>130</sup>

IR (KBr): 2937<sub>s</sub>, 2857<sub>s</sub>, 2566<sub>s</sub>, 2232<sub>m</sub>, 1629<sub>m</sub>, 1560<sub>m</sub>, 1455<sub>m</sub>, 1394<sub>m</sub>, 1070<sub>s</sub>, 981<sub>m</sub>, 915<sub>m</sub>, 820<sub>m</sub>

NMR  $\delta_{\text{H}}$  (200 MHz, D<sub>2</sub>O): 5.8 (1H, m, CH<sub>2</sub>CHCH<sub>2</sub>O), 5.18 (1H, dd, <sup>2</sup>J<sub>HH</sub> = 17.1 Hz, <sup>3</sup>J<sub>HH</sub> = 1.7 Hz, CH<sub>2</sub>CHCH<sub>2</sub>O), 5.02 (1H, dd, <sup>2</sup>J<sub>HH</sub> = 10.4 Hz, <sup>3</sup>J<sub>HH</sub> = 1.4 Hz, CH<sub>2</sub>CHCH<sub>2</sub>O), 4.12 (2H, *psuedo-t*, CH<sub>2</sub>CHCH<sub>2</sub>O), 2.99 (2H, m, H<sub>3</sub>N<sup>+</sup>CH(CH<sub>2</sub>R)<sub>2</sub>), 1.80-1.95 (4H, m, CH<sub>x</sub>NH<sub>3</sub><sup>+</sup>), 1.55-1.75 (4H, m, CH<sub>x</sub>NH<sub>3</sub><sup>+</sup>), 1.45-1.55 (2H, m, CH<sub>x</sub>NH<sub>3</sub><sup>+</sup>), 0.90-1.35 (10H, m, CH<sub>x</sub>NH<sub>3</sub><sup>+</sup>).  $\delta_{\text{C}}$  (50.3 MHz, D<sub>2</sub>O) (ppm): 24.03 (CH<sub>2</sub>, CH<sub>x</sub>NH<sub>3</sub><sup>+</sup>), 24.53 (CH<sub>2</sub>, CH<sub>x</sub>NH<sub>3</sub><sup>+</sup>), 30.57 (CH<sub>2</sub>, CH<sub>x</sub>NH<sub>3</sub><sup>+</sup>), 50.59 (CH, CH<sub>x</sub>NH<sub>3</sub><sup>+</sup>), 65.55 (CH<sub>2</sub>CHCH<sub>2</sub>O, d, <sup>2</sup>J<sub>C-P</sub> = 4.42 Hz), 116.29 (CH<sub>2</sub>CHCH<sub>2</sub>O), 135.61 (CH<sub>2</sub>CHCH<sub>2</sub>O, d, <sup>3</sup>J<sub>C-P</sub> = 6.99 Hz).  $\delta_{\text{P}}$  {<sup>1</sup>H} (81.0 MHz, D<sub>2</sub>O): 5.64 (s).

ESI-MS (ES<sup>-</sup>): 297 (7 %), 275 (4 %), 157 (4 %), 143 (8 %), 137 (M + H, 100 %), 115 (8 %), 79 (66 %). (ES<sup>+</sup>): 100 (M, 100 %), 83 (M - NH<sub>3</sub>, 33 %).

#### Allylphosphate mono(triethylamine) salt (**167**)<sup>130</sup>



**167**

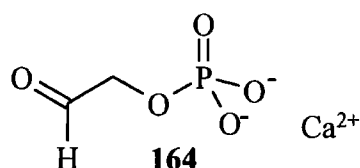
Dowex 50X8 (H<sup>+</sup>) was added to an aqueous solution of allylphosphate bis(cyclohexylamine) salt (**166**) (4.00 g, 11.9 mmol) until the pH remained constant. The solution was stirred at room temperature for 20 minutes before the resin was removed by filtration, and washed with water (150 ml). The washings were combined



in a separating funnel and mixed with a solution of triethylamine (17 ml, 10 mol equivalents) in diethyl ether (250 ml). The aqueous layer was separated from the organics and the solvent removed under reduced pressure. The product (**167**) oil, 2.8 g (43.9 %) was reacted on immediately due to the potential instability of the product.

NMR  $\delta_{\text{H}}$  (300 MHz, D<sub>2</sub>O): 5.79 (1H, m, CH<sub>2</sub>CHCH<sub>2</sub>O), 5.17 (1H, d, CH<sub>2</sub>CHCH<sub>2</sub>O, *trans*-<sup>3</sup>J<sub>HH</sub> = 17.1 Hz), 5.03 (1H, d, CH<sub>2</sub>CHCH<sub>2</sub>O, *cis*-<sup>3</sup>J<sub>HH</sub> = 10.5 Hz), 4.19 (2H, *psuedo*-t, CH<sub>2</sub>CHCH<sub>2</sub>O), 3.00 (6H, q, CH<sub>3</sub>CH<sub>2</sub>N, <sup>3</sup>J<sub>HH</sub> = 7.40 Hz), 1.07 (9H, t, CH<sub>3</sub>CH<sub>2</sub>N, <sup>3</sup>J<sub>HH</sub> = 7.35 Hz).  $\delta_{\text{p}}$  {<sup>1</sup>H}(81.0 MHz, D<sub>2</sub>O): 1.36 (s).

### Glycolaldehyde phosphate, calcium salt (**164**)<sup>130</sup>



A stream of O<sub>3</sub> (generated from O<sub>2</sub> @ 60 l.hr<sup>-1</sup>) was passed through a solution of allylphosphate mono(triethylamine) salt (**167**) (2.8 g, 5.2 mmol) in methanol (150 ml) at -78 °C. After 30 minutes the reaction mixture turned light blue indicating ozone saturation. The ozone stream was replaced by nitrogen and the reaction vessel was allowed to warm to -20 °C. After 10 minutes DMS (5 ml, 13 mol equivalent) was added and the resultant solution was stirred for 24 hours whilst maintaining the temperature at -20 °C. The reaction vessel was then placed in an ice bath, then iced water (80 ml) and Dowex 50 X 8 (H<sup>+</sup>) were added. The resultant mixture was stirred for 30 minutes and the resin removed by filtration and washed with ice-cold water (400 ml). The volume was reduced to approximately 50 ml under reduced pressure, keeping the water bath temperature below 40 °C. After the reaction mixture was cooled in an ice bath, a solution of calcium acetate (1.89 g, 11.9 mmol) in water (25 ml) was added and it was left to stir for 1 hour. Acetone (50 ml) was added and a white precipitate formed. The mixture was then stored at 4 °C for 16 hours. The precipitate was collected by centrifugation (20,000 rpm, 30 minutes, 4 °C), and the supernatant was treated with a further volume of acetone (25 ml). This precipitate was collected by centrifugation and combined, to yield a white amorphous solid (2.1 g, 71 %)

Melting point: > 260 °C (lit. not quoted)<sup>130</sup>

IR (KBr): 3395<sub>s</sub> (br.), 3250<sub>s</sub> (sh.), 3160<sub>s</sub> (sh.), 1719<sub>w</sub>, 1654<sub>w</sub>, 1636<sub>w</sub>, 1458<sub>w</sub>, 1137<sub>s</sub>, 1091<sub>s</sub>, 1024<sub>s</sub>, 913<sub>m</sub>, 828<sub>m</sub> (br.)

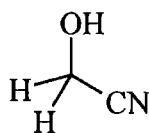
NMR  $\delta_{\text{H}}$  (200 MHz, D<sub>2</sub>O / trace DCl): 4.98 (1H, dt,  $^3J_{\text{HH}} = 4.90$  Hz, OCH<sub>2</sub>CH(OH)<sub>2</sub>), 3.67 (2H, dd,  $^3J_{\text{HH}} = 4.90$  Hz,  $^3J_{\text{HP}} = 6.90$  Hz, OCH<sub>2</sub>CH(OH)<sub>2</sub>);  $\delta_{\text{C}}$  (50.3 MHz, D<sub>2</sub>O / trace DCl) (ppm): 68.09 (OCH<sub>2</sub>CH(OH)<sub>2</sub>, d,  $^3J_{\text{CP}} = 5.53$  Hz), 88.46 (OCH<sub>2</sub>CH(OH)<sub>2</sub>, d,  $^2J_{\text{CP}} = 8.75$  Hz);  $\delta_{\text{p}}$  {<sup>1</sup>H} (81.0 MHz, D<sub>2</sub>O / trace DCl): 1.00 (s).

ESI-MS (ES<sup>-</sup>): 199 (26 %), 197 (M + 1, 50 %), 195 (M - 1, 38 %), 164 (35 %), 162 (100 %), 160 (98 %).

### 5.1.7 Preparation of [*1*-<sup>13</sup>C]- and [*1*-<sup>13</sup>C, 2,2-<sup>2</sup>H<sub>2</sub>]-glycolaldehyde (179) & (182)

Isotopically labelled glycolaldehyde was synthesised following modified versions of the method of Seranni *et al.*<sup>136,140,141,142</sup> and Thirkettle.<sup>137</sup>

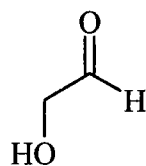
#### Glycolonitrile (178)<sup>137</sup>



178

The pH of a solution of KCN (0.5 g, 7.8 mmol) in H<sub>2</sub>O (40 ml) was adjusted from 10.5 to 8.5 with concentrated acetic acid. A solution of formaldehyde (177) (0.23 g, 7.8 mmol, 0.62 ml of a 37 % aqueous solution) in water (15 ml) was added dropwise and the solution was vigorously stirred over 1 hour, maintaining the pH at 8.5 ± 0.2 (with 10 % aqueous acetic acid or 1 M aqueous NaOH). The resultant solution was stirred for a further 40 minutes before the reaction was quenched by the addition of concentrated acetic acid, such that the pH was 4.2. Complete reaction was confirmed by TLC (acetonitrile : water : acetic acid, 40:10:0.5, glycolonitrile (178) R<sub>f</sub> = 0.9), and a negative result on a cyanide precipitate test. Glycolonitrile (178) was reacted on immediately without further manipulation as it can decompose to yield toxic gases.

## Glycolaldehyde (176)<sup>137</sup>

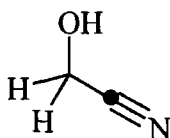


176

Solid Pd-BaSO<sub>4</sub> (0.47 g, 5 %, 60 mg per mmol of nitrile) was suspended in H<sub>2</sub>O (15 ml) and stirred vigorously under a hydrogen atmosphere. After 30 minutes the glycolonitrile (178) solution prepared above was added and the pH adjusted to pH 1.7 with concentrated H<sub>2</sub>SO<sub>4</sub>. The resultant solution was then stirred under a hydrogen atmosphere for 16 hours before the pH was again returned to pH 1.7 and stirred under a hydrogen for a further 24 hours. TLC analysis (acetonitrile : water : acetic acid, 40:10:0.5) demonstrated complete conversion of glycolonitrile (178) to glycolaldehyde (176) (spot at R<sub>f</sub> = 0.9 replaced by R<sub>f</sub> = 0.6). The catalyst was removed by filtration through a hyflo plug and the resultant solution was treated with excess Dowex 50X8 (H<sup>+</sup>) until pH = 1.0, was stirred and the resin removed by filtration. Slow and careful addition of BaCO<sub>3</sub> to this solution, ensuring that any effervescence ceased before the subsequent addition, so that at pH = 4.3 a fine, sticky precipitate formed which was removed by centrifugation (20,000 rpm, 10 minutes, 25 °C). The supernatant was treated with excess Dowex 2X8 (AcO<sup>-</sup>), with no change in pH, and the resin removed by filtration. The solution was then treated with Dowex 50X8 (H<sup>+</sup>) until pH = 0.9, the resin was removed by filtration and the solvent removed under reduced pressure (ensuring that the temperature did not exceed 45 °C). This yielded a colourless syrup of the product (176), containing acetic acid and water (0.8 g).

NMR, δ<sub>H</sub> (300 MHz, D<sub>2</sub>O): 4.89 (1H, t, <sup>3</sup>J<sub>HH</sub> = 5.25 Hz, HOCH<sub>2</sub>C(OH)<sub>2</sub>H), 3.35 (2H, d, <sup>3</sup>J<sub>HH</sub> = 5.10 Hz, HOCH<sub>2</sub>C(OH)<sub>2</sub>H).

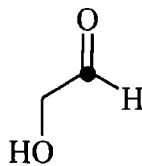
### [1-<sup>13</sup>C]-Glycolonitrile



The pH of a solution of [<sup>13</sup>C]-KCN (0.5 g, 7.8 mmol) in H<sub>2</sub>O (40 ml) was adjusted from 10.5 to 8.5 with concentrated acetic acid and reacted with formaldehyde (177) as described above for glycolonitrile (178). Complete reaction was confirmed by TLC (acetonitrile : water : acetic acid, 40:10:0.5, glycolonitrile R<sub>f</sub> = 0.9) and a negative result on a cyanide precipitate test. [1-<sup>13</sup>C]-Glycolonitrile was reacted on immediately without further manipulation as it can decompose to yield toxic gases.

NMR δ<sub>C</sub> (50.3 MHz, H<sub>2</sub>O): 119.5 (s).

### [1-<sup>13</sup>C]-Glycolaldehyde (179)



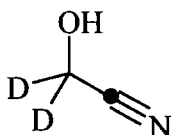
179

Solid Pd-BaSO<sub>4</sub> (0.47 g, 5 %, 60 mg per mmol of nitrile) was suspended in H<sub>2</sub>O (15 ml) and stirred vigorously under a hydrogen atmosphere. After 30 minutes the [1-<sup>13</sup>C]-glycolonitrile solution was added and the pH adjusted to pH 1.7 with concentrated H<sub>2</sub>SO<sub>4</sub>. The resultant solution was then stirred under hydrogen for 16 hours before the pH was again returned to pH 1.7 and stirred under hydrogen for a further 24 hours. TLC analysis (acetonitrile : water : acetic acid, 40:10:0.5) demonstrated complete conversion of [1-<sup>13</sup>C]-glycolonitrile to [1-<sup>13</sup>C]-glycolaldehyde (179) (spot at R<sub>f</sub> = 0.9 replaced by R<sub>f</sub> = 0.6) and so the catalyst was removed by filtration through a hyflo plug. The resultant solution was treated with excess Dowex 50X8 (H<sup>+</sup>) until pH = 1.0, stirred and the resin removed by filtration. The solvent was then removed under reduced pressure (ensuring that the temperature did not exceed 45 °C). This yielded a dark brown syrup of the product (179), containing acetic acid, some water and sulphate (2.2 g). Quantitative

conversion from [ $^{13}\text{C}$ ]-KCN would generate 0.48 g of product (**179**) (22 % of the recovered mass). The sample was used in biological feeding experiments taking this into account.

NMR  $\delta_{\text{H}}$  (200 MHz,  $\text{D}_2\text{O}$ ): 4.88 (1H, dt,  $^1J_{\text{HC}} = 163.6$  Hz,  $^3J_{\text{HH}} = 5.20$  Hz,  $\text{HOCH}_2^{13}\text{C}(\text{OH})_2\text{H}$ ), 3.34 (2H, m,  $\text{HOCH}_2^{13}\text{C}(\text{OH})_2\text{H}$ ).  $\delta_{\text{C}}$  (50.3 MHz,  $\text{D}_2\text{O}$ ): 89.8 (s).

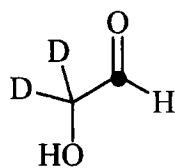
#### [1- $^{13}\text{C}$ , 2,2- $^2\text{H}_2$ ]-Glycolonitrile (**184**)



**184**

The pD of a solution of [ $^{13}\text{C}$ ]-KCN (0.52 g, 7.9 mmol) in  $\text{D}_2\text{O}$  (40 ml) was adjusted from 10.5 to 8.5 with concentrated [1- $^2\text{H}$ ]-acetic acid ( $\text{CH}_3\text{CO}_2\text{D}$ ). A solution of [ $^2\text{H}_2$ ]-formaldehyde (**181**) (0.25 g, 7.9 mmol, 1.25 ml of a 20 % solution in  $\text{D}_2\text{O}$ ) in  $\text{D}_2\text{O}$  (15 ml) was added to this vigorously stirred solution dropwise over 1 hour, maintaining the pD at  $8.5 \pm 0.2$  (with 10 % [1- $^2\text{H}$ ]-acetic acid in  $\text{D}_2\text{O}$  or 1 M NaOD in  $\text{D}_2\text{O}$ ). The resultant solution was stirred for a further 40 minutes before the reaction was quenched by the addition of concentrated [1- $^2\text{H}$ ]-acetic acid such that the pD was 4.2. Complete reaction was confirmed by TLC (acetonitrile : water : acetic acid, 40:10:0.5, glycolonitrile  $R_f = 0.9$ ), and a negative result on a cyanide precipitate test. [1- $^{13}\text{C}$ , 2,2- $^2\text{H}_2$ ]-Glycolonitrile (**184**) was reacted on immediately without further manipulation as it can decompose to yield toxic gases.

**[1-<sup>13</sup>C, 2,2-<sup>2</sup>H<sub>2</sub>]-Glycolaldehyde (182)**



**182**

Solid Pd-BaSO<sub>4</sub> (0.47 g, 5 %, 60 mg per mmol of nitrile) was suspended in D<sub>2</sub>O (15 ml) and stirred vigorously under a hydrogen atmosphere. After 30 minutes the [1-<sup>13</sup>C, 2,2-<sup>2</sup>H<sub>2</sub>]-glycolonitrile (**184**) solution was added and the pD adjusted to pD 1.7 with concentrated D<sub>2</sub>SO<sub>4</sub>. The resultant solution was then stirred under hydrogen for 16 hours before the pD was again returned to pD 1.7 and stirred under hydrogen for a further 24 hours. TLC analysis (acetonitrile : water : acetic acid, 40:10:0.5) demonstrated complete conversion of [1-<sup>13</sup>C,2,2-<sup>2</sup>H<sub>2</sub>]-glycolonitrile (**184**) to [1-<sup>13</sup>C,2,2-<sup>2</sup>H<sub>2</sub>]-glycolaldehyde (**182**) (spot at R<sub>f</sub> = 0.9 replaced by R<sub>f</sub> = 0.6) and so the catalyst was removed by filtration through a hyflo plug. The resultant solution was treated with excess Dowex 50X8 (H<sup>+</sup>) until pD = 1.0, stirred and the resin removed by filtration. Slow and careful addition of BaCO<sub>3</sub> to this solution, so that pD = 4.3, ensuring that any effervescence ceased before the subsequent addition. A fine, sticky precipitate formed, which was removed by centrifugation (20,000 rpm, 10 minutes, 25 °C). The supernatant was treated with excess Dowex 2X8 (AcO<sup>-</sup>), with no change in pD, and the resin removed by filtration. The solution was then treated with Dowex 50X8 (H<sup>+</sup>) until pD = 0.9, the resin was removed by filtration and the solvent removed under reduced pressure (ensuring that the temperature did not exceed 45 °C). This yielded a colourless syrup of the product (**182**), containing acetic acid and some D<sub>2</sub>O (1.0 g).

NMR δ<sub>H</sub> (200 MHz, D<sub>2</sub>O): 4.86 (1H, d, <sup>1</sup>J<sub>HC</sub> = 164.0 Hz, HOCD<sub>2</sub>C(OH)<sub>2</sub>H), 3.47 (0.187H, <sup>1</sup>J<sub>HC</sub> = 142.02 Hz, HOCD<sub>2</sub>CH<sub>2</sub>NH<sub>2</sub>). δ<sub>C</sub> (50.3 MHz, D<sub>2</sub>O): 89.8 (s, HOCD<sub>2</sub>C(OH)<sub>2</sub>H), 62.5 (s, HOCD<sub>2</sub>CH<sub>2</sub>NH<sub>2</sub>).

## 5.2 Biological Preparations

### 5.2.1 General details

*Streptomyces cattleya* manipulation was carried out in a Gallenkamp flowhood, with surfaces washed with 70 % ethanol (v/v) and all flask rims flame sterilised. Glassware, media and consumables were sterilised in a portable universal gas model pressure steam steriliser at 121 °C for 20 minutes (50 minutes for liquids greater than 100 ml in volume). Cultures were incubated in a temperature controlled Gallenkamp orbital incubator and resting cells on a temperature controlled Innova 2000 platform shaker. Cells were harvested in a Beckman J2-2IM/E centrifuge with a J14 head at 14,000 rpm. Other requirements for centrifugation used either the above centrifuge with a J20 head (20,000 rpm), an Eppendorf 5415C microcentrifuge or Beckman L-70 ultracentrifuge. Cells were disrupted using either a Status S70 homogeniser or a Constant Systems Ltd., French Press Cell Disruption Equipment. Aqueous solutions were reduced *in vacuo* on an FTS systems flexi-dry freeze dryer.

#### 5.2.1.1 <sup>19</sup>F NMR analysis of resting cell experiments

**Isotope incorporation:** Supernatants of resting cell experiments was lyophilised (except for 2 ml which was sent to Belfast for GCMS analysis). The residues were resuspended in D<sub>2</sub>O (0.7 ml), and particulate matter was filtered by passing the solutions through a cotton wool plug and transferred into an NMR tube. Spectra were recorded on a Varian Inova 500 MHz, <sup>19</sup>F NMR spectra were recorded at 375 MHz and <sup>1</sup>H decoupled by irradiating the sample at 500 MHz. Samples were typically analysed for 8 - 10 hours (approximately 20,000 repetitions).

**Fluorometabolite analysis:** Supernatants of resting cell or cell free experiments were transferred to an NMR tube (0.7 ml) and the spectrometer (Mercury 200 MHz spectrometers) locked and shimmed to a external sample of D<sub>2</sub>O (0.7 ml). The sample was irradiated at 188 MHz for 64 repetitions. Spectra were referenced to fluoride (-119 ppm, if present) and baseline corrected.

### 5.2.1.2 GCMS analysis of resting cell feeding studies

Culture supernatants (2 ml) were sent to Belfast for GCMS analysis by Dr J. T. G. Hamilton.

**Fluoroacetate (1):** Culture supernatants (1 ml) were mixed with an internal standard (0.25 ml, sodium propionate, final concentration 1 mM) and lyophilised. The residue was resuspended in toluene / acetonitrile (1:1 v/v) (1 ml) and both 18-crown-6 (10 mg) and 2-bromo-4'-phenylacetophenone (**101**) (10 mg) were added. The resultant solution was heated to 75 °C for 12 hours and allowed to cool. The sample was then analysed on a Hewlett Packard 5890 gas chromatograph with a Hewlett Packard Ultra 2 capillary column (12 m x 0.2 mm i.d.), 0.17 µm film thickness and a Hewlett Packard 5970B mass selective detector. Helium was used as a carrier gas at 0.8 ml.min<sup>-1</sup> and the samples (0.1 µl) were injected in the split mode (80:1). The injection port and transfer line were maintained at 280 °C. The oven was held at 130 °C for 1 minute was then ramped at 10 °C min<sup>-1</sup> up to 300 °C, and was held for a further 5 minutes. The phenylphenacyl derivatives of fluoroacetate (**102**) and propionate (**103**) had retention times of 11.8 and 12.1 minutes respectively. Splitless injections were utilised for concentrations of less than 0.2 mM fluoroacetate (**1**). The mass spectrometer operated in selected ion monitoring mode to observe mass currents m/z 272 (M, molecular ion), 273 (M+1), 274 (M+2), 33 (-CH<sub>2</sub>F), 34 (-CH<sub>2</sub>F +1) and 35 (-CH<sub>2</sub>F +2). All values were then corrected for natural abundance of stable isotope by comparison with standard (unenriched) fluoroacetate (**1**).

**4-Fluorothreonine (2):** Culture supernatants (0.25 ml) were lyophilised and the residue derivatised by heating to 100 °C for 1 hour in the presence of N-methyl-N-(trimethylsilyl)-trifluoroacetamide (MSTFA) (0.25 ml). The GC conditions employed were the same as that for the fluoroacetate derivative (**102**), although a split ratio of 50:1 was used (splitless injections were used for concentrations less than 0.2 mM). The mass spectrometer operated in selected ion monitoring mode to observe mass currents m/z 218 (C-1 and C-2), 219 (as before +1), 219 (as before +2), 236 (C-2, C-3 & C-4), 237 (as before +1), 238 (as before +2) and 239 (as before +3). All values were then corrected for natural abundance of stable isotope by comparison with standard (unenriched) 4-fluorothreonine (**2**).



### 5.2.2 *Microorganism maintenance and growth*

*Streptomyces cattleya* NRRL 8057 was obtained from The Queen's University of Belfast, Microbial Biochemistry Section, Food Science Department, Belfast (originally from United States Department of Agriculture, Agricultural Research Service, Midwest Area Northern Regional Research Laboratories, Peoria, Illinois, USA). Cultures were maintained on agar slants containing soybean flour (2 % w/v), mannitol (2 % w/v), agar (1.5 % w/v) and tap water, grown for 14 days at 28 °C before the static cultures were stored at 4 °C.

Starter and batch cultures are grown on chemically defined media, which was prepared by combining previously prepared stock solutions.

**Ion Solution**, sterilised by autoclaving

NH<sub>4</sub>Cl (6.75 g), NaCl (2.25 g), MgSO<sub>4</sub>·7H<sub>2</sub>O (2.25 g), CaCO<sub>3</sub> (1.13 g), FeSO<sub>4</sub>·7H<sub>2</sub>O (0.113 g), CoCl<sub>2</sub>·6H<sub>2</sub>O (45 mg), ZnSO<sub>4</sub>·7H<sub>2</sub>O (45 mg) and distilled water (900 ml).

**Carbon Source Solution**, sterilised by filtration (Nalgene filter sterilisation units) into 75 ml portions in presterilised Schott bottles.

Glycerol (45 g), monosodium glutamate (22.5 g), *myo*-inositol (1.8 g), *para*-aminobenzoic acid (450 µl of freshly prepared 1 mg / ml solution) and distilled water (450 ml)

**Phosphate Buffer Solution**, sterilised by autoclaving.

KH<sub>2</sub>PO<sub>4</sub> (20 g l<sup>-1</sup>) pH adjust to 7.0 (± 0.02) with KOH (2 M)

**Fluoride Solution**, sterilised by autoclaving.

NaF (0.5 M)

The previously prepared solutions were added (ion solution 150 ml, carbon source solution 75 ml, phosphate buffer solution 75 ml, fluoride solution 3 ml) to distilled water (450 ml) sterilised in a 1 l Erlenmeyer flask. After mixing 90 ml was decanted into a 500 ml Erlenmeyer flask and this was inoculated with a loop of vegetative mycelium from the maintenance cultures. The remainder of the medium was stored at 4 °C until required. The starter culture was incubated for 4 days at 28 °C on an orbital shaker at 175 rpm. The sterile defined medium was decanted into 500 ml Erlenmeyer flasks (7 x 90 ml) which were inoculated from the starter culture (0.3 ml) and then incubated for 8 days at 28 °C on an orbital shaker at 175 rpm.

### ***5.2.2.1 Variations of pH and fluoride uptake during growth of S. cattleya***

Batch cultures (4 x 90 ml) were each inoculated from a starter culture (0.3 ml) and grown under standard conditions. An aliquot (1.0 ml) was removed every 12 hours over a period of 14 days and the cells were removed by centrifugation. The supernatant was frozen (-10 °C) pending analysis. On thawing the pH of each sample was recorded and the fluoride concentration measured by the following method. An aliquot (0.5 ml), 1.0M H<sub>2</sub>SO<sub>4</sub> (aq) (0.5 ml) and of a solution of 0.5 M KNO<sub>3</sub> (4.0 ml) and 0.5 M trisodium citrate, were mixed by vortexing. The potential difference was then measured using a fluoride selective electrode, calibrated to 1.0 mM and 2.0 mM NaF.

### ***5.2.3 Resting cell experiments with isotopically labelled putative precursors***

Resting cell experiments were carried out under aseptic conditions, with all equipment and buffer autoclaved prior to use. All manipulations were carried out in a lamina flow hood. Cells were harvested by centrifugation (25 minutes, 14,000 rpm, 25 °C) and the pellet was washed three times in 50 mM MES buffer pH 6.5 (4-morpholineethanesulfonic acid monohydrate) using one third of the original culture volume, to yield cells (between 10 -15 g wet weight). The bacterial pellet was resuspended in 50 mM MES buffer pH 6.5 at a concentration of 0.176 g.ml<sup>-1</sup>. The cell suspension (5 ml) was supplemented with a putative precursor and the total volume adjusted to 23 ml with 50 mM MES buffer pH 6.5. Putative precursors were administered by filter sterilisation through a nylon membrane. If there was no organically bound fluorine in the administered precursor then fluoride was added (as NaF) at a final concentration of 2 mM. Resting cell experiments were incubated for 48 hours (unless stated otherwise) at 28 °C on an orbital shaker at 180 rpm. Prior to analysis the resting cell experiments were stopped by removal of the cells (centrifuge, 25 minutes, 20,000 rpm, 25 °C) and the supernatants stored at -15 °C. Experiments were carried out in duplicate (whenever possible) and 10 mM [2-<sup>13</sup>C]-glycine (**91**) employed as a control, as the assimilation of this label into the fluorometabolites is well established. The supernatants were then studied by <sup>19</sup>F NMR and GCMS.

### [6,6-<sup>2</sup>H<sub>2</sub>]-Glucose (105)

Cells (5 ml), 40 mM NaF (1 ml, 2 mM), MES buffer (16.5 ml) and 200 mM [6,6-<sup>2</sup>H<sub>2</sub>]-glucose (105) (0.5 ml, 5 mM). <sup>19</sup>F {<sup>1</sup>H} NMR (D<sub>2</sub>O, 470 MHz): -218.95 (O<sub>2</sub>CCH<sub>2</sub>F, 76.9 % of FAc), -218.97 (O<sub>2</sub>CCHDF, 3.3 % of FAc), -219.53 (O<sub>2</sub>CCD<sub>2</sub>F, 19.8 % of FAc), -232.71 (RCH(OH)CH<sub>2</sub>F, 75.6 % of 4-FT), -233.29 (RCH(OH)CHDF, 3.9 % of 4-FT), -233.88 (RCH(OH)CD<sub>2</sub>F, 20.6 % of 4-FT).

GCMS (ion 218, positions 1 & 2 of 4-FT, % corrected for natural abundance): 99.8, 99.7 (M); 0, 0 (M+1); 0.2, 0.3 (M+2).

GCMS (ion 236, positions 2, 3 & 4 of 4-FT, % corrected for natural abundance): 74.6, 74.5 (M); 2.7, 3.0 (M+1); 22.6, 22.6 (M+2); 0, 0 (M+3).

### D<sub>2</sub>O

Cells (5 ml), 40 mM NaF (1 ml, 2 mM), MES buffer (12.0 ml) and D<sub>2</sub>O (5 ml). <sup>19</sup>F {<sup>1</sup>H} NMR (D<sub>2</sub>O, 470 MHz): -215.47 (O<sub>2</sub>CCH<sub>2</sub>F, 79.4 % of FAc), -216.05 (O<sub>2</sub>CCHDF, 19.8 % of FAc), -216.63 (O<sub>2</sub>CCD<sub>2</sub>F, 0.8 % of FAc), -229.89 (RCH(OH)CH<sub>2</sub>F, 61.1 % of 4-FT), -230.13 (RCD(OH)CH<sub>2</sub>F, 16.7 % of 4-FT), -230.47 (RCH(OH)CHDF, 14.8 % of 4-FT), -230.71 (RCD(OH)CHDF, 5.6 % of 4-FT), -231.05 (RCH(OH)CD<sub>2</sub>F, 1.9 % of 4-FT)

### [1-<sup>13</sup>C]-Acetate (20)

Cells (5 ml), 40 mM NaF (1 ml, 2 mM), MES buffer (16.0 ml) and 200 mM [1-<sup>13</sup>C]-acetate (20) (1.0 ml, 10 mM). <sup>19</sup>F {<sup>1</sup>H} NMR (D<sub>2</sub>O, 470 MHz): -221.65 (O<sub>2</sub>CCH<sub>2</sub>F, 94.9 % of FAc), -221.73 (d, <sup>1</sup>J<sub>CF</sub> = 177.4 Hz, O<sub>2</sub>C<sup>13</sup>CH<sub>2</sub>F, 5.1 % of FAc), -235.94 (RCH(OH)CH<sub>2</sub>F, 95.0 % of 4-FT), -236.02 (d, <sup>1</sup>J<sub>CF</sub> = 168.0 Hz, RCH(OH)<sup>13</sup>CH<sub>2</sub>F, 5.0 % of 4-FT).

GCMS (ion 33, positions 2 FAc, % corrected for natural abundance): 97.4 (M), 2.6 (M+1); (ion 272, positions 1 & 2 of FAc, % corrected for natural abundance): 94.0 (M), 5.9 (M+1), 0.1 (M+2).

### [1,2-<sup>13</sup>C<sub>2</sub>]-Acetate (21)

Cells (5 ml), 40 mM NaF (1 ml, 2 mM), MES buffer (16.0 ml) and 200 mM [1,2-<sup>13</sup>C<sub>2</sub>]-acetate (21) (1.0 ml, 10 mM). <sup>19</sup>F {<sup>1</sup>H} NMR (D<sub>2</sub>O, 470 MHz): -221.64 (O<sub>2</sub>CCH<sub>2</sub>F, 68.9 % of FAc), -221.74 (dd, <sup>1</sup>J<sub>CF</sub> = 177.4 Hz, <sup>2</sup>J<sub>CF</sub> = 17.4 Hz, O<sub>2</sub><sup>13</sup>C<sup>13</sup>CH<sub>2</sub>F,

31.1 % of FAc), -235.88 (RCH(OH)CH<sub>2</sub>F, 75.3 % of 4-FT), -235.97 (dd, <sup>1</sup>J<sub>CF</sub> = 167.0 Hz, <sup>2</sup>J<sub>CF</sub> = 17.9 Hz, R<sup>13</sup>CH(OH)<sup>13</sup>CH<sub>2</sub>F, 24.7 % of 4-FT).

GCMS (ion 33, position 2 of FAc, % corrected for natural abundance): 81.5 (M), 18.5 (M+1); (ion 272, positions 1 & 2 of FAc, % corrected for natural abundance): 73.4 (M), 11.6 (M+1), 15.0 (M+2).

#### **[2,2,2-<sup>2</sup>H<sub>3</sub>]-Acetate (122)**

Cells (5 ml), 40 mM NaF (1 ml, 2 mM), MES buffer (16.0 ml) and 200 mM [2,2,2-<sup>2</sup>H<sub>3</sub>]-acetate (122) (1.0 ml, 10 mM). <sup>19</sup>F {<sup>1</sup>H} NMR (D<sub>2</sub>O, 470 MHz): -221.64 (O<sub>2</sub>CCH<sub>2</sub>F, 97.1 % of FAc), -222.23 (O<sub>2</sub>CCHDF, 2.9 % of FAc), -235.91 (RCH(OH)CH<sub>2</sub>F, 95.6 % of 4-FT), -236.50 (RCH(OH)CD<sub>2</sub>F, 4.4 % of 4-FT).

GCMS (ion 33, position 2 of FAc, % corrected for natural abundance): 97.3 (M), 2.7 (M+1); (ion 272, positions 1 & 2 of FAc, % corrected for natural abundance): 97.4 (M), 2.6 (M+1), 0.1 (M+2).

#### **[2-<sup>2</sup>H]-Glycerol (128)**

Cells (5 ml), 40 mM NaF (1 ml, 2 mM), MES buffer (16.5 ml) and 200 mM [2-<sup>2</sup>H]-glycerol (128) (0.5 ml, 5 mM): -215.45 (100 % of FAc signal), -229.72 (100 % of 4-FT signal).

#### **[2-<sup>2</sup>H]-Glycerate (129)**

Cells (5 ml), 40 mM NaF (1 ml, 2 mM), MES buffer (16.0 ml) and 200 mM [2-<sup>2</sup>H]-glycerate (129) (1.0 ml, 10 mM): -215.45 (100 % of FAc signal), -229.72 (100 % of 4-FT signal).

GCMS (ion 218, positions 1 & 2 of 4-FT, % corrected for natural abundance): 96.1 (M), 1.3 (M+1), 2.6 (M+2); (ion 236, positions 2, 3 & 4 of 4-FT, % corrected for natural abundance): 97.9 (M), 1.4 (M+1), 0.7 (M+2).

Cells (5 ml), 40 mM NaF (1 ml, 2 mM), MES buffer (16.75 ml) and 200 mM [2-<sup>2</sup>H]-glycerate (129) (0.25 ml, 2.5 mM): -215.45 (100 % of FAc signal), -229.72 (100 % of 4-FT signal).

GCMS (ion 218, positions 1 & 2 of 4-FT, % corrected for natural abundance): 100.8 (M), 1.4 (M+1), 2.3 (M+2); (ion 236, positions 2, 3 & 4 of 4-FT, % corrected for natural abundance): 98.2 (M), 0.9 (M+1), 0.8 (M+2).

Cells (5 ml), 40 mM NaF (1 ml, 2 mM), MES buffer (16.0 ml). After 1 hour 200 mM [2-<sup>2</sup>H]-glycerate (**129**) (1 ml, 10 mM) was added.

GCMS (ion 218, positions 1 & 2 of 4-FT, % corrected for natural abundance): 96.0 (M), 1.3 (M+1), 2.7 (M+2); (ion 236, positions 2, 3 & 4 of 4-FT, % corrected for natural abundance): 97.9 (M), 1.4 (M+1), 0.7 (M+2).

Cells (5 ml), 40 mM NaF (1 ml, 2 mM), MES buffer (16.0 ml), 200 mM glycolate (**50**) (1 ml, 10 mM). After 1 hour 200 mM [2-<sup>2</sup>H]-glycerate (**129**) (1 ml, 10 mM) and 40 mM NaF (1 ml, 2 mM) was added.

GCMS (ion 218, positions 1 & 2 of 4-FT, % corrected for natural abundance): 95.7 (M), 1.4 (M+1), 3.0 (M+2); (ion 236, positions 2, 3 & 4 of 4-FT, % corrected for natural abundance): 98.5 (M), 0.7 (M+1), 0.8 (M+2).

Cells (5 ml), 40 mM NaF (1 ml, 2 mM), MES buffer (16.0 ml), 200 mM glycerol (**87**) (1 ml, 10 mM). After 1 hour 200 mM [2-<sup>2</sup>H]-glycerate (**129**) (1 ml, 10 mM) and 40 mM NaF (1 ml, 2 mM) was added.

GCMS (ion 218, positions 1 & 2 of 4-FT, % corrected for natural abundance): 96.0 (M), 1.4 (M+1), 2.7 (M+2); (ion 236, positions 2, 3 & 4 of 4-FT, % corrected for natural abundance): 97.8 (M), 1.3 (M+1), 0.9 (M+2).

### **3-Fluoro-1-hydroxypropanone (133)**

Cells (5 ml), MES buffer (17 ml) and 3-fluoro-1-hydroxypropanone (1 ml) (**133**).

Time = 18 hours, Fluoride release: 0.25 mM.

<sup>19</sup>F NMR (188 MHz): -119.0 (14.9 % of total signal, F<sup>-</sup>), -216.25 (4.4 % of total signal, t, <sup>2</sup>J<sub>FH</sub> = 48.6 Hz, FAc), -229.62 (39.4 % of total signal, t, <sup>2</sup>J<sub>FH</sub> = 46.7 Hz), -231.78 (31.9 % of total signal, td, <sup>2</sup>J<sub>FH</sub> = 46.7 Hz, <sup>3</sup>J<sub>FH</sub> = 21.9 Hz), -235.87 (9.4 % of total signal, t, <sup>2</sup>J<sub>FH</sub> = 46.3 Hz).

Time = 48 hours, <sup>19</sup>F NMR (188 MHz): -119.0 (3.1 % of total signal, F<sup>-</sup>), -216.68 (18.1 % of total signal, t, <sup>2</sup>J<sub>FH</sub> = 48.1 Hz, FAc), -228.18 (16.6 % of total signal, t, <sup>2</sup>J<sub>FH</sub> = 46.9 Hz), -230.10 (19.5 % of total signal, t, <sup>2</sup>J<sub>FH</sub> = 46.9 Hz), -232.28 (26.9 % of total signal, td, <sup>2</sup>J<sub>FH</sub> = 46.9 Hz, <sup>3</sup>J<sub>FH</sub> = 22.3 Hz), -236.39 (15.5 % of total signal, t, <sup>2</sup>J<sub>FH</sub> = 46.5 Hz).

Cells (5 ml), MES buffer (17.5 ml) and 3-fluoro-1-hydroxypropanone (0.5 ml) (**133**).

Time = 18 hours,  $^{19}\text{F}$  NMR (188 MHz): -119.0 (6.0 % of total signal, F<sup>-</sup>), -216.59 (30.1 % of total signal, t,  $^2J_{\text{FH}} = 47.8$  Hz, FAc), -230.00 (37.7 % of total signal, t,  $^2J_{\text{FH}} = 46.5$  Hz), -232.17 (24.1 % of total signal, td,  $^2J_{\text{FH}} = 47.0$  Hz,  $^3J_{\text{FH}} = 22.3$  Hz), -236.28 (2.1 % of total signal, t,  $^2J_{\text{FH}} = 46.0$  Hz).

Time = 48 hours,  $^{19}\text{F}$  NMR (188 MHz): -119.0 (13.3 % of total signal, F<sup>-</sup>), -216.61 (13.2 % of total signal, t,  $^2J_{\text{FH}} = 48.3$  Hz, FAc), -230.01 (24.0 % of total signal, t,  $^2J_{\text{FH}} = 46.3$  Hz), -232.25 (40.0 % of total signal, td,  $^2J_{\text{FH}} = 46.9$  Hz,  $^3J_{\text{FH}} = 22.2$  Hz), -236.29 (9.5 % of total signal, t,  $^2J_{\text{FH}} = 46.3$  Hz).

### **[1- $^{13}\text{C}$ ]-Glycolaldehyde (179)**

Cells (5 ml), MES buffer (16 ml), 40 mM NaF (1 ml, final concentration 2 mM), < 200 mM [1- $^{13}\text{C}$ ]-glycolaldehyde (**179**) (1 ml, < 10 mM).  $^{19}\text{F}$  { $^1\text{H}$ } NMR (D<sub>2</sub>O, 470 MHz): -216.46 (100 % of FAc signal), -230.78 (100 % of 4-FT signal).

GCMS (ion 236, positions 2, 3 & 4 of 4-FT, % corrected for natural abundance): 97.0, 96.8 (M), 2.8, 2.9 (M+1), 0.2, 0.3 (M+2).

Cells (5 ml), MES buffer (16 ml), 40 mM NaF (1 ml, final concentration 2 mM), < 200 mM [1- $^{13}\text{C}$ ]-glycolaldehyde (**179**) (2 ml, < 20 mM).  $^{19}\text{F}$  { $^1\text{H}$ } NMR (D<sub>2</sub>O, 470 MHz): -216.53 (100 % of FAc signal), -230.85 (100 % of 4-FT signal).

GCMS (ion 236, positions 2, 3 & 4 of 4-FT, % corrected for natural abundance): 96.7, 96.3 (M), 3.1, 3.3 (M+1), 0.2, 0.3 (M+2).

Cells (5 ml), MES buffer (16 ml), 40 mM NaF (1 ml, final concentration 2 mM), < 200 mM [1- $^{13}\text{C}$ ]-glycolaldehyde (2 ml, < 20 mM).  $^{19}\text{F}$  { $^1\text{H}$ } NMR (D<sub>2</sub>O, 470 MHz): -215.95 (100 % of FAc signal), -230.20 (100 % of 4-FT signal).

GCMS (ion 236, positions 2, 3 & 4 of 4-FT, % corrected for natural abundance): 95.0, 94.9 (M), 4.9, 4.9 (M+1), 0.1, 0.2 (M+2).

### **[1- $^{13}\text{C}$ -2,2- $^2\text{H}_2$ ]-Glycolaldehyde (182)**

Cells (5 ml), MES buffer (16 ml), 40 mM NaF (1 ml, final concentration 2 mM), < 200 mM [1- $^{13}\text{C}$ -2,2- $^2\text{H}_2$ ]-glycolaldehyde (**182**) (1 ml, < 10 mM).  $^{19}\text{F}$  { $^1\text{H}$ } NMR (D<sub>2</sub>O, 470 MHz): -215.77 (100 % of FAc signal), -230.11 (100 % of 4-FT signal).

GCMS (ion 33, position 2 of FAc, % corrected for natural abundance): 100 (M).

GCMS (ion 272, positions 1 & 2 of FAc, % corrected for natural abundance): 98.8, 99.2 (M), 1.3, 1.3 (M+1).

GCMS (ion 236, positions 2, 3 & 4 of 4-FT, % corrected for natural abundance): 97.0, 96.6 (M), 3.0, 3.5 (M+1), 0.0, 0.0 (M+2).

Cells (5 ml), MES buffer (13.2 ml), 40 mM NaF (1 ml, final concentration 2 mM), < 200 mM [1-<sup>13</sup>C-2,2-<sup>2</sup>H<sub>2</sub>]-glycolaldehyde (**182**) (3.8 ml, < 10 mM). <sup>19</sup>F {<sup>1</sup>H} NMR (D<sub>2</sub>O, 470 MHz): -215.39 (100 % of FAc signal), -229.69 (100 % of 4-FT signal).

GCMS (ion 33, position 2 of FAc, % corrected for natural abundance): 100 (M).

GCMS (ion 272, positions 1 & 2 of FAc, % corrected for natural abundance): 98.3, 99.4 (M), 1.7, 1.7 (M+1).

GCMS (ion 236, positions 2, 3 & 4 of 4-FT, % corrected for natural abundance): 96.5, 96.5 (M), 3.2, 3.1 (M+1), 0.3, 0.3 (M+2).

#### **5.2.4 Whole cell studies with fluoroacetaldehyde (40)**

Studies on whole cell metabolism of fluoroacetaldehyde (**40**) were carried out in the same manner as the resting cell experiments for isotopically labelled putative precursors.

#### **Fluoroacetaldehyde (40)**

Cells (5 ml), MES buffer (16 ml) and 40 mM fluoroacetaldehyde (**40**) (1 ml, final concentration 2 mM). Aliquots removed (1 ml) and the cells removed by centrifugation (microcentrifuge, 14000 rpm, 5 minutes) and stored at 4 °C pending analysis.

<sup>19</sup>F NMR (376 MHz): Ratio of fluoroacetate (**1**) vs fluoroacetaldehyde (**40**) vs 2-fluoroethanol (**71**) (which is constant). T = time that aliquot removed.

**T = 0:** 0.074, 0.218, 1.00; **T = 10 minutes:** 0.183, 0.154, 1.00; **T= 20 minutes:** 0.228, 0.103, 1.00; **T= 30 minutes:** 0.226, 0.043, 1.00; **T= 40 minutes:** 0.322, 0.00, 1.00; **T= 50 minutes:** 0.320, 0.00, 1.00; **T= 60 minutes:** 0.327, 0.00, 1.00; **T= 70 minutes:** 0.362, 0.00, 1.00; **T= 80 minutes:** 0.323, 0.00, 1.00; **T= 90 minutes:** 0.329, 0.00, 1.00.

#### **Fluoroacetaldehyde (40) under nitrogen**

MES buffer was degassed by freezing, subjecting to high vacuum and thawing (this cycle was repeated twice). Cells (5 ml), in degassed MES buffer (16 ml) in a 100 ml

Erlenmeyer flask were purged with a stream of N<sub>2</sub> for 5 minutes and stoppered with a septum seal. Fluoroacetaldehyde (**40**) (1 ml, 40 mM, final concentration 2 mM) was injected into the system and the flask was incubated under standard conditions. Aliquots (1 ml) were taken and the cells were removed by microcentrifugation and the supernatants frozen pending analysis after 0, 20, 40 and 60 minutes. <sup>19</sup>F NMR analysis did not indicate the presence of fluoroacetate (**1**).

#### **Fluoroacetaldehyde (**40**) under <sup>18</sup>O<sub>2</sub>**

MES buffer was degassed by freezing, subjecting to high vacuum and thawing (this cycle was repeated twice). Cells (5 ml) and degassed 50 mM MES buffer (17 ml) in a stoppered Erlenmeyer flask with a tapped side arm, were purged for 5 minutes under a stream of N<sub>2</sub>. The flask was then subjected to a light vacuum (aspirator) and the head space above the cells replaced with N<sub>2</sub> / <sup>18</sup>O<sub>2</sub> (50 ml / 50 ml). Fluoroacetaldehyde (**40**) (40 mM, 1 ml, final concentration 2 mM) was injected into the system and the flask incubated for 1 hour. The cells were then removed by centrifugation and the supernatant frozen pending analysis. GCMS analysis (ion 272, FAc, %): 100.0, 100.0 (M), 18.2, 18.1 (M+1), 2.1, 2.0 (M+2). Natural abundance: 100 (M), 18.0 (M+1) & 2.1 (M+2).

#### **Fluoroacetaldehyde (**40**) with amino acids**

**DL-Alanine (**146**):** MES buffer was degassed by freezing, subjecting to high vacuum and thawing (this cycle was repeated twice). Cells (5 ml), degassed 50 mM MES buffer (16 ml) and 200 mM DL-alanine (**146**) (1 ml, final concentration 10 mM) in a 100 ml Erlenmeyer flask were purged with a stream of N<sub>2</sub> for 5 minutes and stoppered with a septum seal. Fluoroacetaldehyde (**40**) (1 ml, 40 mM, final concentration 2 mM) was injected into the system and the flask incubated under standard conditions. Aliquots (1 ml) were taken and the cells removed by microcentrifugation, after 1, 3 and 48 hours. The supernatants were frozen pending analysis.

<sup>19</sup>F NMR (376 MHz): Ratio of fluoroacetate (**1**) vs fluoroacetaldehyde (**40**) vs 2-fluoroethanol (**71**) (which is constant). T = time that aliquot removed.

**T = 1 hour:** 0.079, 0.297, 1.00; **T = 3 hours:** 0.24, 0.0, 1.00

Cells (5 ml), 50 mM MES buffer (16 ml) and 200 mM DL-alanine (**146**) (1 ml, final concentration 10 mM) in a 100 ml Erlenmeyer flask were incubated for 2 hours at 28 °C



on an orbital shaker. The cells were then purged with a stream of N<sub>2</sub> for 5 minutes and stoppered with a septum seal. Fluoroacetaldehyde (**40**) (1 ml, 40 mM, final concentration 2 mM) was injected into the system and the flask incubated under standard conditions. Aliquots (1 ml) were taken and the cells were removed by microcentrifugation, after 1, 3 and 48 hours. The supernatants were frozen pending analysis.

<sup>19</sup>F NMR (376 MHz): Ratio of fluoroacetate (**1**) vs fluoroacetaldehyde (**40**) vs 2-fluoroethanol (**71**) (which is constant). T = time that aliquot removed.

**T = 1 hour:** 0.030, 0.090, 1.00; **T = 3 hours:** 0.177, 0.0, 1.00

**DL-Serine (54):** MES buffer was degassed by freezing, subjecting to high vacuum and thawing (this cycle was repeated twice). Cells (5 ml), degassed 50 mM MES buffer (16 ml) and 200 mM DL-serine (**54**) (1 ml, final concentration 10 mM) in a 100 ml Erlenmeyer flask were purged with a stream of N<sub>2</sub> for 5 minutes and stoppered with a septum seal. Fluoroacetaldehyde (**54**) (1 ml, 40 mM, final concentration 2 mM) was injected into the system and the flask incubated under standard conditions. Aliquots (1 ml) were taken and the cells removed by microcentrifugation, after 1, 3 and 48 hours. The supernatants were frozen pending analysis.

<sup>19</sup>F NMR (376 MHz): Ratio of fluoroacetate (**1**) vs fluoroacetaldehyde (**40**) vs 2-fluoroethanol (**71**) (which is constant). T = time that aliquot removed.

**T = 1 hour:** 0.096, 0.0, 1.00; **T = 3 hours:** 0.183, 0.0, 1.00

Cells (5 ml), 50 mM MES buffer (16 ml) and 200 mM DL-serine (**54**) (1 ml, final concentration 10 mM) in a 100 ml Erlenmeyer flask were incubated for 2 hours at 28 °C on an orbital shaker. The cells were then purged with a stream of N<sub>2</sub> for 5 minutes and stoppered with a septum seal. Fluoroacetaldehyde (**40**) (1 ml, 40 mM, final concentration 2 mM) was injected into the system and the flask incubated under standard conditions. Aliquots (1 ml) were taken and the cells removed by microcentrifugation, after 1, 3 and 48 hours. The supernatants were frozen pending analysis.

<sup>19</sup>F NMR (376 MHz): Ratio of fluoroacetate (**1**) vs fluoroacetaldehyde (**40**) vs 2-fluoroethanol (**71**) (which is constant). T = time that aliquot removed.

**T = 1 hour:** 0.054, 0.060, 1.00; **T = 3 hours:** 0.066, 0.0, 1.00

### **[1-<sup>2</sup>H]-Fluoroacetaldehyde (147)**

Cells (5 ml), MES buffer (14 ml), and [1-<sup>2</sup>H]-fluoroacetaldehyde (147) (4 ml).

GCMS (T=0, 4-FT): nd

GCMS (T=1 hours, 4-FT): nd

GCMS (T=2 hours, ion 236, positions 2, 3 & 4 of 4-FT, % corrected for natural abundance): 74.8 (M), 39.7 (M+1), -14.5 (M+2).

GCMS (T=3 hours, ion 236, positions 2, 3 & 4 of 4-FT, % corrected for natural abundance): 63.5 (M), 52.7 (M+1), -16.1 (M+2).

GCMS (T=5 hours, ion 236, positions 2, 3 & 4 of 4-FT, % corrected for natural abundance): 51.4 (M), 51.8 (M+1), -3.2 (M+2).

GCMS (T=7.5 hours, ion 236, positions 2, 3 & 4 of 4-FT, % corrected for natural abundance): 41.8 (M), 59.5 (M+1), -1.3 (M+2).

GCMS (T=21 hours, ion 236, positions 2, 3 & 4 of 4-FT, % corrected for natural abundance): 86.6 (M), 13.7 (M+1), -0.3 (M+2).

GCMS (T=48 hours, ion 236, positions 2, 3 & 4 of 4-FT, % corrected for natural abundance): 87.6, 87.8 (M), 12.6, 12.6 (M+1), -0.2, -0.4 (M+2).

### **[1-<sup>2</sup>H]-Fluoroacetaldehyde (147) and [2-<sup>13</sup>C]-glycine (91)**

Cells (5 ml), MES buffer (16 ml), 40 mM NaF (1 ml, final concentration 2 mM), 200 mM [2-<sup>13</sup>C]-glycine (91) (1 ml, final concentration 10 mM).

GCMS (ion 218, positions 1 & 2 of 4-FT, % corrected for natural abundance): 98.3, 98.5 (M), 1.2, 1.1 (M+1), 0.6, 0.4 (M+2).

GCMS (ion 236, positions 2, 3 & 4 of 4-FT, % corrected for natural abundance): 70.1, 68.5 (M), 9.1, 9.5 (M+1), 20.7, 21.6 (M+2), 0.2, 0.4 (M+3).

Cells (2.5 ml), MES buffer (6.5 ml), 200 mM [2-<sup>13</sup>C]-glycine (91) (0.5 ml, final concentration 10 mM) and [1-<sup>2</sup>H]-fluoroacetaldehyde (147) (2 ml).

GCMS (T=0, 4-FT): nd

GCMS (T=3 hours, 4-FT): nd

GCMS (T=6 hours, ion 236, positions 2, 3 & 4 of 4-FT, % corrected for natural abundance): 46.8 (M), 29.4 (M+1), 22.5 (M+2), 1.3 (M+3).

GCMS (T=9 hours, ion 236, positions 2, 3 & 4 of 4-FT, % corrected for natural abundance): 63.5 (M), 18.4 (M+1), 17.3 (M+2), 0.8 (M+3).

GCMS (T=24 hours, ion 236, positions 2, 3 & 4 of 4-FT, % corrected for natural abundance): 58.7 (M), 15.9 (M+1), 24.6 (M+2), 0.8 (M+3).

GCMS (ion 218): unresolved for all time points.

Cells (2.5 ml), MES buffer (6.5 ml), 200 mM [2-<sup>13</sup>C]-glycine (**91**) (0.05 ml, final concentration 1.0 mM) and [1-<sup>2</sup>H]-fluoroacetaldehyde (**147**) (2 ml).

GCMS (T=0, 4-FT): nd

GCMS (T=3 hours, 4-FT): nd

GCMS (T=6 hours, ion 236, positions 2, 3 & 4 of 4-FT, % corrected for natural abundance): 57.2 (M), 39.0 (M+1), 3.4 (M+2), 0.3 (M+3).

GCMS (T=9 hours, ion 236, positions 2, 3 & 4 of 4-FT, % corrected for natural abundance): 72.0 (M), 24.9 (M+1), 2.5 (M+2), 0.6 (M+3).

GCMS (T=24 hours, ion 236, positions 2, 3 & 4 of 4-FT, % corrected for natural abundance): 87.2 (M), 11.1 (M+1), 1.4 (M+2), 0.3 (M+3).

GCMS (ion 218): unresolved for all time points.

#### **Fluoroacetaldehyde (40) with *Streptomyces cinnamomensis***

*Streptomyces cinnamomensis* was grown from a frozen glycerol cell suspension. Once thawed this suspension was used to inoculate petri dishes containing (g/l): yeast extract (4.0), malt extract (10.0), glucose (4.0) and agar (14.0). This was incubated at 29.5 °C for 10 days. Vegetative mycelia from these petri dishes was then used to inoculate complex media (70 ml) in 250 ml Erlenmeyer flasks, which were incubated for 10 days at 32 °C. The complex media contained (g / l): glucose (24.0), soybean flour (15.0), CaCO<sub>3</sub> (3.0), FeSO<sub>4</sub>·7H<sub>2</sub>O (5.5) and MgCl<sub>2</sub>·6H<sub>2</sub>O (0.029). The cells were then harvested as for *Streptomyces cattleya* (section 5.2.3) and suspended in MES buffer at 0.176 g wet wt. / ml.

High cell density: 40 mM Fluoroacetaldehyde (1 ml, 2 mM) was added to a cell suspension (22 ml) and incubated at 28 °C. Aliquots removed (1 ml) and the cells removed by centrifugation (microcentrifuge, 14000 rpm, 5 minutes) and stored at 4 °C pending analysis.

<sup>19</sup>F NMR (376 MHz): Ratio of fluoroacetate (**1**) vs fluoroacetaldehyde (**40**) vs 2-fluoroethanol (**71**) (assumed to remain constant). T = time that aliquot removed in minutes.

**T = 20:** 0.00, 0.183, 1.00; **T = 40:** 0.00, 0.21, 1.00; **T = 60:** 0.020, 0.166, 1.00.

Low cell density: 40 mM Fluoroacetaldehyde (1 ml, 2 mM) was added to a cell suspension (5 ml) in MES buffer (17 ml) and incubated at 28 °C. Aliquots removed (1 ml) and the cells removed by centrifugation (microcentrifuge, 14000 rpm, 5 minutes) and stored at 4 °C pending analysis.

<sup>19</sup>F NMR (376 MHz): Ratio of fluoroacetate (**1**) vs fluoroacetaldehyde (**40**) vs 2-fluoroethanol (**71**) (assumed to remain constant). T = time that aliquot removed in minutes.

**T = 20:** 0.00, 0.20, 1.00; **T = 40:** 0.00, 0.23, 1.00; **T = 60:** 0.00, 0.19, 1.00.

### ***5.2.5 Cell free studies***

Cells were harvested by centrifugation (25 minutes, 14,000 rpm, 25 °C) and the pellet was washed three times in 50 mM MES buffer pH 6.5 (4-morpholine ethanesulfonic acid monohydrate) using one third the original culture volume, to yield cells (between 10 -15 g wet weight). All subsequent steps were carried out in pre-chilled glassware (in ice water) and the centrifuge cooled to 4 °C.

#### ***5.2.5.1 Protein concentration determination***

Protein concentration was determined by the Bradford assay.<sup>128</sup> The test solution was prepared by dissolving Brilliant Blue Dye (50 mg) in 95 % aqueous ethanol (25 ml) and left to stir for 3 hours. 85 % H<sub>3</sub>PO<sub>4</sub> aq. (50 ml) was added and the resultant solution was then diluted with distilled water so that the final volume was 500 ml. To this solution 1.00 M NaOH (aq) was added at 50 µl / ml. The resultant solution was stored at 4 °C and warmed thoroughly to room temperature before use. An aliquot (1 ml) was added to 20 µl of protein solution and mixed thoroughly. After 5 minutes (and no more than after 15 minutes) the absorbance at  $\lambda = 590$  nm measured. This was then compared with a standard curve derived from known concentrations of bovine serum album (BSA).

#### ***5.2.5.2 Cell disruption by sonication***

The bacterial pellet was resuspended in ice cold 50 mM MES buffer pH 6.5 (2 ml of buffer per g wet wt. of cells) and the thick slurry placed in a thick glass tube (inner diameter 17 mm) suspended in an ice water bath. A sonic probe was lowered into the

slurry so that it protruded no more than 5 mm into it. The cells were disrupted to yield the maximum concentration of protein, which was 3 bursts of 10 seconds each on 60 % power (maximum for probe used). The cell debris was removed by centrifugation (20,000 rpm, 20 minutes, 4 °C) and the supernatant decanted. The protein concentration determined by the Bradford assay and used in a cell-free study.

A typical cell free experiment was prepared as follows: Cell free extract (0.625 ml), and 40 mM fluoroacetaldehyde (**40**) (2 mM), were added to MES buffer to a final volume of 5 ml. The MES buffer contained the following co-factors to give the stated final concentrations: NAD<sup>+</sup> (2 mM), NADP<sup>+</sup> (1 mM), ATP (5 mM), COASH (0.5 mM), DTT (2 mM), FAD (2 mM) and FMN (2 mM). The resultant solution were incubated in a water bath at 29 °C for 24 hours before being placed in water (> 85 °C) for 5 minutes and the protein precipitate removed by centrifugation (20,000 rpm, 10 minutes). The supernatants were then frozen pending analysis. <sup>19</sup>F NMR (376 MHz): In all samples, only fluoroacetaldehyde (**40**) and 2-fluoroethanol (**71**) resonances observed.

### *5.2.5.3 Cell disruption using the French press*

The bacterial pellet was resuspended in ice cold 50 mM MES buffer pH 6.5 containing 2 mM dithiothreitol (100 ml). The cells were disrupted by passing the slurry once through a prechilled (4 °C) French press operating at 26,000 p.s.i. The French press was washed through with MES buffer (50 ml) and the fractions combined. After fifteen minutes the cell debris was removed by centrifugation (20,000 rpm, 4 °C, 20 minutes) and the supernatant decanted. The protein concentration was determined (by the Bradford assay) and used in a cell free study.

Typical examples of cell free experiments were prepared as follows: Cell free extract (5 ml) and 14 mM fluoroacetaldehyde (**40**) (1 ml, 2 mM) were added to 50 mM MES buffer pH 6.5 (1 ml). The MES buffer contained the following co-factors to give the stated final concentrations: NAD<sup>+</sup> (2.0 mM), NADP<sup>+</sup> (1.33 mM), FAD (2 mM), FMN (2 mM), CoASH (0.5 mM) and ATP (5 mM). The resultant solution were incubated in a water bath at 29 °C. Once the time period for that experiment was completed the solutions were placed in water (> 85 °C) for 5 minutes and the protein precipitate removed by centrifugation (20,000 rpm, 10 minutes). The supernatants were then

frozen pending analysis. Specific experiments and results are tabulated in text (**chapter 3**).

In the study of the fluorination of phosphorylated glycolytic intermediates, instead of adding 14 mM fluoroacetaldehyde (**40**) (1 ml), 28 mM of the 'glycolytic intermediate' (0.5 ml, 2 mM) and 28 mM NaF (0.5 mM, 2 mM) were added. In order to dissolve glycolaldehyde phosphate (**164**) in 50 mM MES buffer it was necessary to add one drop of 1 M HCl (aq). This did not significantly alter the pH of the overall solution. Specific experiments and results are tabulated in text (**chapter 4**).

#### **5.2.5.4 Phosphate release assay**<sup>133</sup>

The phosphate concentration of a cell free experiment was measured by the method of Jenkins and Marshall. To an aliquot (1.00 ml) of the solution under analysis was added 1.00 M perchloric acid (200  $\mu$ l). After mixing (by vortex), 0.25 M imidazole (100  $\mu$ l) buffered to pH 5.0 with HCl (aq.) and then 1.5 % (m/v) sodium molybdate (500  $\mu$ l) were added and the resultant solution mixed. Butyl acetate (2.00 ml) was then added and, the solution mixed by vortex for 10 seconds. Phase separation was achieved by centrifugation (5000 rpm, 2 minutes). An aliquot (1.00 ml) was removed from the upper organic layer and the absorbance at  $\lambda = 310$  nm was measured. The phosphate concentration was then determined against a standard curve (**section 4.2, Fig. 4.9**).

## References

---

- 1 J. S. C. Marais, *Onderstepoort J. Vet. Sci. Anim.*, **18** (1943), 203 and J. S. C. Marais, *Onderstepoort J. Vet. Sci. Anim.*, **20** (1944), 67.
- 2 J. J. M. Meyer and D. O'Hagan, *Chem. Br.*, **28** (1992), 785.
- 3 L. Stryer, *Biochemistry*, 3<sup>rd</sup> Ed. (1988), W. H. Freeman & Co., New York.
- 4 B. Alberts, D. Bray, J. Lewis, M. Raff, K. Roberts and J. D. Watson, *The Molecular Biology of the Cell*, 3<sup>rd</sup> Ed. (1994), Garland Publishing, Inc., New York.
- 5 V. Betina, *Folia Microbiol.*, **40** (1995), 51.
- 6 J. W. Bennett and R. Bentley, *Adv. Appl. Microbiol.*, **34** (1989), 1.
- 7 M. J. Stone and D. H. Williams, *Mol. Microbiol.*, **6** (1992), 29.
- 8 J. Mann, *Chemical Aspects of Biosynthesis*, Oxford Chemistry Primers (1994), Oxford University Press, Oxford.
- 9 J. Mann, *Murder, Magic and Medicine*, 1992, Oxford University Press, Oxford.
- 10 S. Wrigley, M. Hayes, R. Thomas and E. Chrystal (Eds.), *Phytochemical Diversity: a source of new industrial products*, (1997), The Royal Society of Chemistry, Cambridge.
- 11 L. J. Nisbet and M. Moore, *Current Opinion in Biotechnology*, **8** (1997), 708.
- 12 J. Davis, *Mol. Microbiol.*, **4** (1990), 1227.
- 13 H. K. Lichtenthaler, J. Schwender, A. Disch and M. Rohmer, *FEBS Lett.*, **400** (1997), 271.
- 14 W. Eisenreich, S. Sagner, M. Zenk and A. Bacher, *Tetrahedron Lett.*, **38** (1997), 3889.
- 15 J. Mann, *Secondary Metabolism*, 2<sup>nd</sup> Ed. (1987), Clarendon Press, Oxford.
- 16 J. Mann and M. J. C. Crabbe, *Bacteria and Antibacterial Agents*, Biochemical and Medicinal Chemistry Series (1996), Spektrum Academic Publishers, Oxford.
- 17 M. J. Stone and D. H. Williams, *Mol. Microbiol.*, **6** (1992), 29.
- 18 quoted in H. G. Derx, *Akad. Wet. Amsterdam, Proc. Sect. Sci.*, **28** (1925), 96.
- 19 C. R. Hutchinson, *Natural Product Reports*, **3** (1986), 133.

- 
- 20 K. B. G. Torssell, *Natural Product Chemistry*, 2<sup>nd</sup> Ed. (1997), Swedish Pharmaceutical Press, Stockholm, Sweden.
- 21 S. Rose and S. Bullock, *The Chemistry of Life*, 3<sup>rd</sup> Ed. (1991), Penguin Group, London.
- 22 J. Oró, *J. Biochem. Biophys. Res. Commun.*, **2** (1960), 407.
- 23 C. W. Cornforth, *Nature*, **191** (1961), 1193.
- 24 M. J. Garson and J. Staunton, *Chem. Soc. Rev.*, **8** (1979), 539.
- 25 J. C. Vederas, *Nat. Prod. Rep.*, (1987), 227.
- 26 L. Fowden, *Proc. Roy. Soc.*, **B171** (1968), 5.
- 27 G. W. Gribble, *Prog. Chem. Org. Nat. Prod.*, **68** (1996), 1.
- 28 G. W. Gribble, *Pure & Appl. Chem.*, **68** (1996), 1699.
- 29 G. W. Gribble, *J. Chem. Edu.*, **71** (1994), 907.
- 30 L. Stryer, *Biochemistry*, 3<sup>rd</sup> Ed. (1988), W. H. Freeman & Co., New York, pp. 1001.
- 31 K.-H. van Pée, *Annu. Rev. Microbiol.*, **50** (1996), 375.
- 32 D. B. Harper, *Nature*, **315** (1985), 55.
- 33 G. W. Gribble, *Acc. Chem. Res.*, **31** (1998), 141.
- 34 M. Morrison and G. R. Schonbaum, *Annu. Rev. Biochem.*, **45** (1976), 861.
- 35 M. Picard, J. Gross, E. Lübbert, S. Tölzer, S. Krauss, K.-H. van Pée and A. Berkessel, *Angew. Chem. Int. Ed. Engl.*, **36** (1997) 1196.
- 36 L. P. Hager, D. R. Morris, F. S. Brown and H. Eberwein, *J. Biol. Chem.*, **241** (1966), 1769.
- 37 T. Dairi, T. Nakano, K. Aisaka, R. Katsumata and M. Hasegawa, *Biosci. Biotechnol. Biochem.*, **59** (1995), 1099.
- 38 S. Kirner, S. Krauss, G. Sury, S. T. Lam, J. M. Ligon and K.-H. van Pée, *Microbiol.*, **142** (1996), 2129.
- 39 N. N. Greenwood and A. Earnshaw, *Chemistry of the Elements*, 1<sup>st</sup> Ed. (1984), Pergamon Press, Oxford.
- 40 P. Venkateswarlu, W. D. Armstrong and L. Singer, *Plant Physiol.*, **40** (1965), 255.
- 41 S. M. Andrews and J. A. Cooke and M. S. Johnson, *Environ. Pollut.*, **60** (1989), 165.



- 
- 42 R. P. Gregson, B. A. Baldo, P. G. Thomas, R. J. Quinn, P. R. Bergquist, J. F. Stephens and A. R. Horne, *Science*, **206** (1979), 1108.
- 43 D. B. Harper and D. O'Hagan, *Nat. Prod. Rep.*, **11** (1994), 123.
- 44 D. O'Hagan and H. S. Rzepa, *J. Chem. Soc., Chem. Commun.*, 1997, 645.
- 45 J. S. C. Marais, *Onderstepoort J. Vet. Sci. Anim.*, **18** (1943), 203.
- 46 J. S. C. Marais, *Onderstepoort J. Vet. Sci. Anim.*, **20** (1944), 67.
- 47 P. F. V. Ward, R. J. Hall and R. A. Peters, *Nature*, **201** (1964), 611.
- 48 D. B. Harper, J. T. G. Hamilton and D. O'Hagan, *Tetrahedron Lett.*, **31** (1990), 1776.
- 49 R. A. Peters and M. Shorthouse, *Nature*, **216** (1967), 80.
- 50 K. Miura, S. Otsuka and K. Honda, *Bull. Agric. Chem. Soc. Japan*, **20** (1956), 219.
- 51 F. L. M. Pattison, *Industrial Toxic Agents*, Elsevier Monographs (1959), Elsevier Publishing Company, Amsterdam.
- 52 R. A. Peters, R. W. Wakelin, P. Buffa and L. C. Thomas, *Proc. Roy. Soc.*, **B140** (1953), 497.
- 53 R. Keck, H. Haas and J. Retey, *FEBS Lett.*, **114** (1980), 287.
- 54 W. C. Stallings, C. T. Monti, J. F. Belvedere, R. K. Preston and J. P. Glusker, *Arch. Biochem. Biophys.*, **203** (1980), 65.
- 55 E. Kun and R. J. Dummel, *Methods Enzymol.*, **13** (1969), 623.
- 56 H. Lauble, M. C. Kennedy, M. H. Emptage, H. Beinert and C. D. Stout, *Proc. atl. Acad. Sci. USA.*, **93** (1996), 13699.
- 57 J. J. M. Meyer, N. Grobbelaar, R. Vlegaar and A. I. Louw, *J. Plant Physiol.*, **139** (1992), 369.
- 58 J. Y. Cheng, M. H. Yu, G. W. Millar and G. W. Welkie, *Environ. Sci. Technol.*, **2** (1968), 367.
- 59 J. N. Eloff and B. von Sydow, *Phytochem.*, **10** (1971), 1409.
- 60 P. Goldman, *J. Biol. Chem.*, **240** (1965), 3434.
- 61 P. Goldman and G. W. A. Milne, *J. Biol. Chem.*, **241** (1966), 5557.
- 62 J. R. L. Walker and B. C. Lien, *Soil Biol. Biochem.*, **13** (1981), 231.
- 63 H. Kawasaki, K. Miyashi and K. Tonomura, *Agric. Biol. Chem.*, **45** (1981), 231.

- 
- 64 J.-Q.Liu, T. Kurihara, S. Ichiyama, M. Miyagi, S. Tsunasawa, H. Kawasaki, K. Soda and N. Esaki, *J. Biol. Chem.*, **273** (1998), 30897.
- 65 R. J. Mead, A. J. Oliver and D. R. King, *Aust. J. Biol. Sci.*, **32** (1979), 15.
- 66 A. I. Soifer and P. J. Kostyniak, *J. Biol. Chem.*, **239** (1984), 10787.
- 67 P. F. V. Ward and N. S. Huskisson, *Biochem. J.*, **130** (1972), 575.
- 68 S. O. Thomas, V. L. Singleton, J. A. Lowey, R. W. Sharpe, L. M. Pruess, J. N. Porter, J. H. Mowat and N. Bohonos, *Antibiotics Annu.*, (1957), 716.
- 69 G. O. Morton, J. E. Lancaster, G. E. van Lear, W. Fulmor and W. E. Meyer, *J. Am. Chem. Soc.*, **91** (1969), 1535.
- 70 I. D. Jenkins, J. P. H. Verheyden and J. G. Moffatt, *J. Am. Chem. Soc.*, **98** (1976), 3346.
- 71 A. R. Maguire, W.-D. Meng, S. M. Roberts and A. J. Willetts, *J. Chem Soc., Perkin Trans. 1*, (1993), 1795.
- 72 M. Sanada, T. Miyano, S. Iwadare, J. M. Williamson, B. H. Arison, J. L. Smith, A. W. Douglas, J. M. Liesch and E. Inamine, *J. Antibiotics*, **39** (1986), 259.
- 73 M. R. Amin, D. B. Harper, J. M. Moloney, C. D. Murphy, J. A. K. Howard and D. O'Hagan, *J. Chem. Soc., Chem. Commun.*, (1997), 1471.
- 74 D. Blaser and D. Seebach, *Liebigs Ann. Chem.*, (1991), 1067.
- 75 R. J. Mead and W. Segal, *Aust. J. Biol. Sci.*, **25** (1972), 327.
- 76 A. S. Seneviratne and L. Fowden, *Phytochem.*, **7** (1968), 1039.
- 77 S. Nigam and C. Ressler, *Biochim. Biophys. Acta*, **93** (1964), 339.
- 78 H. G. Floss, L. Hadwiger and E. E. Conn, *Nature*, **208** (1965), 1207.
- 79 G. A. Maw and C. M. Coyne, *Archs. Biochem. Biophys.*, **127** (1968), 241.
- 80 E. A. Barnsley, *Biochim. Biophys. Acta*, **90** (1964), 24.
- 81 R. J. Mead and W. Segal, *Phytochem.*, **12** (1973), 1977.
- 82 E. Kun, *Carbon-Fluorine Compounds: Chemistry, Biochemistry and Biological Activities*, *CIBA Foundation Symposium* (1972), Ed. K. Elliott and J. Birch, Associated Scientific Publishers, Amsterdam, pp158
- 83 L. S. Leung and P. A. Frey, *Biochem. Biophys. Res. Commun.*, **81** (1978), 274.
- 84 J. J. M. Meyer and D. O'Hagan, *Phytochem.*, **31** (1992), 499.
- 85 J. J. M. Meyer and D. O'Hagan, *Phytochem.*, **31** (1992), 2699.

- 
- 86 R. A. Peters and M. Shorthouse, *Life Sci.*, **6** (1967), 1565.
- 87 R. A. Peters, *Fluoride*, **6** (1973), 189.
- 88 S. L. Neidleman and J. Geigert, *Trends in Biotechnology*, **1** (1983), 21
- 89 S. L. Neidleman and J. Geigert, *Biohalogenation: Principles, Basic Roles and Applications*, 1986, Ellis Horwood Ltd., Chichester, p. 173.
- 90 J. N. Eloff and N. Grobbelaar, *Joernaal van die Suid-Afrikaanse Chemiese Institute*, **25** (1972), 109.
- 91 M. Luckner, *Secondary Metabolism in Microorganisms, Plants and Animals*, 3<sup>rd</sup> Ed. (1990), Springer-Verlag, Berlin.
- 92 D. B. Harper and D. O'Hagan, *Nat. Prod. Rep.*, **11** (1994), 123, ref. 120
- 93 T. D. Brock, D. W. Smith and M. T. Madigan, *Biology of Microorganisms*, 4<sup>th</sup> Ed (1984), Prentice-Hall, Inc., Englewood Cliffs, USA.
- 94 N. N. Gerber and H. A. Lechevalier, *Appl. Microbiol.*, **13** (1965), 935.
- 95 K. F. Chater, *Microbiol.*, **144** (1998), 1465.
- 96 J. S. Kahan, F. M. Kahan, R. Goegelman, S. A. Currie, M. Jackson, E. O. Stapley, T. W. Millar, A. K. Hendlin, S. Mochales, S. Hernandez, H. B. Woodruff and J. Birnbaum, *J. Antibiotics*, **32** (1979), 1.
- 97 E. W. Nester, C. E. Roberts, M. T. Nester, *Microbiology: a Human Perspective*, 1<sup>st</sup> Ed (1995), Wm. C. Brown Publishers, Dubuque, USA.
- 98 J. M. Williamson, E. Inamine, K. Wilson, A. W. Douglas, J. M. Liesch and G. Albers-Schönberg, *J. Biol. Chem.*, **260** (1985), 4637.
- 99 K. A. Reid, J. T. G. Hamilton, R. D. Bowden, D. O'Hagan, L. Dasaradhi, M. R. Amin and D. B. Harper, *Microbiol.*, **141** (1995), 1385.
- 100 M. R. Amin, *Ph.D. thesis*, University of Durham, 1996
- 101 T. Tamura, M. Wada, N. Esaki and K. Soda, *J. Bacteriol.*, **177** (1995), 2265.
- 102 J. T. G. Hamilton, M. R. Amin, D. B. Harper and D. O'Hagan, *J. Chem. Soc., Chem. Commun.*, (1997), 797.
- 103 J. T. G. Hamilton, C. D. Murphy, M. R. Amin, D. O'Hagan and D. B. Harper, *J. Chem. Soc., Perkin Trans. 1*, (1998), 759.
- 104 J. Nieschalk, J. T. G. Hamilton, C. D. Murphy, D. B. Harper and D. O'Hagan, *J. Chem. Soc., Chem. Commun.*, (1997), 799.
- 105 K. Reid, *PhD Thesis*, 1994, The Queen's University of Belfast, Belfast.

- 106 J. T. G. Hamilton, *PhD Thesis*, 1998, The Queen's University of Belfast, Belfast.
- 107 C. D. Murphy, *PhD Thesis*, 1998, The Queen's University of Belfast, Belfast.
- 108 M. R. Amin, *PhD Thesis*, 1996, University of Durham, Durham.
- 109 L. Stryer, *Biochemistry*, 3<sup>rd</sup> Ed. (1988), W. H. Freeman & Co., New York, p354.
- 110 R. V. Chari and J. W. Kozarich, *J. Org. Chem.*, **47** (1982), 2355.
- 111 L. Van Hijfte, V. Heydt and M. Kolb, *Tetrahedron Lett.*, **34** (1993), 4793.
- 112 M.-T. Lai, E. Oh, Y. Shih and H.-W. Liu, *J. Org. Chem.*, **57** (1992), 2471.
- 113 A. Sattler and G. Haufe, *J. Fluorine Chem.*, **69** (1994), 185.
- 114 J. Umezawa, O. Takahashi, K. Furuhashi and H. Norhira, *Tetrahedron: Asymmetry*, **4** (1993), 2053.
- 115 H. Suga, T. Hamatani and M. Schlosser, *Tetrahedron*, **46** (1990), 4247.
- 116 M. J. Manesco, S.-L. Huang and D. Swern., *J. Org. Chem.*, **43** (1978), 2480.
- 117 J. R. Durrwachter, D. G. Drueckhammer, K. Nozaki, H. M. Sweers and C.-H. Wong, *J. Am. Chem. Soc.*, **108** (1986), 7812.
- 118 L. Chen, D. P. Dumas and C.-H. Wong, *J. Am. Chem. Soc.*, **114** (1992), 741.
- 119 R. L. Pederson, K. K.-C. Liu, J. F. Rutan, L. Chen and C.-H. Wong, *J. Org. Chem.*, **55** (1990), 4897.
- 120 F. Effenberger, V. Null and T. Ziegler, *Tetrahedron Lett.*, **33** (1992), 5157.
- 121 B. C. Saunders, G. J. Stacey and I. G. E. Wilding, *J. Chem. Soc.*, 1949, 773.
- 122 L. Lemarie, M. C. Malet-Martino, S. Longo, R. Martino, M. de Forni and M. Carton, *The Lancet*, **337** (1991), 560.
- 123 T. Bugg, *An Introduction to Enzyme and Coenzyme Chemistry*, 1997, Blackwell Science Ltd., Oxford.
- 124 K. A. Reynolds, D. O'Hagan, D. Gani and J. A. Robinson, *J. Chem. Soc., Perkin Trans. 1*, 1998, 3195.
- 125 D. O'Hagan, S. V. Rogers, G. R. Duffin and K. A. Reynolds, *J. Antibiotics*, **48** (1995), 1280.
- 126 S. Rogers, *PhD Thesis*, 1994, University of Durham, Durham.
- 127 D. E. Cane, T. C. Liang and H. Hasler, *J. Am. Chem. Soc.*, **104** (1982), 7274.
- 128 M. M. Bradford, *Anal. Biochem.*, **86** (1976), 544.

- 
- 129 T. G. Appleton, J. R. Hall, D. W. Neale and C. S. M. Thompon, *Inorg. Chem.*, **29** (1990), 3985.
- 130 D. Müller, S. Pitsch, A. Kittaka, E. Wagner, C. E. Wintner and A. Eschenmoser, *Helvetica Chimica Acta*, **73** (1990), 1410.
- 131 K. B. G. Torssell, *Natural Product Chemistry*, 2<sup>nd</sup> Ed. (1997), Swedish Pharmaceutical Press, Stockholm, Sweden, p 39.
- 132 S. G. Carter and D. W. Karl, *J. Biochem. & Biophys. Methods*, (1982), 7.
- 133 W. T. Jenkins and M. M. Marshall, *Anal. Biochem.*, **141** (1984), 155.
- 134 R. K. Scopes, *Protein Purification, Principles and Practice*, 3<sup>rd</sup> Ed. (1994), Springer, New York, p76.
- 135 R. K. Scopes, *Protein Purification, Principles and Practice*, 3<sup>rd</sup> Ed. (1994), Springer, New York, p346.
- 136 A. S. Seranni, H. A. Nunez, M. L. Hayes and R. Barker, *Methods in Enzymol.*, **89** (1982), 64.
- 137 J. E. Thirkettle, *PhD Thesis*, University of Oxford, 1997.
- 138 J. E. Thirkettle, J. E. Baldwin, J. Edwards, J. P. Griffin and C. J. Schofield, *J. Chem. Soc., Chem. Commun.*, 1997, 1025.
- 139 M.-T. Lai, E. Oh, Y. Shih and H.-W. Liu, *J. Org. Chem.*, **57** (1992), 2471.
- 140 A. S. Seranni, J. Pierce and R. Barker, *Carbohydrate Metabolism, Methods in Enzymology*, **89** (1982), D p73
- 141 A. S. Seranni, E. L. Clark and R. Barker, *Carbohydrate Metabolism, Methods in Enzymology*, **89** (1982), D p79
- 142 A. S. Seranni, E. Cadman, J. Pierce, M. L. Hayes and R. Barker, *Carbohydrate Metabolism, Methods in Enzymology*, **89** (1982), D p83.

## ***Appendix I: List of conferences attended***

Post-graduate Bioorganic symposium, Liverpool, December 1996

RSC Perkin Regional (Scotland) Meeting, Glasgow, December 1997

Royal Society of Chemistry, National Congress, Durham, April 1998

Heterocycles symposium, Sunderland, May 1998

Polyketides II: Chemistry, Biochemistry and Molecular Genetics,  
Bristol, July 1998 (*2 poster presentations*)

**RSC Bursary gratefully acknowledged**

EU Project review meeting, Antitumour Antibiotics, Durham, May 1998  
(*oral presentation*)

Post-graduate Bioorganic symposium, Leicester, January 1999 (*oral presentation*)

North-East Postgraduate symposium, Newcastle, May 1999 (*oral presentation*)

EU Project review meeting, Antitumour Antibiotics, Tübingen, March 1999  
(*oral presentation*)

Biodiversity, St. Andrews, September 1999 (*poster presentation*)

**RSC Bursary gratefully acknowledged**

